

DEVELOPING A NOVEL FEEDING STRATEGY FOR ENHANCED LENTIVIRAL VECTOR PRODUCTION

THESIS
submitted for the degree of
Doctor in Engineering (EngD)

by
Hamza Patel

Department of Biochemical Engineering
University College London

2022

DECLARATION

I, Hamza Patel, confirm that the work presented in this thesis is my own. Where information has been derived from other sources, I confirm that this has been indicated in the thesis.

All the work described in this thesis was carried out in the Department of Biochemical Engineering, University College London and GlaxoSmithKline Medicines Research Centre, Stevenage, under the supervision of Dr Qasim Rafiq, Professor Martina Micheletti and Dr Peter Archibald. This thesis is my own work and contains nothing which is the outcome of work done in collaboration with others except as specified in the text and summarised in the Statement of Contributions.

This thesis has not been submitted, either in whole or in part, for another degree or another qualification at any other university.

ACKNOWLEDGMENTS

First and foremost, all praise be to Allah the Almighty, for His Grace and Blessings.

I would like to thank my supervisors, Dr Qasim Rafiq and Professor Martina Micheletti, for sharing their expertise and supporting me throughout this process.

I would like to extend my sincere gratitude and appreciation to Dr Peter Archibald, my industrial supervisor, for his time and dedication to this project and making this an exciting and inspiring experience.

To my mentor, Dr Farlan Veraitch, thank you for introducing me to the field of cell and gene therapy and keeping me interested to this day.

I would also like to acknowledge the vector process development team at GSK for opening your doors and giving me access to state-of-the-art facilities and expertise.

Finally, I am deeply indebted to my amazing wife, Sukaina, for always supporting and encouraging me in my study, my beautiful sons, Abdullah and Yusuf, for being my constant source of joy and motivation, and my parents, Abdullah and Abeda, for all the love and guidance. I could not possibly have done this without their support.

ABSTRACT

Lentiviral vectors (LVV) represent an important tool for cell and gene therapy applications. Most of the current LVV production methods use the HEK293T cell line as it is easily transfected and supports high-level expression of viral proteins. However, the inability to achieve high cell densities (i.e. $>10 \times 10^6$ cells/mL) with HEK293T stable cell lines in a fed batch process have resulted in poor upstream yields. Optimisation of cell culture conditions is needed to improve upstream yields, which can be expedited by high-throughput screening. This thesis describes the use of Liquid Chromatography-Mass Spectrometry (LC-MS) tools and high-throughput screening to develop a novel feed for improving the growth profile of GSK's 277 HEK293T LVV stable producer cell line, thus enabling high titre lentiviral vector production. Firstly, LC-MS analysis was used to generate a profile of metabolite changes during stable cell line cultivation in 2 L stirred tank reactors (STR). A total of 50 metabolites were identified to be depleting with time, and thus possible targets for developing a bespoke feed. Thereafter, the 24 deep square well (24-DSW) microwell platform was used to develop a scale-down mimic of GSK's established stable suspension LVV production process model at 2 L STR scale. Matched mixing time was found to be an effective basis for scale-translation between the STR and microwells. The growth kinetics and LVV productivity profile in the microwell were reproducible and comparable to the 2 L STR process model as defined by the maximum VCD prior to stationary phase ($\sim 6 \times 10^6$ cells/mL) and infectious titre at harvest ($\sim 2 \times 10^7$ TU/mL). A design of experiments (DoE) approach, facilitated by the 24-DSW high-throughput model, was then used to screen and optimise feeds based upon the depleting metabolites identified, and thus develop a novel feed for optimised HEK293T stable cell line culture. Using the novel feed, the period of exponential growth was increased by up to 24 hours which enabled induction at higher cell densities. This resulted in a 2-fold increase in infectious titre for the 277 stable cell line compared to the platform process control. Therefore, the 24-DSW model together with LC-MS analysis provides an important tool for rapid, high-throughput optimization of the LVV production process.

IMPACT STATEMENT

Lentiviral vectors (LVVs) have played an important role in the recent clinical and commercial success of cell and gene therapies. Commercially approved gene-modified cell therapies utilising LVV for gene delivery include Kymriah[®] (Novartis, Basel, Switzerland) for the treatment of lymphoblastic leukemia and Zynteglo[®] (Bluebird bio, Massachusetts, USA) for beta-thalassemia. Although these therapies have demonstrated curing potential, the manufacturing process is far from optimal, which is reflected in the high cost per treatment (\$475,000/dose for Kymriah and \$2.1M/dose for Zynteglo) (Hernandez et al., 2018; Thuret et al., 2022). The cost of manufacturing the LVV for these therapies represents a major component of the total cost. Hence, the main focus of this thesis was to improve GSK's LVV upstream manufacturing process (e.g. increase titres to reduce cost of goods) in order to maximise the commercial feasibility of its pipeline of cell and gene therapy products.

The development of the novel feeding strategy in this project has led to an increase in the exponential growth period of the HEK293T LVV stable producer cell line. Improved growth has enabled cells to be induced at higher cell densities. Induction at higher cell densities has thus resulted in an increase in LVV production by approximately 2-fold compared to the company's platform process. A study by Comisel *et al.*, 2021 has shown that LVV harvest titre has a large impact on the total cost of goods (COG) of these therapies. The LVV cost contribution relative to the chimeric antigen receptor T-cell (CAR-T) therapy COG/patient ranges between 15–20% (Comisel et al., 2021). Decisional tool analysis by the same authors have predicted that LVV harvest titres need only to double for the LVV cost contribution to drop as low as 1%. Hence, the 2-fold increase in titre achieved in this project could significantly reduce the overall cost of these life-changing therapies. However, it is worth noting that the additional 1 day of culture may increase other COGs such as labour. A detailed economic analysis would be required to fully characterise the trade-off between higher titre and longer culture duration.

According to the most recent annual report by the Alliance for Regenerative Medicine (ARM), there are 2,093 active cell and gene therapy trials ongoing globally as of June 2022. The report also states that 48% of the gene therapy and cell-based immunology trials are using LVV as the gene modification vector. The huge demand has put LVV manufacturing under significant strain. A report by McKinsey & Company from March 2022 states that the current state of LVV manufacture through CDMOs is characterised by shortages and long wait times (Capra et al., 2022). The news site Pharmaceutical Technology suggest that delays can be more than 18 months. Thus, the 2-fold increase in harvest titre achieved in this project means that LVV production is effectively doubled for every batch. Increase in vector production can help ease the shortage in LVV supply. Hence, more patients can be treated and benefit from these transformative gene-modified cell therapies.

Another impact of the novel feed is that it helps GSK move away from an off-the-shelf commercial feed and towards a formulation that they own. Commercial feeds are expensive, especially when scaling up the LVV production process to large scale STRs (i.e. > 200 L scales). Having the feed prepared in-house would be more cost-effective for the company. Furthermore, dependence on a commercial feed is risky when there is a supply shortage as experienced during the COVID-19 pandemic. It is also worth noting that the composition of commercial feeds is proprietary knowledge. Hence, there is little to no information of the formulation used. With the novel feed, understanding of the formulation should result in better process control for the company. Lastly, there is a possibility for the formulation of novel feed to be patented and commercialised. This can be an additional source of revenue for the company.

This study is the first demonstration of using LC-MS analysis to develop a feeding strategy for enhancing cell growth and productivity of a HEK293T stable producer cell line. The findings from this study have the potential to be applied to LVV manufacture for other targets (e.g. CAR-T cells and haematopoietic stem cells) used in advanced therapy applications.

STATEMENT OF CONTRIBUTIONS

The work presented in this thesis would not have been possible without the contributions of many brilliant people, to whom I am very grateful. The title and scope of the thesis was conceived by my first EngD supervisor, Dr Farlan Veraitch, with additional input from Bo Kara (GSK) and Dr Peter Archibald (GSK).

In the following I state the contribution of other people to the data presented by chapter:

Chapter 3: Dr Marialuce Maldini (SCIEX) contributed to the LC-MS experiments and spectral library analysis for compound identification.

Chapter 4: Dr Anne de la Motte (UCL) developed the MATLAB script used to analyse mixing time in 2 L STR and 24-DSW plates

CONTENTS

Declaration	i
Acknowledgments	ii
Abstract	iii
Impact Statement	iv
Statement of Contributions	vi
Contents	vii
List of Figures	xiii
List of Tables	xix
Abbreviations	xxiv
Nomenclature	xxix
List of Publications	xxx
1 Introduction	1
1.1 Scope	1
1.2 Cell and Gene Therapy.....	1
1.3 Lentiviral Vectors	3
1.3.1 General Properties and Applications.....	3
1.3.2 Biology and Structure of Lentiviruses	4
1.4 Production of Lentiviral Vectors	12
1.4.1 Cell Lines	12
1.4.2 Lentiviral Vector Production Through Transient Transfection	14
1.4.3 Lentiviral Vector Production Using Stable Producer Cell Lines	16
1.4.4 Adherent vs Suspension Systems	18
1.5 Approaches for Optimisation in LVV Production	19
1.5.1 Cellular Targets for Improved Viral Vector Manufacturing	20

1.5.1.1	Energy Metabolism.....	20
1.5.1.2	Lipid Metabolism.....	22
1.5.1.3	Nucleic Acid Metabolism	23
1.5.1.4	Polyamine Metabolism.....	24
1.5.2	Metabolomic Approaches to Identify Bottlenecks	24
1.5.3	Nutrient Feeding	27
1.6	Small Scale Culture Systems in Bioprocessing.....	29
1.6.1	Miniature Stirred Tank Reactors (STRs).....	30
1.6.2	Shake Flasks	32
1.6.3	Microtiter Plates	32
1.6.3.1	Engineering characterisation of microwells.....	33
1.6.3.2	LVV production in microwells.....	34
1.7	Scaling Parameters Used for Cell Culture	34
1.7.1	Power per Unit Volume (P/V)	35
1.7.2	Oxygen Transfer Rate (k_{La})	35
1.7.3	Mixing Time.....	36
1.8	Thesis Aim and Objectives.....	37
2	Materials and Methods	40
2.1	Cell Line and Media Formulation.....	40
2.2	Feed Preparations	41
2.3	Shake Flask Cultures.....	43
2.4	Stirred-Tank Reactor Cultures	44
2.5	Shaken Microwell Cultures.....	45
2.6	Stable Cell Line Induction and Vector Harvest	47
2.7	Analytical Techniques	48
2.7.1	Viable Cell Density and Viability Measurements	48
2.7.2	Cell Culture Bioanalyser.....	48
2.7.3	Liquid Chromatography-Mass Spectrometry Analysis	49
2.7.4	Quantification of Lentiviral Vector Infectious Titre	51
2.7.5	Quantification of Lentiviral Vector Physical Titre.....	52
2.8	Quantification of Mixing Time.....	52

2.9	Doe Methodology	53
2.10	Statistics	54
2.11	Formulae.....	54
3	Assessment of GSK's 277 HEK293T Stable Cell Line Cultivation in 2 L Stirred Tank Reactor	57
3.1	Introduction and Aims	57
3.2	Chapter Specific Materials and Methods	58
3.2.1	Details for 2 L STR cultures in sections 3.3, 3.4 and 3.6.....	58
3.2.2	Studying of the effect of induction cell density on LVV production in section 3.5.....	59
3.2.3	Method for analysing the LC-MS raw data in section 3.7	60
3.3	Assessment of GSK's 277 Cell Line Growth Profile in 2 L STR	61
3.4	Assessment of GSK's 277 Cell Line Platform LVV Production Process in 2 L STR.....	66
3.5	Effect of Induction Cell Density on LVV Production.....	72
3.6	Effect of Altering Glucose and Lactate Metabolism on 277 Cell Line Growth Profile.....	75
3.7	LC-MS Analysis of Cell Culture Media During 277 Cell Line Growth Culture	85
3.7.1	Metabolites with no significant change in concentration with time	86
3.7.2	Accumulating metabolites with time	91
3.7.3	Depleting metabolites with time.....	95
3.8	Chapter Summary.....	115
4	Developing a High-Throughput Scale-Down Model of GSK's Platform 277 HEK293T Stable Cell Line Cultivation Process in 2 L Stirred Tank Reactors	119
4.1	Introduction and Aims	119
4.2	Chapter Specific Materials and Methods	120
4.2.1	Mixing time characterisation in section 4.5.....	120
4.2.2	Details for 2 L STR and 24-DSW plate cultures in section 4.6.....	121
4.3	Rationale for Selecting the 24-DSW Plate Format.....	121
4.4	Rationale for Using Mixing Time as the Basis for Scale-Translation.....	122

4.5	Mixing Time Characterisation.....	123
4.5.1	Mixing time in 2 L STR.....	123
4.5.2	Mixing time in 24-DSW plate.....	125
4.6	Scale Translation of 277 Stable Cell Line Culture at Matched Mixing Time.....	128
4.6.1	277 cell line growth culture.....	129
4.6.2	GSK's platform LVV production process using the 277 cell line	136
4.6.3	Discussion.....	144
4.7	Chapter Summary	146
5	Developing a Novel Feeding Regime for Enhanced HEK293T Stable Cell Line Growth	149
5.1	Introduction and Aims.....	149
5.2	Chapter Specific Materials and Methods.....	150
5.2.1	Characterising the effect of commercial feed on 277 cell line growth in section 5.3	150
5.2.2	DoE screening studies in section 5.4	151
5.2.3	Optimisation studies in section 5.5	154
5.3	Characterising the Effect of a Commercial HEK293 Feed on 277 Cell Line Growth	156
5.4	Design of Experiments Based Screening of Feed Supplements to Include in the Novel Feed for Enhancing 277 Cell Line Growth....	165
5.4.1	Screening study 1 – Assessment of metabolites groups common to the LC-MS analysis and mammalian cell culture feeds	167
5.4.2	Screening study 2 – Assessment of metabolites commonly present in mammalian cell culture feeds and not identified in the LC-MS analysis	182
5.4.3	Screening study 3 – Assessment of individual effect of important essential and non-essential amino acids identified in the LC-MS analysis	198
5.4.4	Screening study 4 – Assessment of individual effect of important metabolites identified in the LC-MS analysis	208
5.5	Characterising the Optimal Composition and Feeding Regime of the Novel Feed for Enhancing 277 Cell Line Growth	216

5.5.1	Optimisation study 1 – Optimising concentration of essential and non-essential amino acids in the novel feed.....	216
5.5.2	Optimisation study 2 – Assessment of essential amino acids concentration higher than 30X MEM.....	225
5.5.3	Optimisation study 3 – Assessment of the optimal feeding regime of the novel feed.....	228
5.6	Chapter Summary.....	241
6	Assessment of LVV Production at High Induction Cell Densities Using the Novel Feed	243
6.1	Introduction and Aims	243
6.2	Chapter Specific Materials and Methods	244
6.2.1	Characterisation of LVV production at high cell densities in 24-DSW plates using the 277 and GSK-asset stable cell lines.....	244
6.2.2	Quantification of infectious titre for LVV produced using the GSK-asset stable cell line	245
6.3	Characterisation of LVV Production at High Cell Densities in 24-DSW Plates Using the 277 Stable Cell Line	247
6.4	Evaluating the Effect of the Novel Feed on Cell Growth and LVV Production Profile of a GSK-Asset Stable Cell Line Cultivated in 24-DSW Plates.....	259
6.5	Chapter Summary.....	269
7	Conclusion and Future Work	271
7.1	Review of Project Objectives	271
7.2	Recommendations for Future Work	274
7.2.1	Further optimisation of the novel feed process.....	274
7.2.1.1	Improvement in feed design.....	274
7.2.1.2	Feed stability studies	275
7.2.1.3	Assess the effect of the novel feed with other GSK-asset stable cell lines.....	275
7.2.1.4	Optimisation of induction conditions.....	275
7.2.1.5	Explore a two-step feeding strategy for LVV production.....	276
7.2.2	Industrial implementation of the novel feed.....	277

7.2.2.1	Process validation of the novel feed for upstream LVV production.....	277
7.2.2.2	Practical, safety and environmental aspects.....	281
8	References	283
9	Appendix A: Supplementary Material	301
9.1	Cell Population Doubling Time Data.....	301
9.1.1	Cell population doubling time for 277 stable cell line growth culture in 2 L STR (section 3.3)	301
9.1.2	Cell population doubling time for 277 stable cell line platform LVV production process in 2 L STR (section 3.4).....	302
9.1.3	Cell population doubling time for 277 stable cell line growth culture in 2 L STR at different pH and CO ₂ set-point values (section 3.6).....	302
9.1.4	Cell population doubling time for 277 stable cell line growth culture in 24-DSW plate (section 5.3)	303
9.2	Literature References Used to Score Depleting Metabolites in Section 3.7.3.....	303
9.3	Comparison of Sampling Methods Used for 24-DSW Plate Cultures	306
9.4	Design of Experiments Studies	307
9.4.1	Experimental design space for DoE screening studies generated using Design Expert software (section 5.4)	307
9.4.2	Experimental design space for DoE optimisation studies generated using Design Expert software (section 5.5)	312
9.4.3	Complete formulations of the commercially available pre- formulated reagents used in the DoE studies (Section 5.4 and 5.5).....	314
9.4.4	DoE model fit summary data from optimisation studies (section 5.5).....	317

LIST OF FIGURES

Figure 1.1: Schematic representation of a lentivirus particle.....	5
Figure 1.2: Schematic representation of a wild-type HIV-1 genome.....	6
Figure 1.3: Schematic representation of the first generation VSV-G pseudotyped LVV system.	7
Figure 1.4: Schematic representation of the second generation VSV-G pseudotyped LVV system.	8
Figure 1.5: Schematic representation of the third generation VSV-G pseudotyped LVV system.	10
Figure 1.6: Production of VSV-G pseudotyped lentiviral vector by transient transfection.	16
Figure 1.7: Rapid generation of a VSV-G pseudotyped lentiviral vector producer cell line using a single BAC construct.	18
Figure 1.8: Workflow for untargeted and targeted metabolomics.	27
Figure 1.9: Examples of small scale stirred tank systems used in upstream process development.....	31
Figure 2.1: Schematic diagram of 24-DSW microtiter plate.	46
Figure 2.2: 24-DSW plate set-up for HEK293T stable cell line cultivation.	47
Figure 3.1: Viable cell density and cell viability profile for GSK's 277 stable cell line growth culture in 2 L STR.	63
Figure 3.2: Glucose and lactate concentration profile for GSK's 277 stable cell line growth culture in 2 L STR.	66
Figure 3.3: Viable cell density and viability profile for GSK's 277 stable cell line platform LVV production process.....	68
Figure 3.4: Glucose and lactate concentration profiles for GSK's 277 stable cell line platform LVV production process.	71
Figure 3.5: Glutamine and glutamate concentration profiles for GSK's 277 stable cell line platform LVV production process.	72
Figure 3.6: Effect of induction cell density on LVV infectious titre.	75
Figure 3.7: pH profile of the 277 stable cell line cultivated in 2 L STR.	78
Figure 3.8: Effect of pH and CO ₂ on lactate concentration profile of the 277 stable cell line cultivated in 2 L STR.....	79

Figure 3.9: Effect of pH and CO ₂ on glucose concentration profile of the 277 stable cell line cultivated in 2 L STR.	79
Figure 3.10: Effect of pH and CO ₂ on VCD profile of the 277 stable cell line cultivated in 2 L STR.	80
Figure 3.11: Effect of pH shift on lactate concentration profile of the 277 stable cell line cultivated in 2 L STR.	82
Figure 3.12: Effect of pH shift on glucose concentration profile of the 277 stable cell line cultivated in 2 L STR.	83
Figure 3.13: Effect of pH shift on VCD profile of the 277 stable cell line cultivated in 2 L STR.	84
Figure 3.14: Peak area intensity profile of some key vitamins showing no significant change in concentration with time.	90
Figure 3.15: Peak area intensity profile of linoleic acid at three different stages along the cell culture period.	91
Figure 3.16: Peak area intensity profile of lactic acid at three different stages along the cell culture period.	94
Figure 3.17: Peak area intensity profile of isocitric acid, D-sucrose and cytidine monophosphate at three different stages along the cell culture period.	94
Figure 3.18: Peak area intensity profile of the high scoring depleting essential amino acids at three different stages along the cell culture period.	106
Figure 3.19: Peak area intensity profile of the high scoring non-essential amino acids at three different stages along the cell culture period.	107
Figure 3.20: Peak area intensity profile of L-alanyl-L-glutamine at three different stages along the cell culture period.	108
Figure 3.21: Quantitative LC-MS analysis of the proteinogenic amino acids at three different stages along the cell culture period.	109
Figure 3.22: Peak area intensity profile of the high scoring depleting non-proteinogenic amino acids at three different stages along the cell culture period.	109
Figure 3.23: Peak area intensity profile of glucose at three different stages along the cell culture period.	111
Figure 3.24: Peak area intensity profile of the high scoring significantly depleting vitamins at three different stages along the cell culture period.	112
Figure 3.25: Peak area intensity profile of putrescine at three different stages along the cell culture period.	113
Figure 3.26: Peak area intensity profile of the histamine at three different stages along the cell culture period.	114

Figure 3.27: Peak area intensity profile of the D-pipecolic acid at three different stages along the cell culture period.	115
Figure 4.1: Liquid phase mixing times for 2 L STR measured using the dual indicator system for mixing time (DISMT) technique.....	124
Figure 4.2: Liquid phase mixing times for 24-DSW plate measured using the dual indicator system for mixing time (DISMT) technique.	127
Figure 4.3: Comparison between data shown in present study with the mixing time model reported in Rodriguez <i>et al.</i> , 2014.....	128
Figure 4.4: Viable cell density profile for cultivation of the 277 HEK293T stable producer cell line in 24-DSW plate and 2 L STR at matched mixing time of < 10 s.....	132
Figure 4.5: Cell viability profile for cultivation of the 277 HEK293T stable producer cell line in 24-DSW plate and 2 L STR at matched mixing time of < 10 s.....	133
Figure 4.6: Glucose concentration profile for cultivation of the 277 HEK293T stable producer cell line in 24-DSW plate and 2 L STR at matched mixing time of < 10 s.....	134
Figure 4.7: Lactate concentration profile for cultivation of the 277 HEK293T stable producer cell line in 24-DSW plate and 2 L STR at matched mixing time of < 10 s.....	135
Figure 4.8: pH profile for cultivation of the 277 HEK293T stable producer cell line in 24-DSW plate and 2 L STR at matched mixing time of < 10 s.....	136
Figure 4.9: Viable cell density profile for cultivation of GSK's platform LVV production process using 277 cell line in 24-DSW plate and 2 L STR at matched mixing time of < 10 s.	139
Figure 4.10: Cell viability profile for cultivation of GSK's platform LVV production process using 277 cell line in 24-DSW plate and 2 L STR at matched mixing time of < 10 s.	140
Figure 4.11: Glucose concentration profile for cultivation of GSK's platform LVV production process using 277 cell line in 24-DSW plate and 2 L STR at matched mixing time of < 10 s.	141
Figure 4.12: Lactate concentration profile for cultivation of GSK's platform LVV production process using 277 cell line in 24-DSW plate and 2 L STR at matched mixing time of < 10 s.	142
Figure 4.13: pH profile for cultivation of GSK's platform LVV production process using 277 cell line in 24-DSW plate and 2 L STR at matched mixing time of < 10 s.....	143

Figure 4.14: LVV productivity profile in 24-DSW plate and 2 L STR at matched mixing time of < 10 s.....	144
Figure 5.1: VCD profile for the 277 stable cell line cultivated in 24-DSW plate with different feeding regimes of the commercial feed.....	160
Figure 5.2: Cell viability profile for the 277 stable cell line cultivated in 24-DSW plate with different feeding regimes of the commercial feed.	161
Figure 5.3: Glucose concentration profile for the 277 stable cell line cultivated in 24-DSW plate with different feeding regimes of the commercial feed.	162
Figure 5.4: Glucose concentration profile for the 277 stable cell line cultivated in 24-DSW plate with different feeding regimes of the commercial feed.	163
Figure 5.5: Ammonium concentration profile for the 277 stable cell line cultivated in 24-DSW plate with different feeding regimes of the commercial feed.....	164
Figure 5.6: Day 5 VCD response model graph from screening study 1.....	172
Figure 5.7: Day 5 cell viability response model graph from screening study 1.....	173
Figure 5.8: Day 6 VCD response model graph from screening study 1.....	175
Figure 5.9: Day 6 cell viability response model graph from screening study 1.....	176
Figure 5.10: Day 7 VCD response model graph from screening study 1.....	178
Figure 5.11: Day 7 cell viability response model graph from screening study 1.....	179
Figure 5.12: Comparison of VCD profile between top performing feed condition from screening study 1 (Run 6 and 34) and no feed condition (Run 4 and 24).	180
Figure 5.13: Comparison of cell viability profile between top performing feed condition from screening study 1 (Run 6 and 34) and no feed condition (Run 4 and 24).	181
Figure 5.14: Day 5 VCD response model graph from screening study 2.....	186
Figure 5.15: Day 5 cell viability response model graph from screening study 2.....	187
Figure 5.16: Day 6 VCD response model graph from screening study 2.....	189
Figure 5.17: Day 6 cell viability response model graph from screening study 2.....	191
Figure 5.18: Day 7 VCD response model graph from screening study 2.....	193
Figure 5.19: Day 7 cell viability response model graph from screening study 2.....	195
Figure 5.20: Comparison of VCD profile between top performing feed condition from screening study 2 (Run 5 and 31) and no feed condition (Run 13 and 35).....	196

Figure 5.21: Comparison of cell viability profile between top performing feed condition from screening study 2 (Run 5 and 31) and no feed condition (Run 13 and 35).	197
Figure 5.22: Day 5 VCD response model graph from screening study 3.	201
Figure 5.23: Day 6 VCD response model graph from screening study 3.	203
Figure 5.24: Day 6 cell viability response model graph from screening study 3.	204
Figure 5.25: Comparison of VCD profile between top performing feed condition from screening study 3 (Run 21 and 25) with no feed condition (Run 17 and 30) and feed with all amino acids.	206
Figure 5.26: Comparison of cell viability profile between top performing feed condition from screening study 3 (Run 21 and 25) with no feed condition (Run 17 and 30) and feed with all amino acids.	207
Figure 5.27: Day 6 VCD response model graph from screening study 4.	211
Figure 5.28: Day 6 cell viability response model graph from screening study 4.	212
Figure 5.29: Day 7 VCD response model graph from screening study 4.	213
Figure 5.30: Day 7 cell viability response model graph from screening study 4.	214
Figure 5.31: Day 6 VCD response model graph from optimisation study 1.	221
Figure 5.32: Day 6 cell viability response model graph from optimisation study 1.	222
Figure 5.33: Comparison of VCD profile of three top performing feed conditions from optimisation study 1 and no feed condition.	223
Figure 5.34: Comparison of cell viability profile of three top performing feed conditions from optimisation study 1 and no feed condition.	224
Figure 5.35: Effect of essential amino acids concentration on VCD profile.	226
Figure 5.36: Effect of essential amino acids concentration on cell viability profile.	227
Figure 5.37: Day 6 VCD response model graph from optimisation study 3.	233
Figure 5.38: Day 6 cell viability response model graph from optimisation study 3.	235
Figure 5.39: Day 7 VCD response model graph from optimisation study 3.	237
Figure 5.40: Comparison of VCD profile of the top performing feed condition from optimisation study 3 and no feed condition.	238
Figure 5.41: Comparison of cell viability profile of the top performing feed condition from optimisation study 3 and no feed condition.	239

Figure 5.42: Comparison of the VCD profile of the top performing feed condition from optimisation study 3 and the optimal commercial feed condition from section 5.3.....	240
Figure 6.1: Effect of the novel feed on LVV infectious titre profile using the 277 cell line cultured in 24-DSW plates.....	251
Figure 6.2: Effect of the novel feed on LVV physical titre profile using the 277 cell line cultured in 24-DSW plates.	252
Figure 6.3: Effect of the novel feed on VCD profile during LVV production using the 277 cell line cultured in 24-DSW plates.....	253
Figure 6.4: Effect of the novel feed on the cell viability profile during LVV production using the 277 cell line cultured in 24-DSW plates.....	254
Figure 6.5: Assessment of the VCD profile without induction of the 277 cell line used in section 6.3.	257
Figure 6.6: Assessment of the cell viability profile without induction of the 277 cell line used in section 6.3.	257
Figure 6.7: Comparison of the VCD profile of the condition with no feed from this study (i.e. from Figure 6.5) and optimisation study 3 (section 5.5.3).....	258
Figure 6.8: Comparison of the cell viability profile of the condition with no feed from this study (i.e. from Figure 6.5) and optimisation study 3 (section 5.5.3).....	259
Figure 6.9: Effect of the novel feed on the non-induced VCD profile of the GSK-asset stable cell line.....	262
Figure 6.10: Effect of the novel feed on the non-induced cell viability profile of the GSK-asset stable cell line.	263
Figure 6.11: Effect of the novel feed on LVV infectious titre profile using the GSK-asset stable cell line cultured in 24-DSW plates.....	266
Figure 6.12: Effect of the novel feed on LVV physical titre profile using the GSK-asset stable cell line cultured in 24-DSW plates.....	267
Figure 6.13: Effect of the novel feed on the VCD profile using the GSK-asset stable cell line cultured in 24-DSW plates.....	268
Figure 6.14: Effect of the novel feed on the cell viability profile using the GSK-asset stable cell line cultured in 24-DSW plates.....	269
Figure 9.1: Viable cell density profile of HEK293T stable producer cell line culture in 24-DSW plates using same well sampling and sacrificial well sampling methods.	307

LIST OF TABLES

Table 1.1: Summary of the characteristics of Adenovirus, AAV and Lentivirus.	3
Table 1.2: Summary of the differences between the three generations of LVV systems.	11
Table 1.3: Summary of approved biopharmaceutical products manufactured with HEK293 cell line.	13
Table 1.4: Widely used HEK293 variant cell lines.	14
Table 1.5: Common nutrients found in mammalian cell culture media.	29
Table 1.6: A summary of studies which have shown successful use of mixing time as a basis for scale-translation across vessels with different geometries.	37
Table 2.1: List of supplements used to prepare feed mixtures the in the DoE experiments.	42
Table 2.2: Summary of mass spectrometry parameters	50
Table 3.1: Summary of LVV productivity parameters for GSK's 277 stable cell line platform LVV production process	70
Table 3.2: A summary of cell culture media component coverage identified using LC-MS.	86
Table 3.3: List of metabolites in cell culture media showing no significant change in concentration with time.	88
Table 3.4: Basal media concentration and cellular function of some of the key vitamins showing no significant change in concentration with time.	89
Table 3.5: Summary of Student's t-test output for metabolites in cell culture media showing significant accumulation with time.	93
Table 3.6: Summary of Student's t-test output for metabolites in cell culture media showing significant depletion with time.	97
Table 3.7: Summary of scoring analysis of depleting metabolites.	100
Table 4.1: Comparison of mixing times for small/bench scale bioreactors from studies published in literature.	125
Table 4.2: Summary of operating parameters for 24-DSW plate and 2 L STR at matched mixing time.	129
Table 5.1: Table of factors used in screening study 1.	152
Table 5.2: Table of factors used in screening study 2.	153

Table 5.3: Table of factors used in screening study 3.....	153
Table 5.4: Table of factors used in screening study 4.....	154
Table 5.5: Table of factors used in optimisation study 1.....	155
Table 5.6: Conditions tested in optimisation study 2.	156
Table 5.7: Table of factors used in optimisation study 3.	156
Table 5.8: Summary of cell culture parameters and amount of feed used for each feed regime.....	164
Table 5.9: Summary of 22 potential feed targets from depleting metabolites identified using LC-MS analysis.....	166
Table 5.10: ANOVA summary of Day 5 VCD response from screening study 1.	171
Table 5.11: ANOVA summary of Day 5 cell viability response from screening study 1.....	173
Table 5.12: ANOVA summary of Day 6 VCD response from screening study 1.	174
Table 5.13: ANOVA summary of Day 6 cell viability response from screening study 1.....	176
Table 5.14: ANOVA summary of Day 7 VCD response from screening study 1.	177
Table 5.15: ANOVA summary of Day 7 cell viability response from screening study 1.....	179
Table 5.16: Feed formulation of Run 6 and 34 from screening study 1.....	181
Table 5.17: ANOVA summary of Day 5 VCD response from screening study 2.	185
Table 5.18: ANOVA summary of Day 5 cell viability response from screening study 2.....	187
Table 5.19: ANOVA summary of Day 6 VCD response from screening study 2.	188
Table 5.20: ANOVA summary of Day 6 cell viability response from screening study 2.....	190
Table 5.21: ANOVA summary of Day 7 VCD response from screening study 2.	192
Table 5.22: ANOVA summary of Day 7 cell viability response from screening study 2.....	194
Table 5.23: Feed formulation of Run 5 and 31 from screening study 2.....	197

Table 5.24: ANOVA summary of Day 5 VCD response from screening study 3.....	201
Table 5.25: ANOVA summary of Day 5 cell viability response from screening study 3.....	202
Table 5.26: ANOVA summary of Day 6 VCD response from screening study 3.....	202
Table 5.27: ANOVA summary of Day 6 cell viability response from screening study 3.....	203
Table 5.28: ANOVA summary of Day 7 VCD response from screening study 3.....	205
Table 5.29: ANOVA summary of Day 7 cell viability response from screening study 3.....	205
Table 5.30: Feed formulation of Run 21 and 25 from screening study 3.	207
Table 5.31: ANOVA summary of Day 5 VCD response from screening study 4.....	209
Table 5.32: ANOVA summary of Day 5 cell viability response from screening study 4.....	210
Table 5.33: ANOVA summary of Day 6 VCD response from screening study 4.....	210
Table 5.34: ANOVA summary of Day 6 cell viability response from screening study 4.....	211
Table 5.35: ANOVA summary of Day 7 VCD response from screening study 4.....	212
Table 5.36: ANOVA summary of Day 7 cell viability response from screening study 4.....	213
Table 5.37: Summary of the models selected for each response in optimisation study 1.....	220
Table 5.38: ANOVA summary of Day 6 VCD response from optimisation study 1.....	220
Table 5.39: ANOVA summary of Day 6 cell viability response from optimisation study 1.....	222
Table 5.40: Feed formulation of top performing conditions from optimisation study 1.....	224
Table 5.41: Summary of feed formulation used in optimisation study 3.	228
Table 5.42: Summary of the models selected for each response in optimisation study 3.....	231

Table 5.43: ANOVA summary of Day 6 VCD response from optimisation study 3.....	232
Table 5.44: ANOVA summary of Day 6 cell viability response from optimisation study 3.	234
Table 5.45: ANOVA summary of Day 7 VCD response from optimisation study 3.....	236
Table 5.46: Summary of the feed regimes of the top 3 conditions from optimisation study 3.	240
Table 5.47: Summary of the optimised characteristics of the novel feed.....	241
Table 6.1: Formulation of the optimised novel feed.	245
Table 6.2: Summary of conditions used to characterise LVV production at high cell densities in 24-DSW plates using the 277 cell line.....	247
Table 6.3: Summary of conditions used to characterise cell growth and LVV production at high cell densities in 24-DSW plates using the GSK-asset stable cell line.	260
Table 9.1: Cell population doubling time for 277 stable cell line growth culture in 2 L STR (section 3.3).	301
Table 9.2: Cell population doubling time for 277 stable cell line platform LVV production process in 2 L STR (section 3.4).	302
Table 9.3: Cell population doubling time for 277 stable cell line growth culture in 2 L STR (section 3.6).	302
Table 9.4: Cell population doubling time for 277 stable cell line growth culture in 2 L STR (section 5.3).	303
Table 9.5: List of literature references for depleting metabolites used in scoring analysis.	303
Table 9.6: Experimental design space for DoE screening study 1 (section 5.4.1).....	308
Table 9.7: Experimental design space for DoE screening study 2 (section 5.4.2).....	309
Table 9.8: Experimental design space for DoE screening study 3 (section 5.4.3).....	310
Table 9.9: Experimental design space for DoE screening study 4 (section 5.4.4).....	311
Table 9.10: Experimental design space for DoE optimisation study 1 (section 5.5.1).....	312

Table 9.11: Experimental design space for DoE optimisation study 3 (section 5.5.3).	313
Table 9.12: Complete formulation of MEM Essential Amino Acids Solution (50X) (ThermoFisher Scientific, U.S.A).	314
Table 9.13: Complete formulation of MEM Non-essential Amino Acids Solution (100X) (ThermoFisher Scientific, U.S.A).	315
Table 9.14: Complete formulation of MEM Vitamins Solution (100X) (Thermofisher Scientific, U.S.A).	315
Table 9.15: Formulation of Polyamine supplement (1000X) (MilliporeSigma, U.S.A).	315
Table 9.16: Complete formulation of chemically defined lipid concentrate (ThermoFisher Scientific, U.S.A).	316
Table 9.17: Complete formulation of Hanks' Balanced Salt Solution (10X) (ThermoFisher Scientific, U.S.A).	316
Table 9.18: Fit summary data for day 6 VCD from optimisation study 1.	317
Table 9.19: Fit summary data for day 6 cell viability from optimisation study 1.	317
Table 9.20: Fit summary data for day 7 VCD from optimisation study 1.	317
Table 9.21: Fit summary data for day 7 cell viability from optimisation study 1.	318
Table 9.22: Fit summary data for day 6 VCD from optimisation study 3.	318
Table 9.23: Fit summary data for day 6 cell viability from optimisation study 3.	318
Table 9.24: Fit summary data for day 7 VCD from optimisation study 3.	318
Table 9.25: Fit summary data for day 7 cell viability from optimisation study 3.	319

ABBREVIATIONS

AAV	Adeno-associated Virus
ANOVA	Analysis of variance
ARM	Alliance for Regenerative Medicine
ATP	Adenosine triphosphate
BAC	Bacterial Artificial Chromosome
BSE	Bovine Spongiform Encephalopathy
CAEV	Caprine Arthritis and Encephalitis Virus
CaP	Calcium Phosphate
CAR-T	Chimeric Antigen Receptor T cells
CDMO	Contract Development and Manufacturing Organization
cGMP	Current Good Manufacturing Practice
CGT	Cell and Gene Therapy
CHO	Chinese Hamster Ovary
CFD	Computational Fluid Dynamics
CMC	Chemistry, Manufacturing, and Controls

CMP	Cytidine Monophosphate
CMV	Cytomegalovirus
CPP	Critical Process Parameter
CQA	Critical Quality Attributes
ddPCR	Droplet Digital Polymerase Chain Reaction
DISMT	Dual Indicator System for Mixing Time
DNA	Deoxyribonucleic Acid
DoE	Design of Experiments
DO	Dissolved Oxygen
DOT	Dissolved Oxygen Tension
DSW	Deep Square Well
EIAV	Equine Infectious Anemia Virus
ELISA	Enzyme-linked Immunosorbent Assay
EMA	European Medicines Agency
FBS	Foetal Bovine Serum
FDA	Food and Drug Administration
FIV	Feline Immunodeficiency Virus
GC-MS	Gas Chromatography–Mass Spectrometry

GFP	Green Fluorescence Protein
GMP	Good Manufacturing Practice
GS-CHO	Glutamine Synthetase Chinese Hamster Ovary
GSK	GlaxoSmithKline
HEK293T	Human Embryonic Kidney (293T) cell line expressing the SV40 large T antigen
HEK293T _{sa}	Human Embryonic Kidney (293T) suspension adapted cells
HIV-1	Human Immunodeficiency Virus-1
IGF-1	Insulin-like Growth Factor 1
IMDM	Iscove's Modified Dulbecco's Medium
IMPD	Investigational Medicinal Product Dossier
IND	Investigational New Drug
LC-MS	Liquid Chromatography–Mass Spectrometry
LTR	Long Terminal Repeat
LV	Lentivirus
LVV	Lentiviral Vector
MBR	Micro Bioreactor
MDH II	Malate Dehydrogenase 2

MEM	Minimum Essential Media
MS/MS	Tandem mass spectrometry
NIST	National Institute of Standards and Technology
OSR	Orbitally Shaken Reactors
PBS	Phosphate Buffered Saline
PCR	Polymerase Chain Reaction
PEI	Polyethyleneimine
PFA	Paraformaldehyde
PPE	Personal Protective Equipment
PPP	Pentose phosphate pathway
PPQ	Process Performance Qualification
QPCR	Quantitative Polymerase Chain Reaction
RCL	Replication Competent Lentivirus
R&D	Research & Development
RNA	Ribonucleic Acid
RPM	Revolutions Per Minute
RPMI	Roswell Park Memorial Institute Medium
RRE	Rev Response Element

SIN	Self-Inactivating
SIV	Simian Immunodeficiency Virus
SMB	Simulated moving bed
SRW	Standard Round Well
STR	Stirred Tank Reactor
SV-40	Simian Virus 40
ssRNA	single-stranded RNA
ssDNA	single-stranded DNA
TCA	Tri-carboxylic Acid Cycle
TetR	Tetracycline Repressor
THF	Tetrahydrofolate
TOF	Time-of-flight
TSE	Transmissible Spongiform Encephalopathies
TU	Transducing Unit
U.S.A	United States of America
VCD	Viable Cell Density
VLP	Virus-like Particle
VSV-G	Vesicular Stomatitis Virus G protein

NOMENCLATURE

Symbol	Description	Units
d_i	Vessel internal diameter	m
d_s	Orbital shaking diameter	m
Fr	Froude number	Dimensionless
Fr_c	Critical Froude number	Dimensionless
Fr/ Fr_c	Froude number ratio	Dimensionless
$K_L a$	Volumetric oxygen transfer coefficient	s^{-1}
N	Shaking speed/Stirrer speed	rpm
$N.t_m$	Mixing number	Dimensionless
P/V	Power input per unit volume	$W.m^{-3}$
t_m	Mixing time	s
V_L	Vessel volume	L

LIST OF PUBLICATIONS

Publications

Patel, H., Archibald, P., Jung, C., Roszell, B., Veraitch, F., Rafiq, A, Q., Micheletti, M.
Developing an effective scale-down model for a suspension adapted HEK293T-
derived lentiviral vector stable producer cell line. *In preparation*

Conference presentations

International Society Cell and Gene Therapy (ISCT), San Francisco, California, U.S.A;
held 4th – 7th May 2022; **Poster Presentation** - *Developing a novel feeding strategy for
enhanced lentiviral vector production*

ECI Advancing Manufacture of Cell and Gene Therapies, San Diego, California, USA;
held 6th - 10st February 2022: **Poster Presentation** - *Developing an effective scale-down
model for a suspension adapted HEK293T-derived lentiviral vector stable producer cell line*

1 INTRODUCTION

1.1 SCOPE

The scope of this project was to develop a novel feeding strategy for achieving high cell density HEK293T stable cell line cultures to potentially enhance lentiviral vector (LVV) titres. Using tools such as LC-MS analysis, design of experiments (DoE) and high throughput scale-down screening, the goal was to develop a feed tailored to the demands of the cells. This project was a collaboration with GlaxoSmithKline plc (GSK) leveraging their proprietary suspension adapted HEK293T LVV stable producer cell line (patent WO2017/089307 and WO2017/089307).

1.2 CELL AND GENE THERAPY

Gene therapy can be defined as the treatment of a disease by introducing therapeutic genes to cellular targets from a patient to correct specific gene mutations (Belete, 2021). When the aim is to reprogram the cellular function and subsequently introduce the modified cells back into the patient, this is broadly termed ‘cell and gene therapy (CGT)’ (Wang et al., 2021). The source of the cells defines whether the therapy is considered to be ‘autologous’ or ‘allogeneic’. Autologous refers to the source of the cells for modification being from the patient, whereas allogeneic refers to the starting material being sourced from a cell bank or donor (Karantalis et al., 2015). The CGT

field has advanced rapidly over the past three decades and according to the 2022 annual report by the Alliance for Regenerative Medicine (ARM), there are more than 2000 clinical trials ongoing worldwide. The CGT industry continues to demonstrate its rapid rise, despite the recent challenges of the COVID-19 pandemic. According to the same ARM report, the sector raised more than \$6B of investment in the first half of 2022, and projected to exceed \$10B by the end of the year. The European approval of the retroviral vector gene therapy product Strimvelis™ (GSK) as well as the FDA and EMA approvals of the chimeric antigen receptor T cell (CAR-T) therapy products Kymriah™ (Novartis), Tecartus™ (Gilead) and Yescarta™ (Gilead) signals a new therapeutic paradigm for previously unmet medical needs (Labbé et al., 2021). For successful cell and gene therapy, viral vectors have been used to specifically and stably incorporate therapeutic genes into the target cells (Labbé et al., 2021). As a result of the increasing number of cell and gene therapy clinical programs, there is a greater demand to manufacture viral vectors not only to meet capacity, but also produce them with patient safety and effectiveness in mind (Sharon and Kamen, 2018; van der Loo and Wright, 2016). The amount of vector required for effective therapy varies among different conditions as well as between types of vector. For example, around 2×10^9 functional lentiviral vector (LVV) particles are required to produce one dose of CAR-T cell therapy against cancer (Comisel et al., 2021). In the treatment of Haemophilia B using adeno-associated virus (AAV) vector, doses as high as 2×10^{12} viruses per kilogram of patient bodyweight is required (Ledgerwood et al., 2017). Therefore, equally important to engineering the vectors themselves is to develop scalable and cost effective manufacturing platforms in order to commercialise cell and gene therapy products (Sharon and Kamen, 2018). Adenovirus, along with AAV and LVV, are three of the most widely studied viral vectors for CGT applications. Although the scope of this review and thesis focuses on LVV, a summary of the key differences between Adenovirus, AAV and LVV are shown in Table 1.1.

Table 1.1: Summary of the characteristics of Adenovirus, AAV and Lentivirus. Abbreviations: dsDNA – DNA double-stranded, ssDNA - DNA single-stranded, ssRNA - RNA single-stranded. Table adapted from Sharon and Kamen, 2018 and Biovian, 2021.

Property	Adenovirus	AAV	Lentivirus
Size	~90-100 nm	~25 nm	~90-130 nm
Genome	dsDNA	ssDNA	ssRNA
Packaging capacity	~8 – 36 kb	~4-5 kb	8 kb
Transduction	Dividing and non-dividing cells	Dividing and non-dividing cells	Dividing and non-dividing cells
Transduction efficiency	High	Moderate	Moderate
Genomic integration	Non-integrating	Non-integrating	Integrating
Primary therapeutic strategy	<i>In vivo</i>	<i>In vivo</i>	<i>Ex vivo</i>
Enveloped or non-enveloped	Non-enveloped	Non-enveloped	Enveloped (i.e. enclosed within a lipid membrane)

1.3 LENTIVIRAL VECTORS

1.3.1 General Properties and Applications

Lentiviruses (LVs) are an attractive gene delivery mechanism for a wide range of applications (McCarron et al., 2016). They offer many advantages including the ability to transduce dividing and non-dividing cells, their high transduction efficiency, and their low immunogenicity (Kotterman et al., 2015). LVs also have the capacity to permanently integrate into the host cell genome, which enables sustained gene expression in the transduced cells and its progeny (Naldini et al., 1996). However, the

integrative nature of the virus introduces the risk of insertional mutagenesis (IM) leading to activation of the proto-oncogenes (Bokhoven et al., 2009). Extensive precautions have been taken to avoid the generation of replication competent viruses as will be discussed in section 1.3.2 in more detail.

The most extensively characterised human LV has been derived from Human Immunodeficiency Virus-1 (HIV-1). This serves as the backbone to LV vectored gene therapies (Sharon and Kamen, 2018). However, lentiviral vectors (LVVs) derived from other viruses have also been developed such as simian immunodeficiency virus (SIV), feline immunodeficiency virus (FIV), equine infectious anaemia virus (EIAV), and caprine arthritis-encephalitis virus (CAEV) (Schweizer and Merten, 2010).

LVVs are one of the most widely used vectors under development within the CGT industry (McCarron et al., 2016). Their favourable characteristics make them a promising tool for use in the treatment of various genetic and acquired diseases such as beta-thalassemia (Cavazzana-Calvo et al., 2010), Parkinson's disease (Palfi et al., 2014) as well as oncology (Levine, 2015). With the increasing use of LVVs in translational research and clinical programs, robust and scalable production processes are of critical importance in view of implementing these novel therapies for routine use (Merten et al., 2016).

1.3.2 Biology and Structure of Lentiviruses

Lentiviruses are RNA containing viruses measuring 90 - 130 nm in diameter and have a mass of $\sim 2.5 \times 10^8$ Da (Sharon and Kamen, 2018). The viral genome is packaged into a capsid surrounded by a membranous lipid envelope (Figure 1.1). Within the capsid, two copies of the viral RNA are complexed with the nucleocapsid protein as well as the three enzymes required for viral replication i.e. reverse transcriptase, integrase and protease (Sharon and Kamen, 2018). A protein matrix is formed around the capsid which interacts with the membranous lipid envelope (Segura et al., 2013). This envelope has protruding viral glycoproteins that are responsible for the binding and

entry of the virus into the target cell. It is formed of two units: transmembrane domain which anchors the protein in the lipid bi-layer and surface domain which binds to the receptor (Segura et al., 2013).

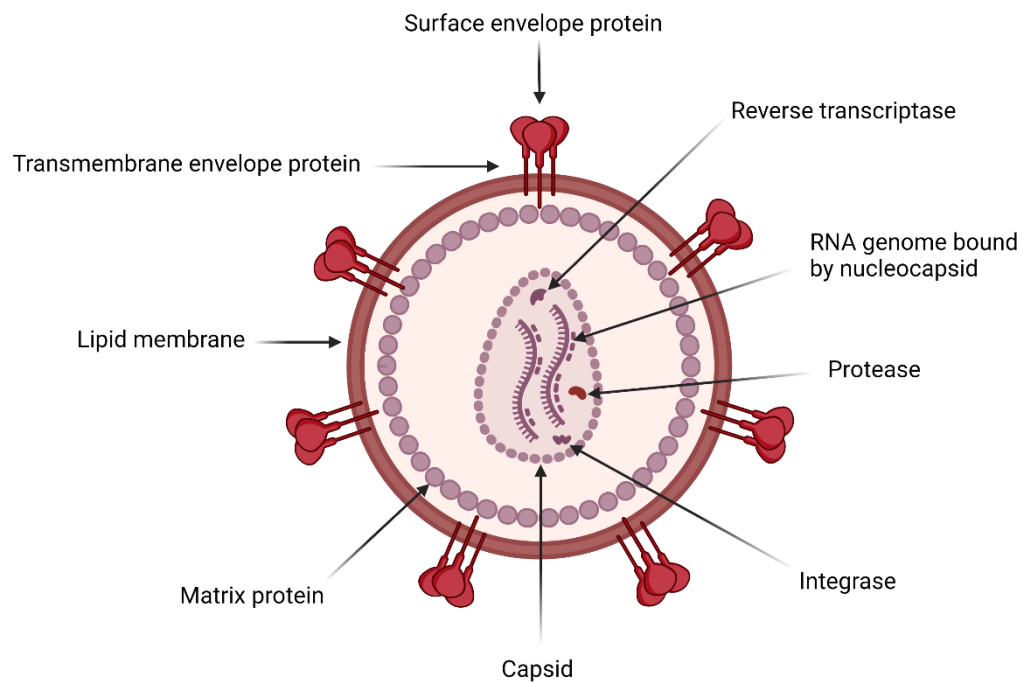


Figure 1.1: Schematic representation of a lentivirus particle. Figure created with BioRender.com.

The linear 9.7 kb RNA HIV-1 genome encodes for nine genes and has long terminal repeat (LTR) sequences on the 5' and 3' ends (Figure 1.2) (Sharon and Kamen, 2018). These LTR sequences function as promoters and facilitate genomic integration. The largest three genes termed *gag*, *pol*, and *env* are common to all retroviruses. *Gag* encodes for the major structural viral components, *pol* encodes LV specific enzymes which include reverse transcriptase, integrase, and protease, and *env* encodes accessory proteins and the virus envelope (Briggs et al., 2003). LVs also contain the regulatory genes *rev* and *tat*. *Rev* is responsible for exporting the viral RNA from the host nucleus whilst *tat* enhances viral RNA transcription (Briggs et al., 2003). The remaining four genes *vpu*, *nef*, *vif* and *vpr* are termed accessory genes and are not necessary for viral

replication (Merten et al., 2016). *Vpu* and *nef* enhance the viruses ability to escape the host immune system and also facilitate viral release (Ansorge et al., 2010). *Vif* (virus infectivity factor) acts against an inhibitory mechanism in the host cell which prevents viral replication (Ansorge et al., 2010). Viral protein R (*vpr*) promotes G2 cell cycle arrest – the phase in which there is optimal viral expression (Quinonez and Sutton, 2002).

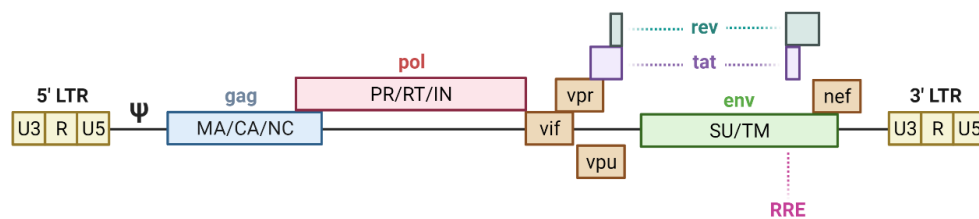


Figure 1.2: Schematic representation of a wild-type HIV-1 genome. Abbreviations: LTR - long terminal repeat; U3 - 3' untranslated region; R - repeat element; U5 - 5' untranslated region; Ψ - packaging signal; MA - Matrix protein; CA - Capsid protein; NC - Nucleocapsid; PR - Protease; RT - Reverse transcriptase; IN - Integrase; SU - Surface envelope protein; TM - Transmembrane envelope protein; RRE - Rev response element. Figure adapted from Tomás *et al.*, 2013 and created with BioRender.com.

The principal aim of developing LVVs was to complement successful features observed in onco-retroviral vectors with the lentivirus-specific ability to transduce non-dividing cells. These features include integration in the chromatin, lack of pre-existing immunity for the virus as well as absence of transferred viral genes (Ansorge et al., 2010).

The first generation of LVVs was developed in 1996 by Naldini et al (Naldini et al., 1996) using a system of three expression cassettes i.e. packaging plasmid, envelope plasmid and a transfer plasmid (Figure 1.3). The packaging plasmid encoded for the core viral genes apart from *env*. The packaging signal, Ψ , was deleted from the packaging plasmid to prevent the packaging of viral elements (Tomás et al., 2013). To reduce homology among the constructs, the 3' LTR was substituted with a poly(A) site (Figure 1.3) (Tomás et al., 2013). In the envelope plasmid, the gp120 envelope protein from the wild type HIV-1 was replaced by heterologous *env* genes (Tomás et al., 2013).

The endogenous HIV-1 viral capsid offers a very narrow natural tropism which is primarily targeted at T cells (Sharon and Kamen, 2018). However, LVVs can be pseudotyped with capsid proteins derived from other viruses. The most commonly used envelope protein is glycoprotein G obtained from the vesicular stomatitis virus (VSV-G) (Sharon and Kamen, 2018). VSV-G not only offers a much broader tropism, but it also stabilises the fragile viral lipid envelope during downstream purification (Sharon and Kamen, 2018). Finally, the transfer plasmid encoded for the transgene of interest within a HIV-1 backbone where in all protein coding regions were silenced or deleted (Merten et al., 2016). The backbone contained all the cis-acting sequences (i.e. non-coding) which include the 3' and 5' LTR, packaging signal (ψ) and the rev responsive element (RRE) (Ansorge et al., 2010). These three plasmids had to be simultaneously expressed in a producer cell to generate the LV vector (Ansorge et al., 2010).

FIRST GENERATION LENTIVIRAL VECTOR SYSTEM

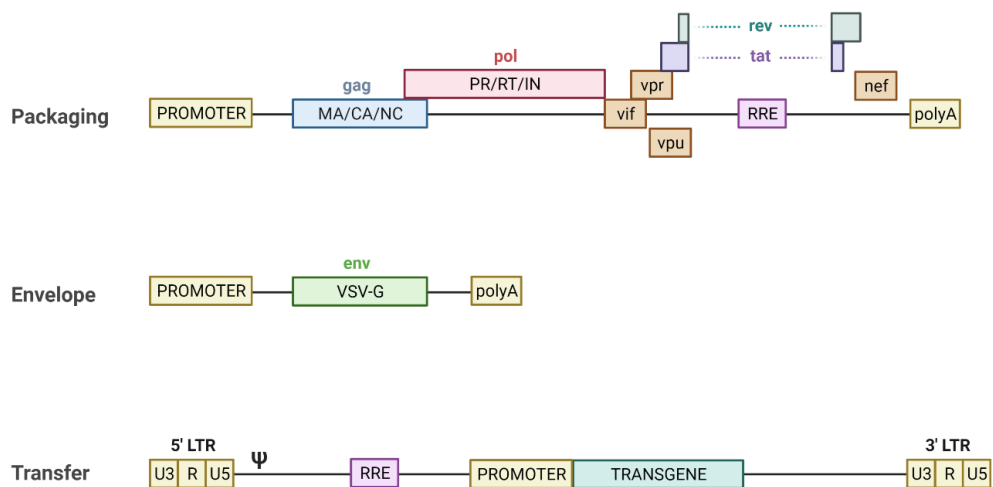


Figure 1.3: Schematic representation of the first generation VSV-G pseudotyped LVV system.

Abbreviations: LTR - long terminal repeat; U3 - 3' untranslated region; R - repeat element; U5 - 5' untranslated region; ψ - packaging signal; MA - Matrix protein; CA - Capsid protein; NC - Nucleocapsid; PR - Protease; RT - Reverse transcriptase; IN - Integrase; RRE - Rev response element. Figure adapted from Tomás *et al.*, 2013 and Labbe *et al.*, 2021 and created with BioRender.com.

As LVVs are based on the highly pathogenic HIV-1 virus, safety was a major concern in the early development phase with respect to the generation of replication competent lentivirus (RCL) via recombination of the encoded sequences on the three plasmids, as RCL could be generated with just three recombination events of homologous sequences (Tomás et al., 2013). These safety concerns had to be addressed by improved vector design. Second generation LVVs came about after the discovery that the accessory genes *vpu*, *nef*, *vif* and *vpr* are not necessary for efficient viral replication (Sharon and Kamen, 2018). The four genes were thus removed from the packaging plasmid in 2nd generation vectors (Figure 1.4). This ensured that any virus produced via recombination would be severely weakened in vivo (Sharon and Kamen, 2018). However, the number of homologous recombination events required to generate RCL was the same as in the first generation (Tomás et al., 2013).

SECOND GENERATION LENTIVIRAL VECTOR SYSTEM

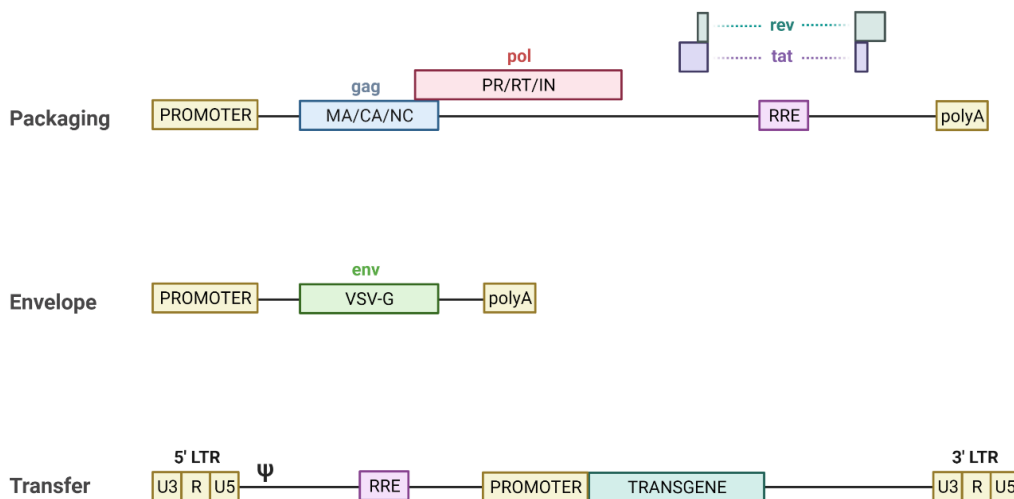


Figure 1.4: Schematic representation of the second generation VSV-G pseudotyped LVV system. Abbreviations: LTR - long terminal repeat; U3 - 3' untranslated region; R - repeat element; U5 - 5' untranslated region; ψ - packaging signal; MA - Matrix protein; CA - Capsid protein; NC - Nucleocapsid; PR - Protease; RT - Reverse transcriptase; IN - Integrase; RRE - Rev response element. Figure adapted from Tomás *et al.*, 2013 and Labbe *et al.*, 2021 and created with BioRender.com.

Although there are no reports of RCLs from 2nd generation constructs, most recent LVV production systems employ 3rd generation plasmid systems for added safety (Figure 1.5). In third generation LVVs, the trans-activation response element (*tar*) in the 5' LTR region was replaced by a strong heterologous promoter (Tomás et al., 2013). Therefore, the TAT protein was no longer necessary for increased transgene expression which allowed eliminating the *tat* gene and hence reducing the wild-type lentiviral elements in the constructs (Tomás et al., 2013). The latest 3rd generation vectors comprise only 10% of the viral genomic RNA, as this is enough to ensure vector functionality (Ansorge et al., 2010). In addition, the packaging plasmid was split into two with *Rev* being expressed on one, while *gag* and *pol* were expressed on the other (Sharon and Kamen, 2018). This increased the number of recombination events required to form an RCL to four, presenting an added level of biosafety (Tomás et al., 2013). The key differences between the three generations of LVV systems are summarised in Table 1.2.

On the transfer plasmid having both LTR's from the wild type virus presented safety problems relating to genotoxicity and hence modifications had to be made (Tomás et al., 2013). The first change was to incorporate a strong heterologous promoter on the 5' LTR in place of *tar* which in turn facilitated the elimination of *tat* (Tomás et al., 2013). In the 3' LTR, the U3 promoter region was deleted to form a self-inactivating (SIN) vector. The SIN design offers transcriptional inactivation since the U3 region of 3' LTR effectively becomes the 5' LTR of the proviral vector following reverse transcription in the target cells (Tomás et al., 2013).

The SIN design offers added safety by preventing vector mobilisation and reduces the risk of insertional mutagenesis, as the possibility of LTR interference with adjacent proto-oncogenes is effectively eliminated (Zufferey et al., 1998). The deletion of the promoter sequences in SIN design led to inefficient transcription termination being observed (Q. Yang et al., 2007). Therefore, heterologous poly A signals have been incorporated in SIN vectors to avoid read-through of adjacent cellular genes (Iwakuma et al., 1999). Chromatin insulators have also been added to reduce interference from

neighbouring genes during expression (Tomás et al., 2013). The woodchuck hepatitis virus post-transcriptional regulatory element (WPRE) can be placed near the 3' LTR to prevent read through in SIN vectors and thereby increasing transgene expression (Tomás et al., 2013).

The viral structural proteins and RNA transgene migrate to the site of assembly stabilised by the actin and tubulin cytoskeleton of the host cell. The LVV particle assembles at cell membrane microdomains known as lipid rafts. They are enriched in cholesterol and sphingolipids and serve as platforms for protein-lipid interactions for the assembly and budding of other enveloped viruses. The MA domain of the gag protein is responsible for the targeting and binding with the lipid raft. The assembled LVV particle is then released from the host cell by budding (Pluta and Kacprzak, 2009).

THIRD GENERATION LENTIVIRAL VECTOR SYSTEM

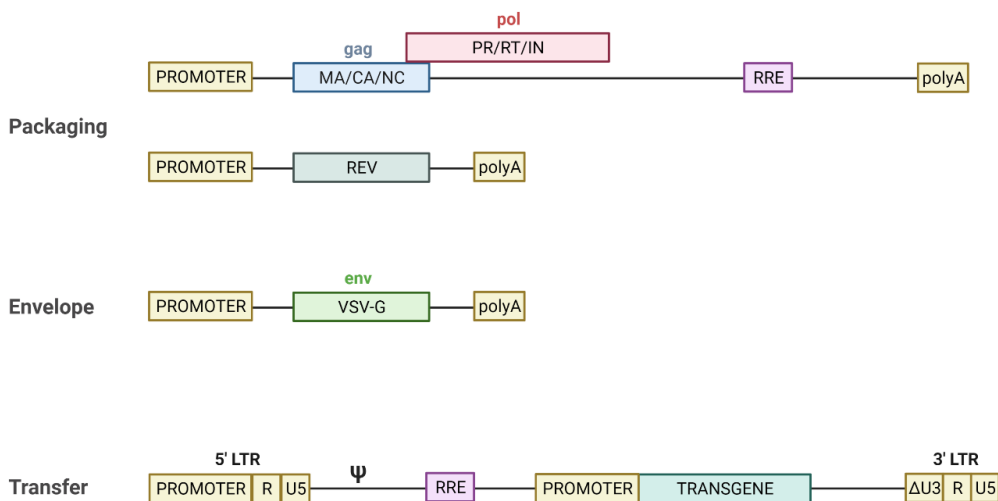


Figure 1.5: Schematic representation of the third generation VSV-G pseudotyped LVV system.

Abbreviations: LTR - long terminal repeat; U3 - 3' untranslated region; R - repeat element; U5 - 5' untranslated region; ψ - packaging signal; MA - Matrix protein; CA - Capsid protein; NC - Nucleocapsid; PR - Protease; RT - Reverse transcriptase; IN - Integrase; RRE - Rev response element. Figure adapted from Tomás *et al.*, 2013 and Labbe *et al.*, 2021 and created with BioRender.com.

Table 1.2: Summary of the differences between the three generations of LVV systems. Table adapted from Addgene: Lentiviral Guide, 2022.

Feature	1st Generation	2nd Generation	3rd Generation
Transfer plasmid	Tat-dependent transgene expression from the LTR	Tat-dependent transgene expression from the LTR	Tat is eliminated through the addition of a chimeric 5' LTR fused to a heterologous promoter
Packaging plasmid	Gag, Pol, Rev, Tat and accessory genes are all on one plasmid	Accessory genes removed. Gag, Pol, Rev and Tat are all on one plasmid	Two plasmids: one encoding Gag and Pol and another encoding Rev
Envelope plasmid	Interchangeable: usually encodes for VSV-G	Interchangeable: usually encodes for VSV-G	Interchangeable: usually encodes for VSV-G
Safety	Safety concern with the presence of viral accessory genes.	Safe. Replication incompetent: Uses 3 separate plasmids encoding various HIV genes.	Safer. Replication incompetent self-inactivating: Uses 4 plasmids instead of 3 and eliminates the requirement for Tat.
LTR viral promoter	Wild type	Wild type	Hybrid: 5'LTR is partially deleted and fused to a heterologous promoter

1.4 PRODUCTION OF LENTIVIRAL VECTORS

1.4.1 Cell Lines

The HEK293 cell line, originally isolated in 1973 (Graham et al., 1977), is now the expression system of choice for the production of LVV as well as several other approved therapeutic products summarised in Table 1.3 (Pulix et al., 2021). A number of HEK293 lineages (Table 1.4) have been engineered from the original parental cell line to express functional properties tailored to the production of specific recombinant products (Pulix et al., 2021). The most commonly used lineage for LVV production is HEK293T as it is highly transfectable and stably expresses the SV-40 T-large antigen (Segura et al., 2013). SV40 DNA replication is initiated by binding of large T-antigen to the origin region of the genome. This is important during transient LVV production as plasmids containing the SV40 origin of replication can be expressed to a high copy number (Segura et al., 2013). HEK293T cells have also been shown to grow faster than the parental cell line and also demonstrate higher vector titres (Stacey and Merten, 2011). Additionally, HEK293T producer cells have also reported higher productivities, appearing to be aided by the low level of constitutive expression of the SV-40 T-large antigen (Gama-Norton et al., 2011). Another important feature is that the HEK293T cells can be suspension adapted and hence are amenable to large scale production (Segura et al., 2013). This also means that cells can be grown in serum-free media, which is advantageous from a quality perspective since there is improved consistency due to avoiding the need for using inherently variable serum. Additionally, the risk of adventitious agents such as Bovine Spongiform Encephalopathy (BSE) and Transmissible Spongiform Encephalopathy (TSE) are also minimised (Chou et al., 2015).

Table 1.3: Summary of approved biopharmaceutical products manufactured with HEK293 cell line. Table adapted from Pilux *et al.*, 2012.

Product type	Example	Therapeutic use
Biopharmaceutical protein [Therapeutic treatment]	Activated protein C (Drotrecogin alpha)	Septic shock
	Factor VIII (rFVIII Fc)	Haemophilia
	Factor IX Fc (rFIX Fc)	Haemophilia
	Glucagon-like peptide 1 (Dulaglutide)	Diabetes (Type 2)
Virus-like particle (VLP) [Vaccine generation]	Rabies virus G protein VLP	Rabies vaccine
	Influenza virus A/Puerto Rico/8/24 (H1N1) VLP	Influenza vaccine
	Hepatitis B virus small surface antigen (HbaAgS) VLP	Hepatitis B vaccine
Viral vector – Lentivirus [Cell and gene therapy]	Kymriah™	Lymphoblastic leukemia
	Zynteglo™	Beta-thalassemia
Viral vector – AAV [Cell and gene therapy]	Luxturna™	Leber congenital amaurosis
	Zolgensma™	Spinal muscular atrophy type 1
Viral vector – retrovirus [Cell and gene therapy]	Rexin-G™	Pancreatic cancer
	Strimvelis™	Adenosine deaminase – immunodeficiency
	Zalmoxis™	Leukemia

Table 1.4: Widely used HEK293 variant cell lines. Table adapted from Pilux *et al.*, 2021.

HEK293 Variant	Derivation	Desirable phenotype
HEK293	Transformation of HEK cells with sheared fragments of adenovirus type 5 (Ad5) DNA selected for immortalization	Parental HEK293 cell line
HEK293S	Adapted for suspension growth	Lack of serum dependency
HEK293T	Stable transfection of the HEK 293 cell line with a plasmid encoding a temperature-sensitive mutant of the SV40 large T antigen	Rapid cell growth, suspension growth, increased protein expression levels during transient transfection
HEK293F	Cloned from the HEK293 cell line and adapted to commercial cell culture medium	Rapid cell growth, suspension growth

1.4.2 Lentiviral Vector Production Through Transient Transfection

In most current research and development (R&D), clinical and commercial manufacturing processes, LVVs are produced by transfecting 3-5 plasmids into a suitable mammalian cell line such as HEK293 or its variants (293T and 293E) (Segura *et al.*, 2013) (Figure 1.6). The plasmids are: (1) one or more packaging plasmids encoding gag-pol and rev (2) an envelope plasmid (3) a transfer plasmid with your gene of interest as well as all the cis-acting elements to produce a functional vector (Segura *et al.*, 2013). Traditionally, LVVs have been produced by co-precipitation of the plasmid DNA with calcium-phosphate (CaP) (Ansorge *et al.*, 2010). However, this procedure requires large quantities of DNA making it difficult to up-scale (Ansorge *et al.*, 2010). Additionally the presence of serum albumin is also required in the media to

reduce CaP toxicity (Ansoerge et al., 2010). Alternatively, CaP toxicity can be minimised by changing the media following transfection, a process that is unfavourable both financially as well as in terms of practicality (McCarron et al., 2016). Alternative transfection reagents which can be used include cationic polymers such as polyethyleneimine (PEI) (Reed et al., 2006) and lipid-based reagent such as lipofectamine™ (Cribbs et al., 2013). Both reagents are shown to be as effective as CaP, however lipofectamine™ may be too costly for large-scale manufacturing (Segura et al., 2013). PEI is relatively inexpensive and is also less toxic than CaP, hence, not necessitating a medium change after transfection (Segura et al., 2013). Electroporation, the use of high-voltage electric shocks to introduce DNA into cells, is another method used for transfection (Potter and Heller, 2018). However, major drawbacks include lack of scalability as well as substantial cell death caused by high voltage (Potter and Heller, 2018).

Using transient transfection, viral titres in the range of $10^7 - 10^8$ TU/mL have been reported (Ansoerge et al., 2010; Witting et al., 2012). Though sufficient to produce material for small scale clinical studies, production methods based on transient transfection may not be optimal for large scale manufacturing. This is due to batch-to-batch variations in both reagents (e.g. plasmids) and vector batches, reliance on expensive transfection reagents and plasmid DNA, and potential of product contamination with residual plasmid DNA (Ansoerge et al., 2010). Therefore, for GMP (good manufacturing practice) purposes, it is important that LVVs are produced with consistent quality and sufficient quantity, making a stable producer cell line approach highly desirable (McCarron et al., 2016).

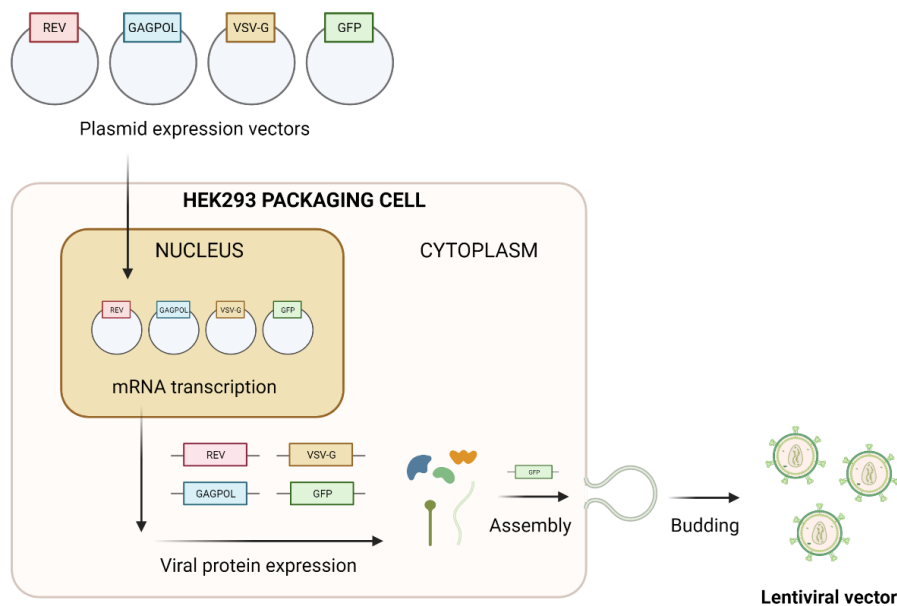


Figure 1.6: Production of VSV-G pseudotyped lentiviral vector by transient transfection. Figure created with BioRender.com.

1.4.3 Lentiviral Vector Production Using Stable Producer Cell Lines

Due to the limitations of transient transfection for LVV production, significant efforts have been undertaken to develop stable packaging and producer cell lines. Packaging cell lines stably express all trans-acting (i.e. protein coding) elements (gag-pol, rev) and envelop protein (env) for LVV packaging (Ansorge et al., 2010; Tomás et al., 2013). However, the transgene cassette is transfected separately which then gets packaged to produce the desired LVV (Segura et al., 2013). Stable producer cell lines can be generated which contain all the genetic elements necessary to generate a viral vector (Sharon and Kamen, 2018). This can be achieved by transfection of all the packaging elements and the transfer vector (Chen et al., 2020).

Over the past 20 years, several LVV producer and packaging cell lines based on HEK293T have been developed, mostly by the sequential introduction of retroviral vector components into the host cell (Chen et al., 2020; Sharon and Kamen, 2018).

This approach has proven to be very laborious and inflexible due to the multiple rounds of screening required to isolate a cell line which is able to express all the required genes (Chen et al., 2020). More recently, GlaxoSmithKline plc (GSK) have developed a stable LVV producer cell line using a single bacterial artificial chromosome (BAC) construct (Chen et al., 2020) (Figure 1.7). With this approach, introduction of the viral genes into the host cell occurs in a single step which allows faster stable clone generation and is also more cost-effective (Chen et al., 2020). Furthermore, by having all the viral genes on a single BAC construct, all genes will integrate at one locus within the host cell genome (Chen et al., 2020). This helps mitigate the problem of gene silencing which becomes apparent if the genes are at various loci (Chen et al., 2020).

The ideal producer cell line should not only generate large quantities of LVVs, but also be stable over extended culture periods (Sharon and Kamen, 2018). Due to the toxicity of some LVV components such as VSV-G, rev and protease, tight regulation is essential in the stable expression systems. This is usually achieved with an inducible promoter requiring the addition of chemical agents such as doxycycline to initiate expression i.e. TET_{on} regulatory system (Throm et al., 2009). In the absence of doxycycline, the tetracycline repressor (TetR) binds and blocks the promoter. However, in the presence of doxycycline, the TetR is removed from the promoter and transcription can proceed. Examples of other mammalian inducible systems include cumate-controlled operator system (Mullick et al., 2006), tamoxifen controlled recombinant system and protein-protein interaction based chimeric system (Kallunki et al., 2019). Compared to the other inducible gene expression systems, the TET_{on} system offers extremely tight regulation where basal expression is extremely low and often undetectable (Das et al., 2016). The TET_{on} system also offers high inducibility and fast response times; gene expression can be detected within 30 minutes after addition of doxycycline to the culture medium (Das et al., 2016). Using stable cell lines, viral titres in the range of $10^6 - 10^7$ TU/mL have been reported. Manceur *et al.*, 2017 achieved an infectious titre of 6×10^6 TU/mL from a suspension cultured HEK293 stable cell line operated in batch mode. In the same study, the stable cell line was also cultivated in perfusion mode from which a higher titre of 2×10^7 TU/mL was

achieved. Greene *et al.*, 2012 achieved titres between $4\text{--}7 \times 10^8$ TU/mL using an adherent stable cell line grown in a 50 L Wave bioreactor with Fibra-Cel disks.

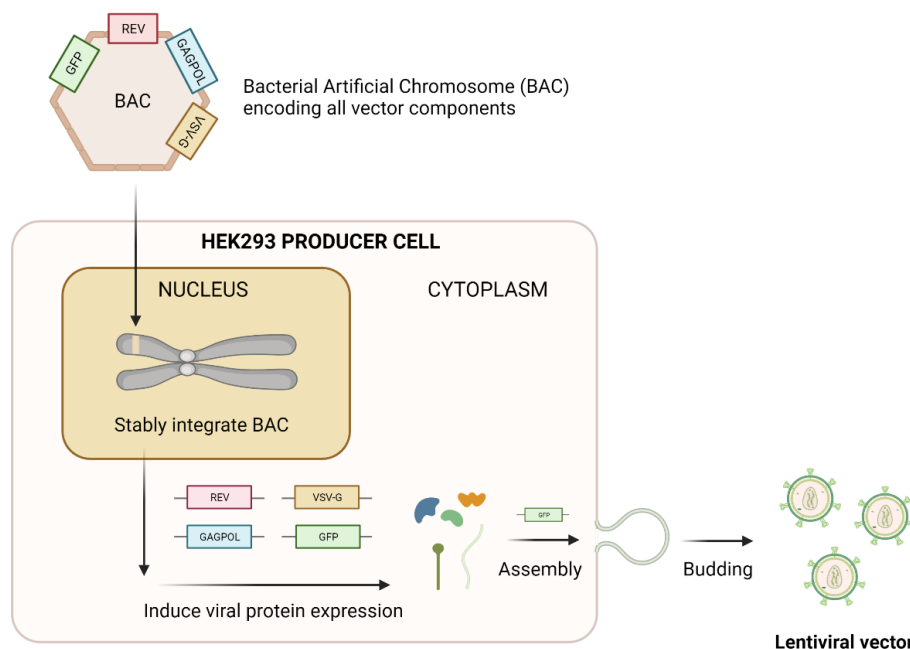


Figure 1.7: Rapid generation of a VSV-G pseudotyped lentiviral vector producer cell line using a single BAC construct. Figure created with BioRender.com.

1.4.4 Adherent vs Suspension Systems

As production needs increase from discovery to late stage animal models, there is an increasing demand for larger quantities of LVV particles. Current adherent cell culture methods, which refers to cells that must be attached to a surface to proliferate, are limited by the surface area required for cell attachment (McCarron *et al.*, 2016). Together with the time consuming manual handling of flasks, adherent systems have little potential for scale-up (Segura *et al.*, 2013). It should be noted that attempts have been made to tackle this issue using various cultivation systems such as: Roller bottles (0.175 m^2 surface area), Multi-layer flasks (e.g. HYPERflasksTM 0.172 m^2 surface area) and Cell factories (e.g. NuncTM CF-10 tray system 0.632 m^2 surface area) (McCarron *et al.*, 2016). The drawback of these systems is that the total number of cells that can be

grown is low due to the limited surface area. This means that scaling out i.e. increasing the number of culture units, is the only feasible option to support large scale production (Segura et al., 2013). This would require significant amount of incubator space and is also very labour intensive (Segura et al., 2013).

For industrial manufacturing, the most convenient approach to overcome this hurdle is to adapt the adherent cell lines to suspension culture (Ansorge et al., 2009). Cells grown in suspension are able to achieve higher cell numbers and hence have greater potential for scale-up. The cells can be expanded in a variety of vessel types to include shake flasks, glass bioreactors, stainless steel bioreactors, wave bags, and disposable stirred tank reactors (Ansorge et al., 2009). In addition, the absence of bovine serum and other animal products in the culture media favours GMP production as it decreases the risk of contamination caused by adventitious agents (Merten et al., 2016). The move to suspension systems also offers the added benefit of reducing batch-to-batch variability by implementation of automated process control of parameters such as temperature, dissolved oxygen and pH as well as eliminating the need for serum which is a major concern in adherent cultures (Geraerts et al., 2005). Additionally, unlike adherent systems, the cell density at transfection/induction can be measured in suspension systems which offers greater reproducibility. In terms of productivity, data thus far suggest that LVV titres in suspension culture are comparable to those achieved with adherent cells, with values ranging from $10^6 - 10^8$ TU/mL (Ansorge et al., 2009; Segura et al., 2007).

1.5 APPROACHES FOR OPTIMISATION IN LVV PRODUCTION

Inefficiencies in LVV manufacturing processing, such as low cell density cultures and accumulation of non-infectious vector particles, have resulted in poor yields during upstream processing (van der Loo and Wright, 2016). The following section discusses

possible approaches for optimising the LVV production process, with a focus on improving cell density and infectious titre.

1.5.1 Cellular Targets for Improved Viral Vector Manufacturing

Understanding the role of host cell metabolism during cell growth and viral vector production can provide possible targets for optimisation. The most active metabolic pathways identified are discussed in this section.

1.5.1.1 Energy Metabolism

Energy metabolism has been manipulated by various groups to increase productivity (Liste-Calleja et al., 2013; Rodrigues et al., 2014; Román et al., 2018). Glucose and glutamine are the main carbon and energy sources for most mammalian cells (Coroadinha et al., 2006b). In HEK293 cells, over 50% of glucose entering glycolysis is converted into lactate (Henry et al., 2011), and hence, only a small amount of glucose-derived carbon enters the tri-carboxylic acid (TCA) cycle (Coroadinha et al., 2006b). As a result, the low glucose oxidation is compensated by the oxidation of glutamine (Coroadinha et al., 2006b), the main amino acid consumed by HEK293 cells (Petiot et al., 2015). Glutamine also plays an important role in the synthesis of nucleotides, lipids, amino acids and proteins (Coroadinha et al., 2006b). Therefore, the use of alternative sugar sources can have a significant impact on the cell's energy metabolism (Coroadinha et al., 2006b).

This strategy has been used in the past to improve recombinant protein production in animal cells where glucose alternatives such as fructose, galactose and sorbitol have been used (Altamirano et al., 2000). Similarly, in the production of retroviral vectors, the use of fructose improved viral titres by up to 3 to 8-fold in several producer cell lines (Coroadinha et al., 2006b). The improvements were not due to nutrient limitation or toxic effects of lactate or ammonia, rather higher uptake of energetic metabolites

was observed, suggesting that cell physiological state is a key parameter for enhancing vector production (Coroadinha et al., 2006b). The authors also observed that cell growth and vector production in fructose supplemented media was gradual and progressive eventually reaching higher titres. Whereas in glucose supplemented media, it was found to be fast and abrupt, and hence the window for the production of infectious particles was much narrower. In the same study, they also found that galactose and sorbitol media resulted in very low infectious titres compared to fructose and glucose media.

In a separate study by Coroadinha *et al.*, 2006a, it was found that reduced cell growth was linked to fructose being poorly metabolised by the producer cells possibly due to low affinity of sugar transporters for fructose. They suggest this is advantageous for vector productivity since there is an accumulation of cells in the G1 phase, wherein the cell energy is being diverted towards the production of viral particles rather than cell growth (Coroadinha et al., 2006a). Reduced lactate production, increased glutamine uptake and increased lipid synthesis were all observed in fructose supplemented media, all of which may have helped improve virus production (Coroadinha et al., 2006a).

As mentioned earlier, HEK293 cell cultures are characterised by high glucose consumption levels and significant accumulation of by-products such as lactate and ammonia (Román et al., 2018). The harmful effects of lactate and ammonia accumulation has been widely documented involving cell growth inhibition and low product titres (Cruz et al., 2000; Ozturk et al., 1992). Increased ammonia levels affects intracellular pH thus inducing apoptotic and necrotic cell death whilst the toxic action of lactate is due to the effect on the pH and osmolarity of the culture medium, only occurring at relatively high concentrations (>5g/L) (Freund and Croughan, 2018). The minimisation of lactate accumulation has been an area of high interest in optimising HEK293 cell culture. However, it is worth noting that the cultivation period of the HEK293T LVV stable cell line is usually around 5 to 7 days which is shorter compared to HEK293 cultivation for recombinant protein production. Hence, the lactate accumulation may not be as high as those processes.

Under certain environmental conditions, studies have shown that HEK293 cells can turn to a more efficient metabolism where lactate and glucose are consumed simultaneously (Liste-Calleja et al., 2015). For HEK293 cell culture in a 2 L stirred tank reactor (STR), a metabolic shift towards glucose and lactate co-consumption was observed at high lactate levels and culture pH below 6.8 (Liste-Calleja et al., 2015). A later study also identified continuous CO₂ flow as a trigger for the co-consumption of glucose and lactate (Román et al., 2018). This metabolic shift is hypothesized to act as a pH detoxification strategy by means of co-transporting extracellular protons together with lactate in the cytoplasm (Liste-Calleja et al., 2015). To illustrate this, for HEK293 cells cultivated in a 2 L STR with no pH control and continuous addition of 1% CO₂, higher cell densities and product titres were achieved compared to a similar pH 7 controlled STR where no metabolic shift was observed (Román et al., 2018). Hence, unravelling the glucose and lactate metabolism provides an exciting possibility for optimising LVV production in HEK293 cells.

1.5.1.2 Lipid Metabolism

Membrane lipids play an active role in the complex process of viral replication and assembly (Heaton and Randall, 2011; Rodrigues et al., 2009). Viruses use lipid scaffolds, also known as lipid rafts, to accumulate viral and cellular proteins at the budding site (Heaton and Randall, 2011). Studies have shown that HIV-1 Gag is a raft associated protein (Lindwasser and Resh, 2001) and it is solely responsible for the assembly of the virus at the host plasma membrane (Kerviel et al., 2013). Lipid rafts are enriched with cholesterol, sphingolipids and other saturated fatty acids which help maintain its stability (Kerviel et al., 2013). Cholesterol depletion has been shown to disrupt lipid rafts which impairs viral particle formation and infectivity (Ono and Freed, 2001; Samuel et al., 2001). This reliance on lipid rafts imposes changes to the host cell lipid metabolism during viral replication (Rodrigues et al., 2014). There is increased biosynthesis of fatty acids and phospholipids through increased expression of respective enzymes as well as reduced lipid oxidation (Seo and Cresswell, 2013). Some viruses cause upregulation of genes encoding proteins responsible for

cholesterol uptake (Rodrigues et al., 2014). The inhibition of these pathways lead to defective viral particles for both enveloped and non-enveloped viruses (Rodrigues et al., 2014).

Lipid metabolism is easily manipulated as, in the presence of an external lipid source such as serum, most cells readily take them up from the culture medium (Rodrigues et al., 2009). In the absence of serum, cells are usually able to activate the lipid biosynthetic pathways to counterbalance lipid deprivation (Rodrigues et al., 2009). Depending on the cell type, the activation of the lipid *de novo* synthesis may take hours or even days (Alberts et al., 1974). In other cases, the cells can no longer synthesize certain lipids (Rodrigues et al., 2009). For instance, HEK293 Flex cells are derived from kidney tissue wherein there is a low activity of cholesterol biosynthetic enzymes and hence low capacity for cholesterol synthesis (Rodrigues et al., 2012). In such cases, lipid supplementation can be used as strategy to overcome the limitations in host cell metabolism. In a study by Cervera *et al.*, 2013, supplementation of lipid mixture containing cholesterol and fatty acids improved the production of HIV-VLP (virus-like particles) by 2.4-fold (Cervera et al., 2013). Furthermore, in a separate study by Chen *et al.*, 2009, cholesterol supplementation before and during virus production improved the infectivity of lentiviral vectors by up to 6-fold. The authors also found that the cholesterol amount in cells without cholesterol supplementation did not decrease during vector production. This suggests that cholesterol supplementation did not act by restoring deficiency, but rather altering the composition of the lipid rafts (Chen et al., 2009). The authors suggest that this may have changed the viral vector membrane fluidity making it more infective.

1.5.1.3 Nucleic Acid Metabolism

There are distinct changes in the nucleic acid metabolism of the producer cell upon the onset of viral replication. There is increased nucleotide biosynthesis which is associated to higher consumption of nucleoside precursor amino acids (glutamine, glycine, and aspartate) and backbone (Munger et al., 2008, 2006). In addition, there is

also increased activity and expression of pentose phosphate pathway enzymes i.e. the preceding route to nucleotide biosynthesis (Diamond et al., 2010; Munger et al., 2008). Therefore, supplementation with nucleosides has been explored as a strategy to improve viral production. In a study by Rodrigues *et al.*, 2013, it was found that adding nucleoside to the culture medium improved murine leukemia virus (MLV) titres by almost 2-fold.

1.5.1.4 Polyamine Metabolism

Polyamines play an active role in viral replication. They can bind onto DNA or RNA and hence stabilizes the viral genome leading to improved encapsidation (Rodrigues et al., 2014). Polyamines also influence the viral membrane rigidity and thereby prevent lipid peroxidation (Rodrigues et al., 2014). Other beneficial properties include their ability to modulate transcription events and also present antioxidant properties (Wallace et al., 2003). Raina *et al.*, 1981 observed that viral RNA polymerase activity was reduced in polyamine depleted cells. By adding spermidine, a polyamine, the RNA polymerase activity was restored. In a study by Rodrigues *et al.*, 2013, supplementation with polyamines improved murine leukemia virus (MLV) titre by 1.8-fold. However, the concentration of polyamines added to the culture is critical, as high concentration of polyamines may lead to oxidation, and oxidised polyamines are known to exhibit potent antiviral activity (Bachrach, 2007).

1.5.2 Metabolomic Approaches to Identify Bottlenecks

Metabolomics has proved to be an invaluable tool to unravel the complexity of cellular function and physiology (Khoo and Al-Rubeai, 2007). This is because the metabolomics data is reflective of the changes in the transcriptome and proteome of the cell (Chong et al., 2010). Metabolomic analysis has been applied across a range of

cell types, including yeast (Allen et al., 2003), bacterial (Villas-Bôas et al., 2006) and mammalian cells (Chong et al., 2011, 2010, 2009).

The first step in most metabolomic experiments involves extraction of metabolites from the biological samples (Lee et al., 2010). To ensure the sample analysed is representative of its biological system at the time of sampling, metabolism must be stopped immediately after sampling (Sake et al., 2020). The process known as quenching aims to completely and immediately halt all metabolic activity without altering the metabolite profile to be analysed (Sake et al., 2020). The most widely used approach is to add the sample into prechilled cold methanol (Sake et al., 2020). The extracted metabolites are then separated by mass spectrometry based techniques such as gas chromatography/MS (GC/MS) or liquid chromatography/MS (LC/MS) (Lee et al., 2010). Efficient desorption and ionisation of metabolites is important, as the resulting ions are then separated by mass analysers such as time-of-flight, ion trap, and quadrupole (Lee et al., 2010). The ions are then detected using a photomultiplier tube and subsequently identified by their exact mass, retention times, and fragmentation patterns. Verification of identity is carried out by comparison with authentic standards and spectral databases (Lee et al., 2010).

Metabolomic approaches can be distinguished as ‘targeted’ or ‘untargeted’ as shown in Figure 1.8. In targeted methods, specific metabolites of interest are pre-selected for analysis (Baig et al., 2016). The advantage with this approach is that the specificity and sensitivity of the mass spectrometry technique is maximised (Lee et al., 2010). The metabolites are then identified and quantified using authentic analytical standards (Baig et al., 2016). In contrast, authentic standards are not used in untargeted metabolomics (Baig et al., 2016). Rather, the aim is to generate a global metabolite profile or maximise the coverage of metabolites (Lee et al., 2010). The untargeted approach involves no prior method development but requires extensive data analysis. In addition, the lack of analytical standards may compromise the accurate identification and quantification of any particular metabolite.

To the author's knowledge, there are currently no published studies that have carried out a metabolomics approach to identify bottlenecks specific for LVV production. However, a study by Lavado-Garcia *et al.*, 2020 has carried out proteomic analysis of HEK293 cells to provide insights into molecular changes associated with virus-like particle (VLP) production. They identified VLP production to be highly dependent on lipid biosynthesis and intracellular protein transport (Lavado-García et al., 2020). It was observed that the overall lipid biosynthesis was reduced when transfection was carried out at high cell densities (i.e. $>4 \times 10^6$ cells/mL) (Lavado-García et al., 2020). In this state, cells that recently acquired the plasmids did not engage in producing VLPs and cells that were already producing start to slow the production rate (Lavado-García et al., 2020). With regards to intracellular protein transport, downregulation of the whole nucleus transport machinery was observed at high cell densities which affected VLP production (Lavado-García et al., 2020). The metabolomic approach has been widely used to optimise antibody producing Chinese Hamster Ovary (CHO) cell cultures (Chong et al., 2011, 2010, 2009). In a study by Chong *et al.*, 2009, metabolomic analysis was used to identify the accumulation of harmful amino acid derivatives, acetylphenylalanine and dimethylarginine, both of which are detrimental to cell growth. In the same study, they also found certain medium components to be limiting, tryptophan and choline. The findings were then used towards improving media design which ultimately increased cell productivity. In another study, metabolomic analysis revealed significant malate accumulation in the culture media which was found to be due to an enzymatic bottleneck at malate dehydrogenase II (MDH II) (Chong et al., 2010). Re-engineering the cell line to overexpress MDH II achieved higher cell densities and improved antibody titre.

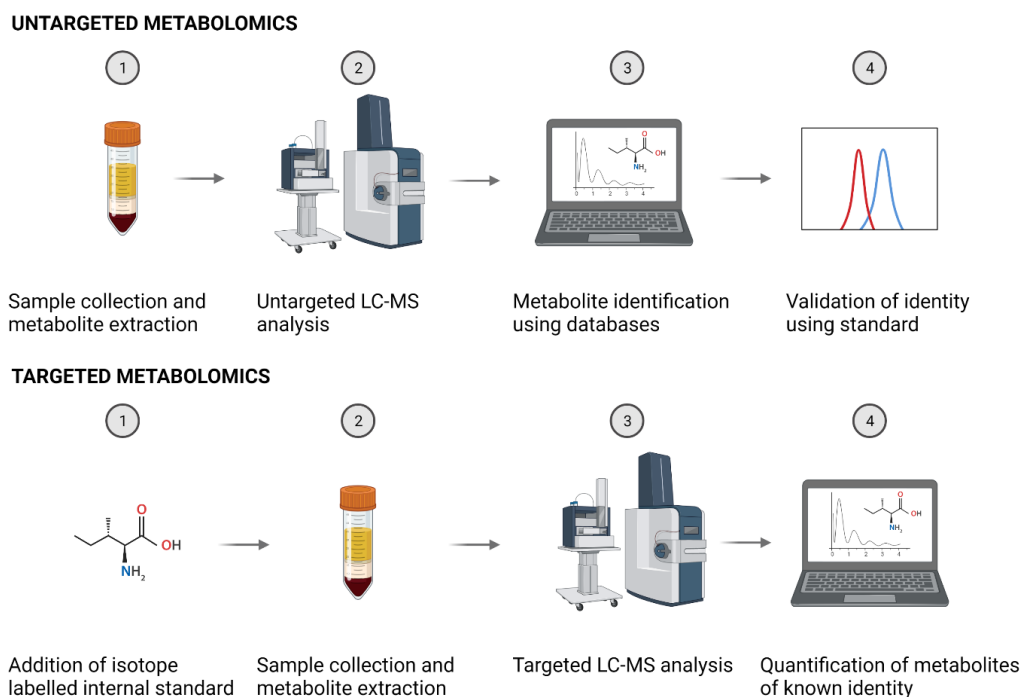


Figure 1.8: Workflow for untargeted and targeted metabolomics. Figure created with BioRender.com.

1.5.3 Nutrient Feeding

Nutrient feeding can be used as a strategy for increasing cell density and productivity (Petiot et al., 2015). The feed can either be added in fed-batch or continuous mode. In a fed-batch process, the basal medium usually supports the initial growth and production, and a feed medium is then added to the cell culture to supply critical nutrients that become depleted (Costa et al., 2014). This results in improved culture longevity and high cell and product yields (Costa et al., 2014). Understanding which nutrients become depleted during the culture is the key to developing the optimal feed for the cells. Metabolomic tools discussed in section 1.5.2 can be used to generate a profile of critical depleting metabolites with time thus enabling accurate feed design. Furthermore, it is important that the nutrient feed is formulated as concentrated as possible in order to reduce feed volume additions which could otherwise lead to cell culture dilution (Costa et al., 2014). Table 1.5 summarises some of the nutrients that are commonly found in most mammalian cell culture feeds.

Continuous feeding, also known as perfusion mode, has also been used to increase cell culture productivity. This approach involves continuously feeding cells with appropriate amount of critical substrates and simultaneously removing accumulated toxic metabolite waste (e.g. lactate and ammonia) (Petiot et al., 2015). For LVV production in particular, a major advantage with continuous feeding is the potential concomitant removal of labile viral products such as LVV from the cell culture vessel (Petiot et al., 2015). This approach has been successfully applied to HEK293 suspension cells grown in 3 L STRs for the production of LVV (Manceur et al., 2017). Not only were cell densities higher in perfusion mode, but a 15-fold increase in titre was achieved compared to batch mode (Manceur et al., 2017). Beyond LVV production, continuous feeding has also led to significant improvement in cell growth and productivity for other mammalian systems e.g. Chinese Hamster Ovary (CHO) cells for monoclonal antibody production (Bielser et al., 2018; Clincke et al., 2013; Tripathi and Shrivastava, 2019).

For LVV production in particular, implementation of continuous feeding at industrial scale is hindered by several bottlenecks. The main challenge with perfusion mode is the difficulty in synchronising upstream and downstream processing (McCarron et al., 2016). The instability of LVV means that it has to be processed as soon as possible after harvest in order to maintain infectivity (Ansorge et al., 2010). However, the current state of LVV downstream processing is not yet capable of processing large quantities of upstream harvest in a continuous manner (McCarron et al., 2016; van der Loo and Wright, 2016). Advancements in LVV downstream processing technologies such as simulated moving bed (SMB) chromatography can enable continuous operation and thus overcome current bottlenecks (Tripathi and Shrivastava, 2019).

Table 1.5: Common nutrients found in mammalian cell culture media. The concentrations in the table is relative to minimum essential media (MEM) (1x). Table adapted from Costa *et al.*, 2014.

Nutrient	Concentration
Glucose	5 – 30 x
Glutamine	5 – 30 x
Essential amino acids ¹	5 – 30 x
Non-essential amino acids ²	0 – 1 x
Vitamins	1 – 4 x
Inorganic salts	1 x
Additional supplements (e.g. lipids, hormones, growth factors and trace elements)	1 x

Essential and non-essential amino acids required for cells in culture as determined by Eagle (Eagle, 1955) include:

¹ Essential amino acids: L-Arginine, L-Cysteine, L-Glutamine, L-Histidine, L-Isoleucine, L-Leucine, L-Lysine, L-Methionine, L-Phenylalanine, L-Threonine, L-Tryptophan, L-Tyrosine, L-Valine

² Non-essential amino acids: Glycine, L-Alanine, L-Asparagine, L-Aspartic acid, L-Glutamic acid, L-Proline, L-Serine

1.6 SMALL SCALE CULTURE SYSTEMS IN BIOPROCESSING

It can take approximately a decade to bring a therapeutic drug product to the market and an estimated \$4.5 billion of investment (Schlander et al., 2021). Unexpected challenges during scale-up are extremely costly and delay the product time-to-market. Therefore, initial optimisation studies should be carried out at small scale under conditions that aim to mimic the large-scale bioreactor environment (Kumar et al., 2004). This is referred to as the scale-down approach. Small scale studies offer advantages in terms of parallelisation, automation and cost reduction (Kumar et al., 2004). The following section reviews the culture systems that are commonly used as scale-down models.

1.6.1 Miniature Stirred Tank Reactors (STRs)

Bioreactors are vessels designed to provide an effective environment for cells to transform biochemicals into products (Erickson, 2011). STRs are one of the most conventional bioreactors used in bioprocessing due to their advantages which include easy scalability, good fluid mixing, oxygen transfer ability and compliance with current Good Manufacturing Practice (cGMP) requirements (Zhong, 2019). They typically consist of a cylindrical vessel with a motor driven central shaft that supports one or more agitators (Chisti and Moo-Young, 2003). The design has been used extensively for microbial and yeast fermentations (Butler, 2003). However, mammalian cells, which are more sensitive than most bacteria or fungi, have also been cultured using STRs for the production of various biopharmaceuticals. For example, the production of recombinant proteins such as insulin (Minteer et al., 2014), monoclonal antibodies (Li et al., 2010) and human factor VIII (Delignat et al., 2018), viral vectors such as LVV (Tang et al., 2021), as well as gene-modified cells used for cell therapy such as CAR-T cells (Costariol et al., 2020).

STRs have been developed commercially in large-scale mammalian cell culture processes up to a volume of 10,000 litres or greater (Butler, 2003). Miniature STRs, based on conventional STRs, have also been developed for early-stage bioprocess development and high-throughput screening (Betts and Baganz, 2006). A variety of small-scale STR systems are now available on the market, with examples including ambr[®]15 and ambr[®]250 (Sartorius), DASGIP[®] (Eppendorf), Applikon MiniBio (Geringe), Multifors2 (Infors-HT), among others (Figure 1.9). The main advantage of small scale STRs is that they have the same features as manufacturing scale vessels (Silk, 2014). Hence, scale translation is relatively straightforward (i.e. compared to vessels which are not geometrically similar e.g. shake flask or microwell to STR) as the engineering environments of the cells (e.g. mixing dynamics, oxygen transfer) are similar (more detail on scale translation is discussed in section 1.7). In addition, they provide the added benefit of online monitoring and control of parameters such as pH, temperature and dissolved oxygen (Silk, 2014).

Some drawbacks with these systems include time-consuming and labour intensive set-up and clean-up especially for glass and stainless steel systems (Silk, 2014). The adoption of single-use technologies with pre-calibrated probes has helped to mitigate this to an extent (Silk, 2014). The investment and operating cost of these systems is also relatively high compared to other small scale systems (Silk, 2014). Lastly, the degree of parallelisation (i.e. number of vessels that can be run at a given time) is still limited in comparison to shake flasks and microwells (Silk, 2014).

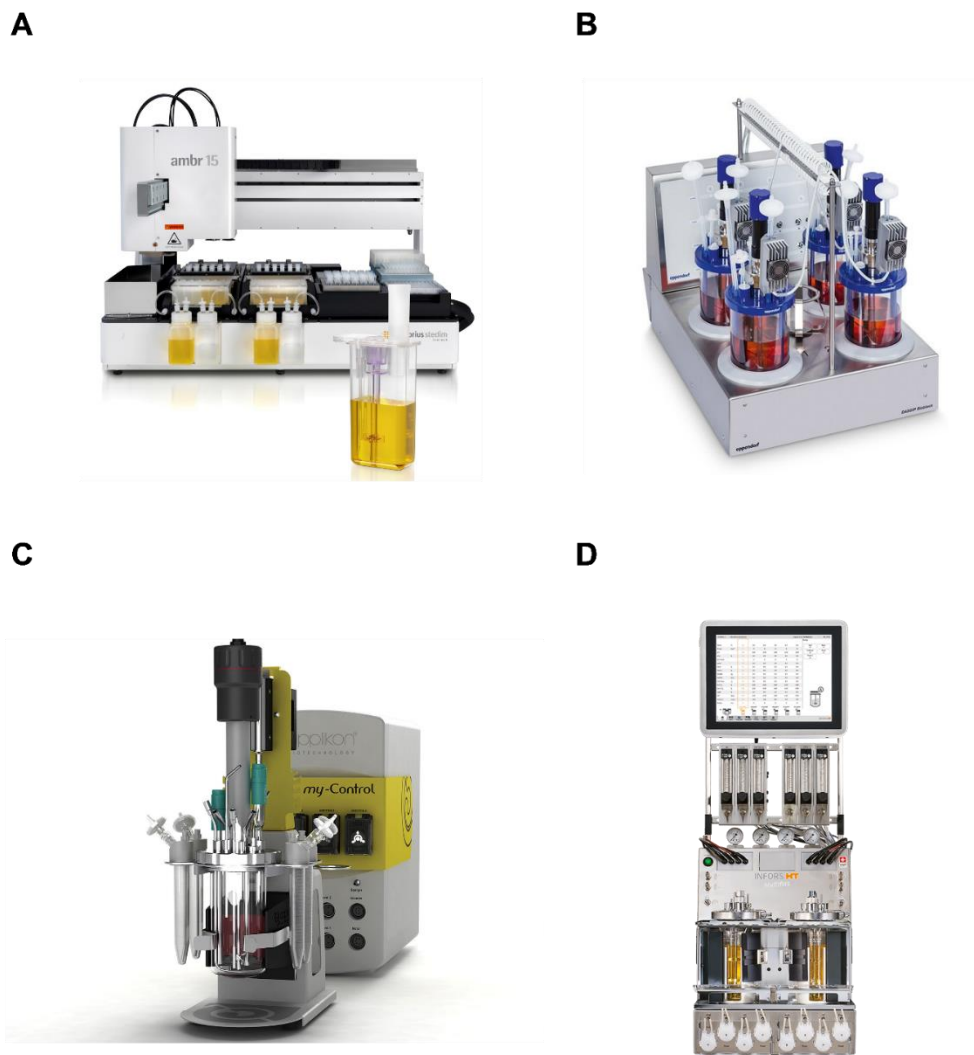


Figure 1.9: Examples of small scale stirred tank systems used in upstream process development. A. Ambr® 15 Cell Culture Generation System (Image source: www.sartorius.com); B. DASGIP® Parallel Bioreactor System (Image source: www.eppendorf.co.uk); C. Applikon MiniBio (Image source: www.getinge.com); D. Multifors2 parallel bioreactor system (Image source: www.infor-ht.com).

1.6.2 Shake Flasks

Shake flasks, also known as Erlenmeyer flasks, are often used for screening and early process development work (Kumar et al., 2004). They have been used to culture a variety of cell types including bacteria, yeast, fungi and animal cells (Kumar et al., 2004). They come in various sizes ranging from 25 mL to 5 L working volumes. The flasks are typically filled to 20% of the nominal volume to promote efficient gas transfer thorough the head-space (Kumar et al., 2004). They are operated within shaking incubators wherein the centrifugal movement provides the liquid mixing and mass transfer. Temperature and dissolved oxygen (DO) is maintained inside the incubator, however pH control is challenging and requires offline pH measurement and manual addition of buffers to maintain the desired pH (Kumar et al., 2004). For sampling, the shake flask has to be removed from the shaking incubator which causes disruption in oxygen supply and concentration of dissolved gases (Kumar et al., 2004). However, the main limitation of these vessels for scale-down work is their limited throughput and the relatively large culture volume required.

1.6.3 Microtiter Plates

Microtiter plates are a series of parallel miniaturized vessels with identical shape and fluid dynamics (Kumar et al., 2004). They offer the potential for carrying out initial high-throughput screening and optimisation studies (Kumar et al., 2004). Other advantages offered are related to logistics and cost. They offer a 50-fold reduction in medium requirements compared to shake flasks and other devices used in early stage bioprocess development (Silk et al., 2010). Knowledge and technology in relation to cell cultivation in microtiter plates has evolved rapidly over the past decade. Various types of plate geometries and sizes are available on the market (Kumar et al., 2004). The wells are either characterised as deep or shallow, and the shape of the well as round or square. Commonly used plates have 6 to 384 wells per plate (Kumar et al., 2004). The typical working volume ranges from 0.025 mL to 5 mL. Due to the relatively small volumes used in microwells, evaporation is of particular concern

particularly for prolonged cultures. To mitigate this, Duetz and co-workers have designed a sandwich lid cover consisting of a layer of silicone with holes above each well and a layer cotton wool covering the plate (Duetz et al., 2000). When compared to an open plate, this system prevented spillage of the culture fluid as well reduced rates of evaporation significantly (Duetz, 2007). In microtiter plates, stopping the shaking incubator is necessary for sampling which disturbs the respiratory profile of the culture organisms (Kumar et al., 2004). In addition, only a small volume of sample can be obtained and hence are only suitable for analytical methods which require low volumes.

1.6.3.1 Engineering characterisation of microwells

Microtiter plates have been extensively characterized in terms of their engineering parameters. For instance, sufficient oxygen transfer is a requirement to support cell growth for any cell culture (Silk, 2014). Doig *et al.*, 2005 have derived a correlation to predict the volumetric oxygen transfer coefficient (k_{La}) in the round well plate operated at a range of shaking speeds (Doig et al., 2005). Adding to this, Duetz and co-workers found that the oxygen transfer rate in round well plates is approximately half of that achieved in square well plates of the same number of wells (Duetz and Witholt, 2004). This is due to the higher turbulence achieved in deep square well (DSW) plates, with the sharp edges acting like baffles promoting greater mixing. It is also important to ensure that bulk mixing is achieved in the microwells in order to have a homogenous culture environment. Zhang *et al.*, 2008 describe the use of computational fluid dynamics (CFD) to characterise fluid flow in microwells (Zhang et al., 2008). The CFD patterns were also used to estimate mean energy dissipation in the 24 standard round well (24-SRW) plate for a range of shaking speeds. The study found that the CFD fluid flow patterns matched closely to those observed using a high speed camera.

1.6.3.2 LVV production in microwells

Previous studies have demonstrated the use of 24-SRW microtiter plates for the suspension cultivation of mammalian cell lines such as hybridoma (Barrett et al., 2010; Micheletti et al., 2006) and GS-CHO (Silk et al., 2010) for antibody production. However, there are very few examples in literature of their use in LVV production. Guy and co-workers describe cultivation of HEK293 cells in 24-SRW plates for LVV production (Guy et al., 2013). In this study, findings from microwell cultures were used to establish operating conditions for LVV production in a 0.5 L wave bioreactor culture. For the proprietary stable producer cell line used (Oxford Biomedica), the authors demonstrated successful cultivation of HEK293 cells and vector production in 24-SRW microtiter plates (Guy et al., 2013). To this authors' knowledge, this is the only publication demonstrating LVV production in microwells and, in particular, no studies have been reported around LVV production in the 24-DSW format. As discussed earlier, square shaped wells have a better mixing and oxygen transfer profile compared to round well plates (Duetz, 2007). Furthermore, the working volume in the deep well plate (i.e. 24-DSW) is 3-4 times greater than the round well plate offering greater volume for analytics.

1.7 SCALING PARAMETERS USED FOR CELL CULTURE

Several scaling parameters have been proposed for cell culture systems including: Aeration rate, impeller tip speed, vessel geometry, k_{La} , mean energy dissipation (P/V) and mixing time (Barrett et al., 2010). Parameters such as aeration rate, impeller tip speed and vessel geometry are mainly used for stirred vessels and are not applicable to microwell systems (Barrett et al., 2010).

1.7.1 Power per Unit Volume (P/V)

Power per unit volume (P/V) is a measure of the power required to agitate a unit volume of liquid and is used to determine if sufficient power is being applied to the liquid in the mixing vessel (Doran, 2013). P/V is a commonly used scaling parameter as it has a direct effect on both liquid phase mixing and gas-liquid mass transfer. Barrett *et al.*, 2010 have demonstrated the use of P/V for scaling a hybridoma cell culture process from a shaken 24-SRW system (800 μL) to a 250 mL shake flask culture. The data was also indicative of results obtained in a 5 L STR, albeit at unmatched P/V. The STR could not be matched at constant P/V due to an unfeasible operating stirrer speed in excess of 300 rpm, at which point excessive foaming and vortexes formed in the vessel. To estimate P/V in the 24-SRW plate, the authors used CFD predictions for mean energy dissipation generated by Zhang *et al.*, 2008. The CFD predictions lacked accuracy as a counter-intuitive trend was observed whereby microwell power consumption was decreasing with increasing shaking speeds. The authors suggested that an increased area of free liquid surface at high shaking speeds may have affected the CFD predictions (Barrett *et al.*, 2010). Due to the inconsistencies in the CFD predictions, it cannot be certain that scaling was at constant P/V in the work of Barrett *et al.*, 2010, even though cell culture performance was comparable across the different culture systems. Therefore, the lack of accurate methods for determining P/V in microwells limits the use of P/V as a scaling parameter for this system.

1.7.2 Oxygen Transfer Rate ($k_{\text{L}}a$)

The oxygen transfer rate or $k_{\text{L}}a$ is mainly used as a scaling parameter for cell cultures where the oxygen demand is very high such as microbial cells (Ferreira-Torres *et al.*, 2005). For mammalian cells, the oxygen demand is relatively low and is typically not growth limiting, hence $k_{\text{L}}a$ is not the preferred choice of scaling parameter. Nienow, 2006 suggests that cell densities of up to 1×10^7 cells/mL can be achieved with $k_{\text{L}}a$ values as low as 1 h^{-1} (Nienow, 2006).

1.7.3 Mixing Time

Mixing is an important operation to achieve homogeneity in bioprocesses (Nienow, 1998). Poor mixing is detrimental for cell culture as it leads to formation of gradients in pH, temperature, dissolved oxygen and nutrients (Nienow, 1998). Mixing time is defined as the time required to achieve a certain degree of homogeneity in a mixed vessel upon addition of a tracer (Xing et al., 2009). 95% is the standard level of homogeneity used by most groups to characterise complete mixing (Li et al., 2020; Rodriguez et al., 2014).

The two commonly used methods for determining mixing time are: pH tracer and decolourisation method (Xing et al., 2009). In the pH tracer method, the addition of acid or base into the bulk medium is used to monitor changes in pH until homogeneity is achieved (Xing et al., 2009). In the decolourisation method, a high speed camera is used to monitor colour changes upon the addition of an acid, base, dye or chemical. The iodine-sodium thiosulfate reaction and dual indicator system for mixing time (DISMT) technique are the two commonly used decolourisation methods (Li et al., 2020). In the latter, mixing time is measured as the time it takes for an iodine bulk solution (blue) to be decolourised (i.e. turn colourless) upon the addition of sodium thiosulfate. The dual indicator system for mixing time (DISMT) technique, first developed by (Melton et al., 2010), has been widely adopted by several groups to characterise mixing time (Li et al., 2020, 2019; Rodriguez et al., 2014; Tissot et al., 2010). The technique is based on pH-dependent colour changes and, as the name suggests, makes use of two acid-base pH indicators. The colour change only occurs when the reagents have been mixed at the molecular level, hence giving a more accurate representation of the actual mixing times within cell cultures (Li et al., 2020). Compared to point-wise methods such as fluorescence based techniques, the DISMT method is superior as it gives information about mixing across the entire volume of the reactor. Furthermore, as a decolourisation method, it enables visualisation of zones that poorly mixed which is not possible with the pH tracer addition method. Finally, the fact that there is a transition of three colour changes instead of two allows for precise characterisation of complete mixing in the vessel.

Previous studies have demonstrated that mixing time is a suitable scaling criterion for scaling between small scale vessels and also across vessels with different geometries i.e. between microwells, shake flask and stirred tank reactor (see Table 1.6). Maintaining constant mixing times (for $t_m < 10s$) ensures a homogenous environment for comparable cell culture performance. The studies all demonstrate close agreement between key cell culture parameters across the different vessels.

Table 1.6: A summary of studies which have shown successful use of mixing time as a basis for scale-translation across vessels with different geometries.

Literature	Cell Line	Vessel Geometry and Scale
Silk, 2014	GS-CHO	24-SRW plate – 50 mL shake flask – 5 L STR
Sani, 2016	GS-CHO	24-SRW plate – 5 L STR
Sani and Baganz, 2016	GS-CHO	0.5 L MBR – 5 L STR

1.8 THESIS AIM AND OBJECTIVES

Although LVVs are an increasingly popular choice for gene therapy vectors, inefficient manufacturing processes have resulted in unsustainably high prices of cell and gene therapy products. Poor yields during LVV upstream processing are typified by low cell densities and low vector productivities. Current processes for fed-batch cultivation of stable cell lines are characterised by a short exponential growth phase and early growth arrest. Hence, cells are typically induced at low cell densities resulting in lower infectious titres. Furthermore, poor virus stability and packaging leads to large amounts of non-infectious vector particles accumulating in the upstream harvest, where the ratio of infectious to total vector particles is often around 1:100. With the low infectious titre and infectivity ratio, a larger number of functional LVV particles are required to achieve the desired transduction efficiency of the target cells. Thus, the lack of optimised upstream processing strategies for highly productive LVV

manufacture forms the motivation for this project, with a specific focus on addressing the former upstream challenge i.e. achieving high viable cell densities. The aim of this thesis is therefore to develop a feeding strategy, using a scale-down model, in order to increase peak viable cell densities achieved for a HEK293T-derived LVV stable producer cell line cultured in fed-batch mode, enabling the potential for increased LVV production.

As described in section 1.5, studying the HEK293 cell metabolism can provide potential targets for optimising cell growth and productivity. In addition to this, a metabolomic approach can be used to identify critical limiting or accumulating metabolites that may cause growth arrest. Thus, by understanding the nutritional demands during cell growth, this project will aim to establish a novel feeding regime to achieve high viable cell densities. This will facilitate induction at higher cell densities potentially resulting in enhanced LVV titres. Testing a variety of feed components and strategies requires high throughput experimentation, however, this is costly and impractical at conventional scales. Therefore, this project will also establish a scale-down model of GSK's 2 L scale LVV stable producer cell line process using microtiter plates. This microwell model will be used to provide a tool for the high throughput evaluation of various feeds to improve LVV productivity. The specific objectives of this project are outlined below.

Objective 1: Assessment of GSK's 277 HEK293T stable cell line cultivation in 2 L stirred tank reactor and identifying potential targets for improving cell growth

Chapter 3 aims to characterise the HEK293T stable cell line growth, metabolite and LVV productivity profiles in the 2 L STR model using GSK's platform operating conditions for the 277 cell line. The data from this study will be used to identify potential targets for improving cell growth. In addition to this, cell culture media analysis using LC-MS will be used to generate a profile of critical depleting and accumulating metabolites during HEK293T stable cell line cultivation.

Objective 2: Developing an effective high-throughput scale-down model of GSK's platform 277 HEK293T stable cell line cultivation process in 2 L stirred tank reactor

In Chapter 4, the microwell model will be assessed as a potential scale-down tool for high-throughput optimisation studies.

Objective 3: Develop a novel feed and feeding regime for enhanced HEK293T stable cell line growth and LVV productivity

In Chapter 5, a design of experiments (DoE) approach, facilitated by the microwell model, will be used to screen and optimise feeds based upon the depleting metabolites identified and thus develop a novel feed for optimised HEK293T stable cell line growth.

In Chapter 6, the effect of the optimised feeding regime on LVV production will be characterised using two different GSK proprietary HEK293T-derived stable producer cell lines.

2 MATERIALS AND METHODS

2.1 CELL LINE AND MEDIA FORMULATION

A GSK proprietary HEK293T suspension-adapted stable LVV producer cell line (SCL) was used for this study (termed ‘277’ hereafter). This cell line has the green fluorescence protein (GFP) transgene as well as the LVV packaging constructs stably integrated in the host genome (Chen et al., 2020). GFP emits green light when excited by specific wavelengths of light, making it a valuable tool for visualising and tracking gene expression and protein localisation in living cells (Tsien, 1998). The green fluorescence emitted by GFP is also easily detectable and can be observed using fluorescence microscopy or flow cytometry, thus enabling both qualitative and quantitative analysis (Chalfie, 2001). However, GFP can also generate background fluorescence which can interfere with the detection of weak signals or result in false-positive results (Chalfie, 2001). The cell line uses a Tet-On system for controlling transcription of the viral genes (Chen et al., 2020). In the absence of doxycycline, a tetracycline repressor (TetR) protein binds to the human cytomegalovirus immediate early (CMV) promoter (Chen et al., 2020). Addition of doxycycline to the culture medium removes TetR from the promoter, thus inducing transcription (Chen et al., 2020). Upon induction, this cell line produces LVV with an RNA genome encoding

for GFP. The cells were cultured and maintained in complete commercial¹ media. Complete media formulation refers to commercial media supplemented with 20 mL/L GlutaMAX™ (Thermo Fisher Scientific, Waltham, U.S.A) and 10 mL/L Pluronic® F-68 (Thermo Fisher Scientific, Waltham, U.S.A). GlutaMAX™ Supplement is an alternative to L-glutamine and is offered as L-alanyl-L-glutamine dipeptide in 0.85% NaCl solution. Unlike L-glutamine, GlutaMAX™ Supplement does not spontaneously break down to form ammonia. Instead, cells cleave the dipeptide bond to release L-glutamine as needed (Krömer et al., 2011). Pluronic® F-68 is a non-ionic surfactant used to control shear forces in suspension cultures (Tharmalingam and Goudar, 2015). For the STR cultures, the media was also supplemented with 0.5 mL/L antifoam (Cytiva, Washington, U.S.A) to allow direct sparging and prevent excessive foaming.

2.2 FEED PREPARATIONS

Concentrated stock solutions were used to prepare the feed conditions for the DoE experiments in Chapter 5. The volume of concentrated stock solution to add in the feed mixture was determined using the formula shown below:

$$V_1 = \frac{C_2 \times V_2}{C_1} \quad (1)$$

Where:

C_1 = Supplement concentration in stock solution

V_1 = Volume of concentrated stock

C_2 = Feed concentration of supplement

¹ Sensitive information pertaining to GSK's LVV manufacturing process such as the name of the media used to culture the HEK293T cells has been redacted from the thesis to comply with the company's confidentiality policy. The generic term 'commercial media' has been used throughout the thesis instead.

V_2 = Total volume of feed mixture

The full list of supplements used to prepare the feed mixtures are outline in Table 2.1. Sterile filtered de-ionised water was used to make up the final volume and concentration of the feed preparation. Where necessary, the pH of feed mixture was adjusted to 7.1 – 7.4 by adding 1.5 M sodium bicarbonate (MilliporeSigma, Burlington, U.S.A). For supplements in solid form, the stock solutions were prepared by dissolving a known quantity of powder into de-ionised water to achieve the desired concentration. The solution was then passed through a 0.2 μm filter (MilliporeSigma, Burlington, U.S.A) to ensure sterility before use. For the conditions where commercial feed² was used, 5% (v/v) feed was added.

Table 2.1: List of supplements used to prepare feed mixtures the in the DoE experiments.

Supplement	Form	Catalogue number	Supplier
MEM Amino Acids Solution (50X)	Liquid	11130051	ThermoFisher Scientific
MEM Non-essential amino Acids Solution (100X)	Liquid	11140050	ThermoFisher Scientific
MEM vitamins solution (100X)	Liquid	11120052	ThermoFisher Scientific
D-Glucose	Solid	G7021	MilliporeSigma
Polyamine Supplement (1000 \times)	Liquid	P8483	MilliporeSigma
GlutaMAX™ Supplement	Liquid	35050061	ThermoFisher Scientific
Chemically Defined Lipid Concentrate	Liquid	11905031	ThermoFisher Scientific

² Details of the commercial feed used in this project has been redacted from the thesis to comply with the company’s confidentiality policy. The generic term ‘commercial feed’ has been used throughout the thesis instead.

Hank's balanced salt solution (HBSS) (10X)	Liquid	14185052	ThermoFisher Scientific
Human insulin solution	Liquid	I9278	MilliporeSigma
Recombinant human IGF-1	Solid	I1271	MilliporeSigma
Sodium pyruvate (100 mM)	Liquid	11360070	ThermoFisher Scientific
L-Ornithine monohydrochloride	Solid	O2375	MilliporeSigma
L-Norvaline	Solid	N7627	MilliporeSigma
2-Aminoisobutyric acid	Solid	850993	MilliporeSigma
Choline chloride	Solid	C7527	MilliporeSigma
Folic acid	Solid	F8758	MilliporeSigma
Putrescine dihydrochloride	Solid	P5780	MilliporeSigma
L-Aspartic acid	Solid	A7219	MilliporeSigma
L-Leucine	Solid	L8912	MilliporeSigma
L-Valine	Solid	V0513	MilliporeSigma
L-Lysine monohydrochloride	Solid	L8662	MilliporeSigma
L-Isoleucine	Solid	I7403	MilliporeSigma
L-Arginine monohydrochloride	Solid	A6969	MilliporeSigma

2.3 SHAKE FLASK CULTURES

The 277 cells were routinely maintained in Erlenmeyer flasks (Corning Inc. New York, U.S.A) at working volumes between 25 – 1000 mL. These were kept in a non-humidified orbital shaking incubator (shaking diameter = 25 mm) (Adolf Kuhner AG, Basel, Switzerland) set at 37°C, 140 rpm and 5% (v/v) CO₂. The cells were seeded at a viable cell density of 0.3 – 0.4 x 10⁶ cells/mL and sub-cultivated every 3 – 4 days.

The cell density pre- and post-passage were determined using the Vi-Cell XR Cell Viability Analyser as outlined in section 2.7.1.

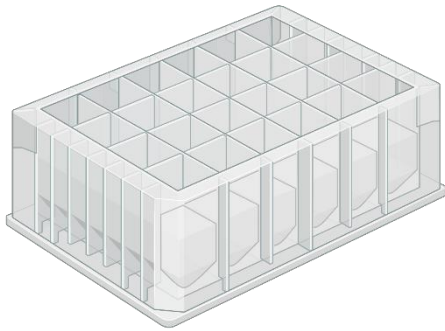
2.4 STIRRED-TANK REACTOR CULTURES

All STR studies were conducted in 2 L UniVessel[®] SU single-use bioreactors (Sartorius AG, Gottingen, Germany) in conjunction with the Biostat[®] B universal benchtop controller (Sartorius AG, Gottingen, Germany). The STR's were run with GSK's platform process operating conditions for the 277 cell line with defined inoculation and induction viable cell densities as well as concentrations of induction agents (i.e. doxycycline and sodium butyrate). In addition, the STR's were also operated with a controlled stirrer speed, temperature, pH and dissolved oxygen. Agitation was provided by two 3-blade segment impellers (diameter = 54 mm) generating a down-flow flow characteristic. Data acquisition and process control was managed using the MFCS/Win 2.0 system (Sartorius AG, Gottingen, Germany). Temperature was controlled using a heating/cooling jacket. The pH was controlled within a deadband of ± 0.1 pH units around the set-point through the addition of sodium carbonate base and CO₂ sparge in the inlet air. The dissolved oxygen tension (DOT) was maintained at the set-point using a cascade of air and oxygen. In order to prime the DOT and pH patch sensors, the STR's were filled with media a day prior to inoculation. Immediately prior to inoculation, the offline pH was measured using the BioProfile[®] FLEX2 analyser (Nova biomedical, Waltham, USA) and the online pH was recalibrated if the offline pH deviated from the online pH by more than 0.05 units. The STR's were seeded at a viable cell density of 0.5×10^6 cells/mL using a diluted mid-exponential phase shake flask culture. The working volume of the STR cultures was between 1.5 to 1.8 L, with the latter being the final working volume after addition of induction agents. Where required, concentrated glucose feed (i.e. 30%) (MilliporeSigma, Burlington, U.S.A) was manually added to the STR. Further details are provided in the relevant results sections.

2.5 SHAKEN MICROWELL CULTURES

Twenty-four deep square well (24 DSW) microtiter plates (Adolf Kuhner AG, Basel, Switzerland) were used in the experiments described in this thesis. The geometry and dimensions of this plate type is illustrated in Figure 2.1. The microwell cultures were inoculated using diluted mid-exponential phase cultures from routinely maintained Erlenmeyer flasks. The plates were sealed with a ‘sandwich lid system’ (Duetz et al., 2000) in conjunction with a metal clamp (Adolf Kuhner AG, Basel, Switzerland) to minimize evaporation over extended periods of culture (Figure 2.2). All microwell plates were incubated in an orbital shaker (shaking diameter = 25 mm) (Adolf Kuhner AG, Basel, Switzerland) with temperature at 37°C and CO₂ at 5%. The well fill volume varied between 5 mL, at the start of culture, and 2.5 mL at the harvest time point. The reduction in volume was due to sampling of cell culture each day for VCD/culture viability and metabolite analysis (see section 2.7.1 and 2.7.2 respectively). For sampling, 0.5 mL of cell culture was removed from multiple wells (i.e. n=2 or n=3 depending on the study). Sacrificial well sampling was not considered for the microwell studies since the 24-DSW plate is not limiting in terms of working volume. Additionally, sacrificial well sampling also leads to a reduction in experimental throughput. To validate the aforementioned well sampling approach, the cell culture performance using sacrificial well sampling was compared against the same well sampling method i.e. where cell culture is removed from the same well for the entire duration of culture (see Figure 9.1 in the Appendix).

A



B

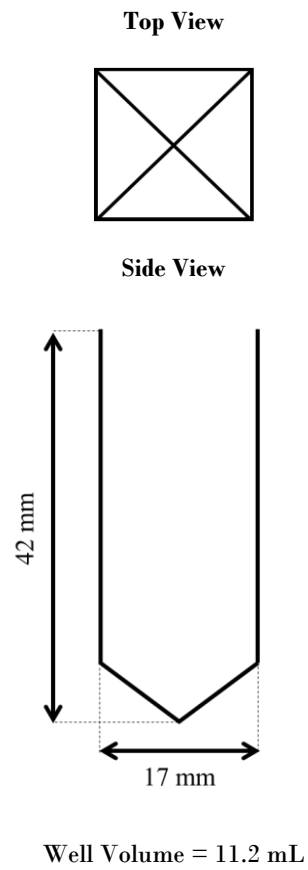


Figure 2.1: Schematic diagram of 24-DSW microtiter plate. (A) Full plate layout (B) Geometry and dimensions of a single well in the 24-DSW plate format. Image generated using Biorender.

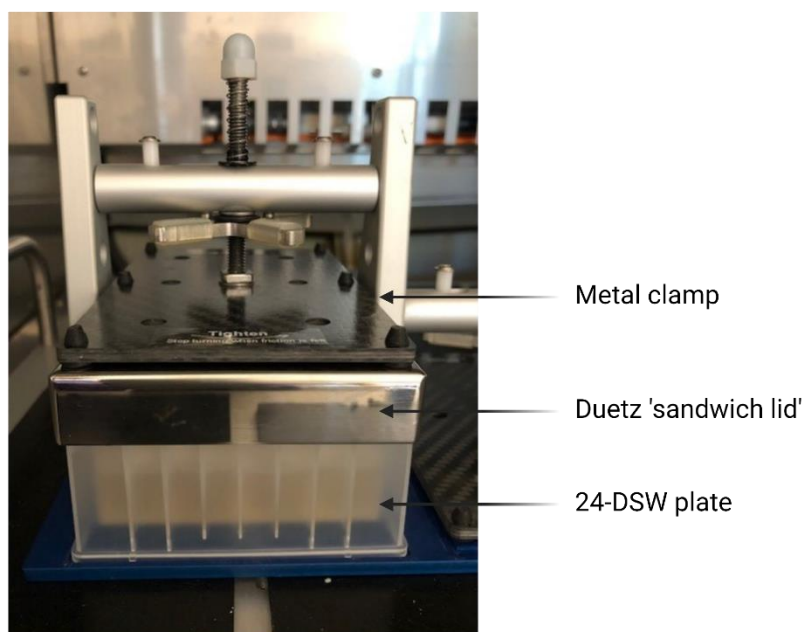


Figure 2.2: 24-DSW plate set-up for HEK293T stable cell line cultivation.

2.6 STABLE CELL LINE INDUCTION AND VECTOR HARVEST

For all culture formats, once the target induction viable cell density was reached, the 277 cell cultures were induced to initiate the production of LVV. Induction was carried out by the addition of 2 $\mu\text{g}/\text{mL}$ Doxycycline (MilliporeSigma, Burlington, U.S.A) and 5 mM Sodium Butyrate (MilliporeSigma, Burlington, U.S.A). Sodium butyrate is a transcription enhancer as it increases gene accessibility to transcription factors (Cuisset et al., 1997). It regulates gene expression by inhibiting histone deacetylase (HDAC) (Cuisset et al., 1997). The resulting hyperacetylated histones form relaxed complexes with the DNA (Cuisset et al., 1997). These relaxed complexes are more accessible by regulatory factors and hence, better transcribed (Cuisset et al., 1997). The induction agents were diluted in complete culture medium prior to being added to the culture vessel. The vector was harvested approximately 48 hours post-induction which has been determined as part of GSK's 277 cell line platform process. Vector harvests were

performed by centrifuging the cell culture in a bench top centrifuge (Eppendorf, Hamburg, Germany) at 1000g for 5 minutes at room temperature. The vector supernatant was aliquoted into cryovials (Corning Inc. New York, U.S.A) and stored in a -80°C freezer.

2.7 ANALYTICAL TECHNIQUES

2.7.1 Viable Cell Density and Viability Measurements

VCD and culture viability measurements were performed immediately post-sampling using an automated cell counting and viability measurement system (Vi-cell XR Cell Viability Analyser, Beckman Coulter, Brea, California, U.S.A). Briefly, 0.5 – 1 mL of cell suspension was aliquoted into a Vi-Cell cup (Beckman Coulter, Brea, California, U.S.A) which was then run on the Vi-Cell system to determine VCD and cell viability measurements by trypan blue exclusion. The method is based on the principle that live cells possess intact cell membranes that exclude certain dyes, such as trypan blue, whereas dead cells do not (Strober, 2001). In this test, the Vi-cell system mixes the cell suspension with trypan blue and then uses a camera to capture images to count the number of viable and non-viable cells.

2.7.2 Cell Culture Bioanalyser

The Nova BioProfile FLEX2 (Nova Biomedical, Brea, California, U.S.A) was used to quantify extracellular metabolites, measure offline pH and gas profiles of cell culture media samples. The full cell culture test menu obtained using the nova include the following: Glucose, Lactate, Glutamine, Glutamate, Ammonium (NH₄⁺), Sodium ion (Na⁺), Potassium ion (K⁺), Calcium ion (Ca⁺⁺), pH, pCO₂, pO₂, and osmolality. A sample volume of 275 µL was required to perform the full analysis. For sample loading,

cell culture collected using a 5 – 10 mL syringe (BD Medical, New Jersey, U.S.A) was injected into the Nova via the inlet port.

2.7.3 Liquid Chromatography-Mass Spectrometry Analysis

Liquid chromatography-mass spectrometry (LC-MS) analysis was performed to generate a profile of depleting and accumulating metabolites during 277 cell culture. The analysis was performed in collaboration with SCIEX (Framingham, U.S.A). A brief description of the method used is provided below.

Prior to shipping to SCIEX, the cell culture media samples were pre-treated in order to inactivate any trace LVV particles in the supernatant. This step was carried out in order to comply with SCIEX's biosafety requirements. The method used was chemical inactivation as outlined by (Sofer, 2003). Briefly, 1 mL of neat sample was mixed with 4 mL solution of 0.1% formic acid (Sigma-Aldrich, St. Louis, Missouri, U.S.A) and 50% acetonitrile (Sigma-Aldrich, St. Louis, Missouri, U.S.A). The mixture was allowed to stand for 4 hours at room temperature to ensure deactivation of virus particles. Quenching is commonly used to rapidly halt cellular metabolism and preserve the metabolite concentrations at the time of sampling. Without quenching, cellular metabolism may continue and the metabolite levels measured after analysis may not reflect the true metabolic state at the time of sampling. As per SCIEX's protocol for cell culture media analysis, a quenching step was not included post sampling. In some situations, such as if the extracellular metabolites are highly stable or if the study aims to investigate their dynamics over time, quenching may not be necessary (Rabinowitz et al., 2011). Instead, samples can be collected at different time points, and the changes in metabolite concentrations can be assessed without immediate quenching. Using a bench top centrifuge (Eppendorf, Hamburg, Germany), the mixture was then centrifuged at 1000g for 5 min at room temperature. The supernatant was collected in a new 5 mL cryovial (Corning Inc. New York, U.S.A) and the sediment discarded.

For the LC-MS analysis, samples were analysed using a TripleTOF[®] 6600 LC-MS/MS system (SCIEX, Framingham, U.S.A) coupled with an ExionLC[™] system (SCIEX, Framingham, U.S.A). Analytes were separated using a Phenomenex Kinetex[®] F5 column (150 mm x 2.1 mm ID, particle size 2.6 μm) (SCIEX, Framingham, U.S.A). Nine samples were analysed in total, which included triplicate samples taken at three different time points during the 277 cell line growth phase. The LC run time was 20 minutes at a flow rate of 200 $\mu\text{L}/\text{min}$. Mobile phase A was 0.1% formic acid in water, and mobile phase B was 0.1% formic acid in acetonitrile. Column oven temperature was 40°C and the injection volume was 5 μL . During mass spectrometry, the data was generated with SWATH[®] acquisition using 20 variable windows. The mass spectrometry method details are outlined in Table 2.2. The data was then analysed using SCIEX OS 1.5 software (SCIEX, Framingham, U.S.A). Peak integration was performed with MQ4 algorithm. For compound confirmation, the acquired MS/MS spectra were matched against MS/MS spectra in the built-in high resolution spectral library. This built-in spectral library contains entries from the SCIEX Accurate Metabolite Spectral library, Antibiotics and NIST library.

Table 2.2: Summary of mass spectrometry parameters

MS Parameter	Value	MS/MS Parameter	Value
MS mass range:	50-700 m/z	MS/MS mass range:	25-700 m/z
MS accumulation time:	100 ms	MS/MS accumulation time:	35 ms
Curtain gas:	30 psi	Source temperature:	400°C
Ion source gas 1:	50 psi	Ion source gas 2:	50 psi
Polarity:	+ or -	Ion spray voltage:	5500 or -4500 V

2.7.4 Quantification of Lentiviral Vector Infectious Titre

To determine the concentration of infectious viral particles (i.e. infectious viral titre measured in transducing units per mL (TU/mL)), HEK293T cells were transduced with serial LV dilutions in the presence of polybrene (8 µg/mL) (MilliporeSigma, Burlington, Massachusetts, U.S.A). Polybrene is a polycation agent which has shown to enhance transduction by retroviral vectors (Davis et al., 2002). The transduced cells were derived from an adherent HEK293T cell line from a GSK in-house research cell bank. The cells were grown in a T-flask (T-125) (Corning Inc. New York, U.S.A) and subsequently seeded into 6-well plates (Corning Inc. New York, U.S.A). For each viral supernatant to be titrated, 3 wells of the 6-well plate were seeded with 3×10^5 viable cells in 2 mL of IMDM media (Thermo Fisher Scientific, Massachusetts, U.S.A). Complete formulation of IMDM was achieved by supplementing with 10% Foetal Bovine Serum (FBS) (Thermo Fisher Scientific, Massachusetts, U.S.A) and 2 mL/L of GlutaMAX (Thermo Fisher Scientific, Massachusetts, U.S.A). An additional 6-well plate was also seeded in the same way, 3 wells to be used for cell counting, to determine the number of viable cells transduced per well, and one well for a negative control. Following transduction, cells were cultured for 3 days at 37°C in a 5% (v/v) CO₂ humidified incubator (Panasonic, Osaka, Japan). After this incubation period, the transduced cells were harvested by transferring 150 µL of cell suspension into a corresponding well of 24 well plate (Corning Inc. New York, U.S.A) containing 1 mL of 2% paraformaldehyde (PFA) which is fixative solution (Alfa Aesar, Haverhill, Massachusetts, U.S.A). The eGFP expression in the transduced cells was measured by flow cytometry using the Accuri c6 Plus system (BD Biosciences, New Jersey, U.S.A). The formula used to calculate the infectious titre is shown as equation 5 in section 2.11. The titre was calculated from dilution factor where the % of GFP positive cells was between 3 – 30% as this falls within the linearity range of the assay.

2.7.5 Quantification of Lentiviral Vector Physical Titre

The p24 protein, located in the LV capsid, is one of four proteins encoded by the HIV-1 gag gene (Ansoerge et al., 2010). Measuring the amount of p24 protein present in cell culture supernatants can be used to infer the LVV physical titre (i.e. total number of vector particles). This assay measured the p24 protein using the Simple Plex HIV-1 Gag p24 ELISA kit (Protein Simple, San Jose, California) following the manufacturer's instructions. The kit consists of the ELLA automated microfluidic glass nano reactors (GNRs) based 72-well cartridge system. The wells of the cartridge are coated with anti-HIV-1 p24 capture antibody, which binds the p24 in the test samples. The ELLA quantifies the p24 protein in triplicate for each sample well. The vector samples were diluted according to the estimated p24 concentration to ensure they were in the linear range of the assay. The first dilution was performed with 0.5% Triton X Lysis buffer (MilliporeSigma, Burlington, Massachusetts, U.S.A). To ensure lysis, the sample preparations were incubated for 1 hour at 37°C in a 5% (v/v) CO₂ humidified incubator (Panasonic, Osaka, Japan). A second dilution was then performed with SD30 dilution buffer (Protein Simple, San Jose, California) prior to loading the samples on the cartridge. Samples were analysed in triplicate and read using the ELLA microfluidic device (Protein Simple, San Jose, California). The p24 concentration (i.e. pg p24/mL) was calculated relative to the factory-calibrated standard curve supplied with the kit. The LVV specific infectivity was calculated as the ratio between infectious titre and physical titre.

2.8 QUANTIFICATION OF MIXING TIME

The dual indicator system for mixing time (DISMT) technique was used to quantify mixing time in the experiments described in Chapter 4. The method used was the same as that reported by Li *et al.*, 2019. The DISMT technique was first developed by Melton *et al.*, 2010 is based around pH dependent colour changes (Melton et al., 2010). As the

name implies, two pH indicator solutions, specifically thymol blue (Fisher Scientific, Loughborough, UK) and methyl red (Fisher Scientific, Loughborough, UK), were used for visualisation of pH change with the fluid appearing red in acidic conditions, yellow at neutral pH and blue in basic conditions. The pH of the working reagent was adjusted until it became neutral (i.e. yellow). After filling the vessel with the working reagent, a stoichiometric amount of 0.075 M hydrochloric acid (HCL) (MilliporeSigma, Burlington, U.S.A) was added to make the colour transition from yellow to red. Thereafter, an equal amount of 0.075 M sodium hydroxide (NaOH) (MilliporeSigma, Burlington, U.S.A) was added to neutralise the acid and return the colour to yellow. The mixing process was recorded using the iCube (NET GmbH, Germany) high speed camera upon the addition of base. Mixing can be visualised since only regions that are well mixed appear yellow. Each condition was repeated five times to reduce statistical error and the average value was used as the mixing time. A universal MATLAB (MathWorks, Massachusetts, U.S.A) script was used to compute the mixing time. The image processing method was the same as that used by Li *et al.*, 2019.

2.9 DOE METHODOLOGY

A Design of Experiments (DoE) approach was used to screen and optimise the composition and the feeding regime of the bespoke feed for enhanced 277 cell growth. The DoE software used for this work was Design Expert v10 (Stat-Ease Inc., Minnesota, U.S.A). For the screening experiments, a factorial design was generated whereby each factor was varied over two levels (high and low). For the optimisation studies, a response surface design was generated as these are better suited to estimate the effects of factors whilst predicting curvature in the response. The experimental runs were performed using the 24-DSW plate high-throughput scale down model. The design summary and conditions generated using Design Expert for all the DoE studies are presented in Table 9.6 – 9.11 in the Appendix (see Chapter 9).

To analyse the data, viable cell density and cell viability responses were entered into the Design Expert software. Data for each response factor was transformed as

appropriate in order to approximate normal distribution (Guy et al., 2013). The automatic model selection tool was used to keep only significant terms in the model. The criterion used was backward p-value selection set at a cut-off value of 0.1. Keeping only significant terms maximises the resulting regression function of the model (Guy et al., 2013). The reduced model was analysed using ANOVA to ensure all the statistical parameters were within the appropriate limits.

2.10 STATISTICS

One-way ANOVA analysis was performed to compare differences between multiple means. Where the overall ANOVA result was significant, post-hoc multiple comparison tests such as Tukey's Honestly Significant Difference (HSD) test and Dunnett's test were also performed. Tukey test was used to determine which pairs of means were significantly different from each other and Dunnett's test was used to compare means of each condition against the control. Student's t-test was also performed for specific pairwise comparisons. All the above statistical tests were performed using Prism 8 (GraphPad, San Diego, U.S.A). Statistical significance was determined using a minimal confidence level of 95% ($p < 0.05$).

2.11 FORMULAE

1. Calculation of cell population doubling time

$$\text{Doubling time} = \frac{\ln(2)}{gr} \quad (2)$$

$$gr = \frac{\ln\left(\frac{N_t}{N_0}\right)}{t} \quad (3)$$

Where:

gr is the growth rate

N_t is the number of cells at time t

N_0 is the number of cells initially at time 0

t is time (days)

2. Calculation of volume of cell suspension required to achieve target induction cell densities in section 3.5

$$\text{Volume of cell suspension} = \frac{\text{Target induction cell density} \times \text{Working volume}}{\text{Cell density of stock culture on day of induction}} \quad (4)$$

3. Calculation of LVV infectious titre

Equation 5 below was used to calculate the infectious titre as the number of LVV transducing units per mL of vector supernatant:

$$\begin{aligned} \text{Infectious titre} &= (\% \text{ GFP positive cells}) \times (\text{number of viable cells transduced}) \\ &\times \left(\frac{\text{Dilution factor}}{\text{Transduciton volume}} \right) \quad (5) \end{aligned}$$

4. Power law relationship for scaling in orbitally shaken reactors (OSRs) described by Rodriguez *et al.*, 2014

$$N \cdot t_m = 100.7 \times \left(\frac{Fr}{Fr_c} \right)^{-1.245} + 25 \quad (6)$$

Where:

N is orbital shaking speed (s^{-1})

t_m is mixing time (s)

Fr is Froude number (dimensionless)

Fr_c is critical Froude number (dimensionless)

5. Calculation of volume of feed addition using concentration of a reference nutrient

The equation below described by Costa *et al.*, 2014 was used to calculate the volume of feed to add to the cell culture in section 5.3:

$$V_{feed} = \frac{C_{r,targ} - C_{r,meas}}{C_{r,feed}} \times V_t \quad (7)$$

Where:

V_{feed} is the volume of feed medium

$C_{r,targ}$ is the target concentration of the reference nutrient in the culture

$C_{r,meas}$ is the measured concentration of the reference nutrient

$C_{r,feed}$ is the concentration of the reference nutrient in the feed medium

V_t is culture volume at the moment of sampling

3 ASSESSMENT OF GSK's 277 HEK293T STABLE CELL LINE CULTIVATION IN 2 L STIRRED TANK REACTOR

3.1 INTRODUCTION AND AIMS

GSK have developed a platform process for the production of LVV in suspension cell culture using a stable producer cell line as described earlier under section 1.4.3. The current process for fed-batch cultivation of the 277 stable cell line is characterised by a short exponential growth phase lasting between 3-4 days and early growth arrest by day 5. Hence, cells are typically induced by day 3 at low viable cell densities (i.e. $2 - 3 \times 10^6$ cells/mL). It is hypothesised that inducing at higher cell densities would yield higher titres.

In this chapter, an assessment of the growth phase of the 277 cell line will first be carried out at the 2 L stirred tank reactor (STR) scale in order to characterise cell growth and metabolite profiles. A key output from this study is to identify the maximum viable cell density (VCD) achieved before cells enter the stationary phase. Thereafter, an assessment of the platform process will be carried out at the 2 L STR scale using the 277 cell line to characterise the LVV productivity profile. To evaluate

the hypothesis that a greater number of cells at induction results in higher infectious titres, a shake flask culture of 277 cells will be used to assess the effect of induction cell density on LVV productivity. Lastly, the spent medium samples from the 277 cell line growth study in the 2 L STR will be analysed using liquid chromatography-mass spectrometry (LC-MS) to generate a profile of critical depleting and accumulating metabolites during the course of the culture. Insights from extracellular metabolite profiles will be used to identify potential targets for improving 277 cell line growth using a bespoke feeding strategy. The specific objectives are:

- Assessment of GSK's 277 cell line growth profile in 2 L STR
- Assessment of GSK's 277 cell line platform LVV production process in 2 L STR
- Assess the effect of induction cell density on LVV production profile
- LC-MS analysis of cell culture media during 277 cell line growth culture

3.2 CHAPTER SPECIFIC MATERIALS AND METHODS

3.2.1 Details for 2 L STR cultures in sections 3.3, 3.4 and 3.6

The method pertaining to STR set-up, operation and sampling has been outlined in section 2.4. For studies in sections 3.3 and 3.4, three 2 L STR's were run in parallel and operated at the platform operating conditions of the 277 cell line. For the study in section 3.6, one STR per condition was set-up. Only the control STR was operated at the 277 cell line platform operating conditions. For the other conditions in section 3.6, the pH set-point and CO₂ flow rate were varied depending on the conditions evaluated

and are specified in more detail in the relevant section. In section 3.4, the induction of the stable cell line and vector harvest were performed using the method outlined in section 2.6. The method for all analytical techniques used in these studies are described in section 2.7. The cell population doubling time was calculated using equations 2 and 3 as shown in section 2.11.

3.2.2 Studying of the effect of induction cell density on LVV production in section 3.5

The 277 cell line was used for this study. The following viable cell densities at induction were examined:

- 2×10^6 cells/mL (control)
- 5×10^6 cells/mL
- 10×10^6 cells/mL
- 15×10^6 cells/mL
- 20×10^6 cells/mL

For each condition, two E-125 shake flasks (Corning Inc. New York, U.S.A) were set-up and operated at 20 mL working volume. The shake flasks were seeded at the target cell densities using a diluted mid-exponential phase shake flask stock culture. The target induction cell densities were achieved by centrifuging the cells and re-suspending them in fresh media. The volume of cell suspension required to achieve the target induction cell densities was calculated using equation 4 in section 2.11. This method has several advantages compared to achieving the target induction cell density through cell growth. Firstly, cells in all conditions would be in the same stage of growth (i.e. from the same mid-exponential phase stock culture) at the time of induction. On the contrary, if the target induction cell density was achieved through growth, cells in the

different conditions would be in different phases of growth which may affect the LVV productivity profile. Furthermore, some of the high cell density cultures (i.e. $> 10 \times 10^6$ cells/mL) would not be possible to reach in the shake flask culture.

The calculated volume of cell suspension was aliquoted into respective centrifuge tubes (Corning Inc. New York, U.S.A) and centrifuged down in a bench top centrifuge (Eppendorf, Hamburg, Germany) at 300g for 5 minutes at room temperature. The cell pellet from each tube was re-suspended into 20 mL of fresh media to obtain the desired seeding density and then transferred into its respective shake flask. The cultures were induced thereafter using the method outlined in section 2.6. The shake flasks were kept in a non-humidified orbital shaking incubator (shaking diameter = 25 mm) (Adolf Kuhner AG, Basel, Switzerland) set at 37°C, 140 rpm and 5% (v/v) CO₂. The method for all analytical techniques used in this study are described in section 2.7.

3.2.3 Method for analysing the LC-MS raw data in section 3.7

The method for LC-MS analysis of cell culture media samples has been outlined in section 2.7.3. The method for analysing the LC-MS raw data is discussed below.

After determining the identity of analytes present in the samples using the built-in spectral libraries, the raw data was further analysed to evaluate trends in the data set. For each analyte, the LC-MS raw data consisted of peak height and peak area. Generally, when peak symmetry is good, there is no significant difference between using peak height or peak area (Kadjo *et al.*, 2017). However in practice, peak symmetry is rarely ideal, and in these cases, using peak area can give more reliable results as the repeatability is much better than with peak heights (Kadjo *et al.*, 2017). Hence, peak area was used for analysing the data set.

Firstly, for each analyte, one-way ANOVA was performed to test for significant difference between the mean peak area of the three time points. For analytes where

3.3 | ASSESSMENT OF GSK'S 277 CELL LINE GROWTH PROFILE IN 2 L STR

the overall ANOVA was significant, the Tukey multiple comparison test was performed to determine which specific pairs of peak area means were significantly different from each other (i.e. day 0 against day 3; day 0 against day 6; day 3 against day 6). The minimal level of confidence at which the results were considered significant was $p < 0.05$. The results from the t-test were used to group the metabolites into three categories:

1. No significant change – metabolites where there was no significant difference in peak area across all days
2. Accumulating – metabolites where the peak area for day 3 and/or day 6 was significantly greater than day 0
3. Depleting – metabolites where the peak area for day 3 and/or day 6 was significantly smaller than day 0

Lastly, within each group, the analytes were sub-divided according to metabolite group i.e. amino acid, protein, lipid etc.

3.3 ASSESSMENT OF GSK'S 277 CELL LINE GROWTH PROFILE IN 2 L STR

Figure 3.1A illustrates the cell growth and culture viability profile of the 277 cell line cultivated in the 2 L STR. The general trend in cell growth and viability was similar in all three vessels as indicated by the small error bars on the graph. To accurately determine the different phases of growth, the natural logarithm of viable cell density was plotted against time as shown in Figure 3.1B. The culture first passes through a short lag phase between day 0 and day 1 where there was little growth. The cell population doubling time during this period was approximately 56 hours as shown in Table 9.1 under Appendix A (section 9.1). During the lag phase, the cells adjust to the replenished supplies of nutrients and undertake all the necessary synthesis prior to cell

division (Bhatia, 2015). Between day 1 and day 3, Figure 3.1B shows the culture passes through the logarithmic phase or exponential phase of growth in which cells divide more rapidly, causing a logarithmic increase in cell number. The average doubling time for this period was approximately 26.5 hours (i.e. average of day 1 to 3 data shown in Table 9.1 under Appendix A). Between day 3 and day 5, the culture went through a further period of cell division that resulted in a linear increase in cell number, slowing as potentially some nutrients became limiting. Figure 3.1B shows the cells are no longer growing exponentially with the population doubling time increasing to approximately 44.4 hours in this period (i.e. average of day 3 to 5 data shown in Table 9.1 under Appendix A). The doubling time values for the 277 cell line during the growth period correlate with the values reported by others in the literature for HEK293 cells grown in suspension culture (Abaandou et al., 2021; Subedi et al., 2015). Subedi *et al.*, 2015 reported a doubling time of 32 hours whilst Abaandou *et al.*, 2021 reported cell doubling every 33 hours. After day 5, the culture reached a stationary phase in which the rate of cell division within the culture decreased significantly until growth finally halts. By this time, the population doubling time was over 150 hours (see Table 9.1 under Appendix A). As nutrients are likely depleted during this phase, some of the cells in the culture begin to show senescent characteristics and a low level of cell division will maintain cell numbers (Bhatia, 2015). The culture was terminated at this point, however, if cells are left in the stationary phase for too long, a death phase is observed as they enter apoptosis.

Figure 3.1 confirms that the 277 cell line is indeed characterised by early growth arrest with cells entering into stationary phase as early as day 5. Under the platform process operating conditions, this cell line is unable to reach high viable cell densities. The maximum VCD before cells entered stationary phase was around 6×10^6 cells/mL. A decline in cell culture viability was also apparent at this stage (i.e. after day 5) indicating that the environment around the cells was no longer suitable to sustain a healthy culture.

3.3 | ASSESSMENT OF GSK'S 277 CELL LINE GROWTH PROFILE IN 2 L STR

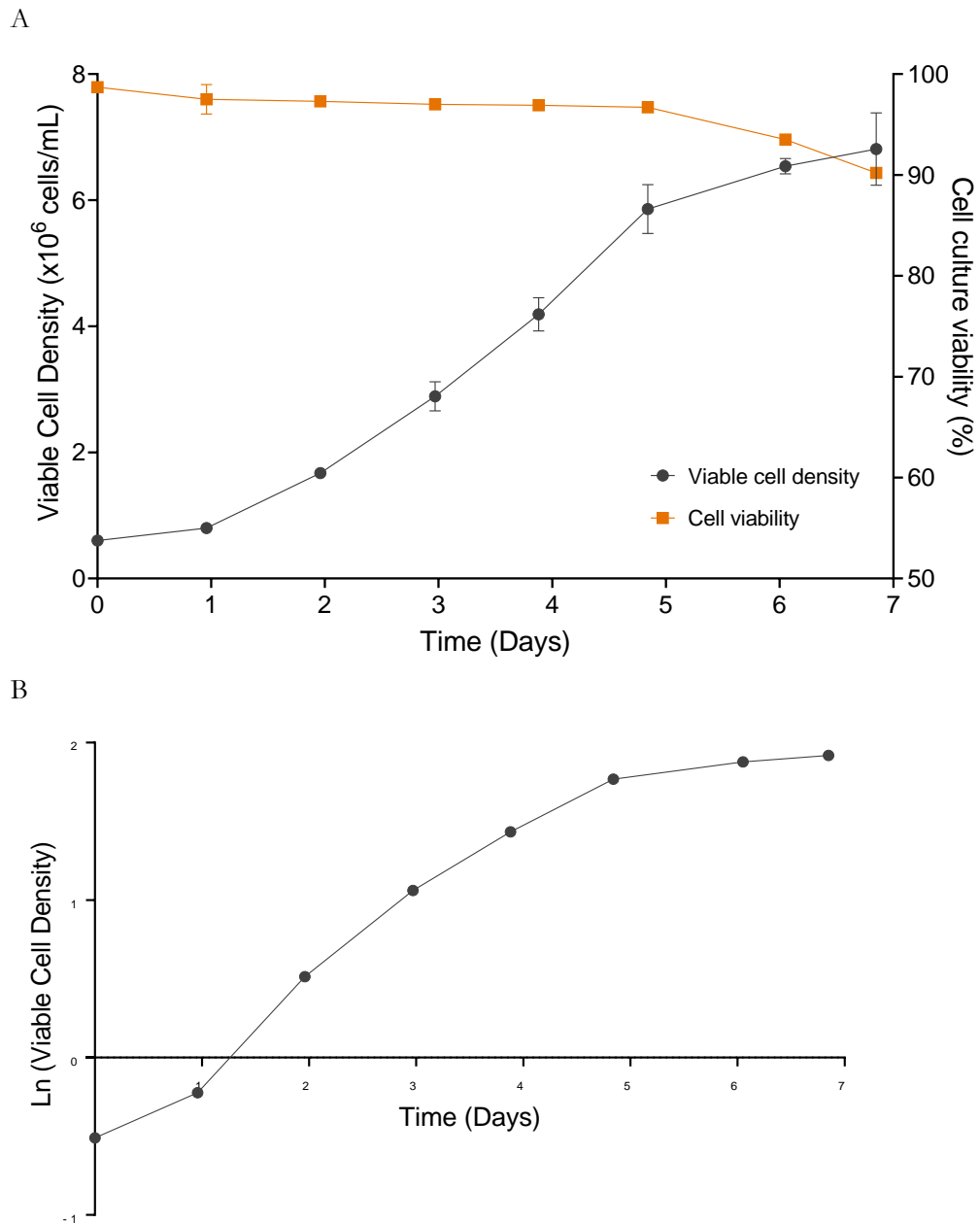


Figure 3.1: (A) Viable cell density and cell culture viability profile for GSK's 277 stable cell line growth culture in 2 L STR. (B) Natural logarithm of viable cell density plotted against time. Error bars represent one standard deviation about the mean (n=3).

Two extracellular metabolites were measured over the culture period, namely glucose and lactate. Figure 3.2 shows the glucose and lactate concentration profiles of the 277 cell line growth culture. The general trend from the graph indicates high levels of glucose consumption and lactate production (i.e. ~ 1 g/L/day glucose consumption

rate and >5 g/L lactate concentration by day 5). This seems to be a common trend associated with HEK293 cells, and the majority of mammalian cell cultures, as reported by several studies in literature (Liste-Calleja *et al.*, 2015; Román *et al.*, 2018). According to Roman *et al.*, 2018, a major disadvantage of HEK293 cells is an inefficient metabolism when growing under usual culture conditions (i.e. pH 7 and 37°C), characterised by consumption of large quantities of glucose and concomitant production of lactate. As seen in Figure 3.2, by day 4, the glucose concentration was below 2 g/L. As per the platform process for 277 cell line culture in 2 L STRs, glucose was fed manually to bring the culture concentration back up to ~ 5 g/L. On day 5, the glucose concentration was again below 2 g/L, hence another manual glucose feed was carried out to bring the concentration up to ~ 5 g/L. During this same period (i.e. between day 4 and day 5), the lactate concentration increased rapidly with concentration exceeding 5 g/L. Ozturk *et al.*, 1992 suggests that lactate concentration values above 5 g/L become growth inhibitory for mammalian cell cultures (Ozturk *et al.*, 1992). On day 6, glucose was depleted in the culture and lactate concentration was approximately 8 g/L. No manual glucose feed was initiated as cells already appeared to be in the stationary phase i.e. no longer actively proliferating.

Comparing Figures 3.1 and 3.2, it can be seen that the transition period between growth and stationary phase (i.e. post-day 5) coincided with the time point when glucose was depleting in the culture medium and also lactate concentration was accumulating at an inhibitory level (i.e. >5 g/L). Liste-Calleja *et al.*, 2015 have demonstrated that culture pH below 6.8 triggers lactate co-metabolism in HEK293 cells. This cellular adaptation is used as a pH detoxification strategy by means of co-transporting extracellular protons together with lactate into the cytoplasm. In a separate study, Roman *et al.*, 2018 demonstrated that CO_2 is also an important trigger that works in tandem with pH. They concluded that pH control in the STR limits the efficient metabolism of glucose and lactate i.e. better HEK293 growth profile was observed in STR's with no pH control. The rationale was to mimic conditions in a shake flask whereby CO_2 in the headspace helps with the media buffering system.

In a STR with no pH control and continuous addition of 1% CO₂, lactate consumption was more pronounced compared to an STR controlled at pH 7.0 and pH 6.8. By altering the glucose and lactate metabolism, both Liste-Calleja *et al.*, 2015 and Roman *et al.*, 2018, demonstrated higher viable cell densities and volumetric productivities mainly due to the effect of pH on triggering the metabolic shift in HEK293 cells. For the optimal condition, which involved no pH control and a 1% CO₂ flow, Roman *et al.*, 2018 achieved an exponential growth period lasting around 6 days and peak VCD of just over 14 x 10⁶ cells/mL. However, it is worth noting that the cell line used in both these studies was a suspension HEK293 cell line expressing hIFN γ protein and not LVV. Hence, the growth kinetics of the two HEK293 cell lines may vary due to the different transgenes. Building upon the work of Liste-Calleja *et al.*, 2015 and Roman *et al.*, 2018, section 3.6 explores the effect of altering the glucose and lactate metabolism using pH and CO₂ on 277 cell line growth in 2 L STR with the aim of increasing viable cell densities.

Beyond glucose and lactate, other metabolites may also be contributing towards the early growth arrest observed in Figure 3.1. Using LC-MS analysis, Chong *et al.*, 2009 identified metabolites that began to accumulate in a CHO cell culture as it entered into stationary phase (Chong et al., 2009). The majority of these were amino acid derivatives such as acetyl phenylalanine and dimethylarginine, which are known to be detrimental to cell growth. In section 3.7, a similar approach has been applied to the 277 cell line where the spent media samples were analysed using LC-MS to generate a more detailed profile of the depleting and accumulating metabolites during the growth phase.

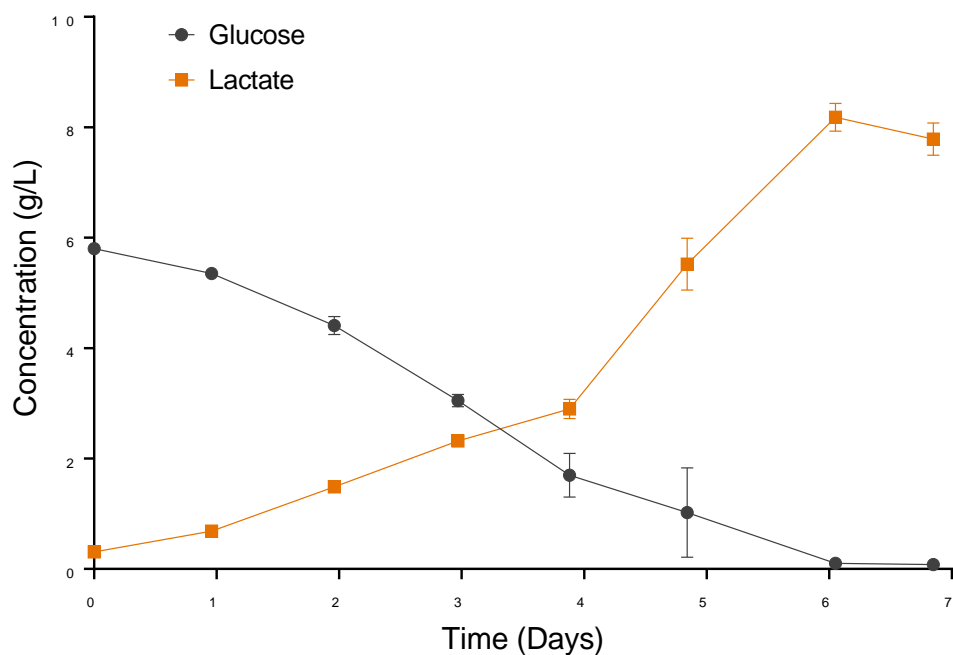


Figure 3.2: Glucose and lactate concentration profile for GSK's 277 stable cell line growth culture in 2 L STR. Error bars represent one standard deviation about the mean (n=3). Note: Post-feed glucose measurements were not taken on day 4 and day 5.

3.4 ASSESSMENT OF GSK'S 277 CELL LINE PLATFORM LVV PRODUCTION PROCESS IN 2 L STR

The company's LVV production platform using the 277 stable cell line has been developed for STR scales ≥ 2 L. For this cell line, the STR is typically inoculated at a seeding cell density of 0.5×10^6 cells/mL. Cells are then cultured for a few days until they reach cell densities in the range of $2 - 3 \times 10^6$ cells/mL. At this point, the culture is induced to initiate the production of LVV. Induction is carried out by the addition of doxycycline and sodium butyrate diluted in media. The vector is then harvested at approximately 48 hours post-induction, which has been characterised as the optimal harvest time point for maximum LVV titre when using the 277 cell line.

Figure 3.3A illustrates the cell growth and viability profile of the 277 cell line over the 5-day culture period. To accurately identify the exponential growth period, the natural logarithm of viable cell density was plotted against time as shown in Figure 3.3B. The general trend in cell growth and viability was similar in all three vessels as indicated by the small error bars on the graph. Between day 0 and day 2, cells appear to be doubling in number every 24 hours with no apparent lag phase observed (see Table 9.2 under Appendix A). By day 2, cells had reached the target induction cell density of 2×10^6 cells/mL. At this point, the cultures were induced to initiate LVV production. The dilution of the culture at induction explains the decrease in viable cell density at day 2.

After induction, a decline in the rate of cell growth was observed which became more apparent between 24 and 48 hours post-induction. A similar plateau in HEK293 cell growth post-transfection has also been described by Ansorge *et al.*, 2011. In the same study, online permittivity measurements were used to define critical transition points in LVV production. The first transition point was identified at 24 hours post-transfection corresponding to the first viral release. The second transition point at 48 hours post-transfection was when maximum functional viral titre was attained. This is also consistent with GSK's platform process using the 277 cell line. The final transition point was observed around 72 hours post-transfection when the LVV titre significantly decreased. A similar study is described by Petiot *et al.*, 2017. Using capacitance monitoring, they identified intracellular accumulation of viral components, i.e. viral proteins, capsids and genomes, between 0 to 15 hours post-transfection. Between 15 to 30 hours post-transfection, the viral production phase was identified by the onset of viral release. Therefore, the plateau in cell growth after 24 hours post-induction observed in the present study may also correspond to the onset of LVV production as shown in Figure 3.3. Perhaps, cellular energy is diverted to virus production rather than cell growth (Coroadinha *et al.*, 2006b). Alternatively, the release of lentiviral vectors can potentially have toxic effects on HEK293 cells which may affect cell growth. For example, the viral proteins and RNA can trigger cellular stress responses or interfere with normal cellular processes (Pfeifer *et al.*, 2001).

3 | ASSESSMENT OF GSK'S 277 HEK293T STABLE CELL LINE CULTIVATION IN 2 L STIRRED TANK REACTOR

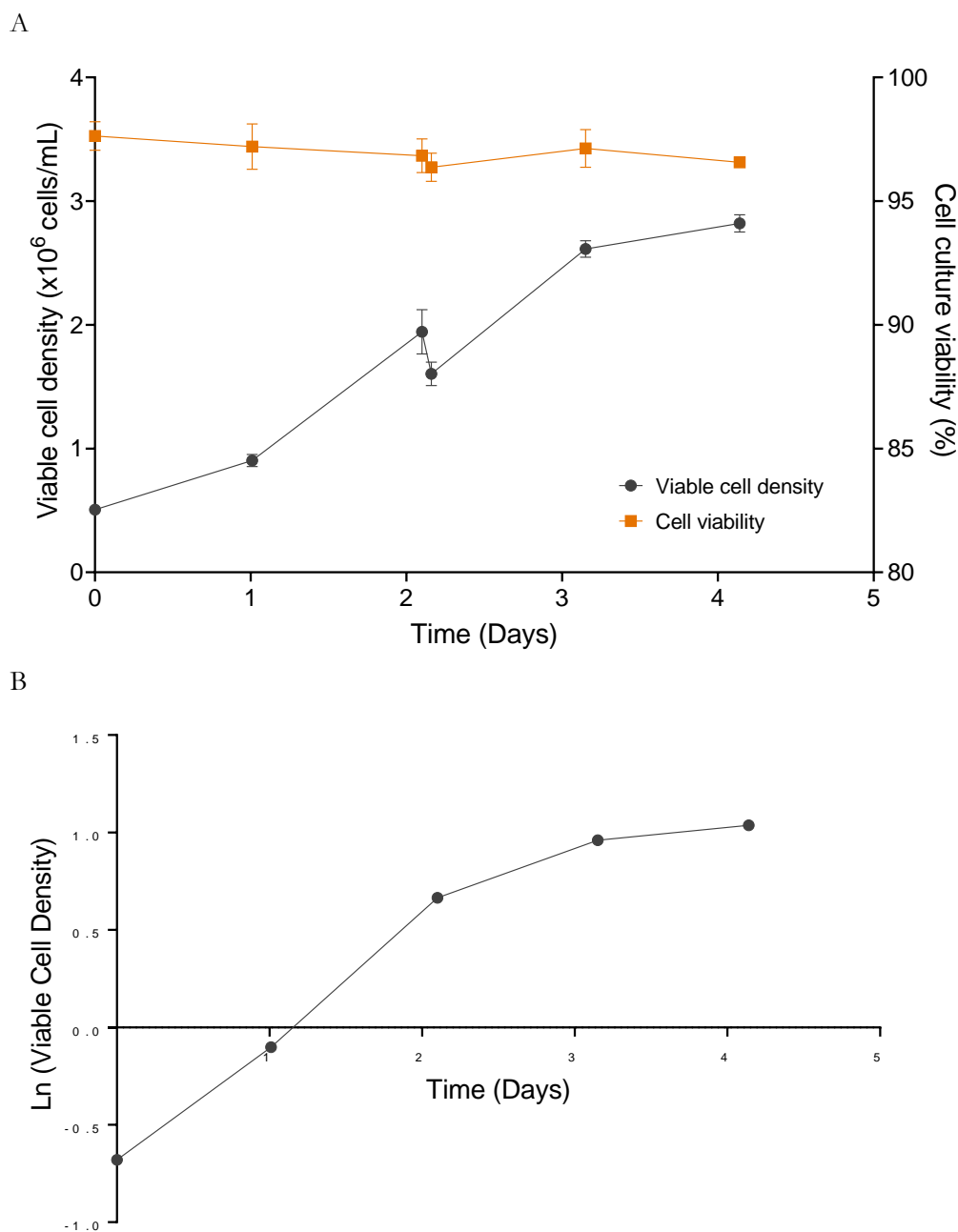


Figure 3.3: (A) Viable cell density and viability profile for GSK's 277 stable cell line platform LVV production process. (B) Natural logarithm of viable cell density plotted against time. Error bars represent one standard deviation about the mean (n=3).

Table 3.1 summarises the key measures of LVV productivity in the vector harvest at 48 hours post-induction. The average infectious and physical titres of the three STR's were 7.76×10^7 TU/mL and 7.16×10^5 pg p24/mL respectively. The coefficient of

variation (CV) around the mean was less than 10% for both titres indicating high comparability between the three STR's. In comparison, Manceur *et al.*, 2017 achieved an infectious titre of 6×10^6 TU/mL from a suspension cultured HEK293 stable cell line operated in batch mode. In the same study, the stable cell line was also cultivated in perfusion mode from which a higher titre of 2×10^7 TU/mL was achieved.

The infectious titre is also comparable to transient transfection where consistently high titres in the range of $10^7 - 10^8$ TU/mL have been reported (Ansorge *et al.*, 2009; Witting *et al.*, 2012). Dividing the infectious titre with the physical titre gives an infectivity ratio in terms of the number of transducing units per pg of p24 protein (TU/pg p24). The ratio provides an indication of the quality of viral particles produced. A higher ratio of TU per pg p24 signifies a higher infectivity since there are more transducing units in a given quantity of virus particles which increases the transduction efficiency. It is worth noting that the p24 method can also measure free p24, not just viral particle associated p24 hence may affect the reliability of the infectivity ratio (Dautzenberg *et al.*, 2020). The infectivity ratio from this study was just over 100 TU per pg p24. It has been estimated that typically there are approximately 1×10^4 physical particles of lentivirus for every pg of p24 antigen (Sigma-Aldrich, 2018). Using this estimation, the infectivity can also be interpreted as 1 transducing unit (i.e. functional LVV) for every 100 LVV particles produced.

Coffin *et al.*, 1997 have also reported a similar ratio of total to infectious vector particles. It is important to note that comparison of titres between different research groups can be challenging due to the lack of a standardised assay protocol and different analytical methods used entirely. Minor modifications in the protocol can lead to significant titre differences. Ansorge *et al.*, 2010 report that vector titre can vary up to 50-fold when modifying conditions such as inoculum volume, type and number of target cells and length of vector exposure to target cells.

Table 3.1: Summary of LVV productivity parameters for GSK's 277 stable cell line platform LVV production process

	Mean	Standard deviation	CV (%)
Infectious Titre (TU/mL)	7.76×10^7	3.68×10^6	4.75
Physical Titre (pg p24/mL)	7.16×10^5	5.18×10^4	7.22
Infectivity (TU/pg p24)	109	6.40	5.90

The metabolite profiles for glucose, lactate, glutamine and glutamate are illustrated in Figure 3.4 and Figure 3.5. During the growth phase (i.e. day 0 to day 2), the average glucose consumption and lactate production rates in the STR's were similar at around 0.7 g/L/day. After induction (i.e. day 2 to day 4), glucose consumption increased at a higher rate compared to lactate production being at 1.7 g/L/day compared to 1.2 g/L/day. This may suggest that the cells are favouring aerobic respiration and efficiently utilising glucose to produce ATP through the TCA cycle and oxidative phosphorylation. This is to provide maximum energy to the cells especially between day 2 and day 3 when cells are both growing and also preparing for virus production. Metabolomic profiling of TCA cycle intermediates, isotope tracing and enzyme assays are some of the techniques that can be used to confirm changes in TCA cycle and electron transport chain activity. In addition, as the cell growth rate was in decline 24 hours post-induction, an increasing glucose consumption rate in this period suggests that cellular energy was being diverted from growth towards virus production. As mentioned earlier, this may be a contributing factor for the plateau in cell growth observed in Figure 3.3.

Glutamine is supplemented in the basal media used in GSK's platform process as the dipeptide L-alanyl-L-glutamine also known as GlutaMAX™. In this formulation, glutamine does not spontaneously breakdown to form ammonia, rather, cells cleave the dipeptide bond to release L-glutamine as needed. This explains the increasing concentration of glutamine between day 0 and day 2. After day 2, the dipeptide is no longer broken down, rather the accumulating L-glutamine is now actively consumed by the cells. A corresponding increase in glutamate production is also observed

between day 2 and day 4. When the cellular energy demands increase, such as after induction, cells can metabolize amino acids for energy. Glutamine is the most consumed amino acid in HEK293 cell culture as it is a major source of energy (Petiot et al., 2015). Glutamine also provides a source of nitrogen atoms which cells require to build molecules such as nucleotides, amino acids, amino-sugars and vitamins (Newsholme et al., 2003). As mentioned earlier, Petiot *et al.*, 2017 describe accumulation of viral components, i.e. viral proteins, capsids and genomes, between 0 and 15 hours post-transfection. Therefore, after induction, in addition to glutamine being consumed to promote cell growth, glutamine may also have been channelled towards the production of viral proteins.

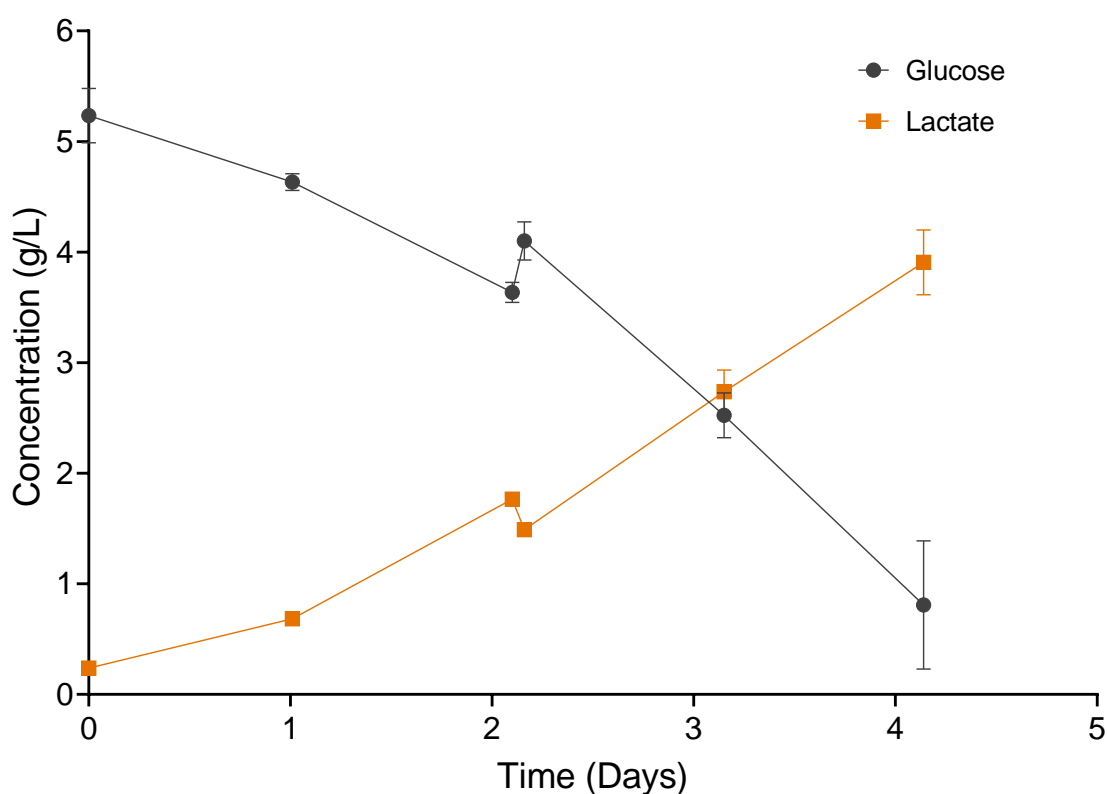


Figure 3.4: Glucose and lactate concentration profiles for GSK's 277 stable cell line platform LVV production process. Error bars represent one standard deviation about the mean (n=3).

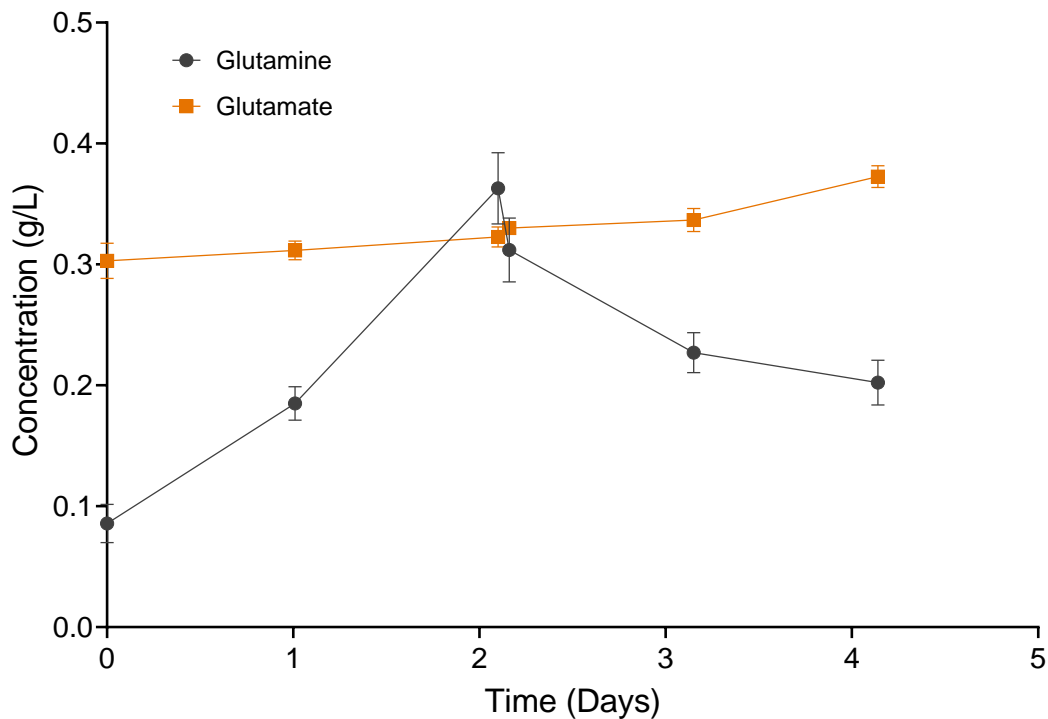


Figure 3.5: Glutamine and glutamate concentration profiles for GSK's 277 stable cell line platform LVV production process. Error bars represent one standard deviation about the mean (n=3).

3.5 EFFECT OF INDUCTION CELL DENSITY ON LVV PRODUCTION

In order to maximise LVV titres, studies have shown that the optimal time point for induction is in the middle of the exponential growth phase when cells are in the most viable state coupled with vector harvest performed around 48 hours post-induction (Ansoerge et al., 2009; Manceur et al., 2017; Petiot et al., 2017). For the 277 cell line, Figure 3.1 indicated a short period of exponential growth wherein cell growth arrest was observed as early as day 5. As a result, GSK's platform process using the 277 cell line has been optimised for induction between Days 2 to 3 (i.e. middle of exponential growth) and vector harvest performed before cells enter into stationary phase (i.e.

between day 4 – 5). This coincides with an induction cell density in the range of $2 - 3 \times 10^6$ cells/mL, which is lower compared to values reported by others in literature. For a similar HEK293T stable LVV producer cell line cultured in suspension, Manceur *et al.*, 2017 have reported an induction cell density of $\sim 5 \times 10^6$ cells/mL.

As already highlighted previously, the 277 cell line is unable to reach high viable cell densities under the current platform process conditions. According to Figure 3.1, the maximum VCD achieved prior to growth arrest was only around 6×10^6 cells/mL. Hence, a key objective of the project is to improve the 277 cell line growth profile by increasing the period of exponential growth beyond day 3. This would then permit the induction of cells after day 3, and consequently at viable cell densities greater than $2 - 3 \times 10^6$ cells/mL. The aim of this study, therefore, was to test the hypothesis that inducing at higher viable cell densities does indeed result in increased LVV production.

As outlined in section 3.2.2, five induction cell densities between 2×10^6 cells/mL (control) and 20×10^6 cells/mL were investigated using a shake flask culture system. The effect of the different induction cell densities on LVV infectious titre is shown in Figure 3.6. The general trend observed was that higher induction cell density correlated to higher infectious titre perhaps due to more virus producing cells present. One-way ANOVA test showed there was a significant difference in the infectious titre between the different induction cell densities. Dunnett's multiple comparison test was then performed to determine if the means of each condition was significantly different from the 277 cell line platform control (i.e. 2×10^6 cell/ml condition). From the Dunnett's test, only the 2×10^6 cell/ml and 5×10^6 cell/ml comparison was not significant at 95% confidence, all other comparisons were significantly different (Figure 3.6). In some cases, Dunnett's test may not have enough statistical power to detect specific differences in these pairwise comparisons, hence a Student's test can be used instead (Midway *et al.*, 2020). For the same two conditions, the Student's t-test showed that the difference in infectious titre was indeed significant at 95% confidence level. .

The data also indicates that up to 10×10^6 cells/mL, the increase in infectious titre was proportional to the increase in induction cell density. The data shows that inducing at

5×10^6 cells/mL gave approximately 2.5-fold higher infectious titre than inducing at 2×10^6 cells/mL. Similarly, inducing at 10×10^6 cells/mL resulted in approximately 5-fold higher infectious titre compared to induction at 2×10^6 cells/mL.

For viable cell densities greater than 10×10^6 cells/mL, a similar proportional increase in LVV production was no longer apparent. Inducing at 15×10^6 cells/mL represents a 7.5-fold increase in induction cell density compared to the 277 cell line platform control. However, the increase in LVV titre between these two conditions was only 6-fold. Similarly, inducing at 20×10^6 cells/mL only resulted in a 5.4-fold increase in titre compared to the control. This phenomenon where cell-specific virus productivity decreases at high cell concentrations is commonly described as the 'cell density effect' and was first identified during the production of adenoviral vectors (Garnier et al., 1994; Nadeau and Kamen, 2003). Although adenovirus cultures have been grown up to 70×10^6 cells/mL, most studies report infection carried out at $12 - 14 \times 10^6$ cells/mL to mitigate the cell density effect. According to Nadeau and Kamen, 2003, this limitation is more related to nutrient limitations and/or accumulation of inhibitors. However, attempts to overcome nutrient limitation and/or by product inhibition in fed-batch mode did not translate into significant yield improvements. The authors concluded that more work was needed to understand basic host cell metabolism. This understanding can be used to develop feeding strategies that provide essential nutrients under conditions that prevent accumulation of inhibiting factors. For LVV production, the 'cell density effect' has not been widely characterised and hence no comparable studies were identified in the literature.

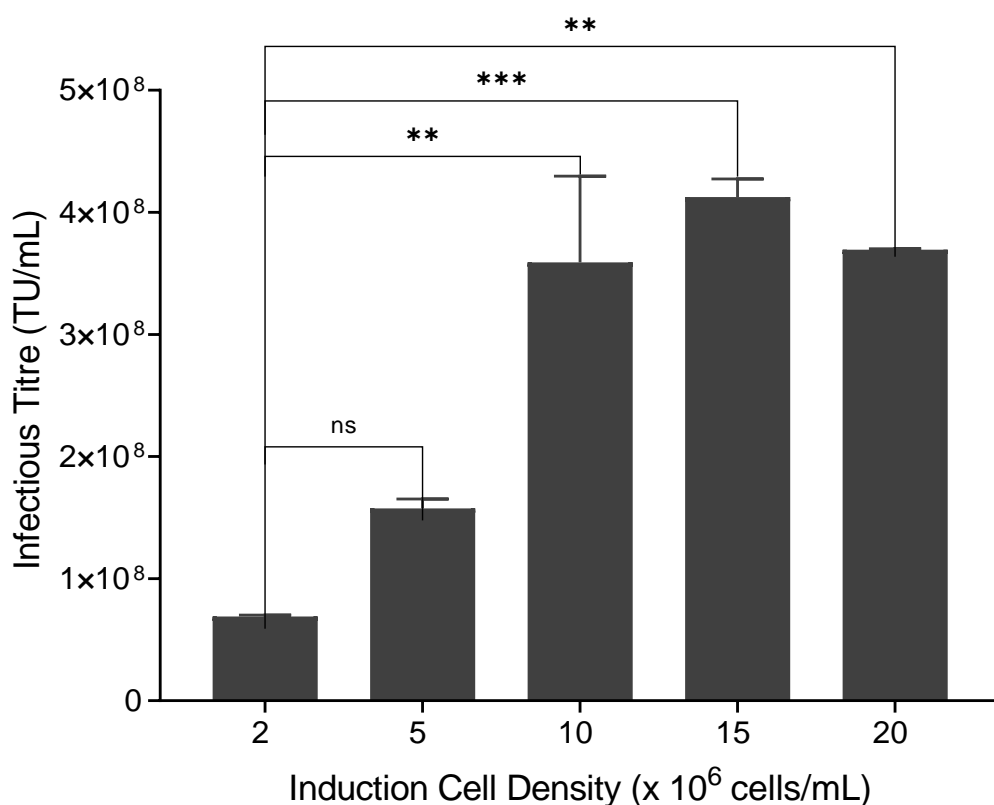


Figure 3.6: Effect of induction cell density on LVV infectious titre. Error bars represent one standard deviation about the mean (n = 2). Statistical comparisons were done using one-way ANOVA followed by post-hoc Dunnett’s multiple comparison test at 95% confidence level: ns: p-value > 0.05; *: p-value ≤ 0.05; **: p-value ≤ 0.01; ***: p-value ≤ 0.001.

3.6 EFFECT OF ALTERING GLUCOSE AND LACTATE METABOLISM ON 277 CELL LINE GROWTH PROFILE

In section 3.3, the growth profile of the 277 cell line was evaluated in the 2 L STR operated at GSK platform operating conditions for this cell line. A plateau in cell growth was observed after 5 days in culture with cells achieving a maximum VCD of $\sim 6 \times 10^6$ cells/mL. The metabolite data showed rapid consumption of glucose with depletion around day 5 and also large accumulation of lactate (i.e. > 5 g/L after day 5).

A study by Roman *et al.*, 2018 showed that in an STR with no pH control and a continuous stream of 1% CO₂, HEK293 cells activate a metabolic switch towards lactate consumption which improved cell growth and productivity. The metabolic profile in the vessel with uncontrolled pH was also more favourable compared to a pH controlled STR, as glucose was not depleted and lactate did not accumulate up to inhibitory levels.

In this study, the aim was to mimic the conditions used by Roman *et al.*, 2018 and assess the impact of altering glucose and lactate metabolism on 277 cell line growth in the 2 L STR. The factors selected to alter their metabolism were pH control and CO₂ addition. According to Roman *et al.*, 2018, more than 1% CO₂ would undesirably lower the medium pH due to the acidic properties of CO₂ and the lack of pH control in the culture system. However, the minimum CO₂ flow rate that could be achieved on the Biostat[®] B (Sartorius, Germany) controller used in this study was 2%. Hence, it was not possible to mimic the exact conditions used by Roman *et al.*, 2018. Nonetheless, 2% CO₂ was still evaluated to confirm the findings by Roman *et al.*, 2018. Two STRs were set up with the following conditions:

- STR 1: No pH control + continuous stream of 2% CO₂
- STR 2: STR operated at GSK's 277 cell line platform operating conditions

Figure 3.7 shows a plot of the change in culture pH with time for both STR's. After day 3, the data indicates a significant decrease in pH for STR 1. By end of the culture, pH for STR 1 was around 6.2, confirming the observations by Roman *et al.*, 2018. The lactate and glucose concentration profiles are shown in Figures 3.8 and 3.9 respectively. In general, the metabolite data shows that having no pH control and adding continuous 2% CO₂ flow prevented glucose depletion, and lactate did not accumulate above growth inhibitory levels (i.e. >5 g/L). Between day 0 and day 3, a steady rate of lactate accumulation was observed in both STR's with comparable profiles. After day 3, accumulation of lactate was more significant in STR 2 compared to STR 1. For STR 1, a plateau in lactate concentration was observed perhaps due to activation of the

metabolic switch towards lactate consumption by the HEK293T cells. For STR 2, as the pH was controlled at a set-point of 7.0 ± 0.1 , a similar metabolic switch was not activated resulting in the significant accumulation of lactate observed during the course of the culture. For glucose, the concentration profiles were also similar for both STRs between day 0 and day 3. At day 3, a manual glucose feed was added to both STR's to bring the concentration up to the target of 5 g/L. Between day 3 and day 4, glucose consumption was greater in STR 2 compared to STR 1, perhaps due to the metabolic switch being activated in STR 1. At day 4, glucose feed was added only to STR 2 as the concentration dropped below 2 g/L. Manual glucose feed was not added to STR 1 as the day 4 concentration was around 4 g/L. Between day 4 and day 5, rapid glucose consumption was observed in STR 2, with glucose being depleted at day 5. For STR 1, glucose consumption was moderate, with the concentration at day 5 being under 3 g/L. At day 5, manual glucose feed was added to both STR's to bring the concentration back to the target value of ~ 5 g/L. Between day 5 and day 6, rate of glucose consumption was higher in STR 2 compared to STR 1. At day 6, manual glucose feed was only added to STR 2 to prevent depletion.

Although STR 1 achieved a favourable metabolite profile (i.e. reduced lactate accumulation), Figure 3.10A shows that this did not translate into improved cell growth as expected. In fact, STR 2 achieved a better growth profile compared to STR 1. During the early stage of culture (i.e. between day 0 and day 3), the growth profile was comparable between the two STR's. After day 3, a noticeable difference in cell growth was observed for the two conditions. A logarithmic plot of viable cell density was also plotted against time to accurately determine exponential growth period as shown in Figure 3.10B. The exponential growth period for STR 2 lasted 24 hours longer (i.e. between day 0 and day 4 with doubling time of 27.7 hours) than STR 1 (i.e. between day 0 and day 3 with doubling time of 26.7 hours). For STR 2, there was a further period of growth until day 5 where the maximum VCD of 7.7×10^6 cells/mL was reached. A plateau in cell growth was observed after day 5. In STR 2, the cells continued to grow until day 6, however the growth rate was no longer exponential after day 3. The population doubling time was around 57 hours in this period (i.e. average of day 3 to 6 data shown in Table 9.3 under Appendix A). The maximum VCD

of 7.0×10^6 cells/mL was comparable with STR 2 although it was reached 24 hours later.

The data shows that the VCD decreased sharply to 4.7×10^6 cells/mL at day 7. Studies have shown that a low pH environment affects mammalian cell growth by inducing G1 phase cell cycle arrest (Hu and Li, 2018). Therefore, the poor cell growth for STR 1 could be due to the increasingly acidic environment around the cells. It is likely that, since the CO₂ flow rate used by Roman *et al*, 2018 was 1%, they did not observe a similar pH profile in their STR with no pH control. Rather, pH only decreased during the first 4 days of culture as lactate was accumulating. At day 4, when pH was around 6.8, the same authors' observed a metabolic switch from lactate accumulation to lactate consumption. The consumption of lactate resulted in a steady increase in culture pH after day 4, eventually stabilising at pH 7.0 around day 6. According Liste-Calleja *et al.*, 2015, HEK293 cells metabolize extracellular lactate as a strategy for pH detoxification, by means of co-transporting extracellular protons together with lactate into the cytosol.

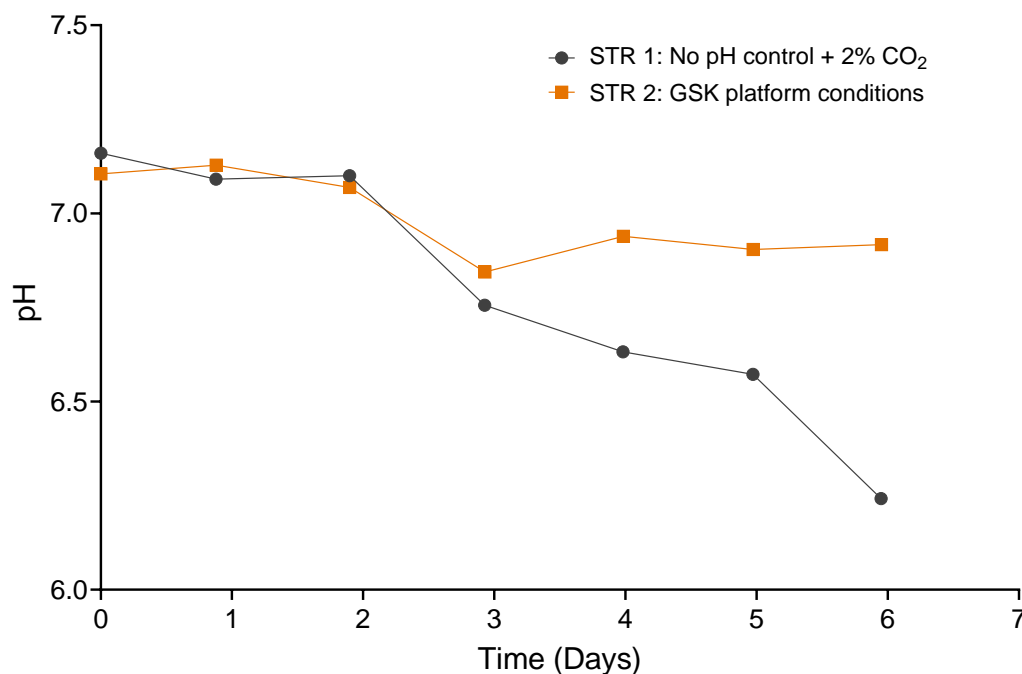


Figure 3.7: pH profile of the 277 stable cell line cultivated in 2 L STR. pH measurements were taken offline using the Nova BioProfile FLEX2. n = 1.

3.6 | EFFECT OF ALTERING GLUCOSE AND LACTATE METABOLISM ON 277 CELL LINE GROWTH PROFILE

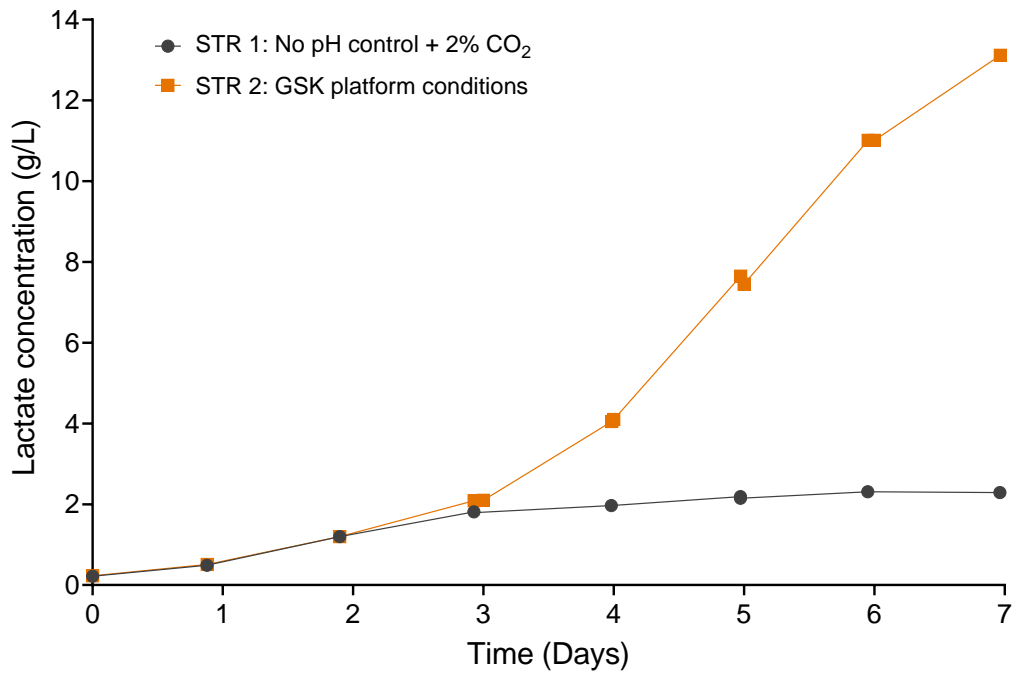


Figure 3.8: Effect of pH and CO₂ on lactate concentration profile of the 277 stable cell line cultivated in 2 L STR. n = 1.

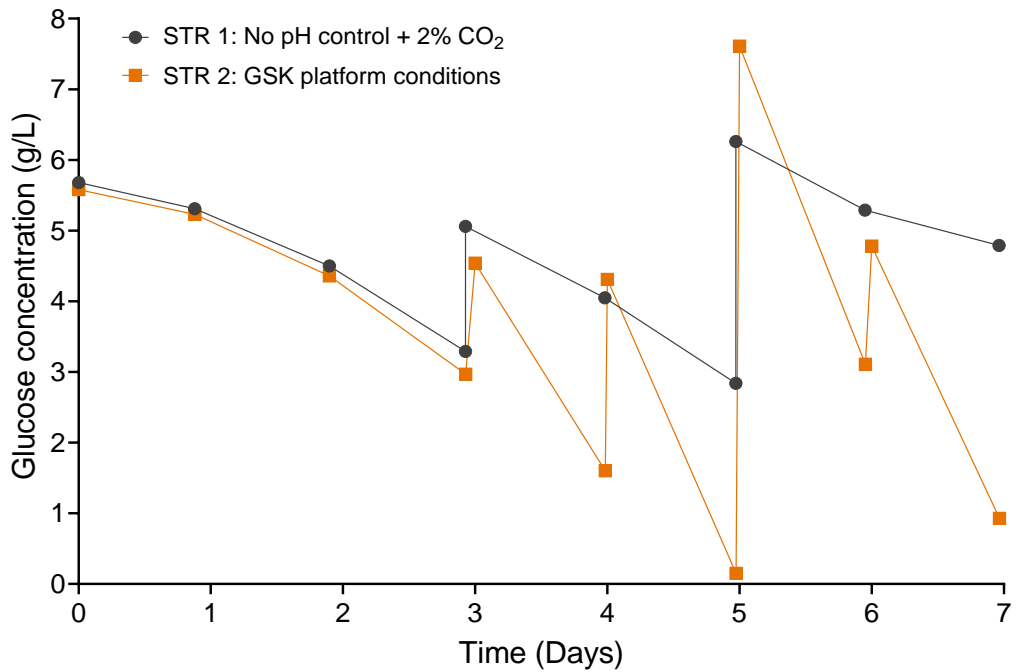


Figure 3.9: Effect of pH and CO₂ on glucose concentration profile of the 277 stable cell line cultivated in 2 L STR. n = 1.

3 | ASSESSMENT OF GSK'S 277 HEK293T STABLE CELL LINE CULTIVATION IN 2 L STIRRED TANK REACTOR

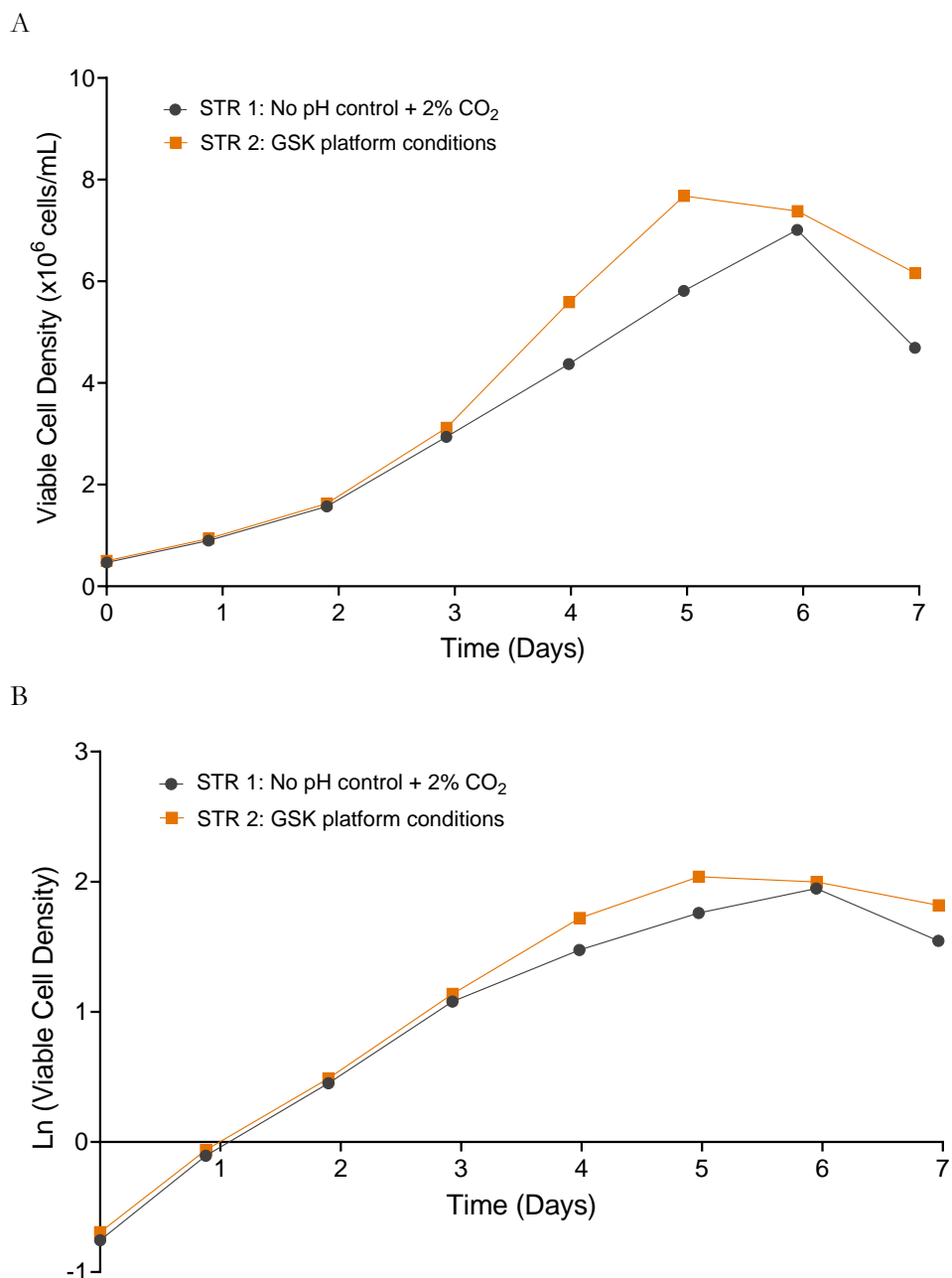


Figure 3.10: (A) Effect of pH and CO₂ on VCD profile of the 277 stable cell line cultivated in 2 L STR. (B) Natural logarithm of viable cell density plotted against time. $n = 1$.

Due to the limitation in minimum CO₂ flow when using the Sartorius BioStat B reactors in this study, a follow-up study was designed with the objective of achieving the desired metabolite profile (i.e. prevent significant lactate accumulation and glucose

depletion) whilst preventing culture pH from becoming increasingly acidic. The idea was to initiate a pH shift from pH 7.0 to 6.8 around day 4 in order to induce a metabolic shift towards lactate consumption. After day 4, the STR would be controlled at 6.8 in order to prevent culture pH from becoming too acidic. Two STRs were set up with the following conditions:

- STR 3: Control at pH 7.0 between day 0 to day 4; after day 4, control at pH 6.8 + continuous stream of 2% CO₂
- STR 4: STR operated at GSK's 277 cell line platform operating conditions

The lactate and glucose concentration profiles are shown in Figures 3.11 and 3.12 respectively. Between day 0 and day 4, a steady rate of lactate accumulation was observed in both STR's with comparable profiles. After day 4, the difference in lactate profiles was evident as this is when pH set point in STR 3 was reduced to 6.8 and CO₂ feed was initiated at 2%. The data shows accumulation of lactate was more significant in STR 4 compared to STR 3 due to the metabolic shift towards lactate consumption in STR 3. By the end of culture, the lactate concentration in STR 4 was just over 10 g/L whilst STR 3 was around 6.5 g/L. Glucose depletion was also prevented in both STR's. Manual glucose feeds after day 3 ensured glucose concentration did not fall below 2 g/L for the entire culture duration.

Figure 3.13A shows that both STR's achieved almost identical growth profiles. A logarithmic plot of viable cell density is also shown in Figure 3.13B. From the logarithmic plot, it is evident that there was no apparent lag phase and cells were in exponential growth phase between day 0 and day 3. In both cultures, there was a period of further growth, albeit non-exponential, until day 5, after which cells transitioned into stationary phase. The maximum VCD prior to growth arrest was also comparable at around 6×10^6 cells/mL.

Once again, the desired metabolite profile in STR 3 did not result in improved growth. Growth arrest was observed in both STR 3 and STR 4 at approximately day 5

suggesting that lactate accumulation and glucose depletion may not be factors limiting 277 cell line growth. Perhaps, the depletion of other critical metabolites and/or accumulation of toxic metabolites may be causing the early growth arrest. Using LC-MS analysis, a more detailed metabolite profile can be generated at different time points in the culture and is discussed in section 3.7.

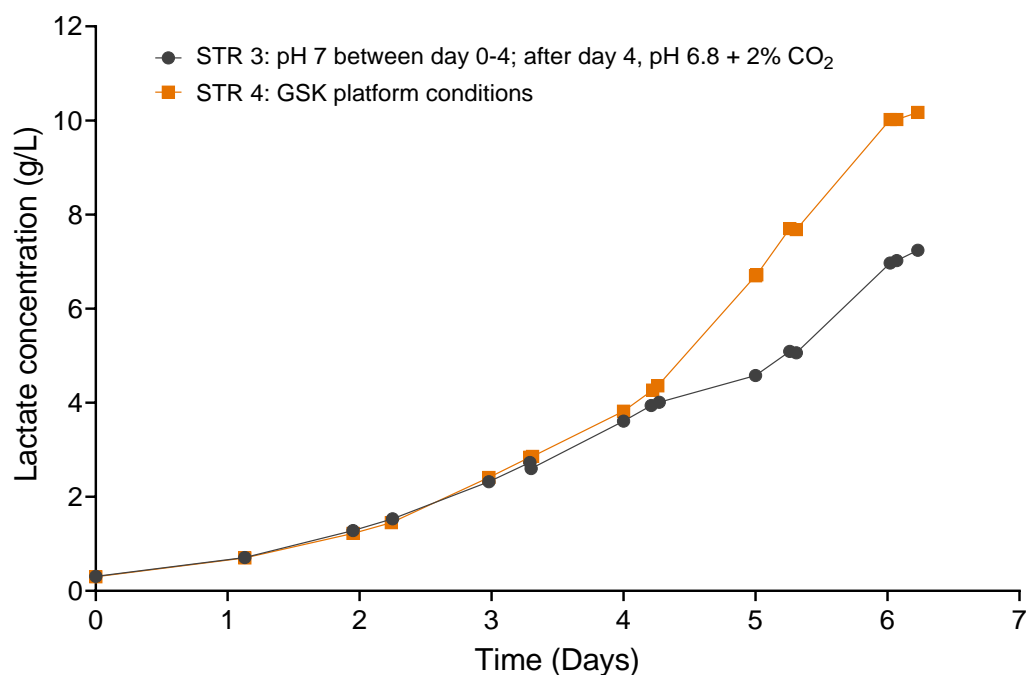


Figure 3.11: Effect of pH shift on lactate concentration profile of the 277 stable cell line cultivated in 2 L STR. n = 1.

3.6 | EFFECT OF ALTERING GLUCOSE AND LACTATE METABOLISM ON 277 CELL LINE GROWTH PROFILE

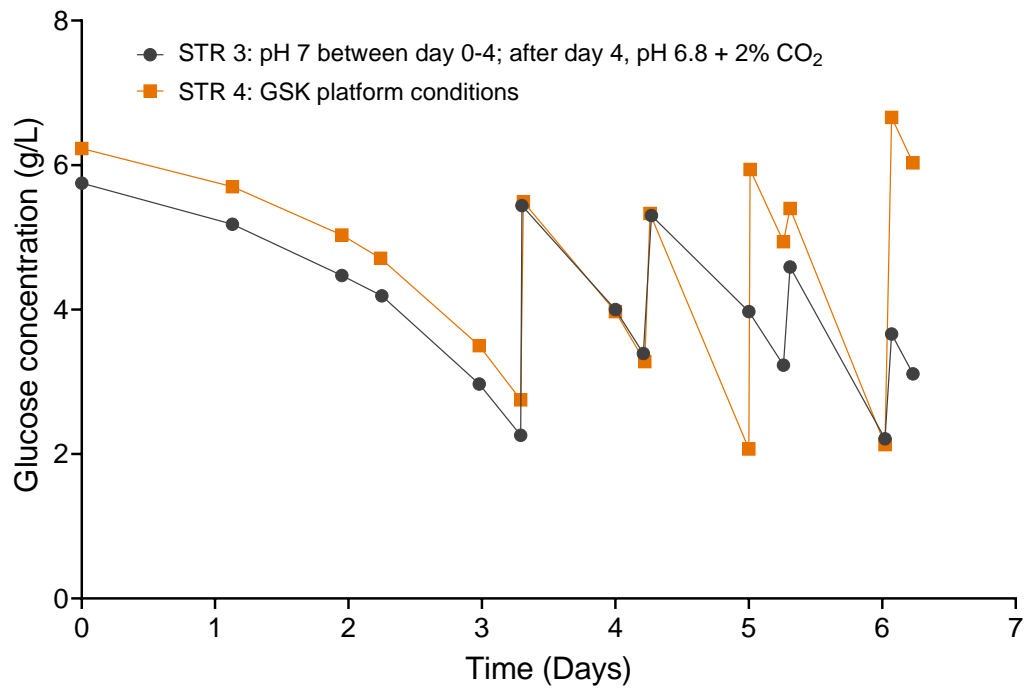
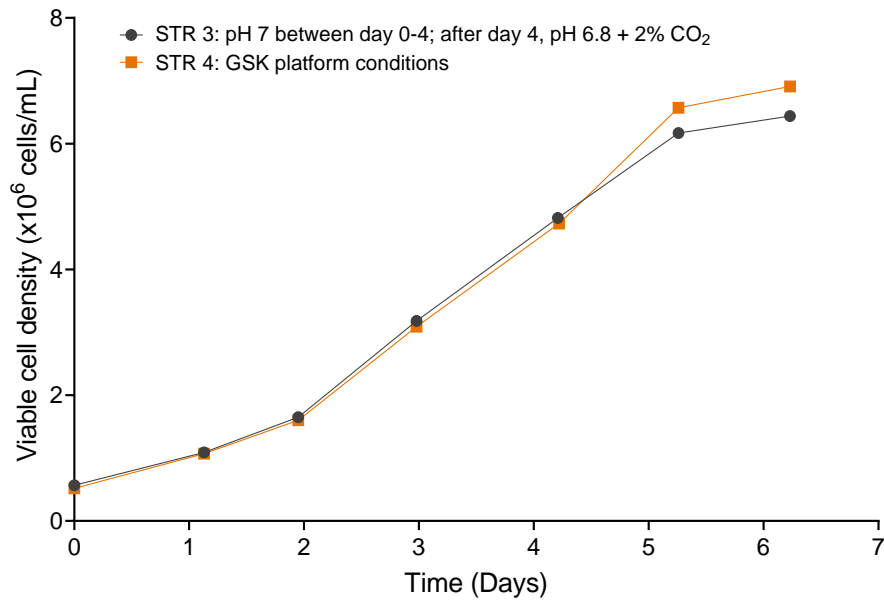


Figure 3.12: Effect of pH shift on glucose concentration profile of the 277 stable cell line cultivated in 2 L STR. n = 1.

3 | ASSESSMENT OF GSK'S 277 HEK293T STABLE CELL LINE CULTIVATION IN 2 L STIRRED TANK REACTOR

A



B

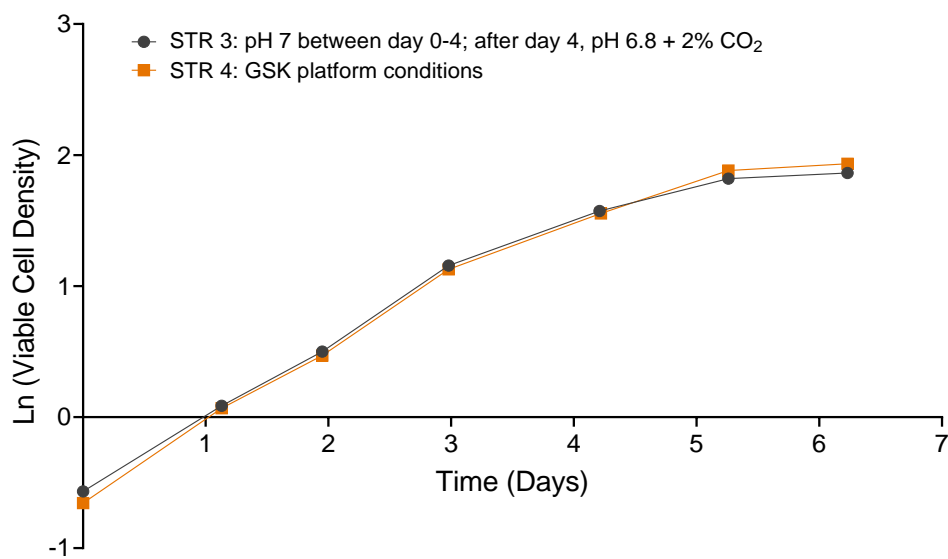


Figure 3.13: (A) Effect of pH shift on VCD profile of the 277 stable cell line cultivated in 2 L STR. (B) Natural logarithm of viable cell density plotted against time. n = 1.

3.7 LC-MS ANALYSIS OF CELL CULTURE MEDIA DURING 277 CELL LINE GROWTH CULTURE

A significant challenge facing process development for LVV upstream processes is the inability to achieve high viable cell densities (e.g. $> 10 \times 10^6$ cells/mL) during HEK293T stable producer cell line cultivation. This observation was confirmed by Figure 3.1 in section 3.3 where a plateau in growth was observed after only 5 days in culture. The maximum cell density achieved prior to growth arrest was around 6×10^6 cells/mL. The metabolite profile indicated significant lactate accumulation (> 10 g/L) as well as glucose depletion towards the end of the culture. In subsequent studies (i.e. section 3.6), adjustments to pH and CO₂ were used to alter the metabolic profile with the aim of preventing lactate accumulation and glucose depletion. However, the data showed that, even in conditions with a favourable metabolite profile (i.e. reduced lactate accumulation and glucose depletion), growth arrest was still observed after 5 days with the culture still not reaching VCD's $> 6 \times 10^6$ cells/mL. This suggests that other factors could be responsible for the decline in cell growth rate.

A possibility for the early growth arrest may be due to depletion of other critical metabolites and/or accumulation of toxic metabolites creating an unfavourable environment for cell growth.

In this study, the aim was to use LC-MS analysis to profile extracellular metabolites at different time points during growth of the 277 cell line culture from section 3.3. The time points selected for analysis were day 0, day 3 and day 6. These specific time points were selected to give coverage of the culture profile over the entire growth period i.e. day 0 provides basal concentration, day 3 provides profile in the middle of exponential growth and day 6 provides profile at the end of the growth period.

A total of 90 metabolites from 10 different compound groups were identified from the cell culture media samples analysed using LC-MS (Table 3.2). 33 of these metabolites showed no significant change in concentration as the culture progressed. 50 metabolites were depleting with time whilst 7 metabolites were accumulating.

Amino acids accounted for one-third of all metabolites analysed, and more importantly, 28 of these were depleted towards the end of the culture. A detailed analysis of the three key trends in metabolite concentrations with time are discussed in the sections below.

Table 3.2: A summary of cell culture media component coverage identified using LC-MS.

Metabolite group	No significant change	Accumulating	Depleting	Total
Amino acid	5	0	28	33
Amino acid derivative	1	0	4	5
Peptide	1	0	3	4
Vitamin	9	0	5	14
Acid	7	3	4	14
Organic compound	0	0	2	2
Fatty acids and Lipids	3	1	2	6
Polyamine	0	0	1	1
Carbohydrate	0	1	1	2
Nucleosides	7	2	0	9
Total	33	7	50	90

3.7.1 Metabolites with no significant change in concentration with time

Table 3.3 lists the metabolites categorised as showing no significant change in concentration with time. For all these metabolites, the one-way ANOVA test showed that the mean peak area intensity for the different time points was not statistically significant i.e. the p-value was greater than 0.05 which was the minimal level of confidence used to determine significance.

According to Table 3.3, several key vitamins important in mammalian cell culture were unchanged with time. Vitamins are essential for cell proliferation and since they cannot

be synthesised in sufficient quantities *in vivo*, they are supplemented in cell culture media (Arora, 2013; Schnellbaecher et al., 2019). Table 3.4 summarises typical basal media concentrations of some key vitamins from Table 3.3, as well as their cellular function. It is worth noting that the selected vitamins are listed based on what is available in the literature and is not a comprehensive list. To gain a better understanding of the relative concentration of these vitamins during the course of culture, the peak area intensity was plotted against time as shown in Figure 3.14. The data indicates a trend for increase in peak area intensity but was not statistically significant. Hence, these vitamins were not considered limiting 277 cell line growth.

Linoleic acid, an unsaturated fatty acid, is another notable metabolite from Table 3.3 important in mammalian cell culture. Fatty acids are important for growth and productivity of mammalian cells, and linoleic acid in particular is a precursor to a number of other fatty acids (Ouellette et al., 2019). It cannot be synthesised by animal cells and must be provided as a nutrient in serum-free cell culture (Haggerty et al., 1965). The basal media for culture of mammalian cell lines typically contains concentration of 0.1 – 0.9 mg/L of linoleic acid (Landauer, 2014). Figure 3.15 shows the trend in peak area intensity of linoleic acid at different time points along the growth phase. As the concentration is fairly constant throughout the culture, this fatty acid was not considered to be limiting for growth of the 277 cell line.

Table 3.3: List of metabolites in cell culture media showing no significant change in concentration with time. Statistical comparisons were done using one-way ANOVA analysis at 95% confidence level (p-value > 0.05 for all metabolites analysed).

Metabolite	Type
DL-2-Aminoadipic acid	Amino acid
Hydroxyproline	Amino acid
L-Cysteine	Amino acid
L-Threonine	Amino acid
Hydroxylysine	Amino acid
Sarcosine	AA derivative
L-Glutathione oxidized	Peptide
Biotin (Vitamin B7)	Vitamin
Ergocalciferol (Vitamin D2)	Vitamin
Niacinamide	Vitamin
Nicotinic acid	Vitamin
Tocopherol acetate	Vitamin
Cyanocobalamin	Vitamin
Pyridoxal hydrochloride (Vitamin B6)	Vitamin
Riboflavin (Vitamin B2)	Vitamin
Aminobenzoic acid	Vitamin
Phosphoascorbic acid	Acid
Folinic acid	Acid
2-Oxovaleric acid	Acid
Citric acid	Acid
Glyceric acid	Acid
Gluconic acid	Acid
L-Threonic Acid	Acid
Linoleic acid	Fatty acids and Lipids
Glycerophosphocholine	Fatty acids and Lipids
Stearic acid	Fatty acids and Lipids
Cytidine	Nucleosides
Deoxycytidine	Nucleosides

3.7 | LC-MS ANALYSIS OF CELL CULTURE MEDIA DURING 277 CELL LINE GROWTH CULTURE

Guanosine monophosphate	Nucleosides
Inosine	Nucleosides
Xanthosine	Nucleosides
Adenine	Nucleosides
Adenosine	Nucleosides

Table 3.4: Basal media concentration and cellular function of some of the key vitamins showing no significant change in concentration with time.

Vitamin type	Basal media concentration (mg/L) ^a	Cellular Function ^b
Biotin (Vitamin B7)	0 – 0.2	Important for amino acid and energy metabolism, and fatty acid synthesis
Niacinamide (also known as nicotinamide)	1 – 4	Converted into the coenzymes NAD and NADP which participate in important redox reactions within the cell
Pyridoxal hydrochloride (Vitamin B6)	0 – 4.1	Important for amino acid, fatty acid and folate metabolism
Riboflavin (Vitamin B2)	0.2 – 0.4	Essential for the metabolism of carbohydrates, amino acid and lipids

^a (Landauer, 2014)

^b (Schnellbaecher et al., 2019)

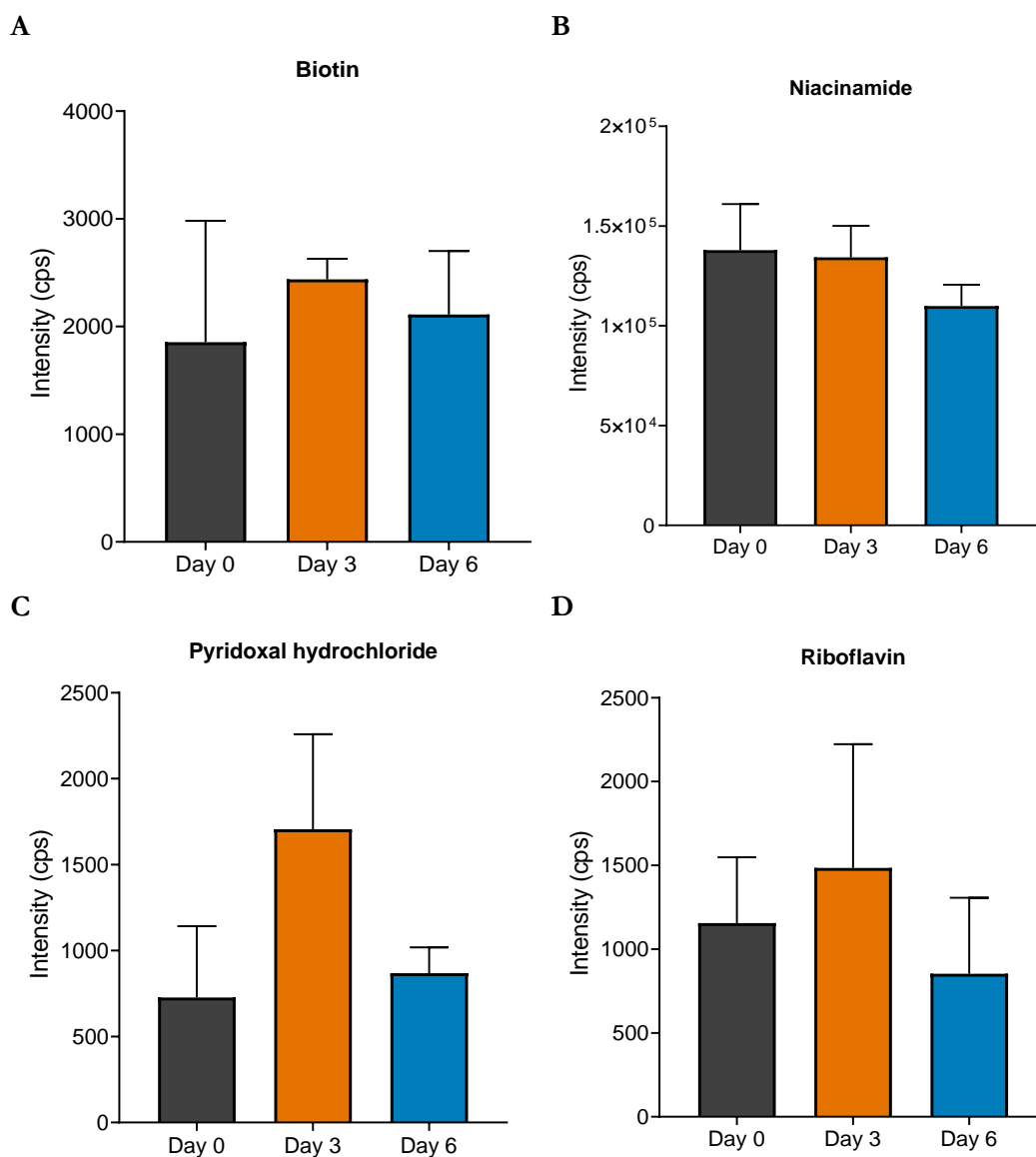


Figure 3.14: Peak area intensity profile of some key vitamins showing no significant change in concentration with time. Error bars represent one standard deviation about the mean (n=3 for day 0 and day 3; n=2 for day 6 due to an error with sample preparation for one of the replicates). Statistical comparisons were done using one-way ANOVA analysis at 95% confidence level. No significant difference (p-value > 0.05) in the peak area intensity at different time points was detected using the one-way ANOVA test. cps means counts per second.

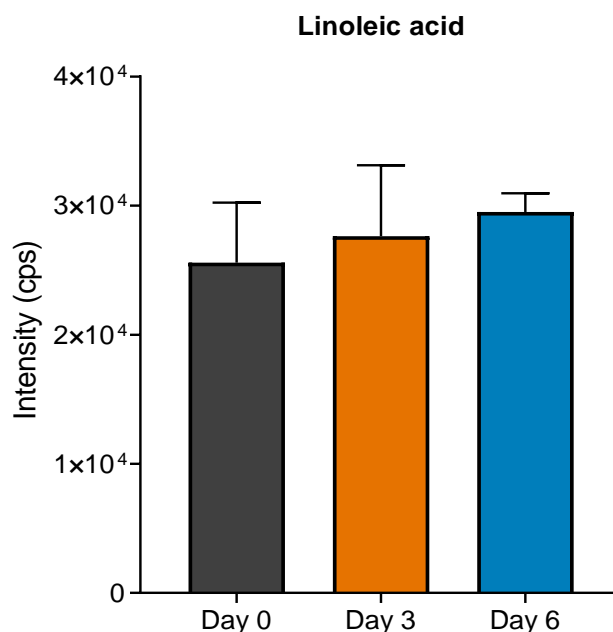


Figure 3.15: Peak area intensity profile of linoleic acid at three different stages along the cell culture period. Error bars represent one standard deviation about the mean (n=3 for day 0 and day 3; n=2 for day 6 due to an error with sample preparation for one of the replicates). Statistical comparisons were done using one-way ANOVA analysis at 95% confidence level. No significant difference (p-value > 0.05) detected in the one-way ANOVA test. cps means counts per second.

3.7.2 Accumulating metabolites with time

The one-way ANOVA output for accumulating metabolites is shown in Table 3.5. For each of these metabolites, the difference in peak area intensity between at least one time interval was found to be statistically significant i.e. the p-value was smaller than 0.05 which was the minimal level of confidence used to determine significance.

Lactic acid (or Lactate) is perhaps the most notable accumulating metabolite from Table 3.5. To better illustrate its trend with time, a plot of the peak area intensity is shown in Figure 3.16. The data not only confirms increasing lactate concentration with time, but also shows that the difference in concentration between the three sample time points was highly significant (i.e. $p < 0.001$). Other groups have reported similar observations and suggest that a major disadvantage of HEK293 cells is the inefficient

metabolism under normal culture conditions (i.e. at pH = 7), characterised by high glucose consumption and accumulation of large quantities of lactate (Martínez et al., 2013; Román et al., 2018). The harmful effects of lactate accumulation in mammalian cell cultures have been extensively documented (Cruz et al., 2000; Liste-Calleja et al., 2015; Martínez-Monge et al., 2019; Ozturk et al., 1992). This involves cell-growth inhibition, increased medium osmolality and, in the absence of pH control, decreased culture pH (Ozturk et al., 1992). Several approaches have been studied with the aim of minimising lactate accumulation. Altamirano *et al.*, 2006 suggest the use of alternative carbon sources like fructose or galactose (Altamirano et al., 2000). Other studies have shown that under certain culture conditions (i.e. pH < 6.8), HEK293 cells can turn to a more efficient metabolism where lactate and glucose are consumed simultaneously (Liste-Calleja et al., 2015; Martínez-Monge et al., 2019; Román et al., 2018). The improved metabolism led to improvements in cell growth and productivity. This approach was evaluated with the 277 cell line with limited success as described earlier in section 3.6.

Other metabolites showing significant accumulation (i.e. $p < 0.001$) for at least one time point are isocitric acid, D-sucrose and cytidine monophosphate. Their peak area intensity profiles are shown in Figure 3.17. Isocitric acid is one of the intermediates of the TCA cycle. Its accumulation towards the end of the culture may suggest that this pathway may not be active and hence glucose is not metabolised efficiently. However, further studies looking into metabolite flux analysis would be required to confirm this observation.

Sucrose is a disaccharide comprised of fructose and glucose (Hossler et al., 2014). It is often used as sugar source in plant based cultures (Wendler et al., 1990). In mammalian cells such as CHO, sucrose has been found to have a role in protein glycosylation (Hossler et al., 2014). It is not clear why sucrose accumulation was observed and no literature references were found to explain this trend. Cytidine monophosphate (CMP) is a nucleotide that is used as a monomer in RNA. Accumulation of nucleotides such as CMP would be expected with time since increase in cell growth is often associated with increase in protein expression (Nordholt et al.,

2017). For each of these metabolites, no literature references were found to suggest that they have any role in mammalian cell growth inhibition.

Table 3.5: Summary of one-way ANOVA output for metabolites in cell culture media showing significant accumulation with time. Tukey multiple comparison test was carried out at 95% confidence level: ns: p-value > 0.05; *: p-value ≤ 0.05; **: p-value ≤ 0.01; ***: p-value ≤ 0.001.

Metabolite	Type	T-test output (p-value significance)		
		Day 0 and Day 3	Day 0 and Day 6	Day 3 and Day 6
DL-P	Acid	ns	**	**
Hydroxyphenyllactic acid				
Isocitric acid	Acid	***	***	**
Lactic acid	Acid	***	***	***
Palmitic acid	Fatty acids and Lipids	*	ns	ns
D-Sucrose	Carbohydrate	**	***	*
Adenosine monophosphate	Nucleotide	ns	*	ns
Cytidine monophosphate	Nucleotide	***	***	**

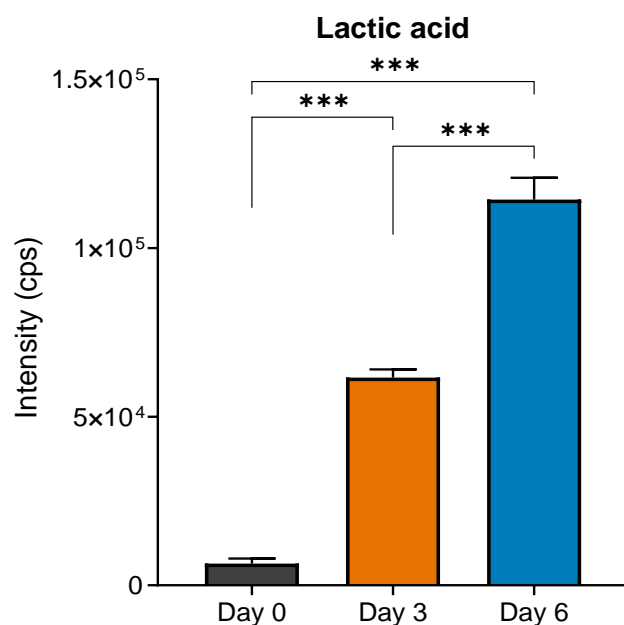


Figure 3.16: Peak area intensity profile of lactic acid at three different stages along the cell culture period. Error bars represent one standard deviation about the mean (n=3 for day 0 and day 3; n=2 for day 6 due to an error with sample preparation for one of the replicates). Statistical comparisons were done using one-way ANOVA analysis followed by post-hoc Tukey multiple comparison test at 95% confidence level: ***: p-value ≤ 0.001. cps means counts per second.

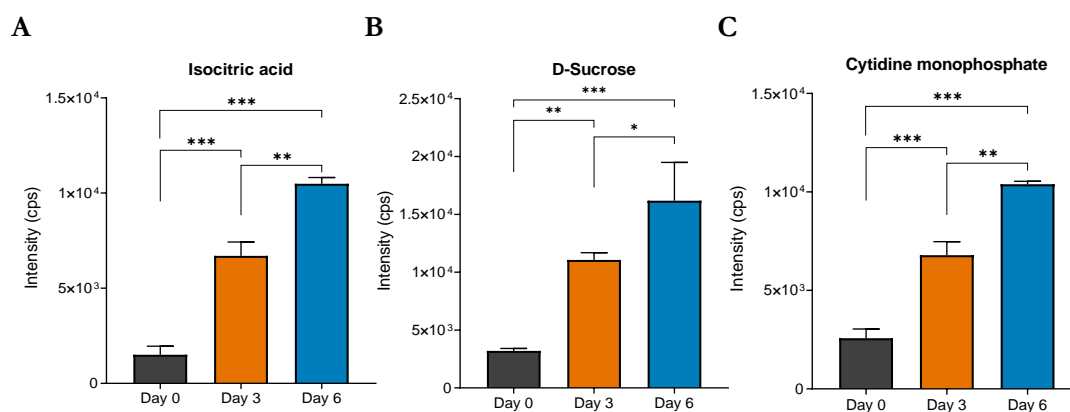


Figure 3.17: Peak area intensity profile of isocitric acid, D-sucrose and cytidine monophosphate at three different stages along the cell culture period. Error bars represent one standard deviation about the mean (n=3 for day 0 and day 3; n=2 for day 6 due to an error with sample preparation for one of the replicates). Statistical comparisons were done using one-way ANOVA analysis followed by post-hoc Tukey multiple comparison test at 95% confidence level: ns: p-value > 0.05; *: p-value ≤ 0.05; **: p-value ≤ 0.01; ***: p-value ≤ 0.001. cps means counts per second.

3.7.3 Depleting metabolites with time

The full list of the 50 metabolites showing significant depletion with time is shown in Table 3.6 together with the one-way ANOVA output for each metabolite. In order to determine which of these metabolites are most important for cell growth, a points-based scoring system consisting of the two metrics, ‘statistical significance’ and ‘literature references’, was devised. Using these two metrics would generate an overall score that takes into account both experimental (i.e. statistical significance) and theoretical (i.e. literature references) value of each metabolite. To this authors’ knowledge, this approach has not been used previously to rank metabolites from LC-MS analysis.

For statistical significance, points were awarded based on the p-value result from the one-way ANOVA analysis i.e. the smaller the p-value, the higher the statistical significance and thus a higher score as summarised below:

- p-value > 0.05 (i.e. not significant): 0 points
- p-value \leq 0.05: 1 point
- p-value \leq 0.01: 2 points
- p-value \leq 0.001: 4 points

As different time points were compared for each metabolite, only the one-way ANOVA output resulting in the highest statistical significance was used for scoring e.g. for 2-Aminoisobutyric acid, the Tukey test output comparing the depletion between day 0 and day 6 was used for scoring as it had the highest statistical significance (i.e. p-value was less than 0.001).

For the literature score, points were awarded in proportion to the number of suitable references in literature. For example, for glutamine and serine, an appropriate reference would be the following quote from Petiot *et al.*, 2015: ‘*glutamine* and *serine* are the most

consumed amino acids in HEK293 cell culture'. To maintain relevance, the scope of the literature search was limited to HEK293, CHO and hybridoma cell cultures. The full list of supporting literature references for each depleting metabolite is shown in Table 9.5 under Appendix A. The allocation of points was as follows:

- No references – 0 points
- 1 to 2 references – 1 point
- 3 to 5 references – 2 points
- More than 5 references – 4 points

For both scoring criteria, a weighted scoring system was used in order to reflect the relative importance of a metabolite i.e. the score assigned was doubled with an increase in each level, to show importance for higher scorers. For a metabolite to be considered as a potential feed target, the benchmark for the combined score of 'statistical significance' and 'literature references' was set at 4. This ensures metabolites which had a high score in only one of the criteria and a negligible score in the other, would also be considered and not overlooked.

The output of the scoring analysis is shown in Table 3.7. A total of 22 metabolites achieved the minimum threshold score of 4. 15 metabolites scored high in both criteria (i.e. total score ≥ 6) with 4 of these attaining a maximum score of 8 i.e. L-Serine, L-Lysine, L-Valine and Choline. With strong evidence in favour of their importance in mammalian cell culture, these 15 metabolites were considered to be suitable targets for a feed supplement to improve 277 cell line growth. However, there were some metabolites that did not score high in the literature criteria but showed very significant depletion towards the end of the culture. These metabolites, which include L-Norvaline, L-Phenylalanine, Histamine, 2-Aminoisobutyric acid and D-Pipecolic acid, could also be considered as potential feed targets. Lastly, pantothenic acid and putrescine both had maximum scores on literature (i.e. 4) but low on statistical significance. For putrescine, it was not because its depletion with time was not

significant, rather the t-test could not be performed as there was only one LC-MS output for each time point. Given that these two metabolites are widely referenced in literature for enhancing mammalian cell growth (Table 9.4), they may also be considered as important targets for feed supplementation.

Table 3.6: Summary of one-way ANOVA output for metabolites in cell culture media showing significant depletion with time. Tukey multiple comparison test was carried out at 95% confidence level: ns: p-value > 0.05; *: p-value ≤ 0.05; **: p-value ≤ 0.01; ***: p-value ≤ 0.001.

Metabolite	Type	T-test output (p-value significance)		
		Day 0 and Day 3	Day 0 and Day 6	Day 3 and Day 6
2-Aminoisobutyric acid	Amino acid	*	***	**
Asparagine	Amino acid	ns	**	**
Aspartic acid	Amino acid	ns	**	**
beta-Alanine	Amino acid	ns	**	**
Citrulline	Amino acid	ns	**	*
Cystathionine	Amino acid	*	ns	*
DL-2-Aminoadipic acid	Amino acid	ns	**	*
Glycine	Amino acid	ns	**	**
Isoleucine	Amino acid	*	***	**
L-Alanine	Amino acid	ns	**	**
L-Arginine	Amino acid	ns	**	*
L-Cystine	Amino acid	ns	**	**
L-Glutamic acid	Amino acid	ns	*	**
L-Glutamine	Amino acid	ns	*	**
L-Histidine	Amino acid	ns	**	**
L-Leucine	Amino acid	ns	**	*
L-Lysine	Amino acid	*	***	***
L-Methionine	Amino acid	***	***	***
L-Norvaline	Amino acid	***	***	***
L-Ornithine	Amino acid	ns	**	**
L-Phenylalanine	Amino acid	ns	***	**
L-Proline	Amino acid	ns	**	**
L-Serine	Amino acid	*	***	**

3 | ASSESSMENT OF GSK'S 277 HEK293T STABLE CELL LINE CULTIVATION IN
2 L STIRRED TANK REACTOR

L-Tryptophan	Amino acid	ns	**	**
L-Tyrosine	Amino acid	ns	**	*
L-Valine	Amino acid	***	***	***
Homocystine	Amino acid	ns	*	*
Gamma-aminobutyric acid	Amino acid	ns	*	ns
L-Pyroglutamic acid	Amino acid derivative	ns	**	**
Acetylcysteine	Amino acid derivative	**	*	ns
DL-Methionine sulfoxide	Amino acid derivative	ns	*	*
Transhydroxyproline	Amino acid derivative	ns	*	*
L-alanyl-L-glutamine	Peptide	***	***	***
Carnosine	Peptide	*	ns	*
GLY-GLN	Peptide	ns	*	ns
Ascorbic acid (VC)	Vitamin	ns	*	ns
Folic acid (VB9)	Vitamin	ns	**	**
Pantothenic acid (VB5)	Vitamin	ns	*	ns
Lipoic acid	Vitamin	ns	*	ns
Choline	Vitamin	ns	***	**
D-Pipecolic acid	Acid	*	***	***
Oleic acid	Acid	*	*	ns
Succinic acid	Acid	ns	*	*
Malic acid	Acid	ns	*	*
Ethylenediamine	Organic compound	ns	**	**
Histamine	Organic compound	ns	***	**
Phosphorylcholine	Fatty acids and Lipids	**	ns	**
2-Aminoethanol	Fatty acids and Lipids	ns	**	**

3.7 | LC-MS ANALYSIS OF CELL CULTURE MEDIA DURING 277 CELL LINE GROWTH CULTURE

Putrescine	Polyamine	n/a ¹	n/a	n/a
Glucose	Carbohydrate	*	ns	**

¹ n/a means there was no t-test output as one of the time points had only one readout from the LC-MS.

Table 3.7: Summary of scoring analysis of depleting metabolites.

Metabolite	Type	Statistical significance score	Literature score	Total
Metabolites above the threshold i.e. Total score ≥ 4				
1 L-Serine	Amino acid	4	4	8
2 L-Lysine	Amino acid	4	4	8
3 L-Valine	Amino acid	4	4	8
4 Choline	Vitamin	4	4	8
5 L-Leucine	Amino acid	2	4	6
6 L-Glutamine	Amino acid	2	4	6
7 Glucose	Carbohydrate	2	4	6
8 L-Arginine	Amino acid	2	4	6
9 Aspartic acid	Amino acid	2	4	6
1 Folic acid 0 (Vitamin B9)	Vitamin	2	4	6
1 L-alanyl-L- 1 glutamine	Peptide	4	2	6
1 Isoleucine 2	Amino acid	2	4	6
1 Asparagine 3	Amino acid	2	4	6
1 L-Ornithine 4	Amino acid	2	4	6
1 L-Methionine 5	Amino acid	4	2	6
1 Pantothenic acid 6 (Vitamin B5)	Vitamin	1	4	5
1 L-Phenylalanine 7	Amino acid	4	1	5
1 Histamine 8	Organic compound	4	0	4
1 L-Norvaline 9	Amino acid	4	0	4

3.7 | LC-MS ANALYSIS OF CELL CULTURE MEDIA DURING 277 CELL LINE GROWTH CULTURE

20	Putrescine	Polyamine	n/a ¹	4	4
21	2-Aminoisobutyric acid	Amino acid	4	0	4
22	D-Pipecolic acid	Acid	4	0	4
Metabolites below the threshold i.e. Total score < 4					
23	Ascorbic acid (Vitamin C)	Vitamin	1	2	3
24	L-Cystine	Amino acid	2	1	3
25	L-Histidine	Amino acid	2	1	3
26	L-Tryptophan	Amino acid	2	1	3
27	L-Tyrosine	Amino acid	2	1	3
28	Acetylcysteine	Amino acid derivative	2	1	3
29	Glycine	Amino acid	2	1	3
30	L-Glutamic acid	Amino acid	2	1	3
31	L-Proline	Amino acid	2	1	3
32	Citrulline	Amino acid	2	1	3
33	L-Alanine	Amino acid	2	1	3
34	2-Aminoethanol	Fatty acids and Lipids	2	1	3
35	Succinic acid	Acid	1	1	2

3 | ASSESSMENT OF GSK'S 277 HEK293T STABLE CELL LINE CULTIVATION IN
2 L STIRRED TANK REACTOR

3 6	Glycyl-L- glutamine	Peptide	1	1	2
3 7	Phosphorylcholin e	Fatty acids and Lipids	2	0	2
3 8	β -Alanine	Amino acid	2	0	2
3 9	DL-2- Aminoadipic acid	Amino acid	2	0	2
4 0	Homocystine	Amino acid	2	0	2
4 1	L-Pyroglutamic acid	Amino acid derivative	2	0	2
4 2	Ethylenediamine	Organic compound	2	0	2
4 3	Lipoic acid	Vitamin	1	1	2
4 4	Transhydroxyprol ine	Amino acid derivative	1	0	1
4 5	Oleic acid	Acid	1	0	1
4 6	Cystathionine	Amino acid	1	0	1
4 7	Gamma- aminobutyric acid	Amino acid	1	0	1
4 8	DL-Methionine sulfoxide	Amino acid derivative	1	0	1
4 9	Carnosine	Peptide	1	0	1
5 0	Malic acid	Acid	1	0	1

¹ For Putrescine, there was only one output from the LC-MS for each time point. Hence a t-test could not be performed.

The peak area data, as well as relevant literature references, for each of the metabolites that met the scoring threshold are discussed below.

Amino acids

From the high scoring proteinogenic amino acids, 8 were essential amino acids (i.e. L-Arginine, L-Leucine, L-Valine, L-Glutamine, L-Lysine, Isoleucine, L-Methionine and L-Phenylalanine) and 3 were non-essential (i.e. L-Serine, Aspartic acid, Asparagine). Essential amino acids cannot be synthesised by cells and these must be included in the culture media (Arora, 2013). They are important for cell proliferation and their concentration determines the maximum cell density that can be achieved (Arora, 2013). Non-essential amino acids can be synthesised by cells. However, they may also be added to the medium to replace those that are depleted (Arora, 2013). Studies have demonstrated that supplementation with non-essential amino acids stimulates growth and prolongs cell viability (Arora, 2013).

The peak area data for the high scoring essential and non-essential amino acids are shown in Figure 3.18 and Figure 3.19, respectively. The general trend observed is a reduction in peak area intensity with time with the exception of L-glutamine where an accumulation was seen at day 3. However, what is common for all the amino acids is a significant decrease in peak area intensity between day 3 and day 6. Notably, this depletion also coincides with the time point when VCD was in decline.

For L-glutamine, this trend in accumulation between day 0 and day 3 is expected as the dipeptide, L-alanyl-L-glutamine (also known as GlutaMAX™), is used in the basal media. Unlike L-glutamine, the GlutaMAX™ supplement does not spontaneously break down to form ammonia. Instead, cells cleave the dipeptide bond to release L-glutamine as needed. As cells were entering exponential growth phase around day 3, there was an increasing demand for L-glutamine hence the higher peak intensity observed for this time point in Figure 3.18 D. Furthermore, the peak area trend for L-alanyl-L-glutamine shows that its concentration was reducing with time with almost complete depletion at day 6 (Figure 3.20).

Within the literature, there is a clear pattern that the same group of amino acids are among the most highly consumed in different mammalian cell lines. In HEK293 cells,

several studies have shown that glutamine and serine are the most highly consumed amino acids, followed by asparagine, aspartic acid, leucine, valine, arginine and lysine (Henry et al., 2011; Martínez-Monge et al., 2019; Nadeau et al., 2000; Petiot et al., 2011; Rodrigues et al., 2013). For CHO cell cultures, Xing et al 2011 reported a similar trend where glutamine was the most highly consumed amino acid, followed by asparagine, serine, leucine, arginine and valine (Xing et al., 2011a). In another study, Fan et al 2015 demonstrated that serine and leucine were the two amino acids with the highest consumption rates (Fan et al., 2015).

In the present study, a quantitative analysis of the amino acids was also performed using LC-MS, as shown in Figure 3.21. For all amino acids except glutamic acid (day 0 to day 3), there is a clear trend of depletion with time. More significantly, six of the amino acids at the highest concentrations in the basal media (i.e. corresponding to day 0) were on the list of high scoring metabolites (i.e. scoring ≥ 4). These include Aspartic acid, Leucine, Valine, Lysine, Isoleucine. Notably, there was no output for glutamine, serine and asparagine from the quantitative LC-MS analysis due to unavailability of internal standards for these metabolites. Both the LC-MS data and supporting literature references highlight the importance of these amino acids in mammalian cell growth and also make them ideal targets for a potential feed or supplementation.

Other depleting amino acids that met the scoring threshold include L-Ornithine, L-Norvaline and 2-Aminoisobutyric acid. Unlike the amino acids discussed above, these three are non-proteinogenic meaning they are not coded for by the genetic code of the cell line. The peak area data for these metabolites are shown in Figure 3.22. The trend shows depletion with time with a significantly lower concentration at day 6 compared to day 0 and day 3. L-Ornithine is the starting point in the formation of polyamines such as spermine, spermidine and putrescine. Its importance in mammalian cell culture has been well documented in the literature, thus its depletion could be detrimental for cell growth (Hölttä and Pohjanpelto, 1982; Roca et al., 2019). From the literature search, no relevant sources were found to indicate any correlation between L-Norvaline and 2-Aminoisobutyric acid concentrations and mammalian cell growth.

3.7 | LC-MS ANALYSIS OF CELL CULTURE MEDIA DURING 277 CELL LINE GROWTH CULTURE

However, they are also considered to be suitable targets to test in the feeding study given their significant depletion at the end of the culture.

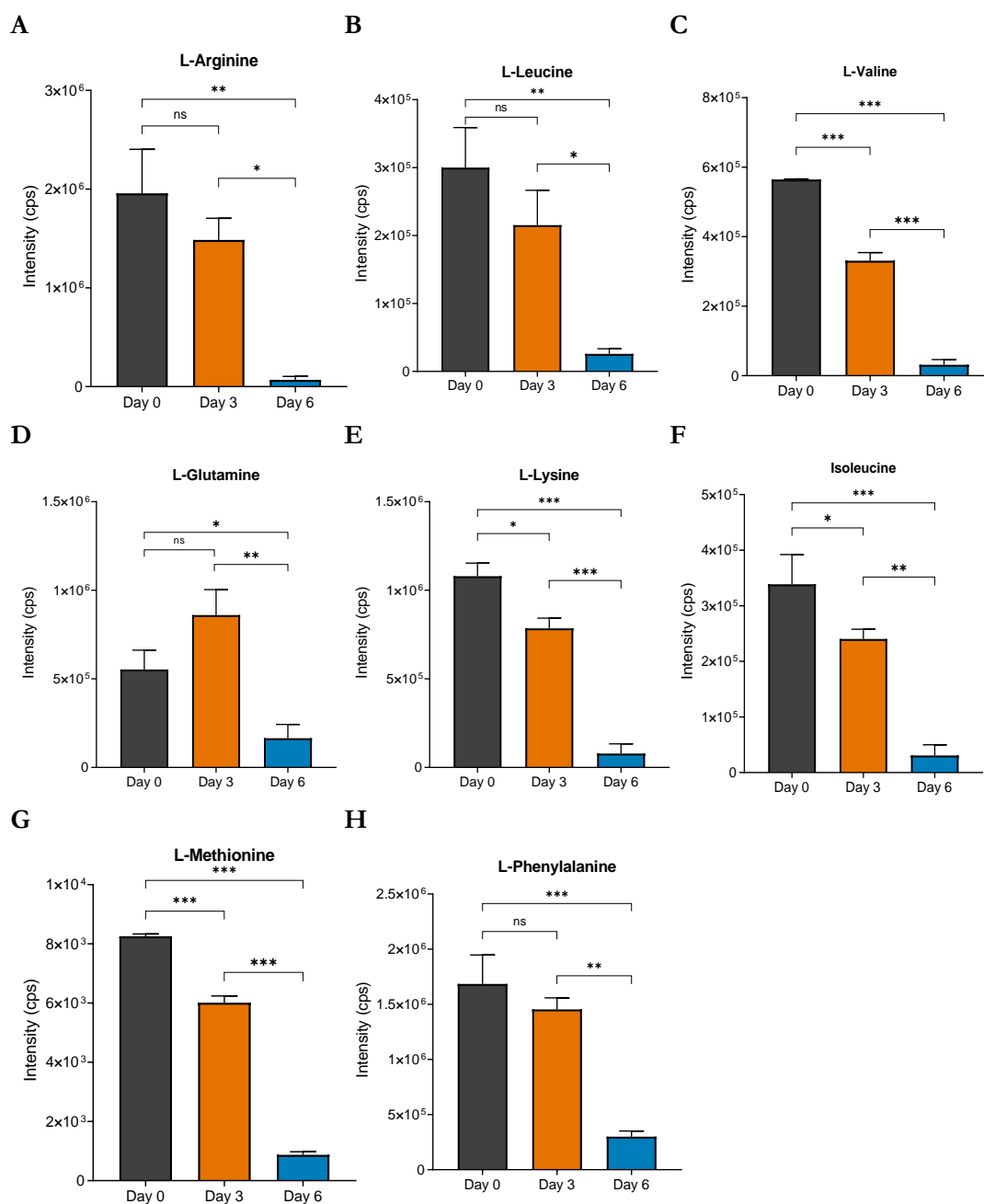


Figure 3.18: Peak area intensity profile of the high scoring depleting essential amino acids at three different stages along the cell culture period. Error bars represent one standard deviation about the mean (n=3 for day 0 and day 3; n=2 for day 6 due to an error with sample preparation for one of the replicates). Statistical comparisons were done using one-way ANOVA analysis followed by post-hoc Tukey multiple comparison test at 95% confidence level: ns: p-value > 0.05; *: p-value ≤ 0.05; **: p-value ≤ 0.01; ***: p-value ≤ 0.001. cps means counts per second.

3.7 | LC-MS ANALYSIS OF CELL CULTURE MEDIA DURING 277 CELL LINE GROWTH CULTURE

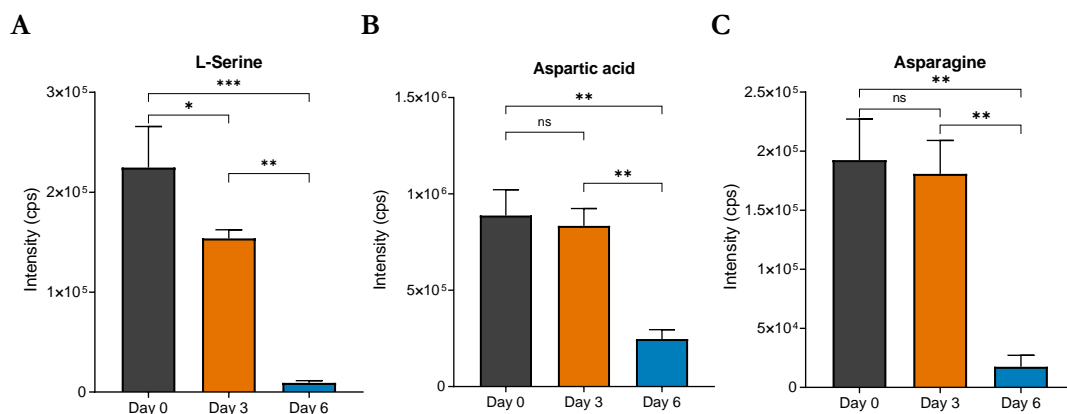


Figure 3.19: Peak area intensity profile of the high scoring non-essential amino acids at three different stages along the cell culture period. Error bars represent one standard deviation about the mean (n=3 for day 0 and day 3; n=2 for day 6 due to an error with sample preparation for one of the replicates). Statistical comparisons were done using one-way ANOVA analysis followed by post-hoc Tukey multiple comparison test at 95% confidence level: ns: p-value > 0.05; *: p-value ≤ 0.05; **: p-value ≤ 0.01; ***: p-value ≤ 0.001. cps means counts per second.

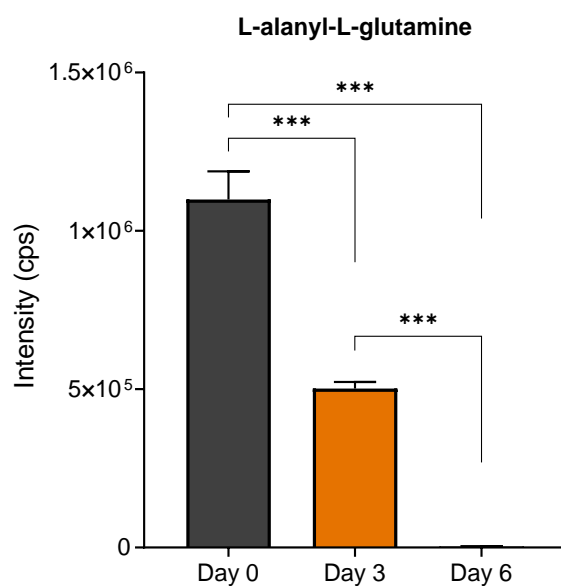


Figure 3.20: Peak area intensity profile of L-alanyl-L-glutamine at three different stages along the cell culture period. Error bars represent one standard deviation about the mean (n=3 for day 0 and day 3; n=2 for day 6 due to an error with sample preparation for one of the replicates). Statistical comparisons were done using one-way ANOVA analysis followed by post-hoc Tukey multiple comparison test at 95% confidence level: ns: p-value > 0.05; *: p-value ≤ 0.05; **: p-value ≤ 0.01; ***: p-value ≤ 0.001. cps means counts per second.

3.7 | LC-MS ANALYSIS OF CELL CULTURE MEDIA DURING 277 CELL LINE GROWTH CULTURE

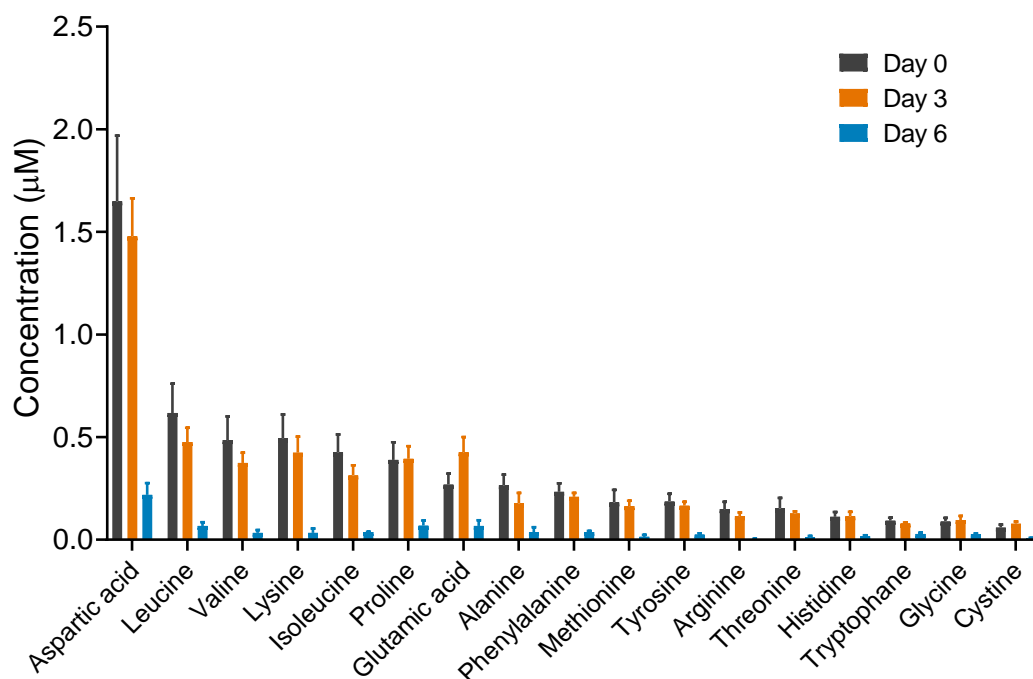


Figure 3.21: Quantitative LC-MS analysis of the proteinogenic amino acids at three different stages along the cell culture period.

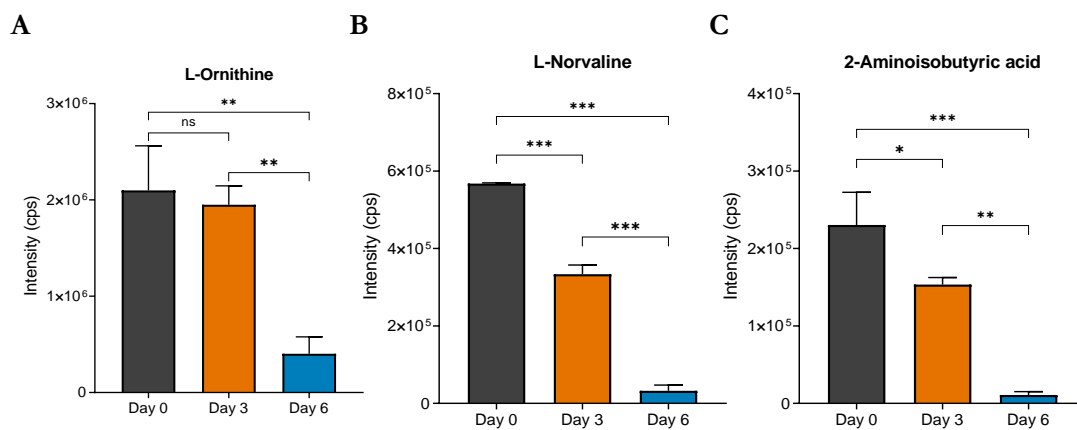


Figure 3.22: Peak area intensity profile of the high scoring depleting non-proteinogenic amino acids at three different stages along the cell culture period. Error bars represent one standard deviation about the mean (n=3 for day 0 and day 3; n=2 for day 6 due to an error with sample preparation for one of the replicates). Statistical comparisons were done using one-way ANOVA analysis followed by post-hoc Tukey multiple comparison test at 95% confidence level: ns: p-value > 0.05; *: p-value ≤ 0.05; **: p-value ≤ 0.01; ***: p-value ≤ 0.001. cps means counts per second.

Glucose

Glucose is the primary sugar source for a majority of cells and is present in most of the commercially supplied mammalian cell culture media (Coroadinha et al., 2006b). Basal media concentrations range from 1 g/L (5.5 mM) to as high as 10 g/L (55 mM) (Landauer, 2014). When glucose levels are sufficient (i.e. >1 g/L), its metabolites move through metabolic pathways such as glycolysis, tri-carboxylic acid (TCA) cycle and pentose phosphate pathway (PPP) which in turn generates adenosine triphosphate (ATP), the main energy currency of the cell (Rodrigues et al., 2013). The energy released from the breakdown of ATP drives most of the cellular metabolic reactions (Rodrigues et al., 2013).

Figure 3.23 shows the peak area data for glucose over the course of the culture. An increase in peak area intensity is observed at day 3. This is expected since there was a manual glucose feed added to the culture around this time point. However, the peak area at day 6 was significantly lower compared to both day 0 and day 3. As mentioned above, without its main energy source, the cellular machinery cannot function efficiently which may affect cell growth. However, data from section 3.6 showed that even in the presence of glucose late in the culture (i.e. post-day 6), cell growth arrest was still observed after day 5, suggesting that depletion of other metabolites may be contributing to the decline in cell growth.

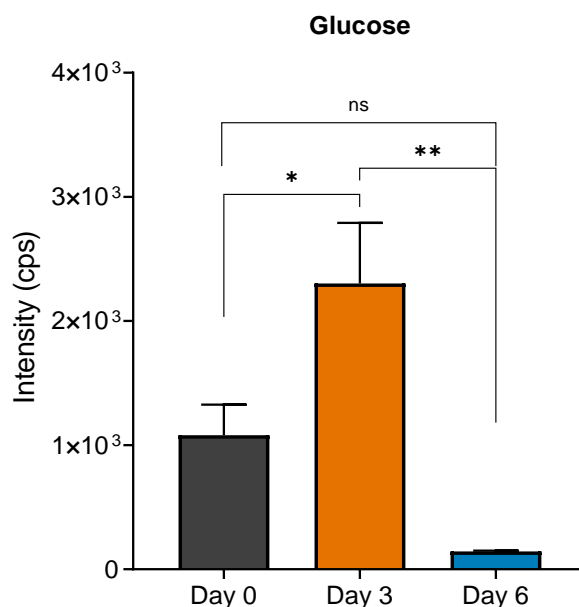


Figure 3.23: Peak area intensity profile of glucose at three different stages along the cell culture period. Error bars represent one standard deviation about the mean (n=3 for day 0 and day 3; n=2 for day 6 due to an error with sample preparation for one of the replicates). Statistical comparisons were done using one-way ANOVA analysis followed by post-hoc Tukey multiple comparison test at 95% confidence level: ns: p-value > 0.05; *: p-value ≤ 0.05; **: p-value ≤ 0.01; ***: p-value ≤ 0.001. cps means counts per second.

Vitamins

As discussed earlier in section 3.7.1, some of the key vitamins in mammalian cell culture showed no significant change in concentration with time. However, there were several other vitamins for which a decrease in concentration was observed and in particular, three of these vitamins met the scoring threshold. These were Choline, Folic acid and Pantothenic acid. All three are from the B complex of vitamins which are commonly added for growth stimulation (Arora, 2013). Their cellular function is to act as cofactors and coenzymes associated with carbohydrate, lipid, protein and nucleic acid metabolism (Ishaque and Al-Rubeai, 2002). The peak area data for the three high scoring vitamins are shown in Figure 3.24. The common trend observed is a significant reduction in peak area intensity at day 6 coinciding with growth decline. Studies in hybridoma and CHO cell culture demonstrated that additional supplementation of B complex vitamins including choline chloride, folic acid and calcium pantothenate

resulted in marked increases in viable cell density and antibody production (Ducommun et al., 2001; Ishaque and Al-Rubeai, 2002; Kim et al., 2005). Hence, these three vitamins would be suitable targets for the potential feed or supplementation during 277 cell line culture.

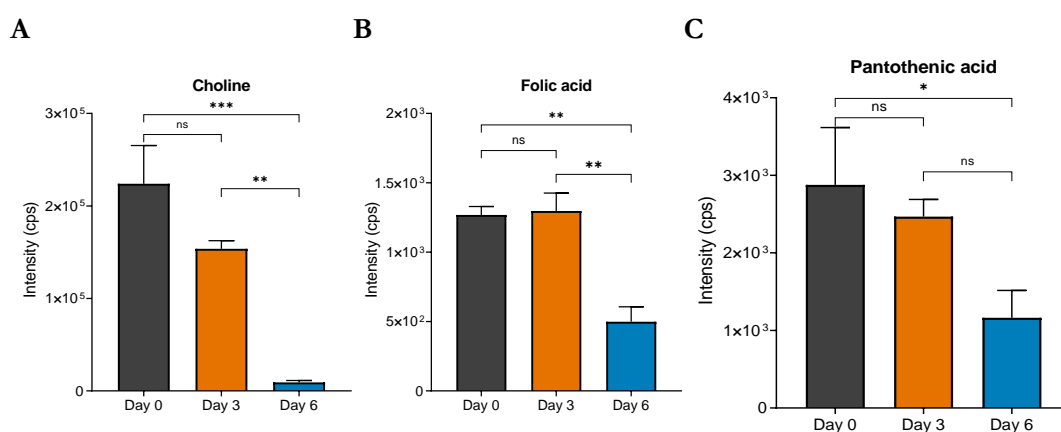


Figure 3.24: Peak area intensity profile of the high scoring significantly depleting vitamins at three different stages along the cell culture period. Error bars represent one standard deviation about the mean (n=3 for day 0 and day 3; n=2 for day 6 due to an error with sample preparation for one of the replicates). Statistical comparisons were done using one-way ANOVA analysis followed by post-hoc Tukey multiple comparison test at 95% confidence level: ns: p-value > 0.05; *: p-value ≤ 0.05; **: p-value ≤ 0.01; ***: p-value ≤ 0.001. cps means counts per second.

Putrescine

Putrescine, along with spermidine and spermine, belongs to the polyamine group (Roca et al., 2019). Polyamines have essential roles in cell proliferation, RNA expression, protein synthesis and DNA replication (Roca et al., 2019). Studies have shown that their depletion results in cell growth arrest and eventual death (Roca et al., 2019). Eukaryotic cell lines such as HEK293 and CHO cultivated in serum-free media require putrescine supplementation, as cells lack the first enzyme of the polyamine production pathway i.e. arginase (Roca et al., 2019). Arginase converts L-arginine to L-ornithine, and ornithine decarboxylase, converts the L-ornithine to finally generate putrescine (HEBY, 1981). The other two polyamines, spermidine and spermine, are subsequently generated from putrescine. Figure 3.25 shows the peak area data of this

essential polyamine, putrescine. A t-test could not be performed to test for significance since there was only one LC-MS output for each time point. However, the trend shows clear depletion with time and more importantly, a very low intensity at day 6 which may have contributed to the growth decline. Hence, putrescine would make a good target for the feed supplement.

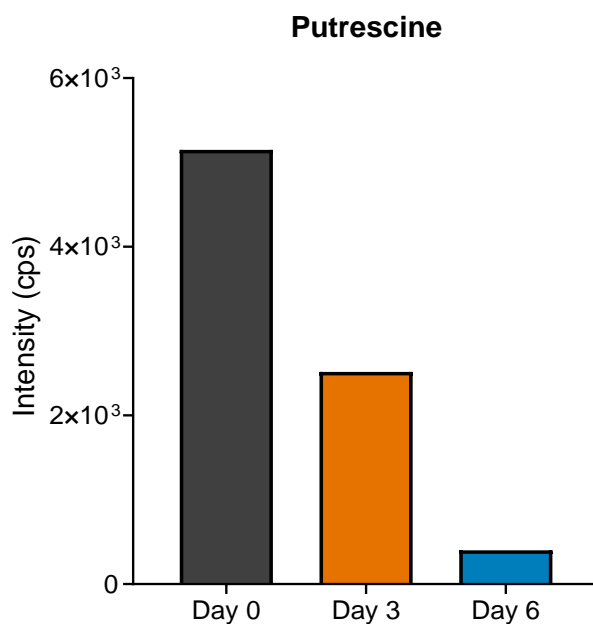


Figure 3.25: Peak area intensity profile of putrescine at three different stages along the cell culture period. n=1 for all days; ANOVA was not performed as there was only one LC-MS output on each day for this metabolite. cps means counts per second.

Histamine

Histamine is an organic compound with recognised roles in allergic and inflammatory reactions (Tetlow and Woolley, 2003). Figure 3.26 shows that this compound was also significantly depleted as the culture progressed. From the literature review performed in the present study, there were no references indicating their role in HEK293, CHO or hybridoma cell culture. However, Tetlow and Woolley, 2003 have reported that histamine is an important modulator of numerous physiological processes, including cell proliferation. In their study, they demonstrated that histamine stimulated the proliferation of human articular chondrocyte cells in culture (Tetlow and Woolley,

2003). Therefore, given that histamine shows very significant depletion towards the end of the culture, it will also be studied as a potential feed target.

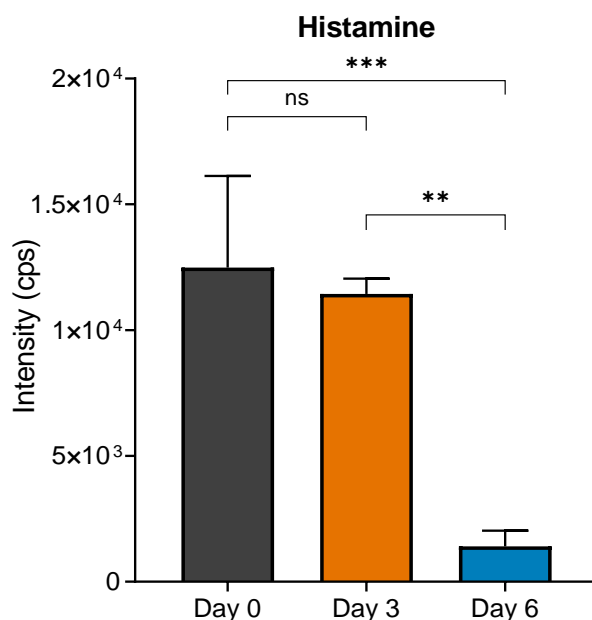


Figure 3.26: Peak area intensity profile of the histamine at three different stages along the cell culture period. Error bars represent one standard deviation about the mean (n=3 for day 0 and day 3; n=2 for day 6 due to an error with sample preparation for one of the replicates). Statistical comparisons were done using one-way ANOVA analysis followed by post-hoc Tukey multiple comparison test at 95% confidence level: ns: p-value > 0.05; *: p-value ≤ 0.05; **: p-value ≤ 0.01; ***: p-value ≤ 0.001. cps means counts per second.

D-Pipecolic acid

D-Pipecolic acid is an imino acid and a metabolite of D-lysine (Matsumoto et al., 2003). Matsumoto *et al.*, 2003 suggest that it has a role as a modulator of synaptic transmission in neuronal cells. However, there were no references indicating their role in HEK293, CHO or hybridoma cell culture. As Figure 3.27 shows, this metabolite was also significantly depleted with time, it can also be studied as a potential feed target.

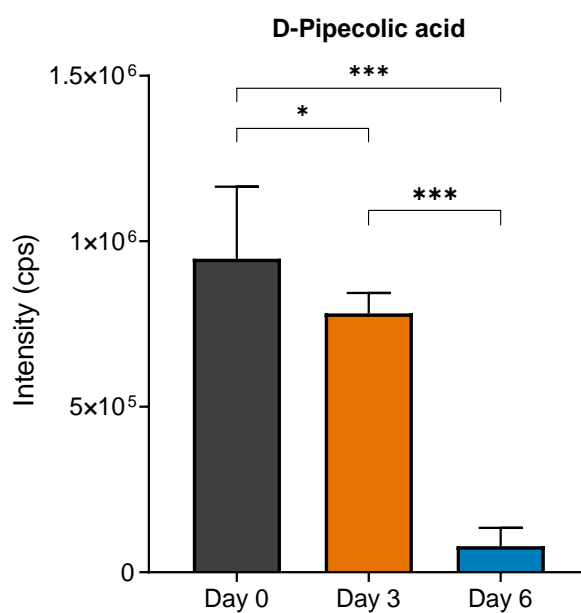


Figure 3.27: Peak area intensity profile of the D-pipecolic acid at three different stages along the cell culture period. Error bars represent one standard deviation about the mean (n=3 for day 0 and day 3; n=2 for day 6 due to an error with sample preparation for one of the replicates). Statistical comparisons were done using one-way ANOVA analysis followed by post-hoc Tukey multiple comparison test at 95% confidence level: ns: p-value > 0.05; *: p-value ≤ 0.05; **: p-value ≤ 0.01; ***: p-value ≤ 0.001. cps means counts per second.

3.8 CHAPTER SUMMARY

This chapter has successfully characterised GSK's 277 HEK293T stable cell line in the 2 L STR model in terms of cell growth, metabolic profile and LVV productivity. Below are the key findings from this chapter:

- In section 3.3, the 277 cell line was characterised by early growth arrest and a short exponential growth phase lasting around 4 days under the current platform operating conditions for this cell line. The maximum VCD achieved before cells entered stationary phase was around 6×10^6 cells/mL.

- The average infectious titre in the vector harvest was around 7×10^7 TU/mL which is greater than titres reported for other stable cell lines in literature (section 3.4).
- The metabolite profile during cell growth was characterised by high levels of glucose consumption and significant lactate accumulation (section 3.3). However, altering the metabolite profile by reducing lactate accumulation and preventing glucose depletion, using pH and CO₂, did not improve cell growth (section 3.6). Growth arrest was still observed after 5 days with the cultures still not reaching VCD's $\geq 7 \times 10^6$ cells/mL.
- Inducing at viable cell densities greater than the current platform induction cell density for the 277 cell line (i.e. $2 - 3 \times 10^6$ cells/mL) resulted in higher infectious titres (section 3.5). Up to 10×10^6 cells/mL, the increase in infectious titre was proportional to the increase in induction cell density. A 'cell density effect' was observed at cell densities greater than 10×10^6 cells/mL.
- In section 3.7, LC-MS analysis was used to profile extracellular metabolites at different time points during growth of the 277 cell line. In total, 90 metabolites were identified belonging to 10 different classes of compounds. 33 metabolites showed no significant change in concentration with time. 7 metabolites were accumulating with time; among these, only lactic acid had growth inhibitory properties. However, section 3.6 confirmed that reducing lactic acid accumulation did not improve cell growth. 50 metabolites were depleting with time; among these, 22 not only showed significant depletion, but also had a correlation with mammalian cell growth based upon literature.

The 22 depleting metabolites identified during the LC-MS analysis described in section 3.7.3 are considered to be suitable targets for developing a feed supplement to improve 277 cell line growth. Before developing a feeding strategy, a high-throughput scale-down system is required to perform design of experiments (DoE) based screening and optimisation studies. Hence, in the next phase of this work, the microwell system

described in section 1.6.3 will be used to develop a high-throughput scale-down model of GSK's platform 277 HEK293T stable cell line process in the 2 L STR.

4 DEVELOPING A HIGH-THROUGHPUT SCALE-DOWN MODEL OF GSK'S PLATFORM 277 HEK293T STABLE CELL LINE CULTIVATION PROCESS IN 2 L STIRRED TANK REACTORS

4.1 INTRODUCTION AND AIMS

Chapter 3 demonstrated that the 277 cell line is unable to reach high viable cell densities under the current platform operating conditions for this cell line. Growth arrest was observed as early as day 5 post-inoculation with a maximum VCD of approximately 6×10^6 cells/mL. LC-MS analysis over the course of culture period identified 50 metabolites which were significantly depleting with time. Among these, 22 metabolites were identified as having an important role in mammalian cell growth based upon literature, making them ideal targets for developing a feed supplement for improving 277 cell line growth.

Testing and developing a feed requires an effective high-throughput scale-down system due to the number of variables to be tested experimentally. As discussed in section 1.6, microtiter plates offers several benefits as well as shortcomings compared

to other scale-down systems, such as shake-flasks and miniature STRs. Shortcomings include lack of parameter control (e.g. pH, DO, temperature), however, the key benefit of the microtiter plate relevant for this work is high throughput. To adopt a microwell system as a scale-down tool for 277 cell line cultivation, cell culture performance such as growth kinetics and LVV productivity must be matched with bench to pilot scale bioreactor processes. If not, there is no guarantee that the optimised process conditions achieved using microwells will be maintained upon scale-up.

From the different microwell formats available, the 24 deep square well (24-DSW) microtiter plate is considered most suitable for this work as discussed in section 4.3. Hence, the aim of this chapter is to use of the 24-DSW plate to develop a scale-down mimic of GSK's established stable suspension LVV production process model at 2 L STR scale. Based on the rationale discussed in section 4.4, mixing time will be used as the basis for scale-translation. To develop the scale-down model, mixing time will first be characterised in the 2 L STR and 24-DSW plate. Thereafter, growth kinetics, LVV productivity and cell metabolism of the 277 cell line will be compared between the microwell and STR cultures at matched mixing time. The specific objectives of this chapter are:

- Characterise mixing time in the bench-scale 2 L STR
- Characterise mixing time in the 24-DSW microtiter plates
- Evaluate scale-translation at matched mixing time

4.2 CHAPTER SPECIFIC MATERIALS AND METHODS

4.2.1 Mixing time characterisation in section 4.5

The dual indicator system for mixing time (DISMT) technique was used to quantify mixing time in the 2 L STR and 24-DSW plate. The DISMT method is outlined in section 2.8.

4.2.2 Details for 2 L STR and 24-DSW plate cultures in section 4.6

In both sections 4.6.1 and 4.6.2, the reactor systems were run in triplicate to account for experimental variability. The STR's were operated at the platform operating conditions of the 277 cell line as outlined in section 2.4. The method pertaining to STR set-up, operation and sampling has also been outlined in section 2.4. For the 24-DSW plate, triplicate wells were used for daily sampling. The method pertaining to 24-DSW plate set-up, operation and sampling has been outlined in section 2.5. The method for all analytical techniques used in these studies are described in section 2.7.

4.3 RATIONALE FOR SELECTING THE 24-DSW PLATE FORMAT

Erlenmeyer shake flasks (Corning) and small scale STR's are commonly used scale-down models in upstream process development. The advantages and limitations of these systems have been discussed in more detail under section 1.6. The common limitation highlighted was the low degree of parallelisation offered, especially in the context of this project, wherein multiple feed supplements need to be tested. Microtiter plates offer a suitable alternative as they provide higher throughput, are more cost-effective and are relatively easy to use. As previously mentioned in section 1.6.3, Guy *et al.*, 2013 describe cultivation of HEK293 cells in 24-SRW plates to establish operating conditions for a 0.5 L wave bioreactor culture and demonstrated that the 24-SRW is an effective scale-down model (Guy *et al.*, 2013). HEK293T stable cell line cultivation in 24-deep square well (24-DSW) plates has yet to be demonstrated in

literature. Compared to the 24-SRW plate, the 24-DSW format is advantageous as it offers 3-6 times greater working volume. Studies have also shown that square shaped wells have a better mixing and oxygen transfer profile compared to round well plates (Duetz and Witholt, 2004). Hence, the 24-DSW plate was the microwell system of choice for this study.

4.4 RATIONALE FOR USING MIXING TIME AS THE BASIS FOR SCALE-TRANSLATION

A variety of approaches for cell culture scale translation have been proposed as described in section 1.7. The commonly used methods are matched mean energy dissipation (P/V), matched $k_L a$ and matched mixing time. Matched $k_L a$ is often used for scaling cell cultures with high oxygen demand (Ferreira-Torres et al., 2005). The oxygen demand for mammalian cells (e.g. HEK293) is relatively low compared to bacterial cell lines (e.g. *E. coli*) (Nienow, 2006), therefore matched $k_L a$ was not considered for the 277 cell line cultures. The use of matched P/V in this study was limited by the lack of accurate methods of determining P/V in microwells. Current methods only provide estimates of the power input using computational fluid dynamics (CFD) predications of the mean energy dissipation (Zhang et al., 2008). As there are no direct methods to compare against, the CFD predictions are yet to be validated as accurate models of the actual P/V . In comparison, there are now more accurate and semi-automated methods for measuring mixing time, such as the dual indicator system for mixing time (DISMT) technique. This method also enables mixing time to be characterised across reactors with different scales and geometries. Furthermore, Sani and Baganz, 2016 demonstrated matched mixing time as a suitable criterion for scaling between 0.5 L micro-bioreactor (MBR) and 5 L STR for a GS-CHO cell line (Sani and Baganz, 2016). However, scale translation for smaller scale vessels with different geometries is yet to be established. Therefore, in this study, mixing time was selected as the basis for 277 cell line scale-translation between 24-DSW microtiter plates and bench-scale 2 L STR.

4.5 MIXING TIME CHARACTERISATION

Mixing time is an important parameter for mammalian cell culture processes. Inadequate mixing results in cells being exposed to different environments within the reactor, which can have adverse consequences on cell growth kinetics and productivity (Gogate et al., 2000; Nienow, 2006). Hence, mixing should be optimised to produce a homogenous cell culture environment whilst avoiding any deleterious effects caused by potential hydrodynamic forces and bubble bursting. Mixing times less than 10s should provide the necessary homogeneity as well as ensuring a fast response to any changes in operating conditions such as pH and temperature (Amanullah et al., 2004; Langheinrich and Nienow, 1999; Silk, 2014). However, a compromise has to be made in selecting the operating stirrer speed i.e. should not be too harsh to cause foaming and shear-related cell death and also not be too gentle to cause cell settling. For fed-batch culture, efficient mixing is particularly important to avoid formation of local nutrient gradients (Enfors et al., 2001; Nienow, 2006). In the present study, mixing times in the 2 L STR and 24-DSW were determined using the DISMT method as described in section 2.8.

4.5.1 Mixing time in 2 L STR

Figure 4.1 shows the mixing time variation in the 2 L STR with varying stirrer speeds and two different working volumes, 1.5 L and 1.8 L, to account for changes in volume through the GSK LVV 277 cell line fed-batch process. As expected, Figure 4.1 shows that mixing time was inversely proportional to the stirrer speed. It can also be seen that, for the two fill volumes evaluated, the mixing times were comparable as demonstrated by the overlapping error bars. The average mixing time ranged from 7 – 17 s for 1.5 L and 7 – 24 s for 1.8 L. At higher agitation rates (i.e. ≥ 225 rpm), the mixing time values were less than 10 s, which is necessary to maintain a homogenous culture environment (Amanullah et al., 2004; Nienow, 2006; Silk, 2014). With respect to the 2 L STR LVV production process model, the 277 cell line platform operating stirrer speed (i.e. 225 rpm) fell in the range of higher agitation rates, hence, was

sufficient to maintain the required homogeneity for optimal HEK293T growth and LVV productivity. In addition, the mixing time values from this work were comparable with those found in literature for other bench-scale bioreactors as summarised in Table 4.1. From this table, it is evident that the variety of mixing time methods used by different groups all produced consistent datasets for a similar range of Reynolds numbers as evaluated in this study.

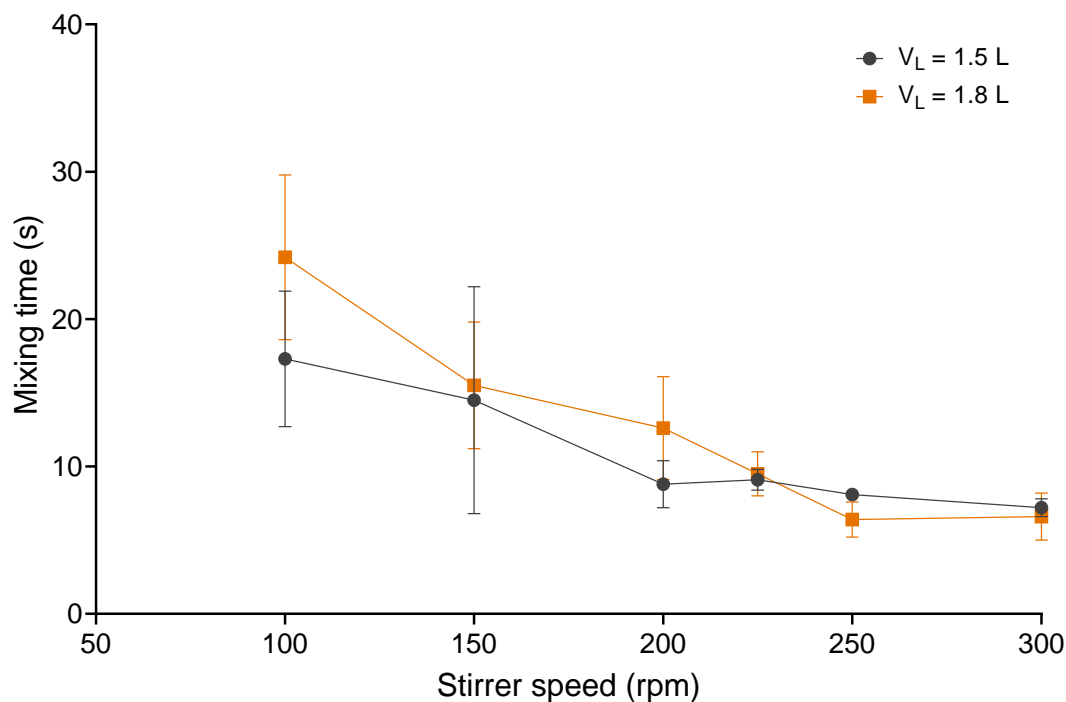


Figure 4.1: Liquid phase mixing times for 2 L STR measured using the dual indicator system for mixing time (DISMT) technique. Mixing time was characterised at stirrer speeds between 100 – 300 rpm and two different bioreactor working volumes, $V_L = 1.5$ L and $V_L = 1.8$ L. Error bars represent one standard deviation about the mean ($n=5$).

Table 4.1: Comparison of mixing times for small/bench scale bioreactors from studies published in literature.

Reactor configuration	Number and type of impeller	Method of mixing time study	Reynolds number [†]	Mixing time (s)	Literature
5 L STR (Sartorius, Germany)	1 x 3-blade segment	Iodine decolourisation	7,000 – 19,000	6 – 19	Silk, 2014
3 L STR (Applikon, Netherlands)	1 x Rushton turbine	Iodine decolourisation	3,000 – 10,000	6 – 20	Betts, 2015
5 L STR (Sartorius, Germany)	1 x Marine	Iodine decolourisation	6,000 – 17,000	6 – 19	Ramadhani, 2015
0.5 L MBR (HEL-BioXplore, United Kingdom)	1 x Marine	pH tracer	4,000 – 10,000	3 – 14	Sani, 2016
2 L STR (Sartorius, Germany)	2 x 3-blade segment	DISMT	7,000 – 21,000	6 – 24	<i>Present study</i>

[†]Reynolds numbers have been rounded to the nearest thousand

4.5.2 Mixing time in 24-DSW plate

Figure 4.2 shows the mixing time variation in the 24-DSW plate with varying shaker speed and four different fill volumes, ranging from 2 – 5 mL. From Figure 4.2, it is evident that mixing time was inversely proportional to shaker speed in the lower end range of shaker speeds investigated i.e. between 175 to 250 rpm. Within this range, mixing time was also reduced for smaller fill volumes. At the lowest shaker speed tested, mixing time for $V_L = 5$ mL was approximately 4 times greater than that of 2 mL. For smaller fill volumes, mixing times are expected to be lower since there is a constant amount of energy being dissipated to a reduced volume, resulting in more

turbulence and hence better circulation (Al-Ramadhani, 2015). At shaker speeds greater than 250 rpm, the mixing process became very rapid with mixing times less than 10 s for all fill volumes evaluated.

For the same 24-DSW format, Li *et al.*, 2020 reported an unexpected increase in mixing time in the higher speed range which was associated with a change in free surface dynamics in the well. The authors attribute this phenomenon to the very small shaking diameter (d_s) used in their study (i.e. 3 mm). A similar increase in mixing time at higher shaker speeds was not observed in this work, perhaps due to the higher shaking diameter of 25 mm being used.

The mixing time results from this work were also compared against the scaling law proposed by Rodriguez *et al.*, 2014 for orbitally shaken reactors (OSRs) (Rodriguez et al., 2014). A comparison between the two studies could be made since the same experimental technique and image processing methodology was used. In their study, Rodriguez *et al.*, 2014 demonstrated good correlation between two dimensionless parameters, mixing number ($N.t_m$) and Froude number ratio i.e. Froude number (Fr)/Critical Froude number (Fr_c). Fr relates the inertia forces in a system to the effects due to gravity and Fr_c is estimated during the change in the flow regime in a shaken reactor from in-phase to out-of-phase flow (Rodriguez et al., 2014). From this, the power law relationship for scaling was derived and is shown in section 2.11 as equation 6. This relationship was found to best fit data from a wide range of operating conditions including reactors of different sizes (Internal diameter, $d_i = 8 - 13$ cm) and orbital shaking diameters ($d_s = 15 - 50$ mm). In the power law relationship, the use of Fr_c was found to be more effective than simply using Fr , since Fr_c considers the flow transition between in- and out-of-phase in the OSR (Li *et al.*, 2020). Li *et al.*, 2020 assessed the applicability of the scaling law, however, the power law function over predicted the mixing numbers for the 24-DSW plate used in their study (Li et al., 2020). This was due to the very small orbital diameter used in which case the different fluid and mixing dynamics within the well meant that the Froude number ratio was not an effective scaling parameter. As the orbital diameter in this work was larger compared to Li *et al.*, 2020, the applicability of the scaling law was re-assessed using the present

data set. Using equation 6 from section 2.11, the mixing number curves for the 24-DSW plate from this study were plotted in Figure 4.3 and compared against the power law function from Rodriguez *et al.*, 2014. From the graph, all the mixing number curves showed good correlation with the power law function, confirming its applicability as a scaling law for OSRs of different sizes and geometries. Furthermore, it also demonstrates confidence in the accuracy of the mixing time values in this work, given that mixing time was selected as the basis for scale-translation.

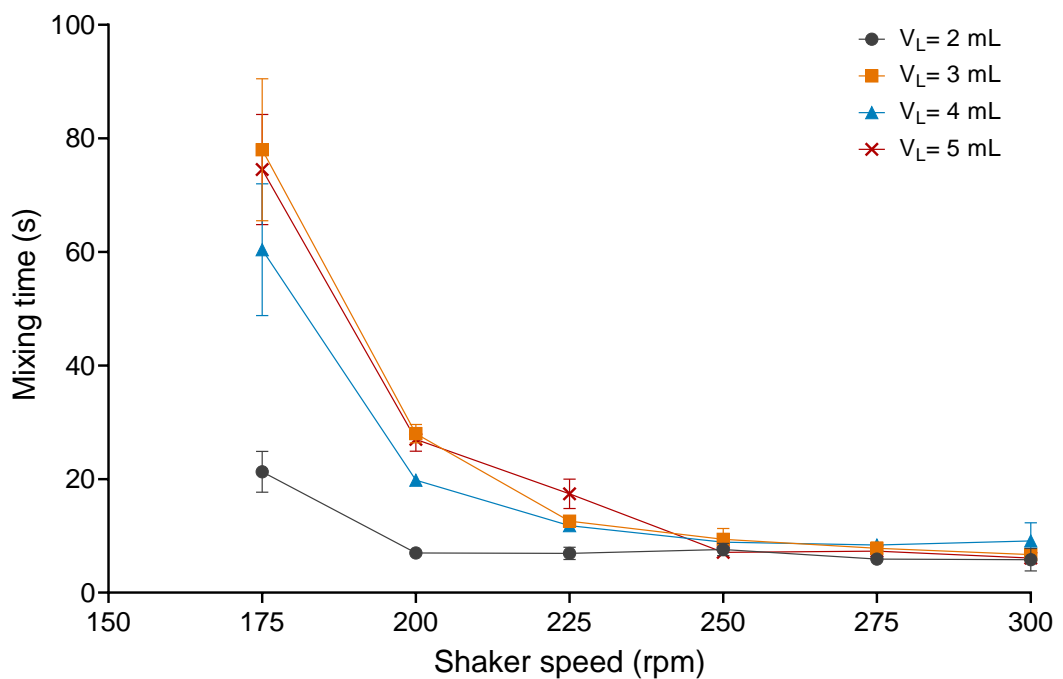


Figure 4.2: Liquid phase mixing times for 24-DSW plate measured using the dual indicator system for mixing time (DISMT) technique. Mixing time was characterised at shaking speeds between 175 – 300 rpm ($d_s = 25$ mm) and four different fill volumes between 2 – 5 mL. Error bars represent one standard deviation about the mean ($n=5$).

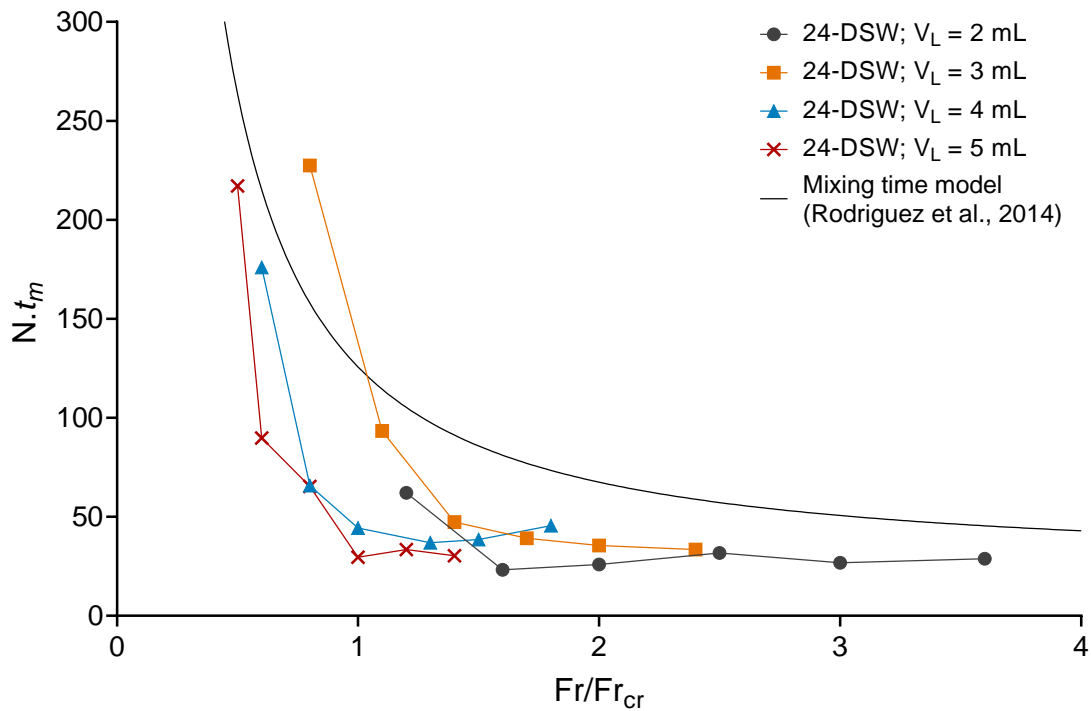


Figure 4.3: Comparison between data shown in present study with the mixing time model reported in Rodriguez *et al.*, 2014. The model is based on the Froude number ratio (Fr/Fr_{cr}) and is used for scaling between OSR's of different sizes and geometries.

4.6 SCALE TRANSLATION OF 277 STABLE CELL LINE CULTURE AT MATCHED MIXING TIME

The scalability of cell culture performance such as growth kinetics and LVV productivity was investigated in 24-DSW microtiter plates (5 mL scale) and stirred tank reactors (2 L scale). As described earlier, mixing time was chosen as the basis for scale translation.

Table 4.2 summarises the operating conditions selected in each of the two vessel formats for operation at matched mixing time of <10 s. The mixing time obtained in the STR under the 277 cell line platform operating conditions was selected as the benchmark. For the 24-DSW plate, the mixing time was matched at shaking speeds \geq

250 rpm for all fill volumes examined. A larger fill volume is more advantageous since there is greater scope for analytics. It also allows for sacrificial well sampling to be avoided thus permitting a higher experimental throughput. Hence, 5 mL was selected as the initial microwell fill volume. This was reduced to 2.5 mL at the harvest time point as the culture was sampled from the same well each day. It should be noted that a constant mixing time is still achieved for this range of working volume at 250 rpm, as supported by Figure 4.2. Comparable cell culture profiles have also been demonstrated between wells with reducing volume (i.e. same well sampling) and the sacrificial well sampling control with 5 mL culture volume as shown in Figure 9.1 under Appendix A (section 9.3). Hence, the reduction in volume up to 2.5 mL does not have any impact on cell culture performance, thus, validating the sampling approach used in this study.

Table 4.2: Summary of operating parameters for 24-DSW plate and 2 L STR at matched mixing time.

Reactor	24-DSW Plate	2 L STR (Sartorius)
Shaker/stirrer speed	250 rpm	225 rpm
Mixing time	7.1 ± 0.1 s	9.5 ± 1.5 s
Aeration system	Headspace	L-type sparger and/or headspace
Working volume	2.5 – 5 mL	1.5 – 1.8 L
pH/DO/Temperature control	n/a [†]	Yes

[†]Parameter control cannot be performed for the 24-DSW plate cultures

4.6.1 277 cell line growth culture

The growth kinetics of 277 cell line cell cultures in 24-DSW plates and 2 L STR are depicted in Figure 4.4A. To accurately determine the period of exponential growth, a logarithmic plot of viable cell density has been plotted against time as shown in Figure 4.4B. In general, the growth profile was comparable between both vessel systems for the entire culture duration. Unlike the 2 L STR culture which had a very short lag phase

between day 0 and day 1, there was no apparent lag phase for the 24-DSW plate culture. Rather, cells appear to be in exponential growth from the start of culture until day 3. For the 2 L STR, cells appear to be in exponential growth between day 1 and day 3. For both cultures, there was a period of further growth until day 5, although not exponential. After day 5, cell growth arrest was observed as cells entered stationary phase. The maximum viable cell density achieved at the end of the culture was similar in both vessels being approximately 6×10^6 cells/mL.

According to Figure 4.5, the culture viability profile was also comparable in both vessel systems. High cell viability (i.e. >95%) was observed between day 0 and day 5. After day 5, a decline in culture viability was observed, however, the viabilities for both systems were still above 90% at the end of the culture.

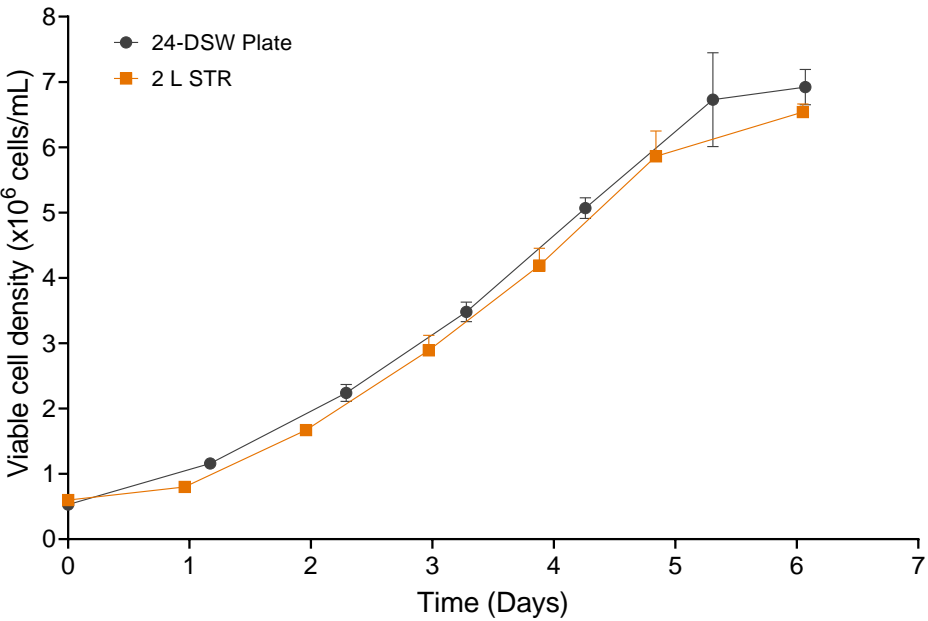
The glucose and lactate concentration profiles for the two vessel systems are shown in Figure 4.6 and 4.7 respectively. The data shows that glucose and lactate concentration profiles were similar in both systems up until day 4. Thereafter, glucose depletion and resulting lactate accumulation was greater in the 2 L STR compared to the 24-DSW plate. This trend in glucose and lactate concentration could be explained by the contrasting pH profiles for both systems.

As discussed earlier in section 3.6, studies by Roman *et al.*, 2018 and Liste-Calleja *et al.*, 2015 have demonstrated that culture pH below 6.8 triggers lactate co-metabolism in HEK293T cells. This cellular adaptation is used as a pH detoxification strategy by means of co-transporting extracellular protons together with lactate into the cytosol. For the STR, the pH was maintained above 6.8 through the controlled addition of sodium carbonate base and CO₂ (Figure 4.8). However, no such control was available in the 24-DSW system which was evident by the steady decrease in culture pH with time, as depicted in Figure 4.8. The spike increase in pH after day 3 and day 5 correspond to the glucose feed time points. After day 3, the microwell pH started to drop below pH 7 as the cellular metabolic activity increased. By day 4, the pH was already below 6.8. At the same time point, a plateau in lactate accumulation for the 24-DSW plate was also observed (Figure 4.7) which is likely due to lactate co-metabolism,

as suggested by Roman *et al.*, 2018 and Liste-Calleja *et al.*, 2015. As shown by the same authors, this change in metabolite profile can be advantageous for HEK293 cells in terms of promoting cell growth. However, more detailed metabolic flux analysis and enzyme assays would be required to confirm the presence of lactate co-metabolism in this study. After day 3, Figure 4.6 shows that the rate of glucose consumption was also significantly lower in the 24-DSW plate compared to the 2 L STR. This was also likely due to the metabolic switch toward lactate co-consumption which reduced the glucose demand for the cells in the 24-DSW plate. However, despite the disparity in pH control between the two vessel systems, the 24-DSW plate still represented a good scale-down model for the 2 L STR with respect to 277 cell line growth.

4 | DEVELOPING A HIGH-THROUGHPUT SCALE-DOWN MODEL OF GSK'S PLATFORM 277 HEK293T STABLE CELL LINE CULTIVATION PROCESS IN 2 L STIRRED TANK REACTORS

A



B

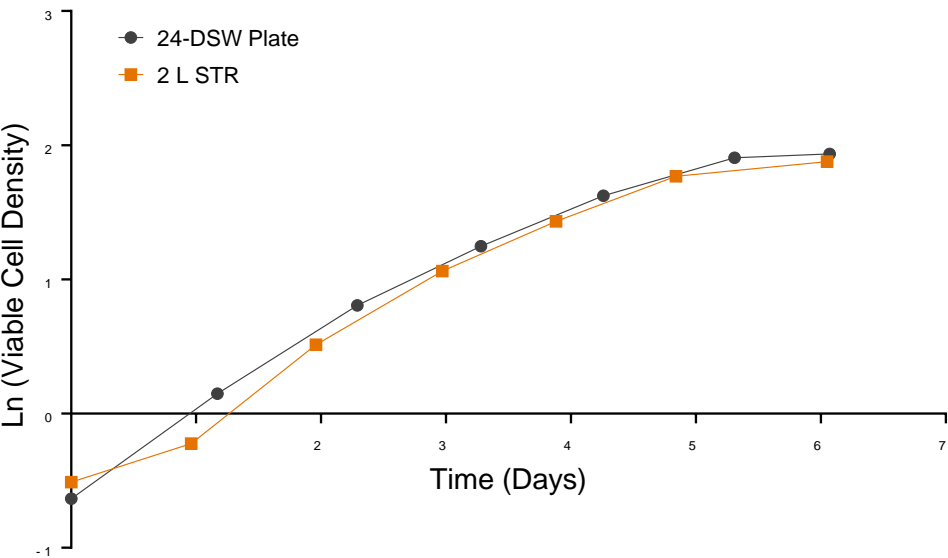


Figure 4.4: (A) Viable cell density profile for cultivation of the 277 HEK293T stable producer cell line in 24-DSW plate and 2 L STR at matched mixing time of < 10 s. (B) Natural logarithm of viable cell density plotted against time. Error bars represent one standard deviation about the mean (n=3).

4.6 | SCALE TRANSLATION OF 277 STABLE CELL LINE CULTURE AT MATCHED MIXING TIME

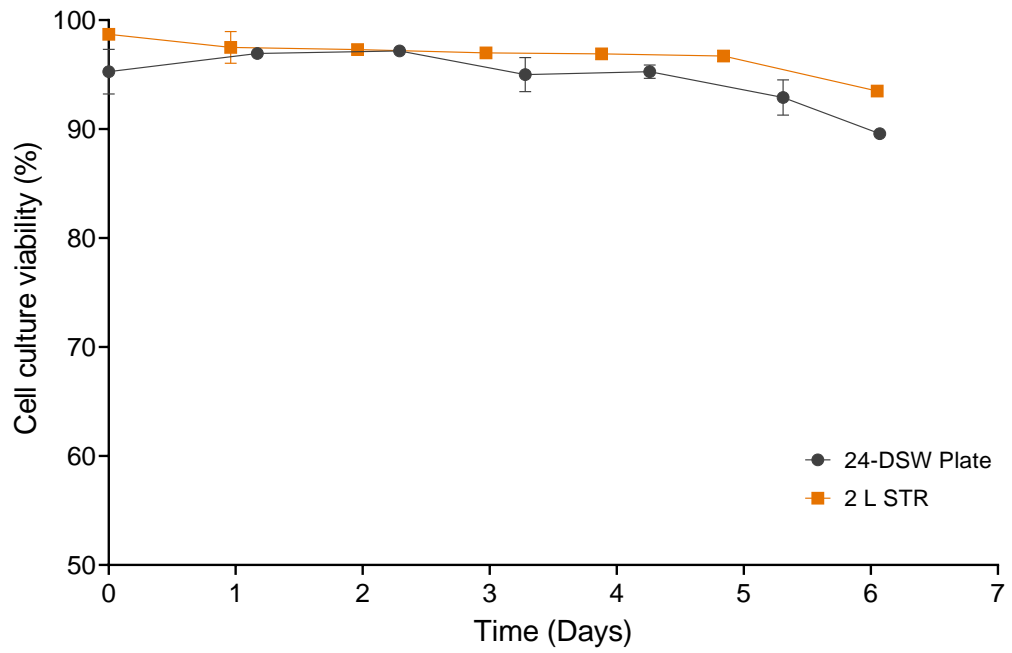


Figure 4.5: Culture viability profile for cultivation of the 277 HEK293T stable producer cell line in 24-DSW plate and 2 L STR at matched mixing time of < 10 s. Error bars represent one standard deviation about the mean (n=3).

4 | DEVELOPING A HIGH-THROUGHPUT SCALE-DOWN MODEL OF GSK'S PLATFORM 277 HEK293T STABLE CELL LINE CULTIVATION PROCESS IN 2 L STIRRED TANK REACTORS

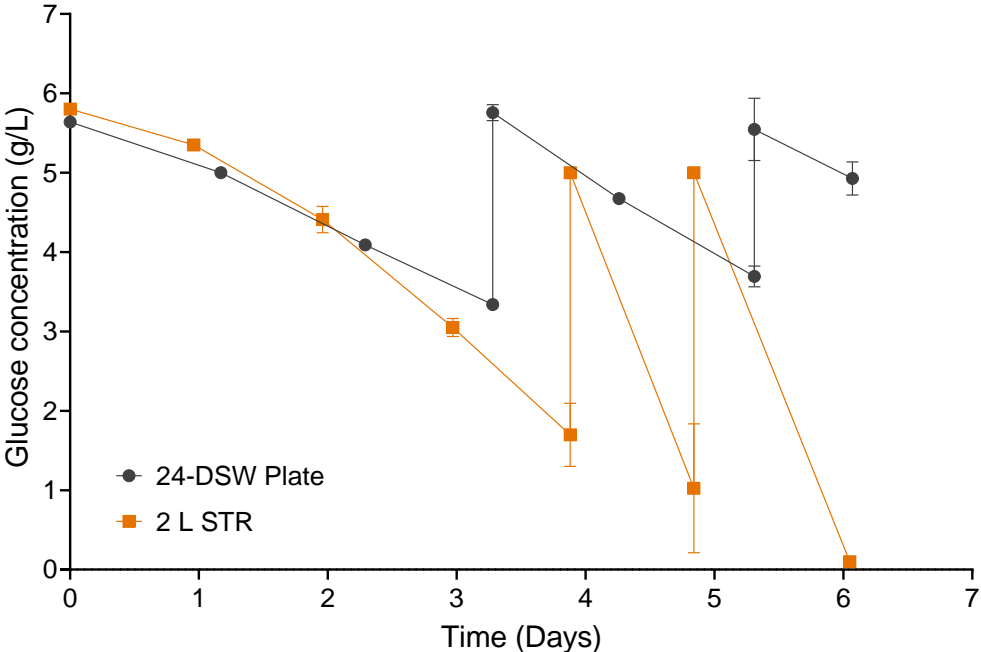


Figure 4.6: Glucose concentration profile for cultivation of the 277 HEK293T stable producer cell line in 24-DSW plate and 2 L STR at matched mixing time of < 10 s. Error bars represent one standard deviation about the mean (n=3).

4.6 | SCALE TRANSLATION OF 277 STABLE CELL LINE CULTURE AT MATCHED MIXING TIME

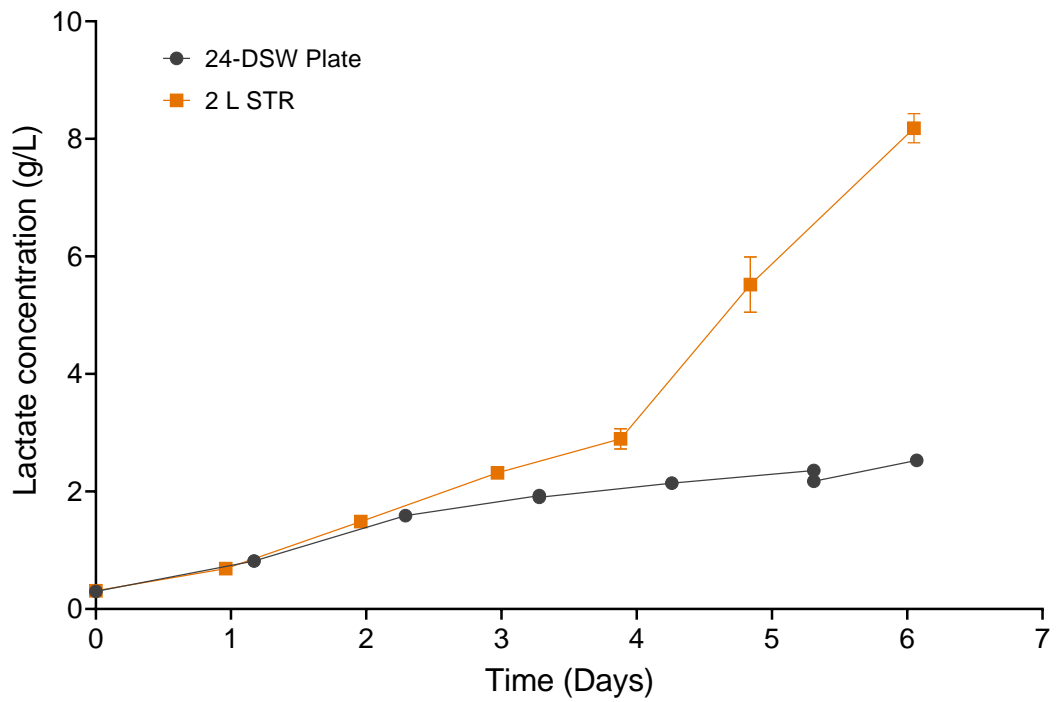


Figure 4.7: Lactate concentration profile for cultivation of the 277 HEK293T stable producer cell line in 24-DSW plate and 2 L STR at matched mixing time of < 10 s. Error bars represent one standard deviation about the mean (n=3).

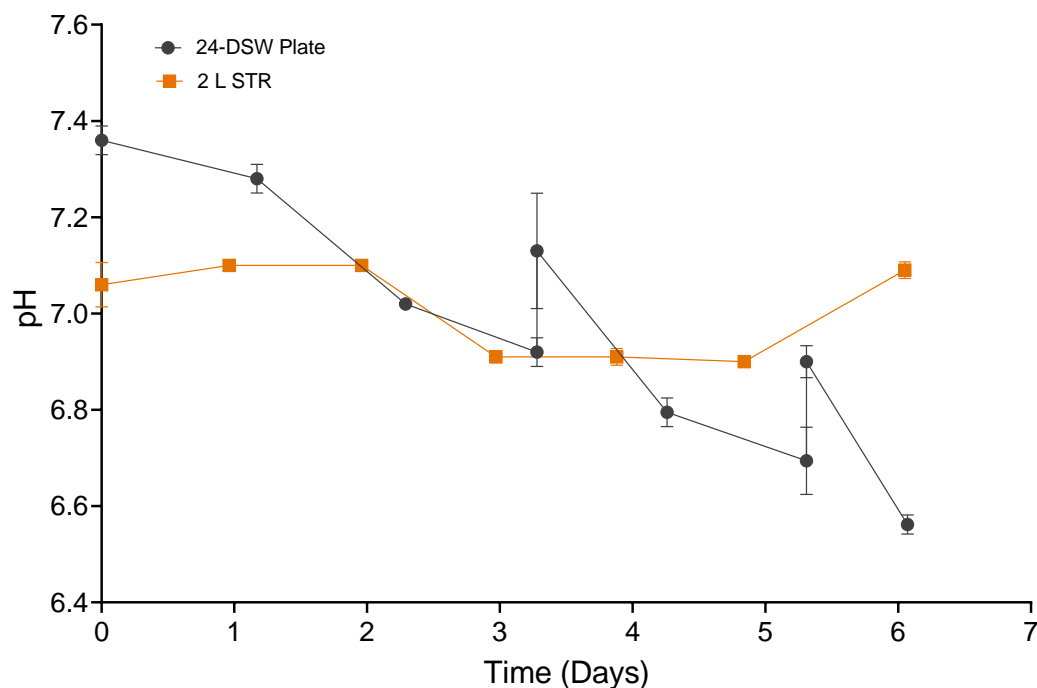


Figure 4.8: pH profile for cultivation of the 277 HEK293T stable producer cell line in 24-DSW plate and 2 L STR at matched mixing time of < 10 s. Error bars represent one standard deviation about the mean (n=3).

4.6.2 GSK's platform LVV production process using the 277 cell line

The 277 cell growth profile of GSK's platform LVV production process in 24-DSW plates and 2 L STR are depicted in Figure 4.9. The viable cell density profile for both vessel systems were comparable for the entire duration of culture. The first two days correspond to the growth phase where cells proliferate before being induced to initiate LVV production. Within 48 hours of culture, cells in both reactor formats reached the target induction cell density of 2×10^6 cells/mL. The decrease in viable cell density at day 2 corresponds to the induction time point; here, the viable cell density decreased due to dilution of the culture upon addition of induction agents. After induction, the viable cell density remained comparable, with both cultures achieving a similar cell density at the harvest time point.

High culture viability values (i.e. > 90 %) were also maintained in both systems throughout the entirety of the culture as shown in Figure 4.10. A 2-5% decrease in culture viability is generally observed after 24 hours post-induction (i.e. day 3). Studies have linked this with the onset of viral release (Ansorge et al., 2011; Petiot et al., 2017). As the LVV buds off from the plasma membrane of the producer cell, the integrity of the membrane is compromised which may lead to apoptosis and a decrease in culture viability. A similar trend was also observed in Figure 4.10, however, it should be noted that the decrease in viability after day 3 was limited, with values still above 90% at the end of the culture.

The glucose and lactate concentration profiles (Figure 4.11 and 4.12 respectively) were comparable in both vessels up until the induction time point (i.e. until day 2). Thereafter, glucose depletion and resulting lactate accumulation was greater in the 2 L STR compared to the microwell plate. As discussed in the previous section, this trend in metabolites post-induction could be explained by the contrasting pH profiles for both systems. For the STR, the pH was maintained around the set-point of pH 7.0 through the controlled addition of sodium carbonate base and CO₂. However, no such control was available in the microwell system. According to Figure 4.13, the microwell pH decreased immediately after induction (i.e. below 6.8) as the cellular metabolic activity increased. Around the same time point, a plateau in lactate accumulation for the 24-DSW plate was also observed, which is likely due to lactate co-metabolism. Perhaps cells may be consuming lactate around this time point to also help towards LVV production. Lactate plays a vital role in providing carbon atoms for acetyl CoA and fatty acid synthesis (Henry et al., 2011). Through the action of lactate dehydrogenase, lactate can be converted back into pyruvate and subsequently acetyl CoA (Henry et al., 2011). In LVV production, fatty acids serve as the building blocks for the lipid components of the viral membrane whilst acetyl CoA is involved in lipid synthesis and is a critical precursor for fatty acid biosynthesis (Rodrigues et al., 2009). Fatty acids and acetyl CoA are also involved in protein synthesis and post-translational modifications, such as glycosylation, which is necessary for proper viral protein function and assembly (Rodrigues et al., 2009).

A comparison of the LVV productivity profile in the 24-DSW plate and 2 L STR is shown in Figure 4.14. Several methods were used to characterise the LVV productivity. The infectious titre method was used to measure the number of functional LVV particles produced whilst the physical titre method was used to estimate the total number of virus particles generated, whether infectious or not, by measuring p24 concentration. In Figure 4.14, both titres were normalised relative to the STR to facilitate easier comparison between both systems. Dividing the infectious titre with the physical titre gives an infectivity ratio in terms of the number of transducing units per pg of p24 protein (TU/pg p24). This ratio provides an indication of the quality of LVV particles produced. A higher ratio of TU per pg p24 signifies a higher infectivity since there are more transducing units in a given quantity of virus particles. Lastly, the cell specific productivity normalises LVV production relative to the cell density at induction. This way, any bias relating to differences in induction cell densities between conditions is removed thus providing an alternative method of comparison. According to Figure 4.14, all four measures of LVV productivity showed good similarity between both vessel formats. In addition, a t-test confirmed any differences between the two systems were statistically insignificant at 95 % confidence level. Overall, these findings demonstrate that mixing time is a good basis for scale translation and yields comparable LVV productivity.

4.6 | SCALE TRANSLATION OF 277 STABLE CELL LINE CULTURE AT MATCHED MIXING TIME

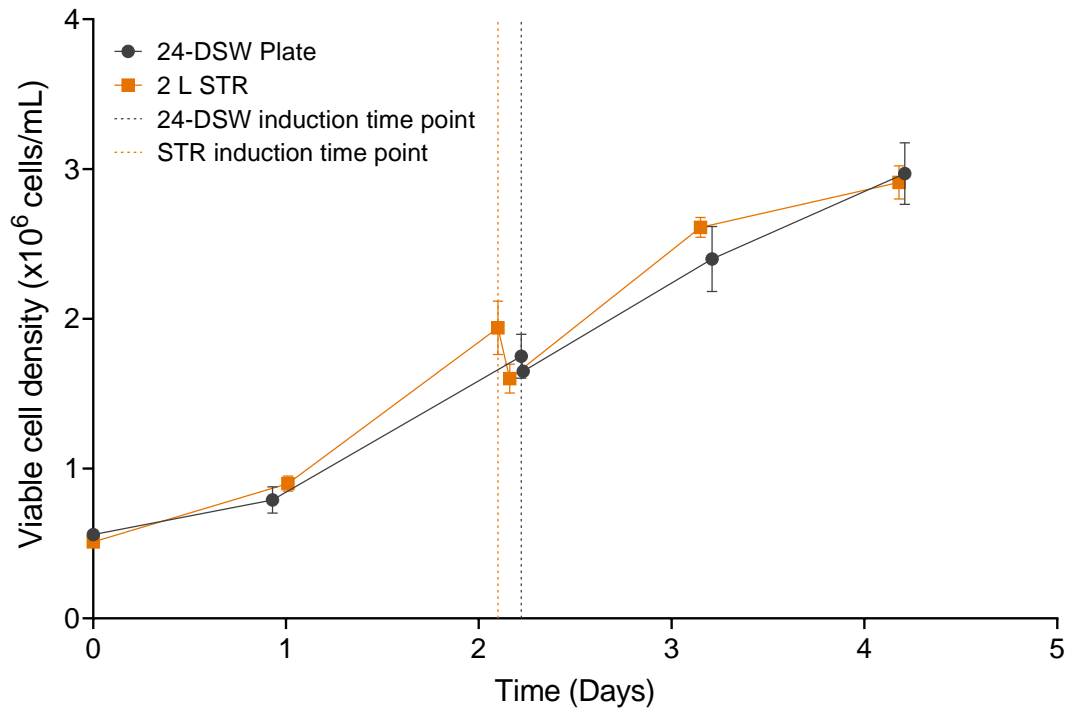


Figure 4.9: Viable cell density profile for cultivation of GSK's platform LVV production process using 277 cell line in 24-DSW plate and 2 L STR at matched mixing time of < 10 s. Error bars represent one standard deviation about the mean (n=3).

4 | DEVELOPING A HIGH-THROUGHPUT SCALE-DOWN MODEL OF GSK'S PLATFORM 277 HEK293T STABLE CELL LINE CULTIVATION PROCESS IN 2 L STIRRED TANK REACTORS

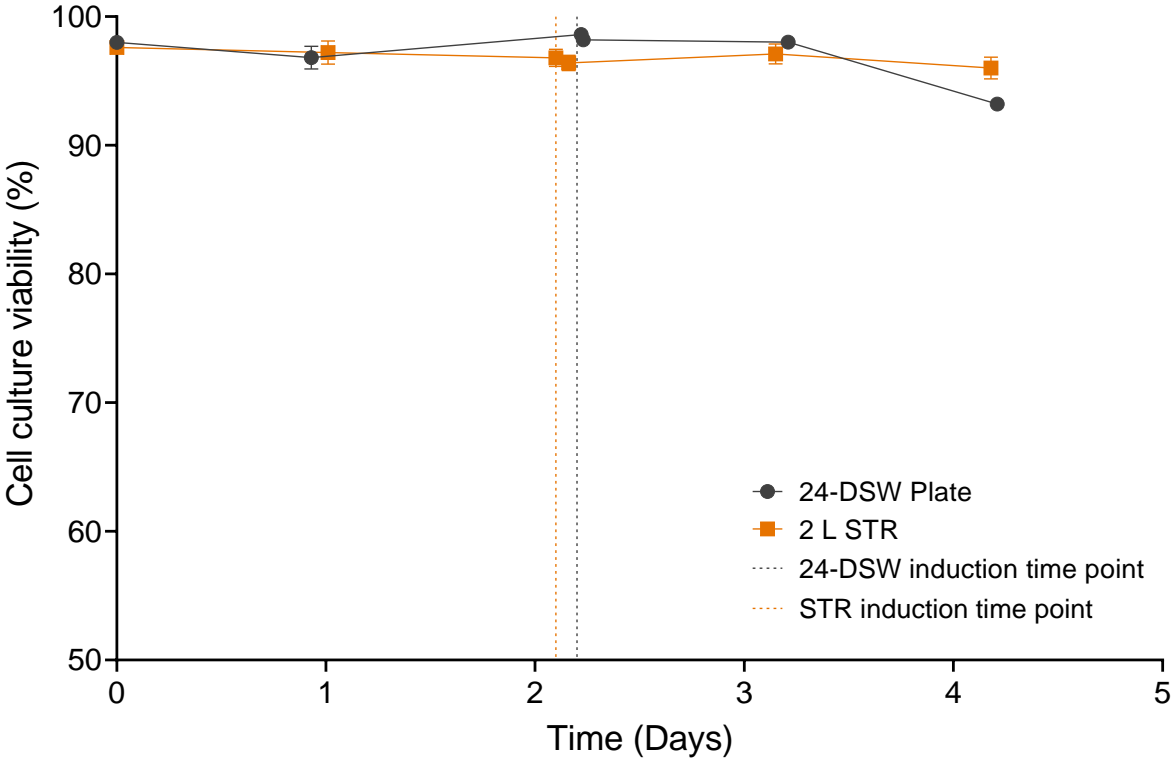


Figure 4.10: Culture viability profile for cultivation of GSK's platform LVV production process using 277 cell line in 24-DSW plate and 2 L STR at matched mixing time of < 10 s. Error bars represent one standard deviation about the mean (n=3).

4.6 | SCALE TRANSLATION OF 277 STABLE CELL LINE CULTURE AT MATCHED MIXING TIME

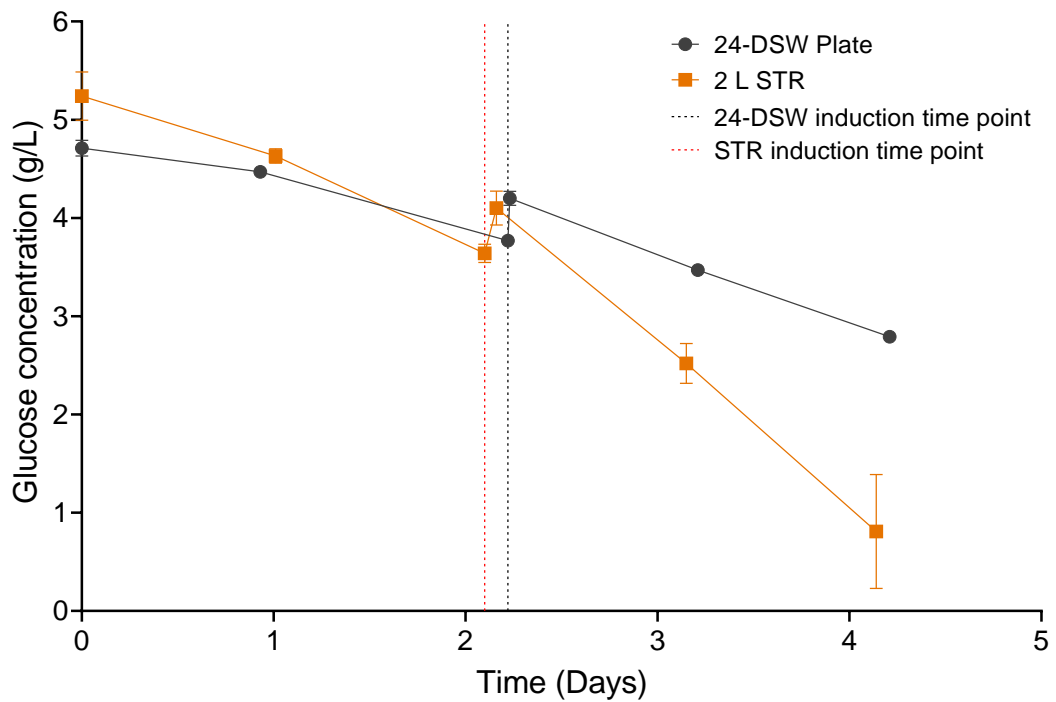


Figure 4.11: Glucose concentration profile for cultivation of GSK's platform LVV production process using 277 cell line in 24-DSW plate and 2 L STR at matched mixing time of < 10 s. Error bars represent one standard deviation about the mean (n=3). Note: For day 0 and day 2 time points, n = 2 is reported as the data for one vessel at each time point was considered to be erroneous i.e. the measurements from the metabolite analyser were below the lower limit detection range suggesting the target metabolites were not detected in the sample.

4 | DEVELOPING A HIGH-THROUGHPUT SCALE-DOWN MODEL OF GSK'S PLATFORM 277 HEK293T STABLE CELL LINE CULTIVATION PROCESS IN 2 L STIRRED TANK REACTORS

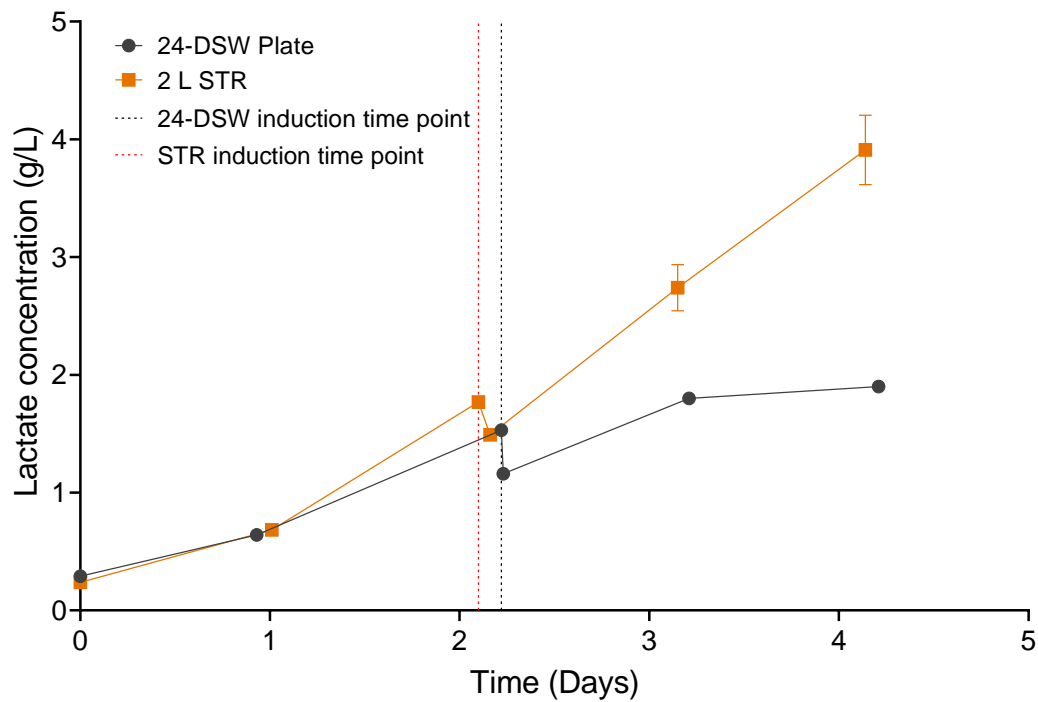


Figure 4.12: Lactate concentration profile for cultivation of GSK's platform LVV production process using 277 cell line in 24-DSW plate and 2 L STR at matched mixing time of < 10 s. Error bars represent one standard deviation about the mean (n=3). Note: For day 0 and day 2 time points, n = 2 is reported as the data for one vessel at each time point was considered to be erroneous i.e. the measurements from the metabolite analyser were below the lower limit detection range suggesting the target metabolites were not detected in the sample.

4.6 | SCALE TRANSLATION OF 277 STABLE CELL LINE CULTURE AT MATCHED MIXING TIME

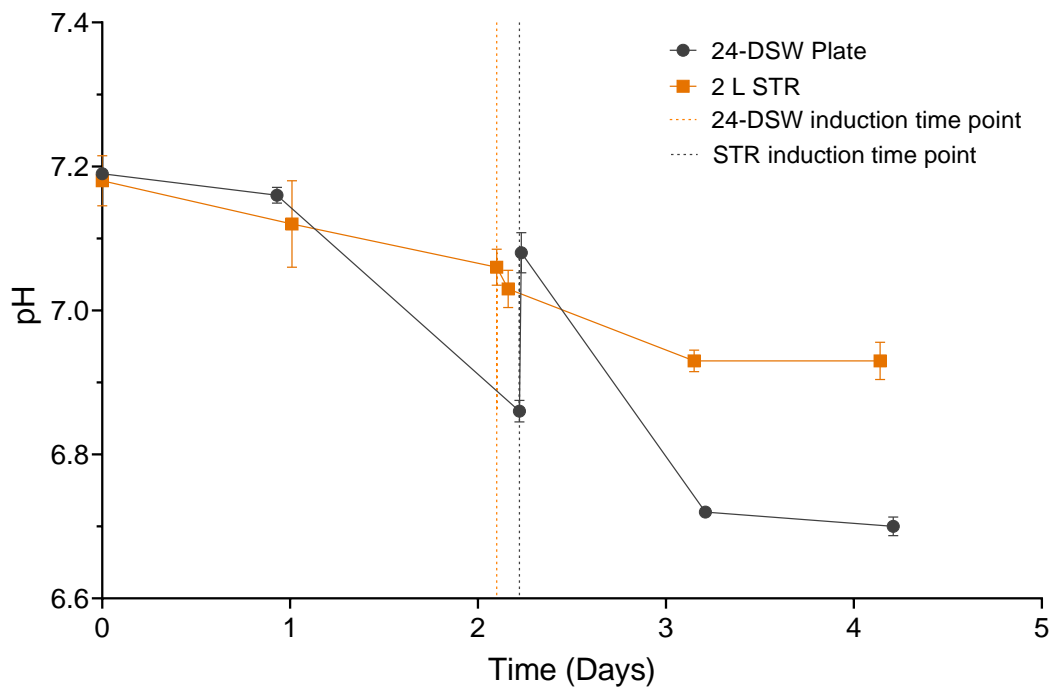


Figure 4.13: pH profile for cultivation of GSK's platform LVV production process using 277 cell line in 24-DSW plate and 2 L STR at matched mixing time of < 10 s. Error bars represent one standard deviation about the mean (n=3).

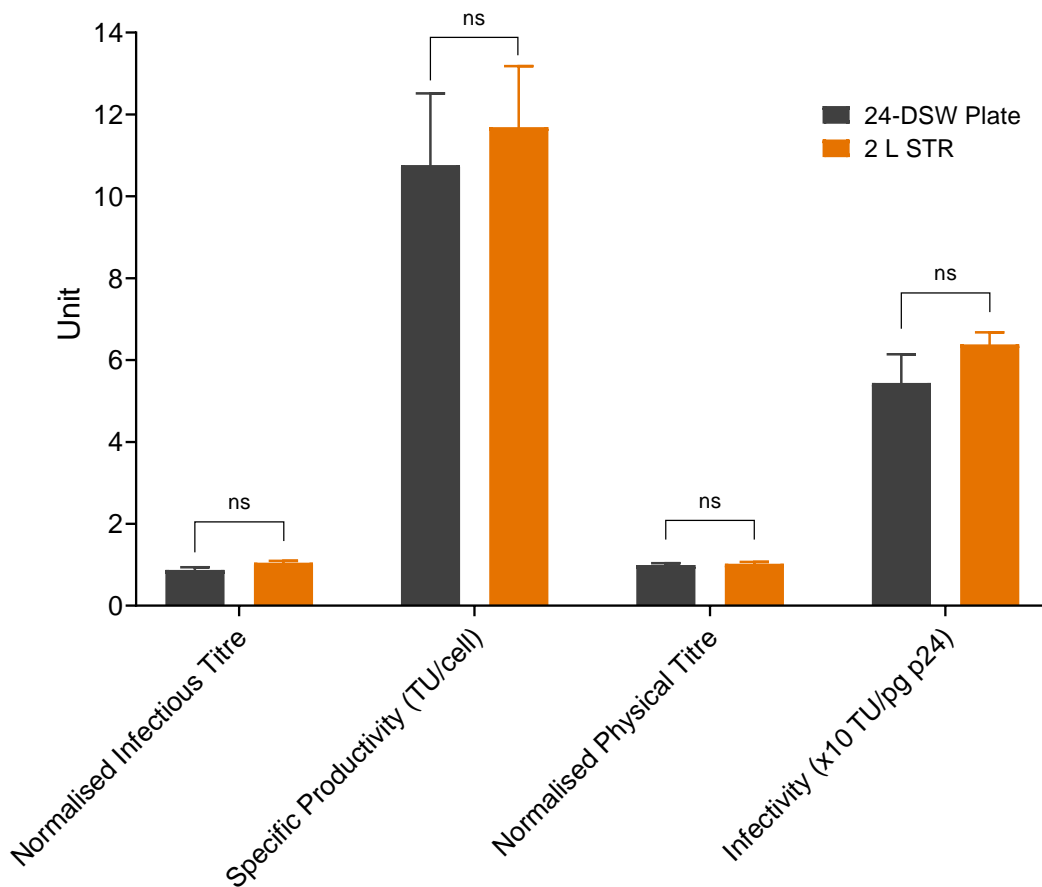


Figure 4.14: LVV productivity profile in 24-DSW plate and 2 L STR at matched mixing time of < 10 s. The infectious titre and physical titre values were normalised relative to the 2 L STR. Error bars represent one standard deviation about the mean (n = 3). Statistical comparisons were done using t-test at 95% confidence level: ns: p-value > 0.05.

4.6.3 Discussion

This work has demonstrated that mixing time can be used as a scaling parameter for HEK293T stable producer cell line culture between 24-DSW plates (operated with a large shaking diameter, $d_s = 25$ mm) and 2 L STRs. Based on the published literature, for geometrically similar reactors, a constant power per unit volume is generally the more preferred scaling option compared to mixing time. This is due to a potentially prohibitive power input requirement for large scale bioreactors in order to achieve short mixing times (Diaz and Acevedo, 1999; Schmidt, 2005; Yang et al., 2007). Larger

fluid volumes result in longer flow paths for bulk circulation, hence higher fluid velocities are required to achieve similar mixing times (Al-Ramadhani, 2015; Nienow, 1998). As the reactor scale increases, more power input is required if higher agitation rates are used in order to achieve higher velocities (Nienow, 1998). For scale-translation at small scale, the power input requirement is not limiting as successfully demonstrated by Sani and Baganz, 2016, who used mixing time as a basis to scale between 0.5 L micro-bioreactor (MBR) and 5 L STR for a GS-CHO cell line (Sani and Baganz, 2016).

In this study, scale translation was required between small scale vessels having very different geometries and flow patterns (i.e. shaken microwells to bench-scale STRs) and matched mixing time was considered as the preferred scaling method. In addition, the use of P/V was limited by the lack of accurate methods to measure the power input in microwell plates as discussed in section 4.4.

The 24-DSW model for LVV production developed in this work offers effective scale-down potential for carrying out initial high-throughput screening and optimisation studies. Compared to other scale-down systems used in early-stage bioprocess development, this 24-DSW model offers several benefits in terms of cost, flexibility and ease of use.

Micro-bioreactors (MBR) are frequently used in upstream processing for cell culture process development work. Applikon's micro-Matrix (Applikon Biotechnology B.V, Delft, Netherlands) is a MBR based on the 24-DSW platform where in each well is individually controlled for pH, DO and temperature (Wiegmann et al., 2020). The micro-Matrix's measurement and control capabilities offer a better insight into the bioprocess compared to the 24-DSW model from this study. The incorporation of pH control also means that similar metabolite profiles to the STRs could also be achieved with the micro-Matrix. However, the investment and operating costs are greater than the more simplistic 24-DSW model.

In terms of ease of use and flexibility, the 24-DSW model is also advantageous compared to MBR platforms, as these require time-consuming set-up with steps such as sterilisation and probe calibration. Furthermore, MBRs are often limited in terms of the number of vessels/wells that can be run simultaneously for a particular run. In contrast, the metal clamp system (EnzyScreen BV, AL Leiden, Netherlands) holding the 24-DSW system accommodates up to four plates giving a total of 96 wells. Hence, the 24-DSW model offers a higher degree of parallelisation making it more suitable for high-throughput screening work. Other microwell based models have also been developed using the 24-SRW plate as the model system (Barrett et al., 2010; Guy et al., 2013; Silk et al., 2010). In comparison to the 24-SRW plate, this 24-DSW scale-down model offers over 6-fold greater working volume which increases the volume for sampling and analytics. In addition, it also offers a higher experimental throughput since the larger working volume means several wells do not have to be sacrificed for a single condition.

4.7 CHAPTER SUMMARY

This work has successfully demonstrated the use of mixing time as a suitable criterion for scale translation between a microwell model and bench scale STRs. The DISMT technique was used to characterise mixing time in both vessels. Below are the key findings from this chapter:

- The mixing data exhibited a comparable pattern to the power law function proposed by Rodriguez *et al.*, 2014, affirming its suitability as a scaling law for OSRs of different sizes and geometries.
- At matched mixing time, comparable 277 HEK293T stable producer cell line growth kinetics and LVV productivity profiles were achieved in 24-DSW plate and 2 L STR cultures.

- The lack of pH control in the microwells likely contributed to differences in glucose and lactate concentration profiles.

Overall, the microwell approach offers many advantages in terms of reduction in scale of operation (by over 10-fold compared to 50 mL shake flask, and 300-fold compared to 2 L STR), reducing cost and increasing experimental throughput. However, drawbacks such as lack of parameter control (e.g. pH) mean metabolite profiles are not comparable to the more controlled environment of the 2 L STR. However, in the context of this project, given its high throughput, as well as proven scalability with STR's in terms of cell growth and LVV productivity, the 24-DSW scale down model provides an ideal platform for screening feeds based upon the depleting metabolites identified in section 3.7, and therefore developing a novel feed for enhanced 277 cell line growth.

5

DEVELOPING A NOVEL FEEDING REGIME FOR ENHANCED HEK293T STABLE CELL LINE GROWTH

5.1 INTRODUCTION AND AIMS

In Chapter 3, spent cell culture medium analysis using LC-MS identified 50 significantly depleting metabolites over the course of 277 cell line growth culture. Among these, 22 metabolites may have an important role in mammalian cell growth, making them ideal targets for developing a novel feed for improving 277 cell line growth. In Chapter 4, the 24-DSW plate was used to develop a scale-down mimic of GSK's established stable suspension LVV production process model at 2 L STR scale. The microwell model demonstrated effective scalability in terms of both cell growth and LVV productivity. The aim of this chapter is to utilise the high throughput microwell model and a DoE approach to develop a novel feed for improving 277 cell line growth based on the depleting metabolites identified from Chapter 3.

First, a commercial feed will be used to characterise a suitable feeding regime that can be employed in the initial DoE experiments. Furthermore, the commercial feed will also be used as a benchmark for assessing the performance of the novel feed. In the DoE approach, feed optimisation will be performed sequentially, starting with a screening design to identify feed supplements with a strong positive effect on cell

growth. This will be followed by additional experiments to optimise the composition of the feed as well as feeding strategy (i.e. timing and volume of feed addition). The specific objectives of this chapter are:

- Characterise the effect of commercial feed on 277 cell line growth
- Use DoE to screen feed supplements that have a positive effect on 277 stable cell line growth (DoE screening studies)
- Use DoE to optimise feed composition and feeding strategy for enhanced 277 cell line growth (Optimisation studies)

5.2 CHAPTER SPECIFIC MATERIALS AND METHODS

5.2.1 Characterising the effect of commercial feed on 277 cell line growth in section 5.3

For 277 cell line culture in the 24-DSW plates, triplicate wells were used to allow for daily sampling. The method pertaining to 24-DSW plate set-up, operation and sampling has been outlined in section 2.5. Different feeding regimes involving multiple feeding time points were evaluated when using the commercial feed in this study. According to the vendor, it is suggested to start adding the feed once cells are in exponential growth (i.e. around day 3). Thereafter, the feed can be added every 24 hours or 48 hours, depending on the requirements of the particular cell line. The vendor also recommends a 5% (v/v) feed addition volume in order to avoid cell culture dilution.

Costa *et al.*, 2014 describe a more calculated approach for determination of feed volume. This involves firstly assessing the concentration of a reference nutrient (e.g.

glucose) and using this value to determine the volume of feed medium to add to the culture in order to return the concentration of the reference nutrient to the established target value (see Equation 7 in section 2.11). The approach described by Costa *et al.*, 2014 was applied in the present study for one of the feeding regimes tested (Feeding regime 4). Glucose was selected as the reference nutrient and a constant target value of chosen 5 g/l (i.e. glucose concentration at the start of the culture) was used throughout the culture period. It is worth noting that the reference nutrient target value can potentially be adapted if consumption rates are known e.g. use a higher target value during exponential growth when glucose consumption is expected to be higher. The conditions evaluated in this study were therefore as follows:

1. **Feeding regime 1:** Add 5% (v/v) feed at day 3 and every 24 hours thereafter
2. **Feeding regime 2:** Add 5% (v/v) feed at day 3 and every 48 hours thereafter
3. **Feeding regime 3:** Add 5% (v/v) feed at day 3 and day 5 and every 24 hours thereafter
4. **Feeding regime 4:** Add calculated amount of feed in relation to concentration of glucose
5. **Negative control:** No feed addition

The methods for all analytical techniques used in this study are described in section 2.7. Cell population doubling time was calculated using equations 2 and 3 as shown in section 2.11.

5.2.2 DoE screening studies in section 5.4

For all screening studies, Design Expert v10 (Stat-Ease, Inc., Minnesota, USA) was used to generate a regular two-level factorial design whereby each factor was varied over a high and low concentration value. Table 5.1 to 5.4 summarises the factors and

concentration range tested in each study. The limits selected for each factor were adapted from relevant literature references which are detailed in the Table legend. In all the DoE designs, each condition was duplicated (i.e. $n = 2$) and five centre point replicates were also added to check for curvature in the responses. The experimental design space for all studies are shown in Table 9.6 to 9.9 under Appendix A (section 9.4.1). More details on DoE design and model evaluation are described in section 2.9. All experiments were performed using the 24-DSW plate high-throughput scale down model with operating conditions and sampling method outlined in section 2.5. The feeding regime used in the DoE studies was adapted from the optimal commercial feed regime determined in section 5.3. The method for preparing the feed conditions is discussed in section 2.2.

Table 5.1: Table of factors used in screening study 1. Minimum and maximum levels for each factor were adapted from Costa *et al.*, 2014. × MEM refers to relative to concentration in minimum essential media.

Factor	Name	Units	Minimum	Maximum
A	Essential amino acids	× MEM	0	15
B	Non-essential amino acids	× MEM	0	1
C	L-alanyl-L-glutamine	× MEM	0	15
D	Vitamins	× MEM	0	4
E	Glucose	× MEM	0	0
F	Polyamines	× MEM	0	1

Table 5.2: Table of factors used in screening study 2. Feed mixture comprises of non-essential amino acids, vitamins, glucose and polyamines. For essential amino acids, L-alanyl-L-glutamine, inorganic salts and components of feed mixture, the minimum and maximum levels were adapted from Costa *et al.*, 2014. The limits tested for lipids, insulin and sodium pyruvate were adapted from MilliporeSigma. The limits for IGF-1 was adapted from the vendor Repligen (U.S.A). × MEM refers to relative to concentration in minimum essential media.

Factor	Name	Units	Minimum	Maximum
A	Essential amino acids	× MEM	0	15
B	L-alanyl-L-glutamine	× MEM	0	15
C	Lipids	dilution	0	0.05 (1 in 20)
D	Inorganic salts	× MEM	0	1
E	Insulin	mg/mL	0	2.5
F	IGF-1	µg/mL	0	2.5
G	Sodium pyruvate	mM	0	1
H	Feed mixture	Relative concentration ¹	0	1

¹ For feed mixture, the upper limit value of 1 corresponds to the following concentration of the constituent components: non-essential amino acids (0.5× MEM), vitamins (2× MEM), glucose (4× MEM) and polyamines (0.5× MEM).

Table 5.3: Table of factors used in screening study 3. Minimum and maximum levels for each factor were adapted from Salazar *et al.*, 2016.

Factor	Name	Units	Minimum	Maximum
A	L-Aspartic acid	g/L	0	0.4
B	L-Leucine	g/L	0	1.6
C	L-Valine	g/L	0	1.4
D	L-Lysine hydrochloride	g/L	0	2.2
E	L-Isoleucine	g/L	0	1.6
F	L-Arginine hydrochloride	g/L	0	3.8
G	L-Serine	g/L	0	0.3
H	L-Asparagine	g/L	0	0.4

Table 5.4: Table of factors used in screening study 4. Minimum and maximum levels for essential amino acids, choline chloride, folic acid and putrescine dihydrochloride were adapted from Costa *et al.*, 2014. Limits tested for L-Ornithine was adapted from Cell Guidance Systems (www.cellgs.com). No references were available for L-Norvaline and 2-Aminoisobutyric acid; the range defined for L-Ornithine was also tested for these metabolites. × MEM refers to relative to concentration in minimum essential media.

Factor	Name	Units	Minimum	Maximum
A	Essential amino acids	× MEM	0	15
B	L-Ornithine	g/L	0	5
C	L-Norvaline	g/L	0	5
D	2-Aminoisobutyric acid	g/L	0	5
E	Choline chloride	g/L	0	5
F	Folic acid	g/L	0	0.5
G	Putrescine dihydrochloride	g/L	0	1

5.2.3 Optimisation studies in section 5.5

In optimisation study 1, a DoE approach was used to optimise the amino acid concentration for enhanced cell growth. A central composite design was generated where each factor was set to 5 levels: plus and minus alpha (axial points), plus and minus 1 (factorial points) and the centre point. The design summary is shown in Table 5.5.

In optimisation study 2, operating conditions were selected manually to test high concentrations of essential amino acids. Conditions tested are summarised in Table 5.6. In optimisation study 3, a DoE approach was used to optimise the feeding regime of the novel feed. A D-optimal response surface design was generated. D-optimal designs are best suited to estimate the effects of factors whilst predicting curvature in the response. The design summary is shown in Table 5.7. For the DoE studies,

conditions in optimisation study 1 were run in triplicate (i.e. $n = 3$), whilst conditions in optimisation study 3 were run in duplicate (i.e. $n = 2$). The experimental design space for the two DoE studies are shown in Table 9.10 and 9.11 respectively under Appendix A (section 9.4.2). Further details on DoE design and model evaluation are described in section 2.9.

For optimisation study 2, each condition was duplicated (i.e. $n = 2$). All experiments were performed using the 24-DSW plate high-throughput scale down model with operating conditions and sampling method outlined in section 2.5. The feeding regime used in optimisation study 1 was adapted from the optimal commercial feed regime determined in section 5.3. In optimisation study 2, the day 6 feed from the commercial feed regime was excluded due to cell toxicity observed with high essential amino acids concentration at day 6. The method for preparing the feed conditions is discussed in section 2.2.

Table 5.5: Table of factors used in optimisation study 1.

Factor	Name	Units	-alpha	+alpha	Minimum	Maximum
A	Essential amino acids	× MEM	0	30	4.4	25.6
B	Non-essential amino acids	× MEM	0	10	1.5	8.5

Table 5.6: Conditions tested in optimisation study 2.

Condition	Essential amino acid concentration (× MEM)
1	30
2	35
3	40
4	45
5	50
6	No feed

Table 5.7: Table of factors used in optimisation study 3.

Factor	Name	Units	Minimum	Maximum
A	Day 3 feed amount	%	0	5
B	Day 4 feed amount	%	0	5
C	Day 5 feed amount	%	0	5
D	Day 6 feed amount	%	0	5

5.3 CHARACTERISING THE EFFECT OF A COMMERCIAL HEK293 FEED ON 277 CELL LINE GROWTH

According to the vendor, the commercial feed used in this study has been formulated to increase viable cell density and culture duration in suspension-adapted HEK293 cell lines. The feed is chemically-defined and free of animal components. In this study, the aim was to characterise the effect of the commercial feed on 277 cell line growth, as well as comparing different feeding regimes. The conditions evaluated in this study have been outlined in section 5.2.1.

The viable cell density and natural logarithmic plot of viable cell density are demonstrated in Figure 5.1A and Figure 5.1B respectively. The cell culture viability profile is shown in Figure 5.2. The general trend observed is that all conditions where commercial feed was added performed better than the control condition i.e. no feed. Figure 5.1 shows that for the ‘no feed’ condition, the maximum VCD of 5×10^6 cells/mL was achieved at day 5. A steep decline in viability was also observed thereafter. For the four feeding regimes, the maximum VCD was not only 2-fold higher (i.e. $\sim 10 \times 10^6$ cells/mL) but it was also achieved 48 hours later. Figure 5.2 also shows that culture viability only started to decrease between day 6 and day 7. Therefore, the period of exponential growth was extended by 2 days. This shows that essential nutrients that could be depleting around day 5 were being supplemented by the feed and hence promoting prolonged cell growth.

Figure 5.1 also shows that feed regimes 1, 2 and 3 had similar growth profiles. For all conditions, there was no apparent lag phase as cells were doubling approximately every 24 hours until day 2 as shown in Table 9.4 under Appendix A (section 9.1.4). After day 2, feed regimes 1, 2 and 3 had similar growth profiles. Between day 2 and day 6, cells were actively growing where the average population doubling time was 46.9, 54.7 and 58.2 hours respectively (i.e. average of day 2 to day 6 data shown in Table 9.4 under Appendix A). Between day 6 and day 7, the average population doubling time increased to 116.6, 161.8 and 109.5 hours respectively (i.e. average of day 6 and day 7 data shown in Table 9.4 under Appendix A) indicating the cultures were transitioning into stationary growth period. The mean maximum VCD for feed regime 1 (i.e. 9.4×10^6 cells/mL), was higher compared to regimes 2 (8.6×10^6 cells/mL) and 3 (8.8×10^6 cells/mL). However, a Student’s t-test showed that the difference was not statistically significant at 95% confidence level. In terms of culture viability, feed regime 3 had the most favourable profile with culture viability greater than 90% even at day 8. For feed regimes 1 and 2, the decline in culture viability was more pronounced; culture viability started to decline after day 6 and were just below 90% at day 7.

After day 2, feed regime 4 had a different cell growth trajectory compared to the other feed regimes, but achieved similar endpoints. Up until day 5, feed regime 4 had a similar

growth profile to the 'no feed' condition despite initiating feeding at day 3. For the other feed regimes, the addition of feed at day 3 seemed to have an immediate effect with higher VCD's measured on day 4. However, the cells in feed regime 4 continued to grow beyond day 5 unlike the 'no feed' condition, demonstrating the feed was indeed effective. A maximum VCD of 9.6×10^6 cells/mL was achieved at day 7 similar to the other feed regimes. The lower VCD's observed for feed regime 4 compared to other feed regimes up to day 6 could be a result of cell culture dilution upon addition of the feed in this regime. For the other feed regimes (i.e. 1, 2 and 3), the method recommended by the vendor (i.e. 5% v/v feed addition) required an equal amount of cell culture to be removed in order to maintain the final volume. Therefore, the effects of cell culture dilution were not as apparent for these feed regimes.

For all four feed regimes, the VCD profile (Figure 5.1A) indicates a rapid decline in cell growth after day 7. From Figure 5.1B, it is evident that cells in feed regimes 1, 2 and 3 had transitioned from stationary phase into death phase around day 7. However, no apparent stationary phase is evident for feed regime 4, rather cells appear to have transitioned directly from exponential phase into death phase. The steep decline may have been exaggerated by the effects of cell culture dilution; there was no increase in VCD after day 7 to offset the dilution caused by feed addition resulting in lower cell counts. Nutrient limitation may be ruled out as a possible reason for the cell growth arrest since feed was added in all four feed regimes at day 7.

Glucose depletion is also not likely to be the root cause for growth arrest as Figure 5.3 shows that glucose concentration was kept above 3 g/L for the entire culture duration. Therefore, the accumulation of growth inhibiting toxic metabolites is likely to be a factor contributing to the growth arrest. In mammalian cell culture, it has been widely reported that lactate and ammonium accumulate to levels that inhibit cell growth and productivity (Freund and Croughan, 2018). Lactate is a by-product of glucose metabolism, whilst ammonium is produced by the metabolism of amino acids such as glutamine. The lactate profile (Figure 5.4) shows that the maximum concentration reached was around 2.5 g/L, which is well below the growth inhibitory level reported by Freund and Croughan, 2018 (i.e. 5–10 g/L). At low pH conditions (i.e. $\text{pH} < 6.8$),

HEK293 cells trigger a shift in metabolism towards lactate consumption as a way to self-regulate culture pH around the cells (Liste-Calleja et al., 2015; Román et al., 2018). This explains why lactate did not accumulate to high levels in the uncontrolled pH environment of the microwell culture. However, the ammonium profile (Figure 5.5) indicates significant accumulation as the culture progressed. According to Freund and Croughan, 2018, ammonium concentration above 0.07 g/L (i.e. 4 mM) can be detrimental for mammalian cell culture. For all four feed regimes, the ammonium concentration after Day 7 was in excess of 0.08 g/L which is above the acceptable threshold. Hence, significant ammonium accumulation after day 7 may have contributed to the observed cell growth arrest.

In order to determine the most suitable feed regime, the cell growth performance was evaluated against the total amount of feed used in each condition. This is summarised in Table 5.8. Feed regime 1 and 4 utilised the most amount of feed and hence may not be as cost effective compared to other conditions upon scale-up. Although maximum VCDs were higher in feed regime 1 and 4, the Student's t-test confirmed that they were still comparable to those achieved with conditions that used lower feed volumes. Hence, the increased amount of feed used in feed regime 1 and 4 may not be justified. Feed regime 2 utilised the least amount of feed and hence may be considered the most cost-effective among the four methods. Although it achieved a high maximum VCD, the less frequent feeding led to lower viability values after day 6 compared to the other conditions. Feed regime 3 was the second most cost-effective method in terms of the total volume of feed utilised. Not only did it achieve a high maximum VCD, but the cell culture was also most viable with this feed regime. Hence, feed regime 3 will be implemented in the subsequent DoE screening studies.

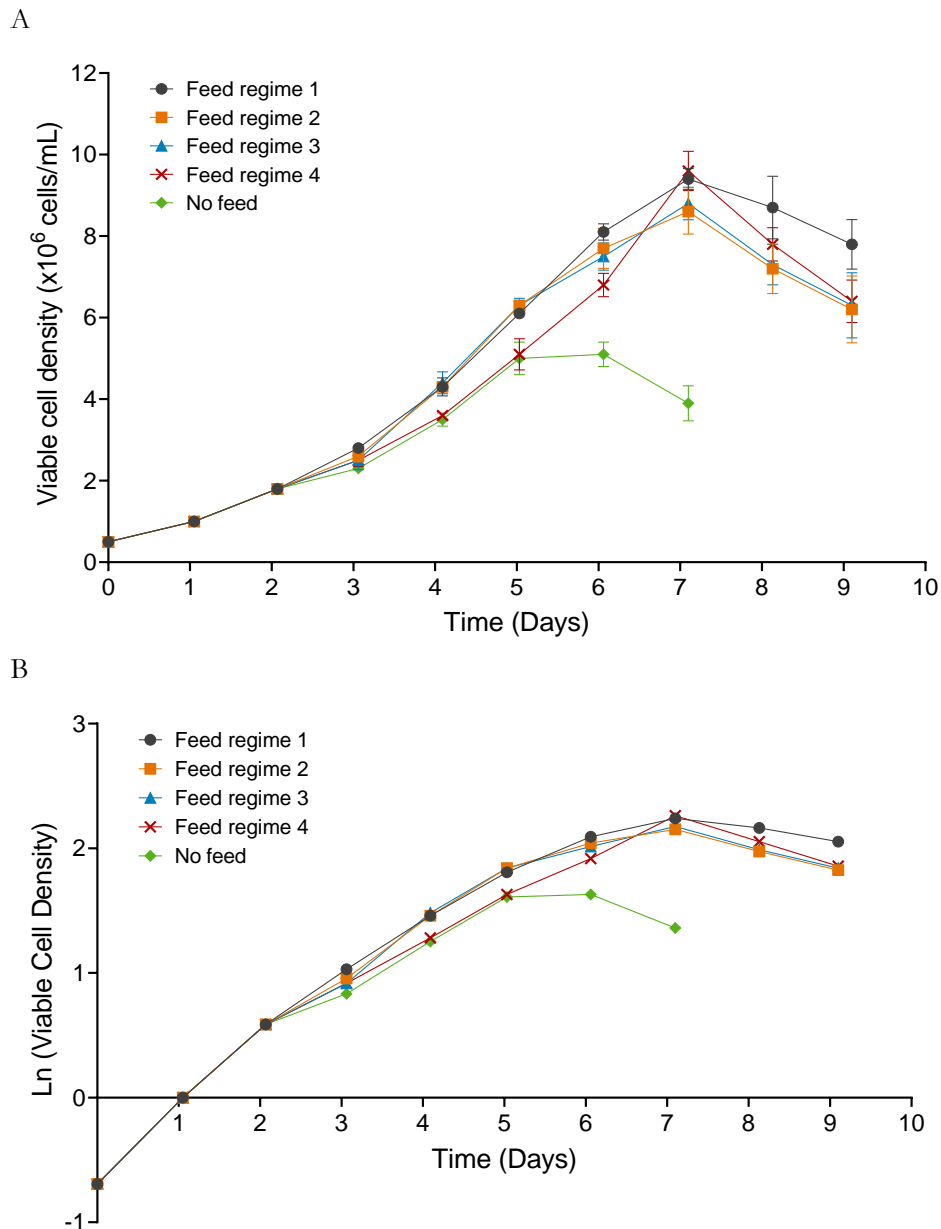


Figure 5.1: (A) VCD profile for the 277 stable cell line cultivated in 24-DSW plate with different feeding regimes of the commercial feed. (B) Natural logarithm of viable cell density plotted against time. Feed regime 1: 5% (v/v) feed addition at day 3 and every 24 hours thereafter; Feed regime 2: 5% (v/v) feed addition at day 3 and every 48 hours thereafter; Feed regime 3: 5% (v/v) feed addition at day 3 and day 5 and every 24 hours thereafter; Feed regime 4: Add calculated amount of feed in relation to concentration of glucose. Error bars represent one standard deviation about the mean (n=3).

5.3 | CHARACTERISING THE EFFECT OF A COMMERCIAL HEK293 FEED ON 277 CELL LINE GROWTH

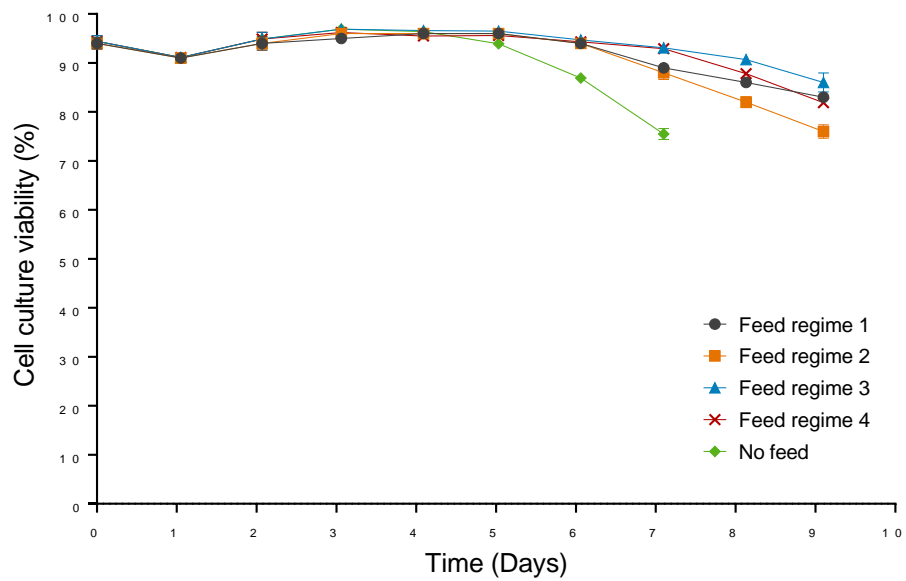


Figure 5.2: Culture viability profile for the 277 stable cell line cultivated in 24-DSW plate with different feeding regimes of the commercial feed. Feed regime 1: 5% (v/v) feed addition at day 3 and every 24 hours thereafter; Feed regime 2: 5% (v/v) feed addition at day 3 and every 48 hours thereafter; Feed regime 3: 5% (v/v) feed addition at day 3 and day 5 and every 24 hours thereafter; Feed regime 4: Add calculated amount of feed in relation to concentration of glucose. Error bars represent one standard deviation about the mean (n=3).

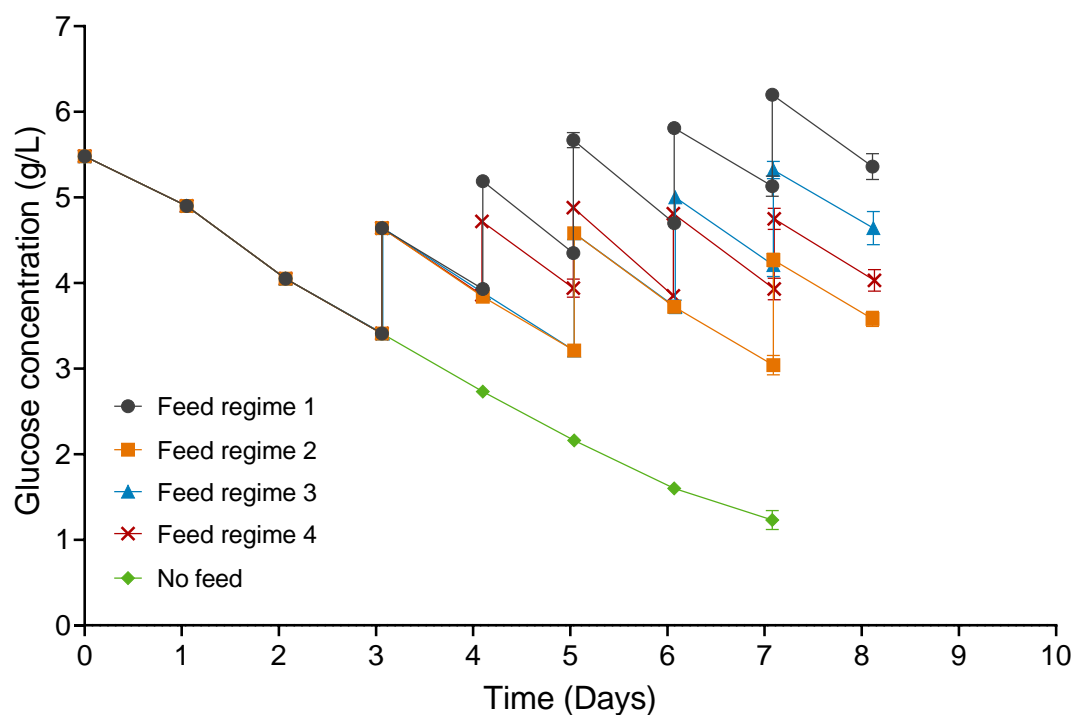


Figure 5.3: Glucose concentration profile for the 277 stable cell line cultivated in 24-DSW plate with different feeding regimes of the commercial feed. Feed regime 1: 5% (v/v) feed addition at day 3 and every 24 hours thereafter; Feed regime 2: 5% (v/v) feed addition at day 3 and every 48 hours thereafter; Feed regime 3: 5% (v/v) feed addition at day 3 and day 5 and every 24 hours thereafter; Feed regime 4: Add calculated amount of feed in relation to concentration of glucose. Error bars represent one standard deviation about the mean (n=3).

5.3 | CHARACTERISING THE EFFECT OF A COMMERCIAL HEK293 FEED ON 277 CELL LINE GROWTH

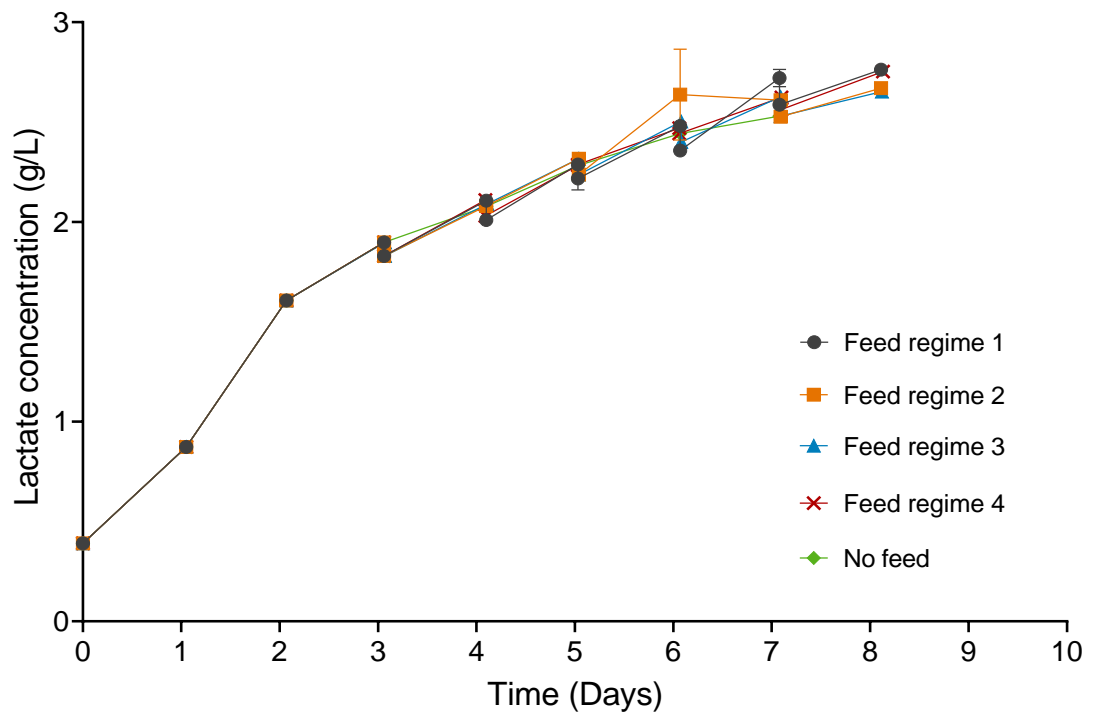


Figure 5.4: Glucose concentration profile for the 277 stable cell line cultivated in 24-DSW plate with different feeding regimes of the commercial feed. Feed regime 1: 5% (v/v) feed addition at day 3 and every 24 hours thereafter; Feed regime 2: 5% (v/v) feed addition at day 3 and every 48 hours thereafter; Feed regime 3: 5% (v/v) feed addition at day 3 and day 5 and every 24 hours thereafter; Feed regime 4: Add calculated amount of feed in relation to concentration of glucose. Error bars represent one standard deviation about the mean (n=3).

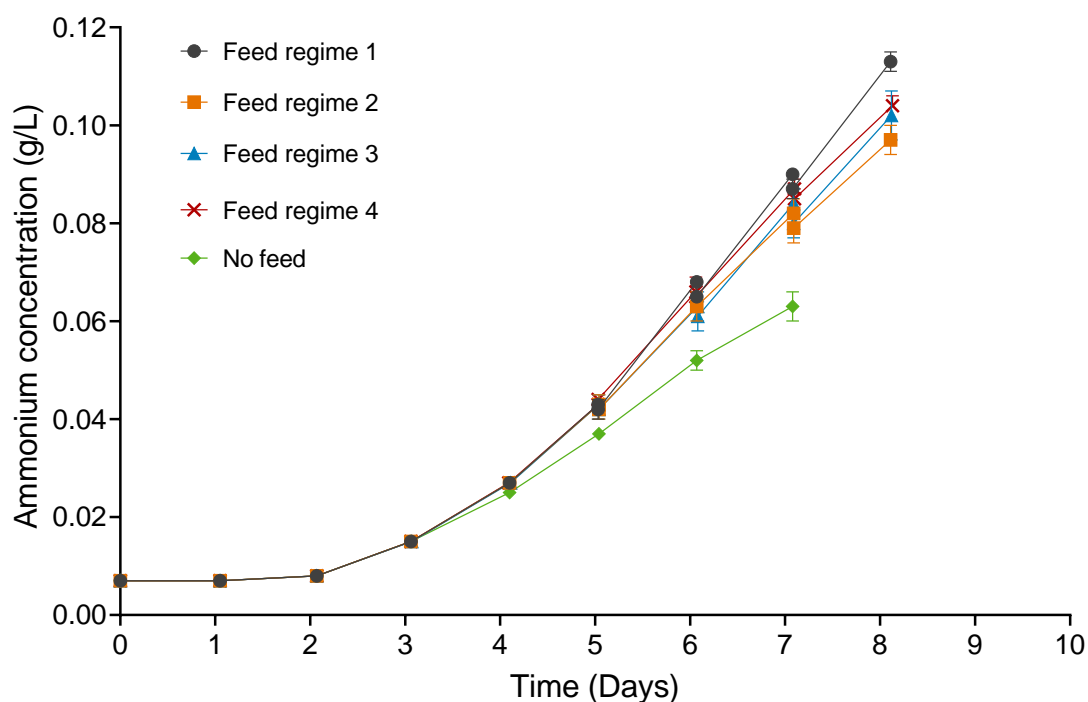


Figure 5.5: Ammonium concentration profile for the 277 stable cell line cultivated in 24-DSW plate with different feeding regimes of the commercial feed. Feed regime 1: 5% (v/v) feed addition at day 3 and every 24 hours thereafter; Feed regime 2: 5% (v/v) feed addition at day 3 and every 48 hours thereafter; Feed regime 3: 5% (v/v) feed addition at day 3 and day 5 and every 24 hours thereafter; Feed regime 4: Add calculated amount of feed in relation to concentration of glucose. Error bars represent one standard deviation about the mean (n=3).

Table 5.8: Summary of cell culture parameters and amount of feed used for each feed regime.

	Total volume of feed used per well (μL)	Maximum VCD (×10 ⁶ cells/mL)	Culture viability at maximum VCD (%)
Feed regime 1	510	9.4 ± 0.3	89.9 ± 0.1
Feed regime 2	294	8.6 ± 0.6	88.8 ± 1.4
Feed regime 3	408	8.8 ± 0.4	93.1 ± 0.9
Feed regime 4	495.2	9.6 ± 0.5	92.9 ± 0.3
No feed	0	5.0 ± 0.4	93.9 ± 0.9

5.4 DESIGN OF EXPERIMENTS BASED SCREENING OF FEED SUPPLEMENTS TO INCLUDE IN THE NOVEL FEED FOR ENHANCING 277 CELL LINE GROWTH

Earlier in section 3.7, 22 of the 50 significantly depleting metabolites were either widely referenced in literature to have an important role in mammalian cell growth and/or demonstrated very significant depletion prior to growth arrest. Hence, these 22 metabolites outlined in Table 5.9 have been identified as potential targets for developing a novel feed for improving 277 cell growth.

In this study, the aim was to use DoE to screen the 22 depleting metabolites in order to assess which of them demonstrate a strong positive effect on cell growth. In addition to the depleting metabolites from LC-MS, a few additional compounds from literature known to be included in mammalian cell culture feeds were included in the screening studies. To evaluate all the compounds in a single screening experiment, a very high experimental throughput would be required, which is not feasible even using the 24-DSW plate model. Hence, the DoE screening was carried out over multiple studies as discussed in the following sections.

Table 5.9: Summary of 22 potential feed targets from depleting metabolites identified using LC-MS analysis.

	Metabolite	Type
1	L-Lysine	Essential amino acid
2	L-Valine	Essential amino acid
3	L-Leucine	Essential amino acid
4	L-Arginine	Essential amino acid
5	Isoleucine	Essential amino acid
6	L-Phenylalanine	Essential amino acid
7	L-Methionine	Essential amino acid
8	L-glutamine	Essential amino acid
9	Asparagine	Non-essential amino acid
10	Aspartic acid	Non-essential amino acid
11	L-Serine	Non-essential amino acid
12	L-alanyl-L-glutamine	Peptide
13	Choline	Vitamin
14	Pantothenic acid (Vitamin B5)	Vitamin
15	Folic acid (Vitamin B9)	Vitamin
16	L-Ornithine	Non proteinogenic Amino acid
17	L-Norvaline	Non proteinogenic Amino acid
18	2-Aminoisobutyric acid	Non proteinogenic Amino acid
19	Histamine	Organic compound
20	Glucose	Carbohydrate
21	Putrescine	Polyamine
22	D-Pipecolic acid	Acid

5.4.1 Screening study 1 – Assessment of metabolites groups common to the LC-MS analysis and mammalian cell culture feeds

Costa *et al.*, 2014 have summarised some of the nutrients that are commonly found in most mammalian cell culture feeds as shown earlier in Table 1.5. In the first screening study, the aim was to assess common metabolite groups from Table 1.5 and the depleting metabolites from Table 5.9. These include:

1. Essential amino acids
2. Non-essential amino acids
3. L-alanyl-L-glutamine
4. Vitamins
5. Glucose
6. Polyamines

The separate essential amino acids, non-essential amino acids, vitamins and polyamines from Table 5.9 were grouped together and considered as individual factors. Grouping the compounds enabled the number of factors to be reduced from 16 to 6, thus permitting a more manageable experimental design space. As a first screen, use of the complete formulations was justified since the goal was to identify compound groups with a positive response on cell growth. However, it is worth mentioning that the metabolites from Table 5.9 have also been studied separately in later screening studies to assess their individual effect on growth. Commercially available pre-formulated solutions of essential amino acids, non-essential amino acids, vitamins and polyamines were used in this study. The complete formulation of these solutions are shown in Table 9.12 – 9.15 under Appendix A (section 9.4.3). For all four compound groups, the solutions include additional elements to those from Table 5.9. For example, for

essential amino acids, the Gibco™ MEM Essential Amino Acids solution (ThermoFisher Scientific, U.S.A) contains all 12 essential amino acids rather than only the 8 from Table 5.9.

The Gibco™ MEM Essential Amino Acids solution does not contain L-glutamine as part of the formulation. Hence, L-glutamine in the form of the dipeptide L-alanyl-L-glutamine was considered as a separate factor in the DoE design. As mentioned previously, in this form, glutamine does not spontaneously breakdown to form ammonia, rather, cells cleave the dipeptide bond to release L-glutamine as needed.

With feeding only initiated at day 3, the effect of the feed on cell growth would be most apparent around the timepoint when cells transition into stationary phase (i.e. day 5). Hence, the responses analysed included the VCD and culture viability from day 5 until the end of the culture (i.e. day 7). All 6 responses generated significant models (i.e. model p-value < 0.05) where the lack of fit was also not significant. The ANOVA summary for all the responses are shown in Table 5.10 to 5.15. Two important values from the ANOVA table are the F-statistic and the corresponding p-value. The F-statistic is the ratio of the mean squares to the mean squares error. In other terms, it is the variation between sample means divided by the variation within samples. The larger the F-statistic, the greater the variation between sample means relative to the variation within the samples. Thus, the larger the F-statistic, the greater the evidence that there is a difference between the group means. The p-value that corresponds to the F-statistic is used to determine if the difference between group means is statistically significant. For example, at 95% confidence level, a p-value less 0.05 means there is a statistically significant difference between the means of sample groups. According to the ANOVA data, the only factor which was a significant model term in every response was essential amino acids (A-term). In most responses, essential amino acids also had the largest F-statistic and smallest p-value indicating it was the most sensitive factor affecting 277 cell growth.

Model graphs were generated to illustrate the trend in each response, as shown in Figure 5.6 to 5.11. All the models suggest that essential amino acids had a strong

positive effect on VCD and culture viability i.e. increasing the concentration of essential amino acids resulted in higher VCD and cell viability values. Essential amino acids are critical for the growth and maintenance of cells (Salazar et al., 2016). According to Arora, 2013, their concentration also determines the maximum achievable VCD. Given that cells cannot synthesise essential amino acids, the data from this study confirms their importance of these being included as a component of the 277 cell growth feed.

Other significant model terms with positive effects on growth included non-essential amino acids (B-term), L-alanyl-L-glutamine (C-term), vitamins (D-term) and polyamines (F-term). Non-essential amino acids was significant in the models for day 5 and day 7 VCD. L-alanyl-L-glutamine was only significant when interacting with essential amino acids (AC-term) for day 5 VCD. Vitamins only showed significance in the models for day 6 VCD and culture viability. In particular, the vitamin-essential amino acid interaction (AD-term) had a greater impact on the model than vitamins alone. Polyamines had a positive effect on day 5 and day 6 cell growth models. The polyamine-essential amino acid interaction (AF-term) was also a significant term in these models. For all these factors, it is important to note that their contribution to the model (i.e. effect on VCD) was less significant compared to essential amino acids.

Glucose was a significant model term for both day 6 and day 7 models with a strong negative effect on cell growth and viability. Its effect on day 7 cell health was particularly significant as it achieved the largest F-statistic and smallest p-value. The model graphs show a strong correlation between low glucose concentration and increased cell growth. Additionally, the two factor interaction term between essential amino acids and glucose (AE-term) returned a large F-statistic on the day 6 response. Model graphs show that cell growth was reduced when glucose was present at high essential amino acid concentrations. There is no mention in the literature of any toxic by-product or interaction that forms between glucose and essential amino acids that may hinder cell growth. However, Salazar *et al.*, 2016 suggest that nutrients supplied externally during the cell culture process are capable of altering the equilibria of metabolic pathways. Perhaps, the presence of these two metabolites together may

affect the metabolic balance of the HEK293 cells causing a negative effect on cell growth. Data from section 3.6 has shown that glucose does not get fully depleted in an uncontrolled HEK293T cell culture due to initiation of lactate and glucose concomitant consumption at pH less than 6.8. Hence, for an uncontrolled cell culture system like the 24-DSW plate, glucose addition in the feed may not be necessary. Perhaps, the addition of the glucose-rich feed after day 3 may have resulted in a disruption of medium osmolality and thus affecting cell growth negatively. It has been well documented that high concentration of glucose in the medium can create osmotic stress on the cells, affecting their osmotic balance and leading to cellular damage or even cell death (Lin et al., 1999). Perhaps, the osmotic balance in conditions with high glucose and amino acid concentrations may be affected and detrimental to the cells.

To better visualise the effect of the feed on 277 cell growth, the condition with highest maximum VCD (i.e. Run 6 and 34) was plotted against the condition where no feed was added (i.e. Run 4 and 24). Table 5.16 outlines the feed composition of run 6 and 34. As shown in the table, a key feature of its feed formulation is that it has the highest concentration of essential amino acids (i.e. 15× MEM) and contains no glucose. The cell growth profile shows that higher VCD's (Figure 5.12) and culture viability (Figure 5.13) values were achieved for the cell culture where feed was added compared to 'no feed'. The maximum VCD of 5.2×10^6 cells/mL for the culture with feed addition was also higher than 4.5×10^6 cells/mL achieved for the culture with no feed. Furthermore, cells continued to grow until day 6 for the feed culture whilst growth arrest was observed by day 5 for the no feed culture.

Overall, out of the 6 factors screened, essential amino acids has the strongest effect on enhancing cell growth. Glucose was the only factor that resulted in a negative response in terms of cell growth. For the remaining factors, although a positive response was achieved, their effect on cell growth was not as significant as that of essential amino acids.

5.4 | DESIGN OF EXPERIMENTS BASED SCREENING OF FEED SUPPLEMENTS TO INCLUDE IN THE NOVEL FEED FOR ENHANCING 277 CELL LINE GROWTH

Table 5.10: ANOVA summary of Day 5 VCD response from screening study 1. Data generated using Design Expert v10 (Stat-Ease, Inc., Minnesota, U.S.A). df is degrees of freedom.

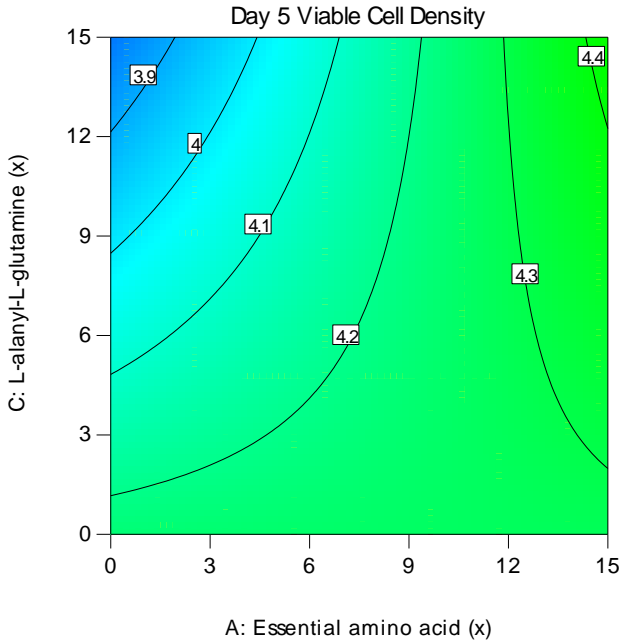
Source	Sum of Squares	df	Mean Squares	F-statistic	p-value
Model	2.77	5	0.55	5.71	0.0008
A-Essential amino acid	0.85	1	0.85	8.80	0.0059
B-Non-essential amino acid	0.62	1	0.62	6.37	0.0171
F-Polyamines	0.54	1	0.54	5.59	0.0247
AC	0.62	1	0.62	6.37	0.0171
Lack of Fit	2.78	26	0.11	3.29	0.1271
Pure Error	0.13	4	0.033		

A

Day 5 VCD ($\times 10^6$ cells/mL)



Concentration of other model terms:
 B: Non-essential amino acid = $0 \times$ MEM
 F: Polyamines = $0 \times$ MEM



B

Day 5 VCD ($\times 10^6$ cells/mL)



Concentration of other model terms:
 B: Non-essential amino acid = $1 \times$ MEM
 F: Polyamines = $1 \times$ MEM

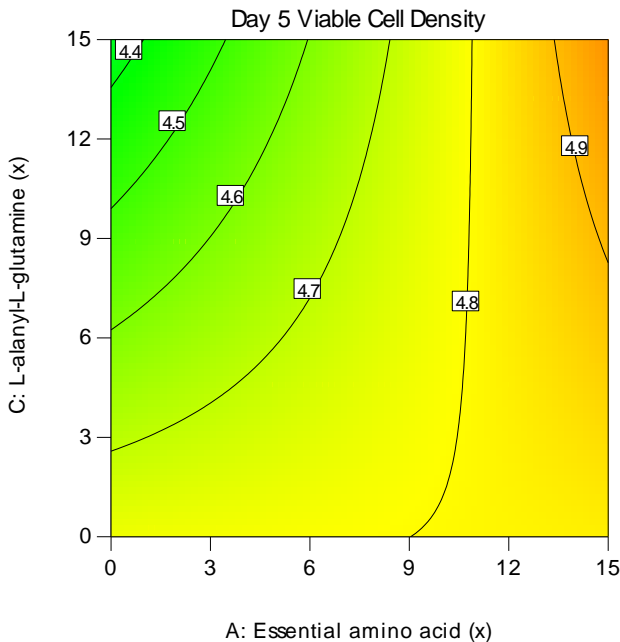


Figure 5.6: Day 5 VCD response model graph from screening study 1. Graph shows AC-term two-factor interaction i.e. between essential amino acids (A-term) and L-alanyl-L-glutamine (C-term). Interaction with the other significant model terms i.e. non-essential amino acids (B-term) and Polyamines (F-term) is also shown. (A) Low level for B and F terms (B) High level for B and F terms. The x and y-axes unit 'x' refers to times the minimum essential media (MEM) concentration. VCD is viable cell density.

5.4 | DESIGN OF EXPERIMENTS BASED SCREENING OF FEED SUPPLEMENTS TO INCLUDE IN THE NOVEL FEED FOR ENHANCING 277 CELL LINE GROWTH

Table 5.11: ANOVA summary of Day 5 culture viability response from screening study 1. Data generated using Design Expert v10 (Stat-Ease, Inc., Minnesota, U.S.A). df is degrees of freedom.

Source	Sum of Squares	df	Mean Squares	F-statistic	p-value
Model	17.43	3	5.81	2.91	0.0496
A-Essential amino acid	6.39	1	6.39	3.20	0.0832
F-Polyamines	10.47	1	10.47	5.24	0.0288
Lack of Fit	52.97	28	1.89	0.69	0.7559
Pure Error	10.97	4	2.74		

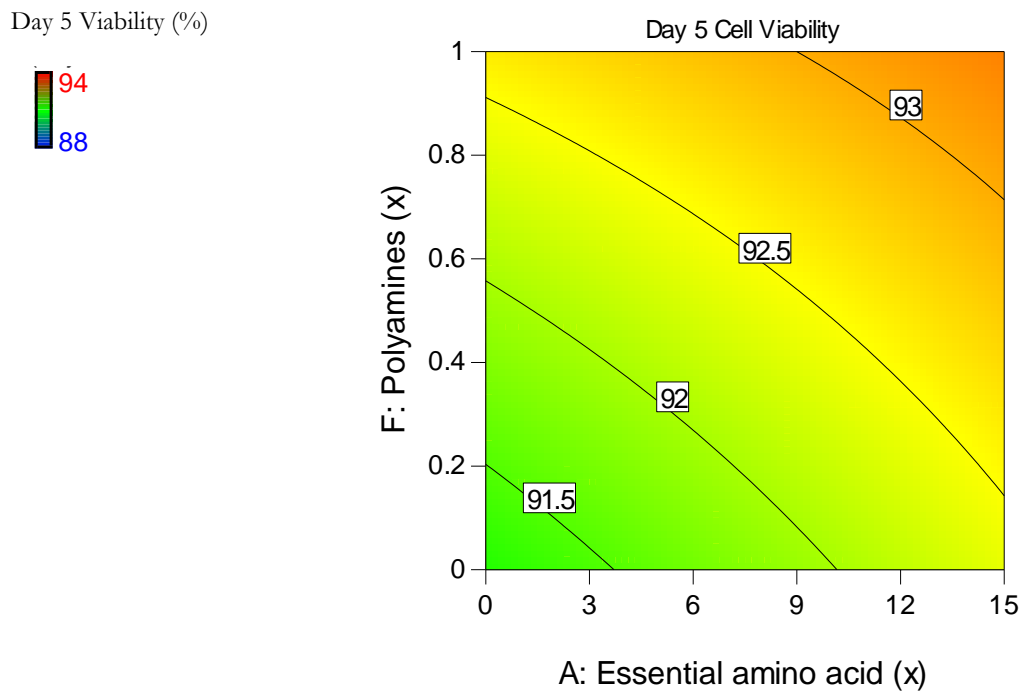


Figure 5.7: Day 5 culture viability response model graph from screening study 1. Graph shows AF-term two-factor interaction i.e. between essential amino acids (A-term) and Polyamines (F-term). The x and y-axes unit ‘x’ refers to times the minimum essential media (MEM) concentration. VCD is viable cell density.

Table 5.12: ANOVA summary of Day 6 VCD response from screening study 1. Data generated using Design Expert v10 (Stat-Ease, Inc., Minnesota, U.S.A). df is degrees of freedom.

Source	Sum of Squares	df	Mean Squares	F-statistic	p-value
Model	5.63	6	0.94	5.77	0.0005
A-Essential amino acid	3.05	1	3.05	18.76	0.0002
F-Polyamines	0.88	1	0.88	5.44	0.0268
AD	0.55	1	0.55	3.36	0.0772
AE	0.93	1	0.93	5.73	0.0234
Lack of Fit	4.12	25	0.16	1.10	0.5259
Pure Error	0.60	4	0.15		

5.4 | DESIGN OF EXPERIMENTS BASED SCREENING OF FEED SUPPLEMENTS TO INCLUDE IN THE NOVEL FEED FOR ENHANCING 277 CELL LINE GROWTH

A

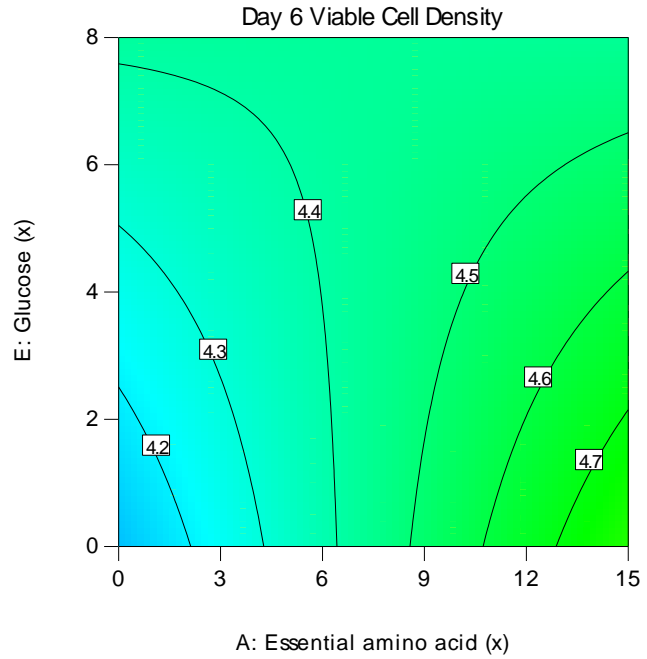
Day 6 VCD ($\times 10^6$ cells/mL)



Concentration of other model terms:

D: Vitamins = $0 \times$ MEM

F: Polyamines = $0 \times$ MEM



B

Day 6 VCD ($\times 10^6$ cells/mL)



Concentration of other model terms:

D: Vitamins = $4 \times$ MEM

F: Polyamines = $1 \times$ MEM

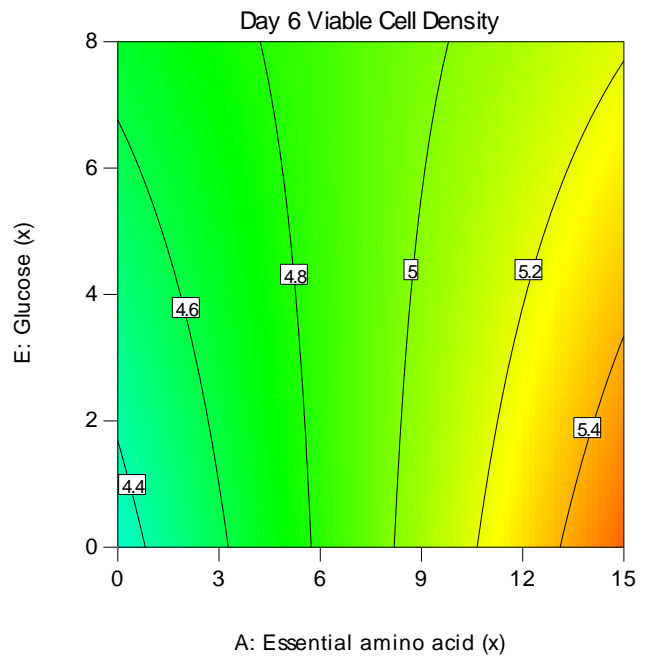


Figure 5.8: Day 6 VCD response model graph from screening study 1. Graph shows AE-term two-factor interaction i.e. between essential amino acids (A-term) and Glucose (E-term). Interaction with the other significant model terms i.e. vitamins (D-term) and polyamines (F-term) is also shown. (A) Low level for D and F terms (B) High level for D and F terms. The x and y-axes unit 'x' refers to times the minimum essential media (MEM) concentration. VCD is viable cell density.

Table 5.13: ANOVA summary of Day 6 culture viability response from screening study 1. Data generated using Design Expert v10 (Stat-Ease, Inc., Minnesota, U.S.A). df is degrees of freedom.

Source	Sum of Squares	df	Mean Squares	F-statistic	p-value
Model	80.74	3	26.91	7.49	0.0006
A-Essential amino acid	64.70	1	64.70	18.02	0.0002
AF	11.16	1	11.16	3.11	0.0874
Lack of Fit	104.87	28	3.75	1.49	0.3822
Pure Error	10.05	4	2.51		

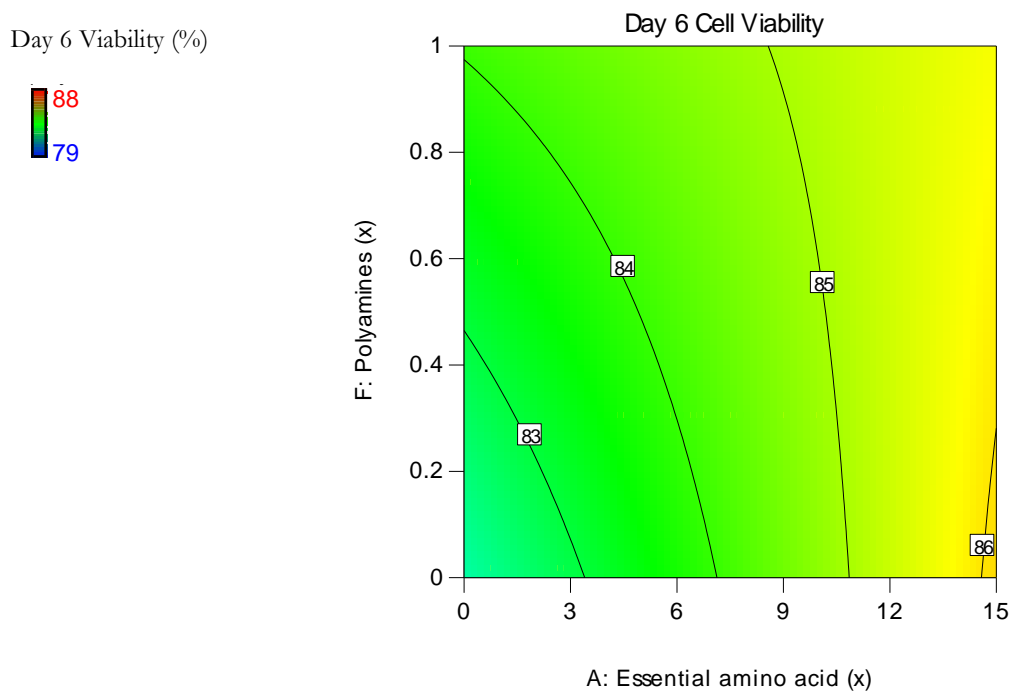


Figure 5.9: Day 6 culture viability response model graph from screening study 1. Graph shows AF-term two-factor interaction i.e. between essential amino acids (A-term) and Polyamines (F-term). The x and y-axes unit 'x' refers to times the minimum essential media (MEM) concentration. VCD is viable cell density.

5.4 | DESIGN OF EXPERIMENTS BASED SCREENING OF FEED SUPPLEMENTS TO INCLUDE IN THE NOVEL FEED FOR ENHANCING 277 CELL LINE GROWTH

Table 5.14: ANOVA summary of Day 7 VCD response from screening study 1. Data generated using Design Expert v10 (Stat-Ease, Inc., Minnesota, U.S.A). df is degrees of freedom.

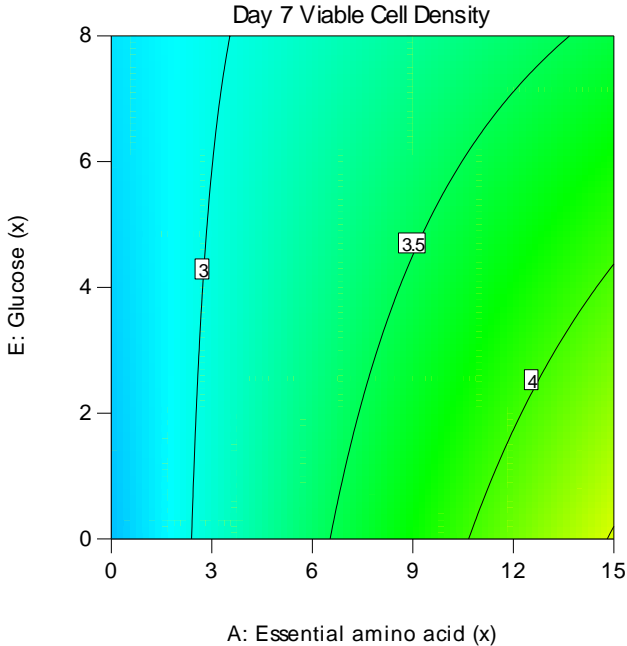
Source	Sum of Squares	df	Mean Squares	F-statistic	p-value
Model	17.68	4	4.42	14.54	< 0.0001
A-Essential amino acid	13.04	1	13.04	42.90	< 0.0001
B-Non-essential amino acid	0.91	1	0.91	2.99	0.0939
E-Glucose	1.42	1	1.42	4.68	0.0383
AE	2.31	1	2.31	7.58	0.0098
Lack of Fit	8.85	27	0.33	2.29	0.2192
Pure Error	0.57	4	0.14		

A

Day 7 VCD ($\times 10^6$ cells/mL)



Concentration of other model terms:
 B: Non-essential amino acid
 = $0 \times$ MEM



B

Day 7 VCD ($\times 10^6$ cells/mL)



Concentration of other model terms:
 B: Non-essential amino acid
 = $1 \times$ MEM

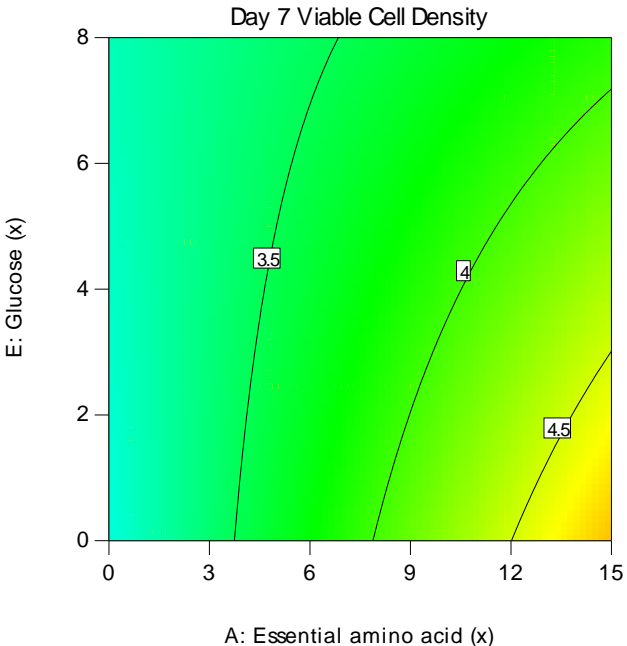


Figure 5.10: Day 7 VCD response model graph from screening study 1. Graph shows AE-term two-factor interaction i.e. between essential amino acids (A-term) and Glucose (E-term). Interaction with the other significant model term i.e. non-essential amino acids (B-term) is also shown. (A) Low level for B-term (B) High level for B-term. The x and y-axes unit ‘x’ refers to times the minimum essential media (MEM) concentration. VCD is viable cell density.

5.4 | DESIGN OF EXPERIMENTS BASED SCREENING OF FEED SUPPLEMENTS TO INCLUDE IN THE NOVEL FEED FOR ENHANCING 277 CELL LINE GROWTH

Table 5.15: ANOVA summary of Day 7 culture viability response from screening study 1. Data generated using Design Expert v10 (Stat-Ease, Inc., Minnesota, U.S.A). df is degrees of freedom.

Source	Sum of Squares	df	Mean Squares	F-statistic	p-value
Model	839.46	3	279.82	39.06	< 0.0001
A-Essential amino acid	320.68	1	320.68	44.76	< 0.0001
E-Glucose	412.56	1	412.56	57.59	< 0.0001
Lack of Fit	210.90	28	7.53	1.64	0.3404
Pure Error	18.35	4	4.59		

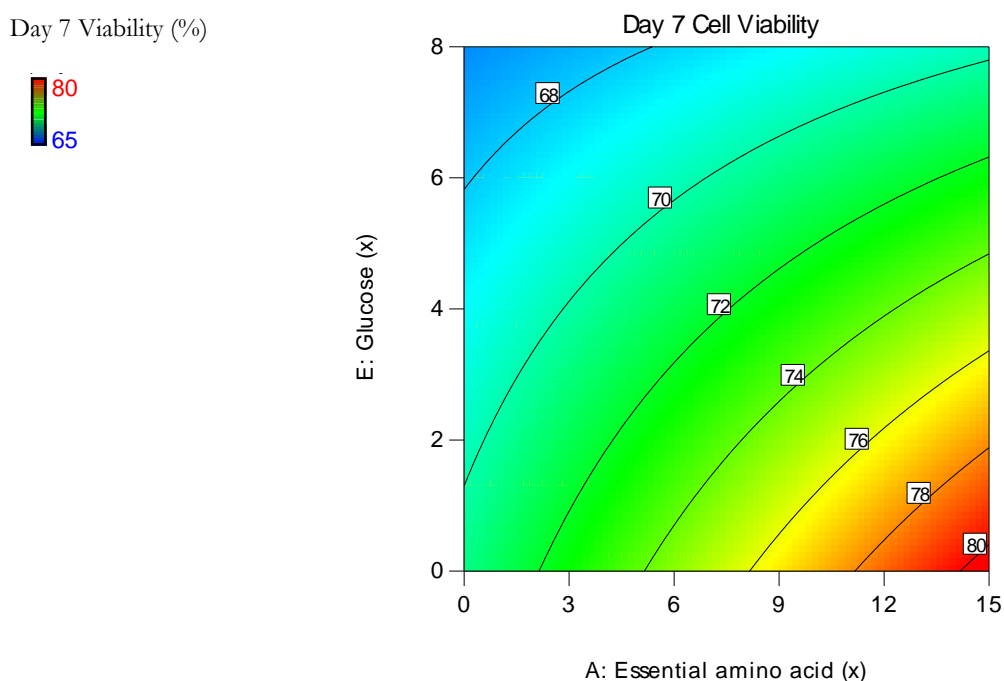


Figure 5.11: Day 7 culture viability response model graph from screening study 1. Graph shows AE-term two-factor interaction i.e. between essential amino acids (A-term) and Glucose (E-term). The x and y-axis unit 'x' refers to times the minimum essential media (MEM) concentration. VCD is viable cell density.

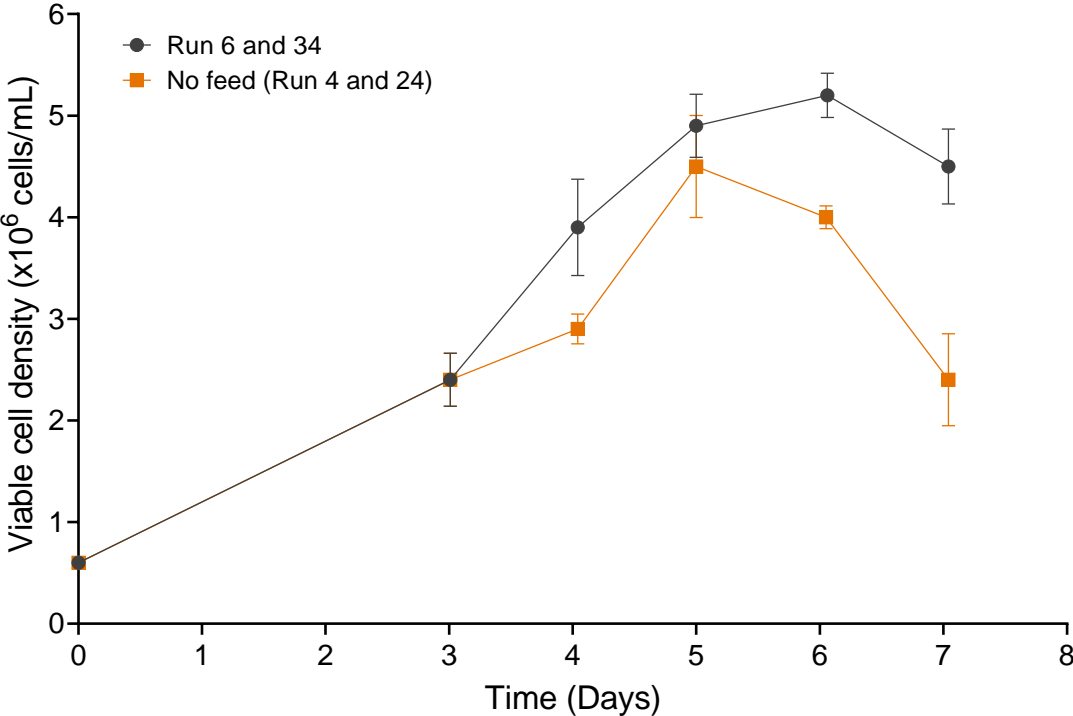


Figure 5.12: Comparison of VCD profile between top performing feed condition from screening study 1 (Run 6 and 34) and no feed condition (Run 4 and 24). Error bars represent one standard deviation about the mean (n=2).

5.4 | DESIGN OF EXPERIMENTS BASED SCREENING OF FEED SUPPLEMENTS TO INCLUDE IN THE NOVEL FEED FOR ENHANCING 277 CELL LINE GROWTH

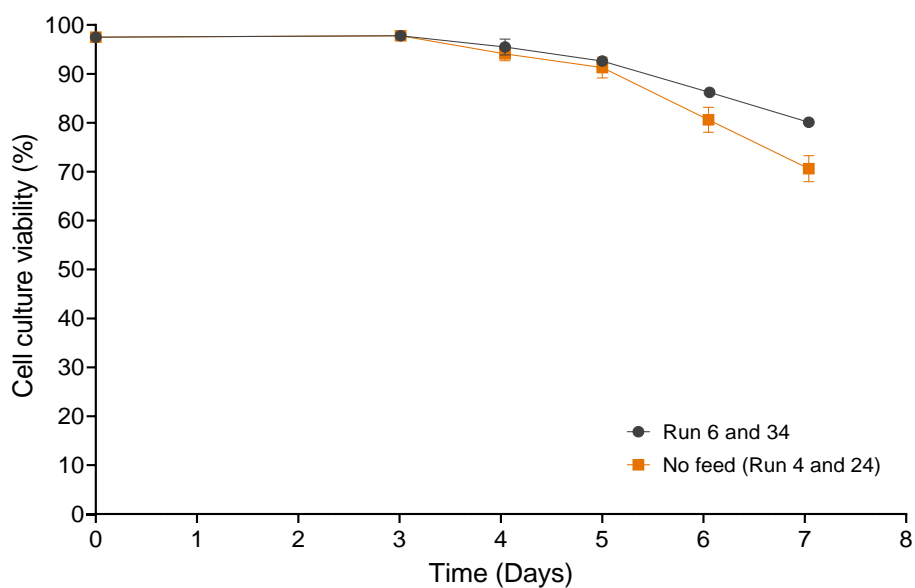


Figure 5.13: Comparison of culture viability profile between top performing feed condition from screening study 1 (Run 6 and 34) and no feed condition (Run 4 and 24). Error bars represent one standard deviation about the mean (n=2).

Table 5.16: Feed formulation of Run 6 and 34 from screening study 1. MEM is concentration of minimum essential media.

Run	Essential amino acid (× MEM)	Non-essential amino acid (× MEM)	L-alanyl-L-glutamine (× MEM)	Vitamins (× MEM)	Glucose (× MEM)	Polyamines (× MEM)
6 and 34	15	0	15	0	0	1

5.4.2 Screening study 2 – Assessment of metabolites commonly present in mammalian cell culture feeds and not identified in the LC-MS analysis

In this study, a new set of feed supplements were screened to assess their effect on 277 cell growth. The focus was to evaluate supplements commonly found in mammalian cell culture feeds as identified by Costa *et al.*, 2014 but were not identified in the LC-MS analysis. The new metabolites that were screened included lipids, inorganic salts, insulin, insulin-like growth factor-1 (IGF-1) and sodium pyruvate.

Cells need lipids for survival and membrane integrity (Yao and Asayama, 2017). In media containing serum, cells derive almost all of their lipids from the serum (Savonnière *et al.*, 1996). In serum-free media, lipids have to be supplemented to maintain cell proliferation (Savonnière *et al.*, 1996). Inorganic salts in the media are important in retaining the osmotic balance and help in regulating membrane potential by providing sodium, potassium, and calcium ions (Arora, 2013). Commercially available pre-formulated solutions of lipids and inorganic salts were used in this study. The complete formulation of these solutions can be found in Table 9.16 and 9.17 respectively under Appendix A (section 9.4.3). Recombinant insulin is a common supplement in serum-free mammalian cell culture media. It is involved in a number of cellular functions, including the stimulation of cell growth, cell cycle progression and glucose uptake (Wong *et al.*, 2004). IGF-1 is an important growth factor responsible for stimulating growth of all cell types (Ren *et al.*, 2008). In CHO cells, it has been shown to promote cell proliferation and inhibit apoptosis of cells (Adamson and Walum, 2007). Sodium pyruvate is a supplement added to improve cell survival in culture. It functions as a key molecule in energy production and as an antioxidant (Yako *et al.*, 2021).

The factors from screening study 1 were also included in the design in order to study possible interactions. Essential amino acids, including L-alanyl-L-glutamine, were

5.4 | DESIGN OF EXPERIMENTS BASED SCREENING OF FEED SUPPLEMENTS TO INCLUDE IN THE NOVEL FEED FOR ENHANCING 277 CELL LINE GROWTH

evaluated as separate factors in this study. This is because they demonstrated significant positive effects on cell growth in screening study 1. The remaining metabolites from screening 1 were included as a single factor termed 'feed mixture' which contains the following metabolites: non-essential amino acids, vitamins, glucose and polyamines. The full list of factors for this study is shown below:

1. Essential amino acids
2. L-alanyl-L-glutamine
3. Lipids solution
4. Inorganic salts
5. Insulin
6. IGF-1
7. Feed mixture (includes non-essential amino acids, vitamins, glucose and polyamines)

Similar to screening study 1, the responses analysed included VCD and culture viability from day 5 until the end of the culture (i.e. day 7). All the responses generated significant models (i.e. model p-value < 0.05). The ANOVA summary for all the responses are shown in Table 5.17 to 5.22. Essential amino acids (A-term), IGF-1 (F-term) and 'feed mixture' (H-term) were significant model terms in most responses. Additionally, the interaction of IGF-1 and 'feed mixture' with essential amino acids (AF and AH terms respectively) were also significant model terms. L-alanyl-L-glutamine (B-term) was only significant in the day 5 VCD response. All other factors screened in this study i.e. lipids, insulin, inorganic salts and sodium pyruvate had p-values greater than 0.05 for all the responses analysed. Hence, their effect on cell growth was insignificant and not included in the respective models.

Model graphs were generated to illustrate the trend in each response as shown in Figure 5.14 to 5.19. Similar to the observation from screening study 1, all the models suggest that essential amino acids had a strong positive effect on VCD and culture viability i.e. increasing the concentration of essential amino acids resulted in higher VCD and culture viability values. The other significant model terms, IGF-1 and 'feed mixture', both had a strong negative effect on cell growth. Lower VCD and viability values were observed when these two factors were present at high concentrations compared to conditions where they were not present at all. The IGF-1 used in this study (LONG[®] R³ IGF-1) is a recombinant analog of human insulin-like growth factor-1 that has been specifically engineered for the enhancement of cell culture performance.

A study by Repligen has shown that LONG[®] R³ IGF-1 improves volumetric productivity in CHO cell culture by up to 62% over cell culture where the growth factor was not added (Kudugunti et al., 2015). The feed concentration of IGF-1 used in this study was adapted to match the optimal cell culture concentration of 2.5 µg/mL reported by Kudugunti *et al.*, 2015. However, the data from all the DoE models suggest a strong negative correlation between IGF-1 concentration and cell growth. Perhaps the IGF-1 concentration used for screening may not have been suitable for HEK293 cells resulting in poor growth. After all, the concentration used by Kudugunti *et al.*, 2015 was optimised for CHO cell culture.

As discussed in screening study 1, glucose was found to be a significant model term for both day 6 and day 7 models with a strong negative effect on cell growth and viability. Therefore, it is possible that the presence of glucose in the 'feed mixture' may have caused the negative correlation with growth. In particular, the interaction of 'feed mixture' with essential amino acids (i.e. AH term) had a stronger negative response than 'feed mixture' alone. It is worth noting that the glucose concentration used in this study was half of that used in screening 1 (i.e. 4× MEM compared to 8× MEM in screening study 1). In the presence of essential amino acids, it seems even lower glucose concentration compared to screening study 1 in the feed is detrimental to cell growth.

5.4 | DESIGN OF EXPERIMENTS BASED SCREENING OF FEED SUPPLEMENTS TO INCLUDE IN THE NOVEL FEED FOR ENHANCING 277 CELL LINE GROWTH

Run 5 and 31, in which the top performing condition was used, was plotted against the ‘no feed’ condition (Run 13 and 35) to better visualise the effect of the bespoke feed on 277 cell growth. The feed formulation of runs 5 and 31, shown in Table 5.23, highlights that this condition comprised of the highest concentration of essential amino acids and did not contain IGF-1 and ‘feed mixture’. According to the VCD profile (Figure 5.20), cells continued to proliferate until day 6 for the culture with feed addition, whilst growth arrest was observed by day 5 for the no feed culture. The cell viability measurements (Figure 5.21) later in the culture were also higher for the feed condition. The maximum VCD of 5.9×10^6 cells/mL for the feed culture was also higher than 5.2×10^6 achieved for the ‘no feed’ culture at day 6.

In summary, the data from this screening study has confirmed the importance of essential amino acids as a key component of the 277 cell growth feed. None of the new supplements screened had any positive effect on cell growth and thus will not be considered as part of the novel feed formulation.

Table 5.17: ANOVA summary of Day 5 VCD response from screening study 2. Data generated using Design Expert v10 (Stat-Ease, Inc., Minnesota, U.S.A). df is degrees of freedom.

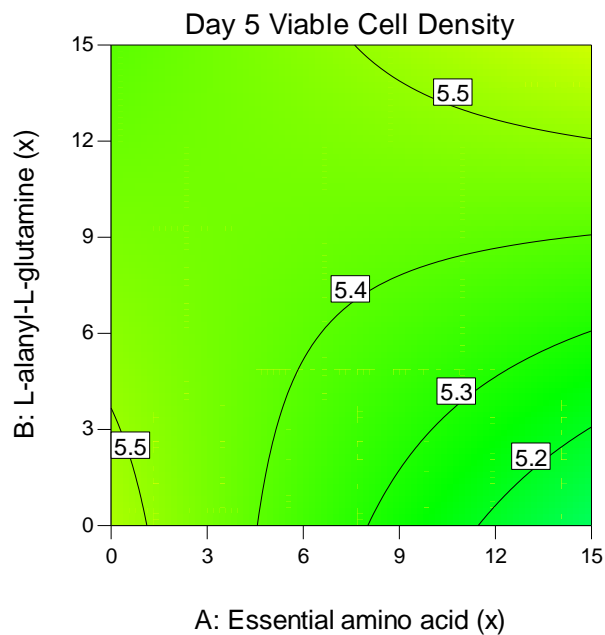
Source	Sum of Squares	df	Mean Squares	F-statistic	p-value
Model	1.45	4	0.36	4.31	0.0067
B-L-alanyl-L-glutamine	0.27	1	0.27	3.21	0.0824
F-IGF-1	0.27	1	0.27	3.17	0.0845
AB	0.80	1	0.80	9.52	0.0042
Lack of Fit	2.09	28	0.075	0.50	0.8765
Pure Error	0.60	4	0.15		

A

Day 5 VCD ($\times 10^6$ cells/mL)



Concentration of other model terms:
F: IGF-1 = 0 $\mu\text{g/mL}$



B

Day 5 VCD ($\times 10^6$ cells/mL)



Concentration of other model terms:
F: IGF-1 = 2.5 $\mu\text{g/mL}$

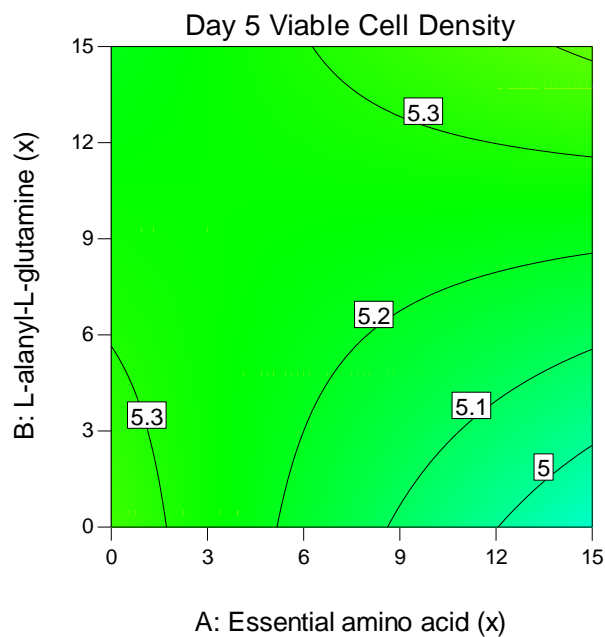


Figure 5.14: Day 5 VCD response model graph from screening study 2. Graph shows AE-term two-factor interaction i.e. between essential amino acids (A-term) and L-alanyl-L-glutamine (B-term). Interaction with the other significant model term i.e. IGF-1 (F-term) is also shown. (A) Low level for F term (B) High level for F term. The x and y-axes unit 'x' refers to times the minimum essential media (MEM) concentration. VCD is viable cell density.

5.4 | DESIGN OF EXPERIMENTS BASED SCREENING OF FEED SUPPLEMENTS TO INCLUDE IN THE NOVEL FEED FOR ENHANCING 277 CELL LINE GROWTH

Table 5.18: ANOVA summary of Day 5 culture viability response from screening study 2. Data generated using Design Expert v10 (Stat-Ease, Inc., Minnesota, U.S.A). df is degrees of freedom.

Source	Sum of Squares	df	Mean Squares	F-statistic	p-value
Model	8.51	1	8.51	13.52	0.0008
H-Feed mixture	8.51	1	8.51	13.52	0.0008
Lack of Fit	21.37	31	0.69	4.22	0.0847
Pure Error	0.65	4	0.16		

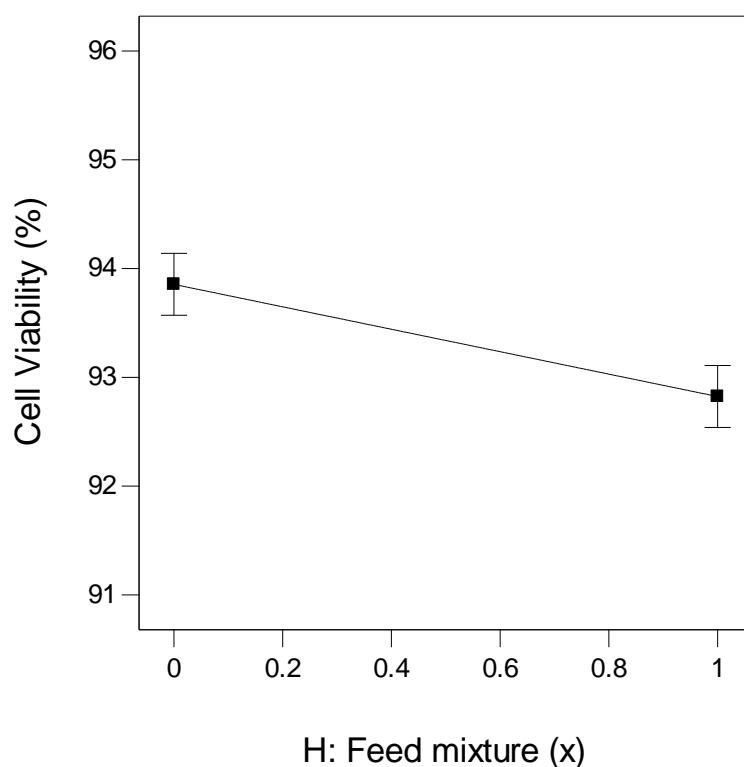


Figure 5.15: Day 5 culture viability response model graph from screening study 2. Graph shows effect of ‘Feed mixture’ (H-term) on day 5 cell viability. The x-axis unit ‘x’ refers to times the minimum essential media (MEM) concentration.

Table 5.19: ANOVA summary of Day 6 VCD response from screening study 2. Data generated using Design Expert v10 (Stat-Ease, Inc., Minnesota, U.S.A). df is degrees of freedom.

Source	Sum of Squares	df	Mean Squares	F-statistic	p-value
Model	2.88	4	0.72	5.14	0.0027
A-Essential amino acid	0.96	1	0.96	6.87	0.0135
F-IGF-1	1.13	1	1.13	8.05	0.0080
H-Feed mixture	0.41	1	0.41	2.90	0.0983
AH	0.39	1	0.39	2.75	0.1076
Lack of Fit	3.99	28	0.15	1.65	0.3375
Pure Error	0.36	4	0.089		

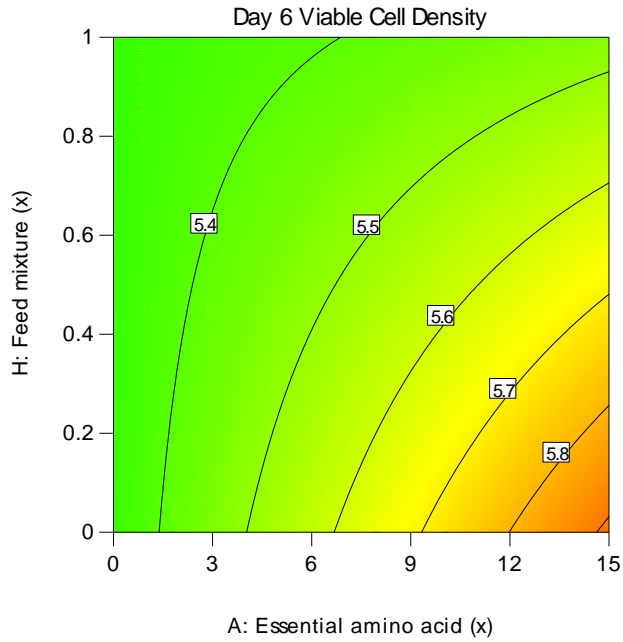
5.4 | DESIGN OF EXPERIMENTS BASED SCREENING OF FEED SUPPLEMENTS TO INCLUDE IN THE NOVEL FEED FOR ENHANCING 277 CELL LINE GROWTH

A

Day 6 VCD ($\times 10^6$ cells/mL)



Concentration of other model terms:
F: IGF-1 = 0 $\mu\text{g/mL}$



B

Day 6 VCD ($\times 10^6$ cells/mL)



Concentration of other model terms:
F: IGF-1 = 2.5 $\mu\text{g/mL}$

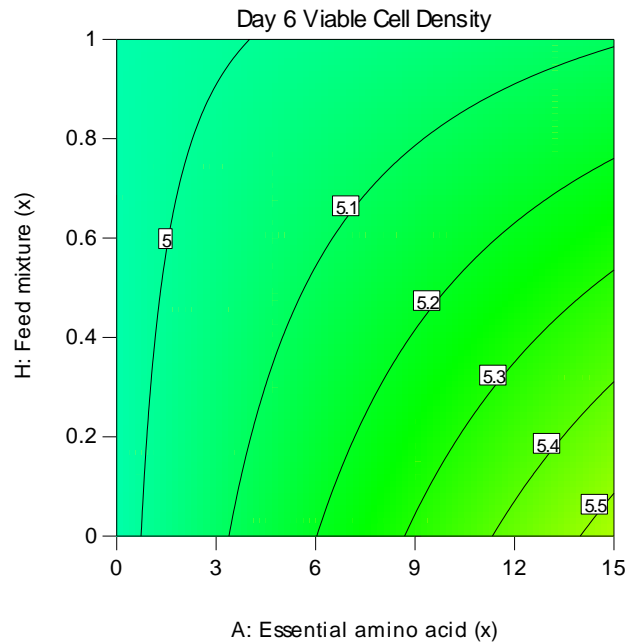


Figure 5.16: Day 6 VCD response model graph from screening study 2. Graph shows AH-term two-factor interaction i.e. between essential amino acids (A-term) and Feed mixture (H-term). Interaction with the other significant model term i.e. IGF-1 (F-term) is also shown. (A) Low level for F term (B) High level for F term. The x and y-axes unit 'x' refers to times the minimum essential media (MEM) concentration. VCD is viable cell density.

Table 5.20: ANOVA summary of Day 6 culture viability response from screening study 2. Data generated using Design Expert v10 (Stat-Ease, Inc., Minnesota, U.S.A). df is degrees of freedom.

Source	Sum of Squares	df	Mean Squares	F-statistic	p-value
Model	35.36	4	8.84	5.07	0.0029
A-Essential amino acid	6.04	1	6.04	3.46	0.0722
F-IGF-1	5.53	1	5.53	3.17	0.0847
H-Feed mixture	18.76	1	18.76	10.76	0.0026
AH	5.04	1	5.04	2.89	0.0990
Lack of Fit	51.13	28	1.89	2.44	0.2002
Pure Error	3.09	4	0.77		

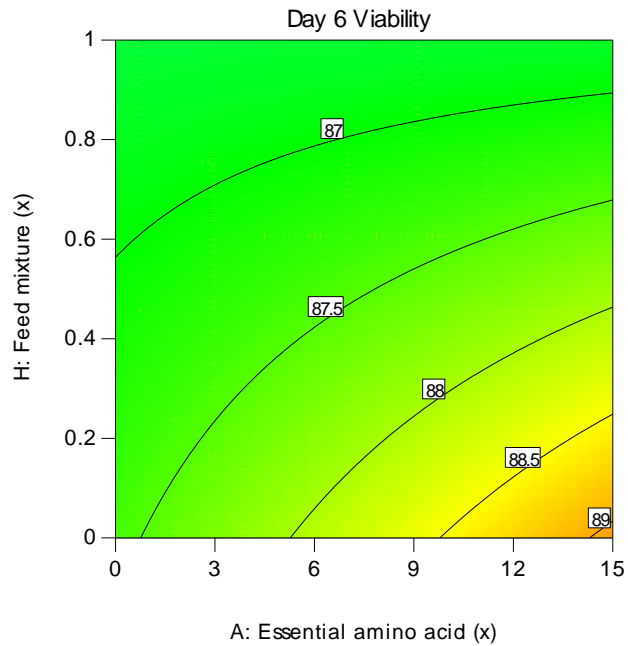
5.4 | DESIGN OF EXPERIMENTS BASED SCREENING OF FEED SUPPLEMENTS TO INCLUDE IN THE NOVEL FEED FOR ENHANCING 277 CELL LINE GROWTH

A

Day 6 Viability (%)



Concentration of other model terms:
F: IGF-1 = 0 $\mu\text{g/mL}$



B

Day 6 Viability (%)



Concentration of other model terms:
F: IGF-1 = 2.5 $\mu\text{g/mL}$

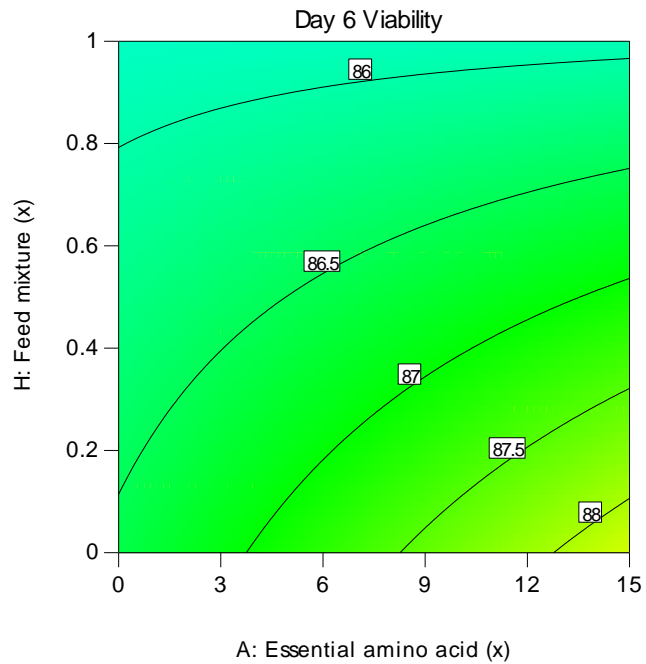


Figure 5.17: Day 6 culture viability response model graph from screening study 2. Graph shows AH-term two-factor interaction i.e. between essential amino acids (A-term) and Feed mixture (H-term). Interaction with the other significant model term i.e. IGF-1 (F-term) is also shown. (A) Low level for F term (B) High level for F term. The x-axis unit 'x' refers to times the minimum essential media (MEM) concentration.

Table 5.21: ANOVA summary of Day 7 VCD response from screening study 2. Data generated using Design Expert v10 (Stat-Ease, Inc., Minnesota, U.S.A). df is degrees of freedom.

Source	Sum of Squares	df	Mean Squares	F-statistic	p-value
Model	26.83	5	5.37	21.58	< 0.0001
A-Essential amino acid	14.42	1	14.42	57.99	< 0.0001
F-IGF-1	4.06	1	4.06	16.33	0.0003
H-Feed mixture	4.29	1	4.29	17.26	0.0002
AF	1.94	1	1.94	7.80	0.0090
AH	2.12	1	2.12	8.53	0.0066
Lack of Fit	6.95	27	0.27	2.11	0.2455
Pure Error	0.51	4	0.13		

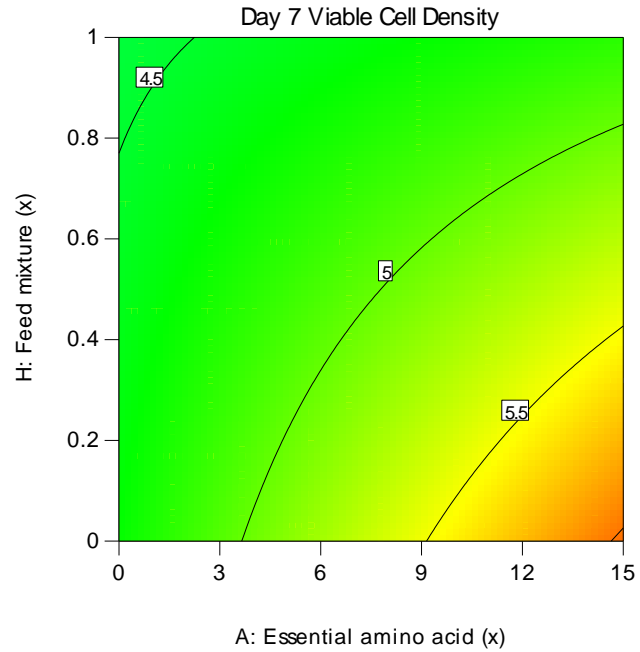
5.4 | DESIGN OF EXPERIMENTS BASED SCREENING OF FEED SUPPLEMENTS TO INCLUDE IN THE NOVEL FEED FOR ENHANCING 277 CELL LINE GROWTH

A

Day 7 VCD ($\times 10^6$ cells/mL)



Concentration of other model terms:
F: IGF-1 = 0 $\mu\text{g/mL}$



B

Day 7 VCD ($\times 10^6$ cells/mL)



Concentration of other model terms:
F: IGF-1 = 2.5 $\mu\text{g/mL}$

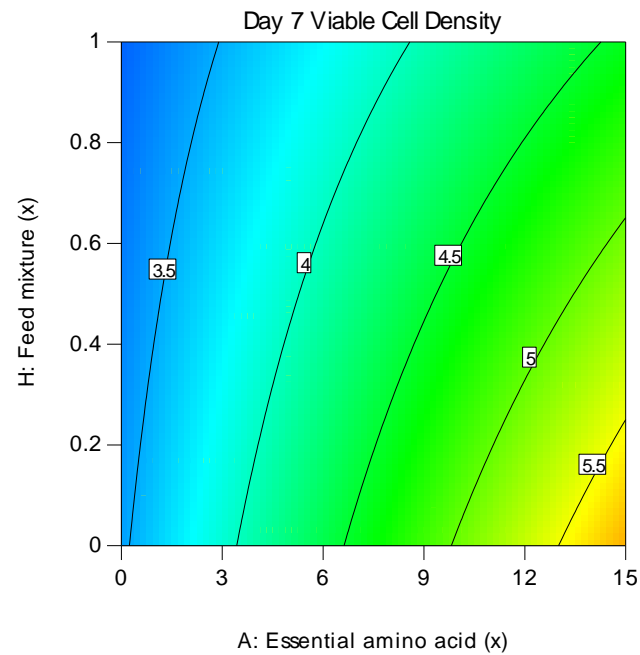


Figure 5.18: Day 7 VCD response model graph from screening study 2. Graph shows AH-term two-factor interaction i.e. between essential amino acids (A-term) and Feed mixture (H-term). Interaction with the other significant model term i.e. IGF-1 (F-term) is also shown. (A) Low level for F term (B) High level for F term. The x-axis unit 'x' refers to times the minimum essential media (MEM) concentration.

Table 5.22: ANOVA summary of Day 7 culture viability response from screening study 2. Data generated using Design Expert v10 (Stat-Ease, Inc., Minnesota, U.S.A). df is degrees of freedom.

Source	Sum of Squares	df	Mean Squares	F-statistic	p-value
Model	1267.51	5	253.50	45.64	< 0.0001
A-Essential amino acid	721.05	1	721.05	129.81	< 0.0001
F-IGF-1	127.60	1	127.60	22.97	< 0.0001
H-Feed mixture	287.40	1	287.40	51.74	< 0.0001
AF	51.77	1	51.77	9.32	0.0047
AH	79.70		79.70	14.35	0.0007
Lack of Fit	164.07	27	6.31	9.83	0.0191
Pure Error	2.57	4	0.64		

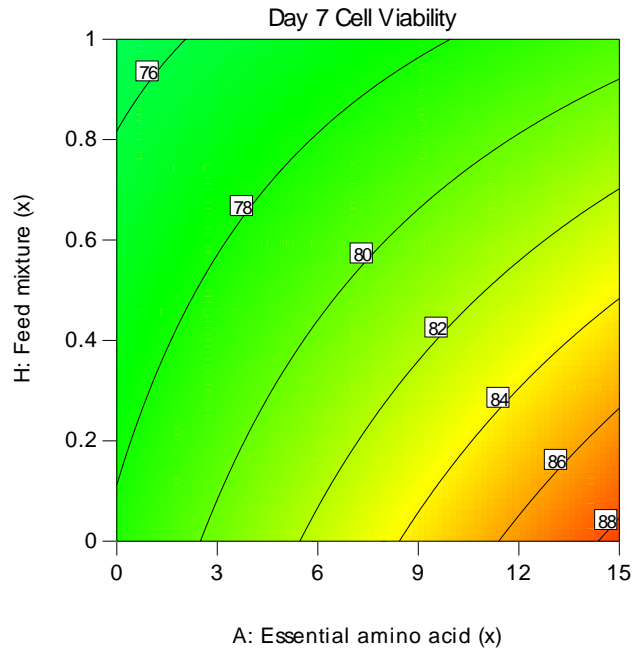
5.4 | DESIGN OF EXPERIMENTS BASED SCREENING OF FEED SUPPLEMENTS TO INCLUDE IN THE NOVEL FEED FOR ENHANCING 277 CELL LINE GROWTH

A

Day 7 Viability (%)



Concentration of other model terms:
F: IGF-1 = 0 µg/mL



B

Day 7 Viability (%)



Concentration of other model terms:
F: IGF-1 = 2.5 µg/mL

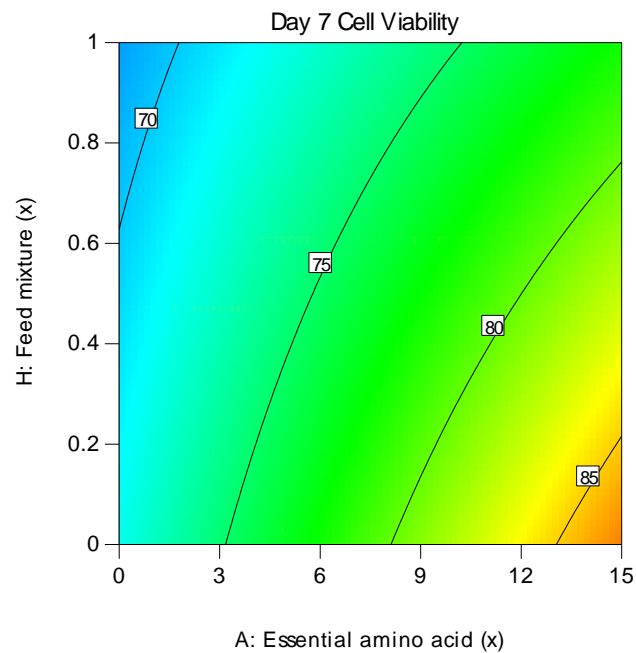


Figure 5.19: Day 7 culture viability response model graph from screening study 2. Graph shows AH-term two-factor interaction i.e. between essential amino acids (A-term) and Feed mixture (H-term). Interaction with the other significant model term i.e. IGF-1 (F-term) is also shown. (A) Low level for F term (B) High level for F term. The x-axis unit 'x' refers to times the minimum essential media (MEM) concentration.

5 | DEVELOPING A NOVEL FEEDING REGIME FOR ENHANCED HEK293T STABLE CELL LINE GROWTH

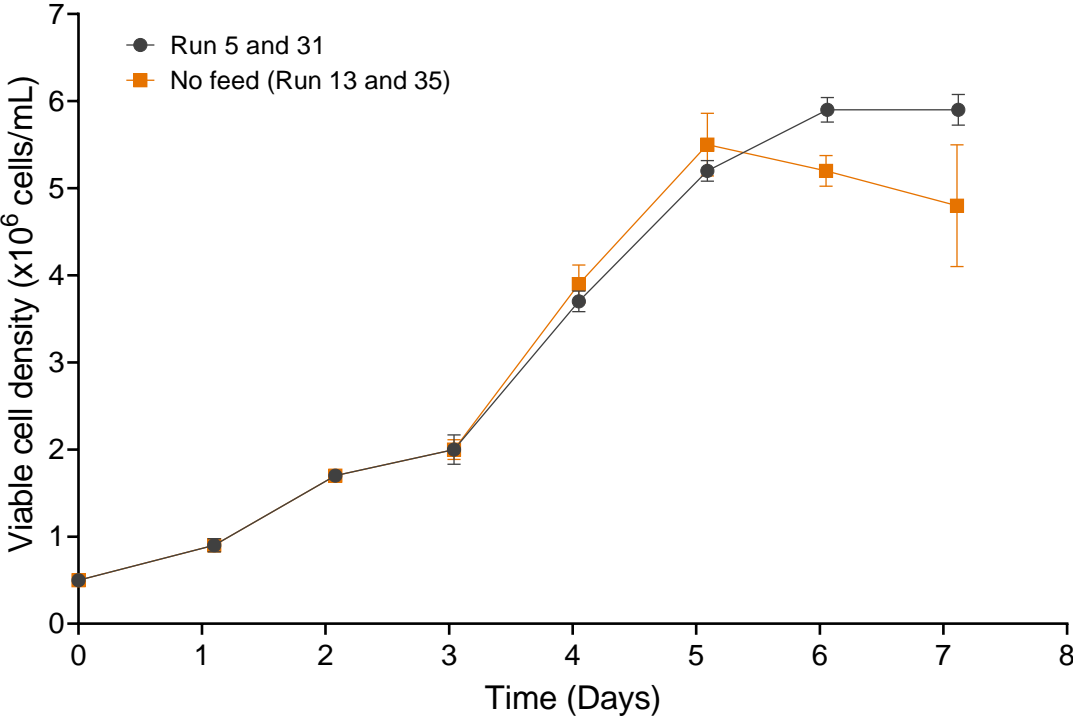


Figure 5.20: Comparison of VCD profile between top performing feed condition from screening study 2 (Run 5 and 31) and no feed condition (Run 13 and 35). Error bars represent one standard deviation about the mean (n=2).

5.4 | DESIGN OF EXPERIMENTS BASED SCREENING OF FEED SUPPLEMENTS TO INCLUDE IN THE NOVEL FEED FOR ENHANCING 277 CELL LINE GROWTH

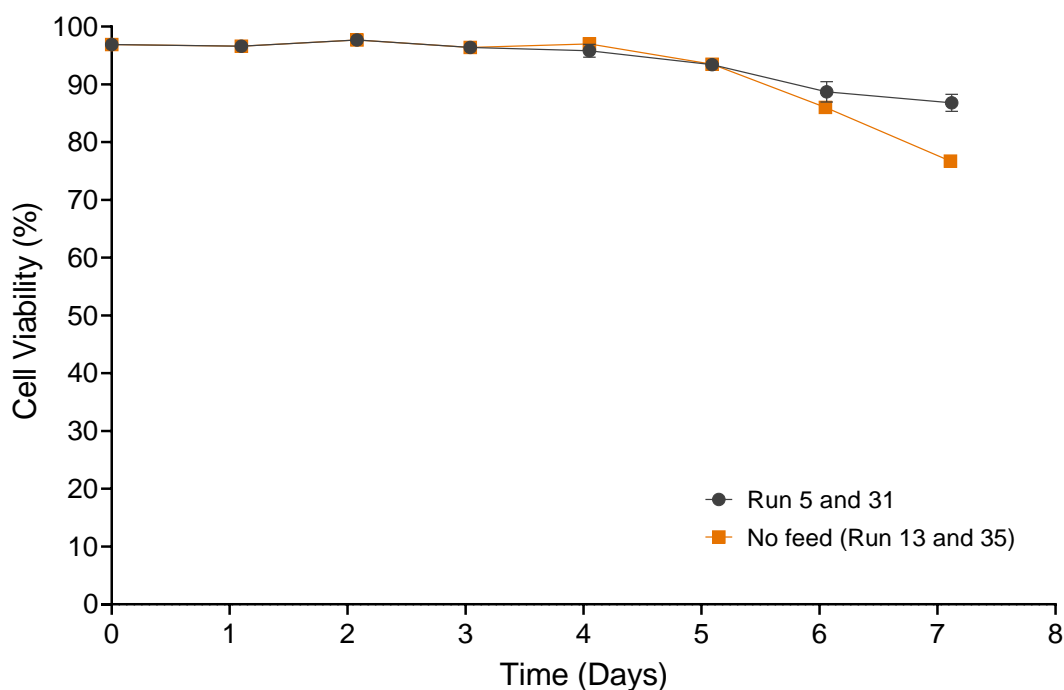


Figure 5.21: Comparison of culture viability profile between top performing feed condition from screening study 2 (Run 5 and 31) and no feed condition (Run 13 and 35). Error bars represent one standard deviation about the mean (n=2).

Table 5.23: Feed formulation of Run 5 and 31 from screening study 2.

Run	Essential amino acid (x MEM)	L-alanyl-L-glutamine (x MEM)	Lipids (dilution)	Inorganic salts (x MEM)	Insulin (mg/mL)	IGF-1 (µg/mL)	Sodium Pyruvate (mM)	Feed Mixture (x MEM)
5 and 31	15	0	1:20	1	0	0	1	0

5.4.3 Screening study 3 – Assessment of individual effect of important essential and non-essential amino acids identified in the LC-MS analysis

In screening study 1, metabolites from Table 5.9 were grouped according to their compound class which were selected as factors in the DoE design. In this study, the individual metabolites from Table 5.9 were screened independently in order to assess their distinct effect on 277 cell growth. To manage the number of factors screened at a time, the essential and non-essential amino acids were evaluated in this study whilst the remaining metabolites were screened in a separate study (see section 5.4.3). The full list of factors evaluated in this study include:

1. L-Aspartic acid
2. L-Leucine
3. L-Valine
4. L-Lysine
5. L-Isoleucine
6. L-Arginine
7. L-Serine
8. L-Asparagine

L-glutamine has already been tested as the dipeptide L-alanyl-L-glutamine in the previous two screening studies. Its effect on growth was not significant and hence not included in this DoE design. L-Methionine and L-phenylalanine were also not included in the study due to unavailability of the reagents at the time of running the experiment.

To assess the efficacy of the individual amino acids, a separate condition independent of the DoE design, comprising of all 20 amino acids (i.e. essential and non-essential) was also included in this study. The concentration of essential and non-essential amino acids in this condition was 15× MEM and 1× MEM respectively.

The responses analysed included the VCD and culture viability from day 5 until the end of the culture (i.e. day 7). Among these, only three responses (i.e. day 5 VCD, day 6 VCD and day 6 cell viability) generated significant models (i.e. model p-value < 0.05). For all other responses, the variation in the growth profile was not sufficiently significant for a model to be generated.

The ANOVA summary for all the responses are shown in Table 5.23 to 5.28. L-Serine (G-term) was the only significant model term for day 5 VCD. L-Lysine (D-term) and L-Arginine (F-term) were significant terms for both day 6 VCD and culture viability. L-Valine (C-term) was only significant in the day 6 culture viability response. All other amino acids screened in this study i.e. L-Aspartic acid, L-Leucine, L-Isoleucine and L-Asparagine had p-values greater than 0.05 for all the responses analysed. Hence, their effect on cell growth was insignificant and not included in the respective models.

Model graphs were generated to illustrate the trend in each response as shown in Figure 5.22 to 5.24. According to Figure 5.22, L-Serine demonstrated a negative linear correlation to cell growth i.e. VCD values at high L-Serine concentration were lower than values at low concentration. L-Serine, a non-essential amino acid, plays an important role in maintaining cell proliferation especially in HEK293 cells with several studies reporting that it is the second most highly consumed amino acid after L-glutamine (Petiot et al., 2015; Rodrigues et al., 2013). According to Salazar *et al.*, 2016, the need for the identification of the optimal concentrations of amino acids is particularly important in fed batch cultures. L-Serine is involved in the metabolism of nucleic acid precursors through the tetrahydrofolate (THF) cycle (Salazar et al., 2016). An imbalance in the L-Serine concentration slows down the THF cycle resulting in the inhibition of cell proliferation (Salazar et al., 2016). Perhaps, the L-Serine concentration tested in this study was not optimal for HEK293T cells which resulted

in the trend observed in Figure 5.22. However, it is important to note that the negative effects on L-Serine were not observed in the day 6 growth profiles. Perhaps, L-Serine was necessary for the cellular metabolic reaction at this time, albeit its effect was not significant enough to be included in the DoE models.

The day 6 models suggest that L-Lysine and L-Arginine had a strong positive effect on both VCD and culture viability. Increasing the concentration of these amino acids resulted in higher VCD and culture viability values. L-Valine was also important for maintaining high cell viability at day 6. Notably, these three are all essential amino acids, a factor that has demonstrated a strong positive effect on cell growth in the previous two screening studies. To further assess the impact of the three significant amino acids identified in the DoE models above, Run 21 and 25, the top performing condition from this study (i.e. consisted of L-Arginine, L-Lysine and L-Valine in its formulation) was plotted against the feed which comprised of all 20 amino acids as well as the 'no feed' condition (i.e. Run 17 and 30). The feed composition of Run 21 and 25 is shown Table 5.29. Immediately after the initiation of feeding at day 3, the cell growth profile shows that higher VCDs (Figure 5.25) and culture viability (Figure 5.26) values were achieved for Run 21 and 25 compared to the culture with no feed. This indicates that the presence of the three essential amino acids in the feed was important for achieving an improved growth profile. However, the data also shows that the feed with all the amino acids outperformed both Run 21 and 25, as well as the 'no feed' condition. Maximum VCD at day 6 was higher in the comprehensive amino acid feed. This suggests that all amino acids have an important role to play in cell growth and maintaining the right balance of all the amino acids in the feed is key to achieving higher cell densities relative to the control.

5.4 | DESIGN OF EXPERIMENTS BASED SCREENING OF FEED SUPPLEMENTS TO INCLUDE IN THE NOVEL FEED FOR ENHANCING 277 CELL LINE GROWTH

Table 5.24: ANOVA summary of Day 5 VCD response from screening study 3. Data generated using Design Expert v10 (Stat-Ease, Inc., Minnesota, U.S.A). df is degrees of freedom.

Source	Sum of Squares	df	Mean Squares	F-statistic	p-value
Model	0.86	1	0.86	10.87	0.0023
G-L-Serine	0.86	1	0.86	10.87	0.0023
Lack of Fit	1.00	15	0.067	0.74	0.7155
Pure Error	1.61	18	0.090		

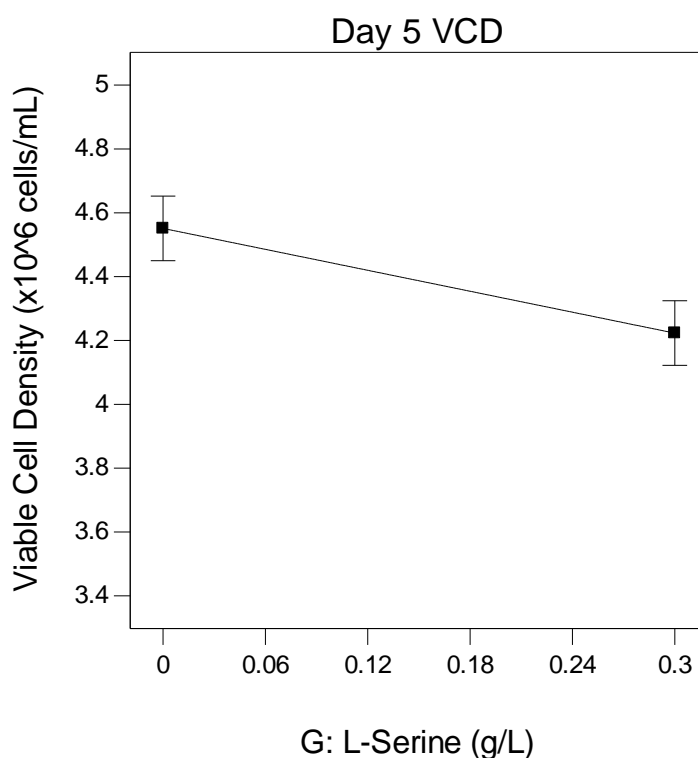


Figure 5.22: Day 5 VCD response model graph from screening study 3. Graph shows effect of L-Serine on day 5 VCD.

Table 5.25: ANOVA summary of Day 5 culture viability response from screening study 3. Data generated using Design Expert v10 (Stat-Ease, Inc., Minnesota, U.S.A). df is degrees of freedom.

Source	Sum of Squares	df	Mean Squares	F-statistic	p-value
Model	4.65	3	1.55	2.58	0.0715 ¹
A-L-Aspartic acid	2.10	1	2.10	3.50	0.0709
AE	2.42	1	2.42	4.03	0.0535
Lack of Fit	6.97	13	0.54	0.83	0.6286
Pure Error	11.65	18	0.65		

¹ Model p-value > 0.05 means the model is not significant

Table 5.26: ANOVA summary of Day 6 VCD response from screening study 3. Data generated using Design Expert v10 (Stat-Ease, Inc., Minnesota, U.S.A). df is degrees of freedom.

Source	Sum of Squares	df	Mean Squares	F-statistic	p-value
Model	2.31	2	1.15	12.09	0.0001
D-L-Lysine hydrochloride	0.94	1	0.94	9.88	0.0037
F-L-Arginine hydrochloride	1.29	1	1.29	13.48	0.0009
Lack of Fit	0.63	14	0.048	0.36	0.9644
Pure Error	2.24	17	0.13		

5.4 | DESIGN OF EXPERIMENTS BASED SCREENING OF FEED SUPPLEMENTS TO INCLUDE IN THE NOVEL FEED FOR ENHANCING 277 CELL LINE GROWTH

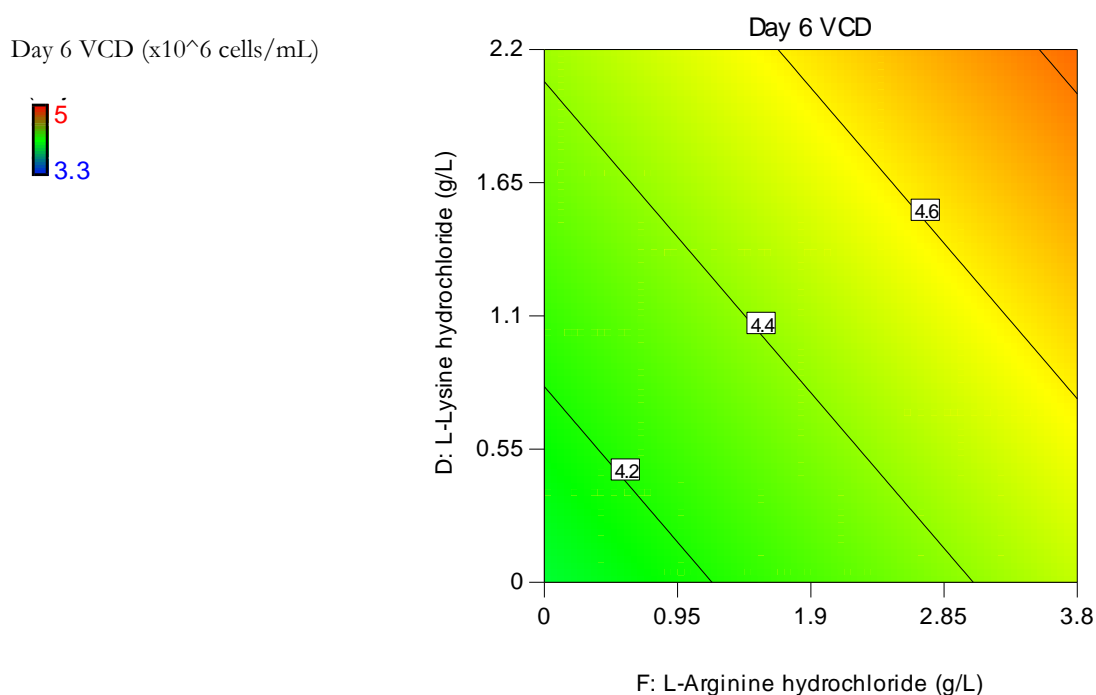


Figure 5.23: Day 6 VCD response model graph from screening study 3. Graph shows effect of L-Lysine hydrochloride (D-term) and L-Arginine hydrochloride (F-term) on day 6 VCD.

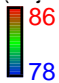
Table 5.27: ANOVA summary of Day 6 culture viability response from screening study 3. Data generated using Design Expert v10 (Stat-Ease, Inc., Minnesota, U.S.A). df is degrees of freedom.

Source	Sum of Squares	df	Mean Squares	F-statistic	p-value
Model	61.79	3	20.60	15.29	< 0.0001
C-L-Valine	9.16	1	9.16	6.80	0.0143
D-L-Lysine hydrochloride	9.97	1	9.97	7.40	0.0109
F-L-Arginine hydrochloride	41.80	1	41.80	31.03	< 0.0001
Lack of Fit	11.57	13	0.96	0.60	0.8170
Pure Error	27.50	17	1.62		

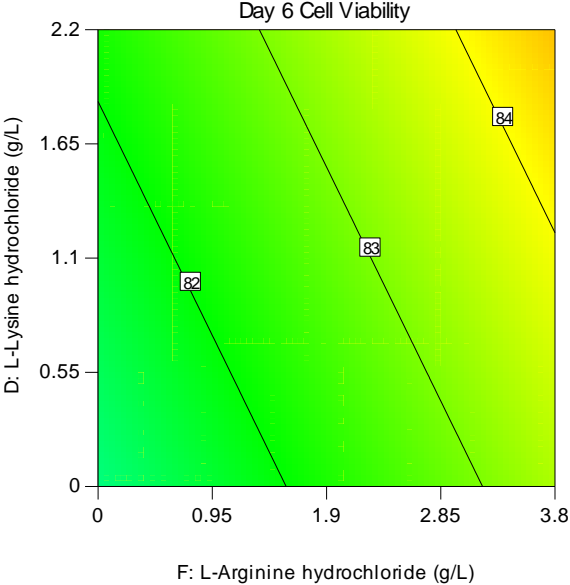
5 | DEVELOPING A NOVEL FEEDING REGIME FOR ENHANCED HEK293T STABLE CELL LINE GROWTH

A

Day 6 Cell Viability (%)

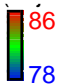


Concentration of other model terms:
C: L-Valine = 0 g/L



B

Day 6 Cell Viability (%)



Concentration of other model terms:
C: L-Valine = 1.4 g/L

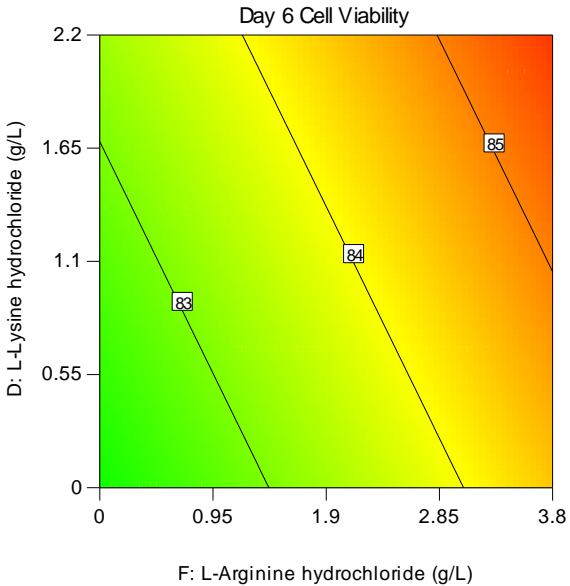


Figure 5.24: Day 6 culture viability response model graph from screening study 3. Graph shows effect of L-Lysine hydrochloride (D-term) and L-Arginine hydrochloride (F-term) on day 6 VCD at low (A) and high (B) concentrations of L-Valine.

5.4 | DESIGN OF EXPERIMENTS BASED SCREENING OF FEED SUPPLEMENTS TO INCLUDE IN THE NOVEL FEED FOR ENHANCING 277 CELL LINE GROWTH

Table 5.28: ANOVA summary of Day 7 VCD response from screening study 3. Data generated using Design Expert v10 (Stat-Ease, Inc., Minnesota, U.S.A). df is degrees of freedom.

Source	Sum of Squares	df	Mean Squares	F-statistic	p-value
Model ¹	0.000	0			
Lack of Fit	6.14	16	0.37	0.62	0.8296
Pure Error	10.57	17	0.62		

¹ There were no significant terms added to the model using backward p-value elimination with the cut-off at 0.1 i.e. all model terms had a p-value greater than 0.1.

Table 5.29: ANOVA summary of Day 7 culture viability response from screening study 3. Data generated using Design Expert v10 (Stat-Ease, Inc., Minnesota, U.S.A). df is degrees of freedom.

Source	Sum of Squares	df	Mean Squares	F-statistic	p-value
Model ¹	0.000	0			
Lack of Fit	12339.3	16	771.2	0.95	0.53
Pure Error	13660.2	17	803.5		

¹ There were no significant terms added to the model using backward p-value elimination with the cut-off at 0.1 i.e. all model terms had a p-value greater than 0.1.

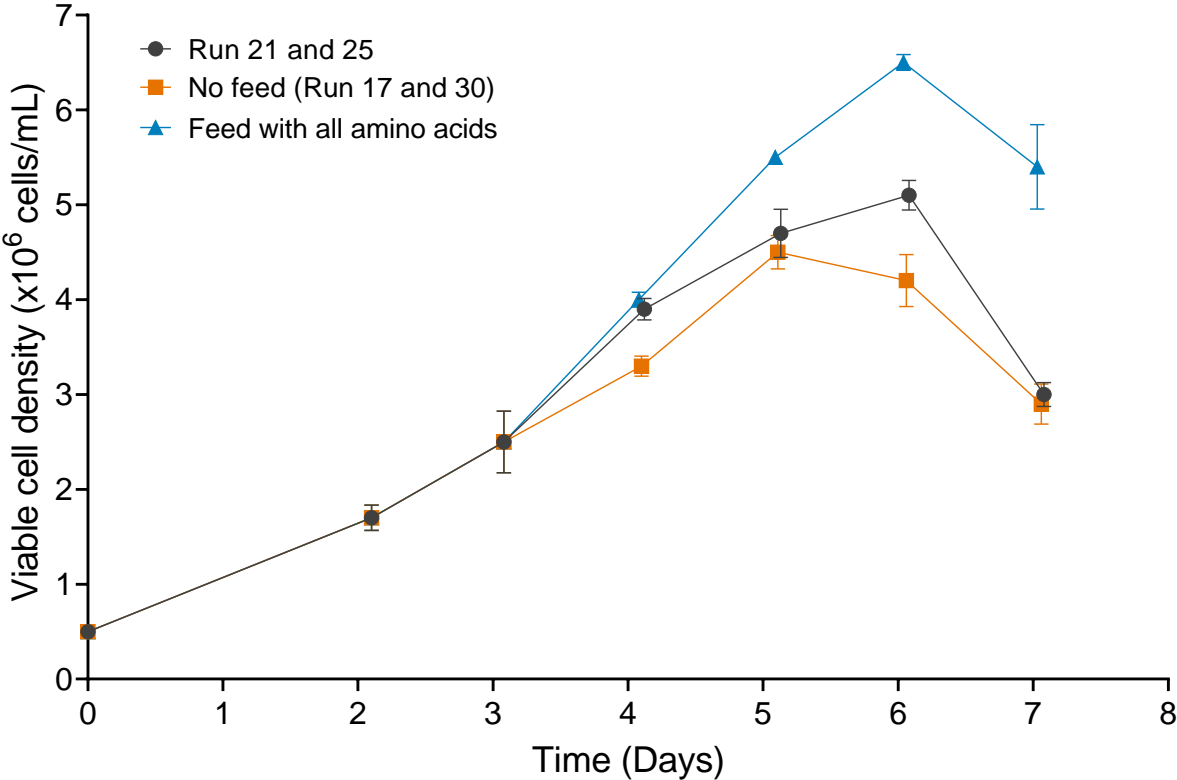


Figure 5.25: Comparison of VCD profile between top performing feed condition from screening study 3 (Run 21 and 25) with no feed condition (Run 17 and 30) and feed with all amino acids. Error bars represent one standard deviation about the mean (n=2).

5.4 | DESIGN OF EXPERIMENTS BASED SCREENING OF FEED SUPPLEMENTS TO INCLUDE IN THE NOVEL FEED FOR ENHANCING 277 CELL LINE GROWTH

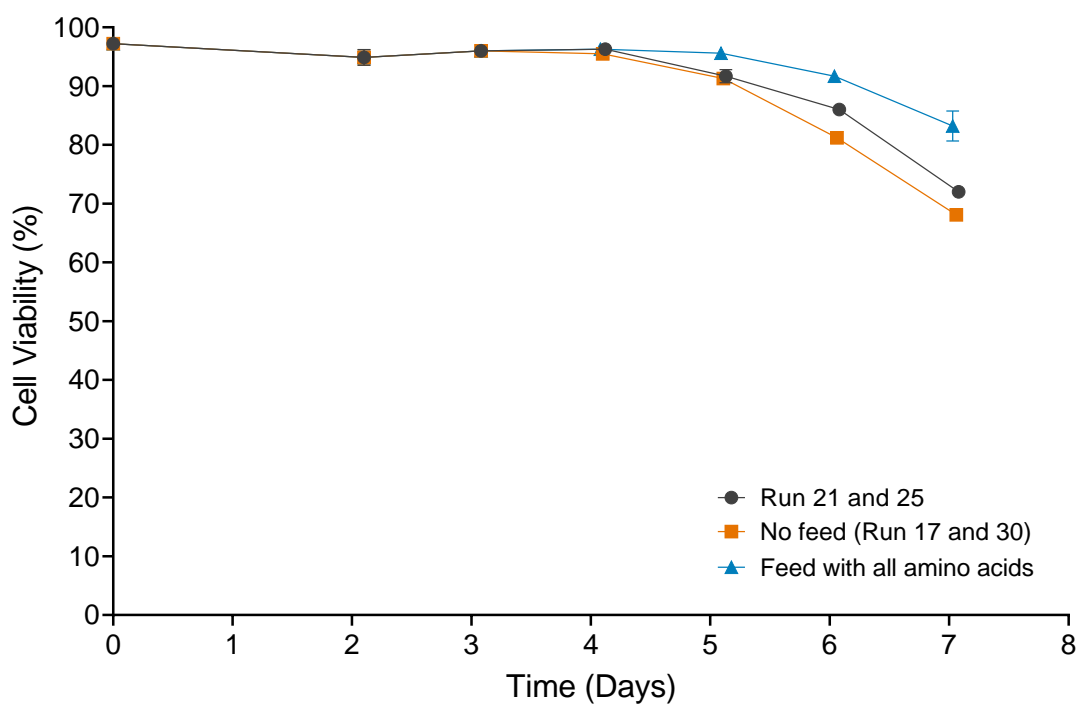


Figure 5.26: Comparison of culture viability profile between top performing feed condition from screening study 3 (Run 21 and 25) with no feed condition (Run 17 and 30) and feed with all amino acids. Error bars represent one standard deviation about the mean (n=2).

Table 5.30: Feed formulation of Run 21 and 25 from screening study 3.

Run	L-Aspartic acid (g/L)	L-Leucine (g/L)	L-Valine (g/L)	L-Lysine hydrochloride (g/L)	L-Isoleucine (g/L)	L-Arginine hydrochloride (g/L)	L-Serine (g/L)	L-Asparagine (g/L)
21 and 25	0	1.6	1.4	2.2	0	3.8	0	0

5.4.4 Screening study 4 – Assessment of individual effect of important metabolites identified in the LC-MS analysis

Following on from screening study 3, the focus of this study was to independently screen the remaining metabolites from Table 5.9 in order to assess their effect on 277 cell growth. To benchmark the performance of the new factors, essential amino acids as a complete formulation was also included as a factor in this design as it has consistently demonstrated a strong positive effect on cell growth in all screening studies. The full list of factors evaluated in this study include:

1. Essential amino acids
2. L-Ornithine
3. L-Norvaline
4. 2-Aminoisobutyric acid
5. Choline chloride
6. Folic acid
7. Putrescine dihydrochloride

L-Ornithine, L-Norvaline and 2-Aminoisobutyric acid are all non-proteinogenic amino acids, which means that they are not coded for by the genetic code of the cell line. These compounds are less commonly found in mammalian cell culture feeds. Of these three amino acids, only the role of L-Ornithine in mammalian cells has been well characterised. L-Ornithine is a key intermediate in the biosynthesis of arginine and also a precursor compound in polyamine synthesis (Roca et al., 2019). It is also indirectly involved in Nitric Oxide (NO) responsiveness through the arginine-NO pathway i.e. L-Ornithine is a precursor for arginine, and arginine is the substrate for nitric oxide

synthase (NOS) to produce NO (Rajapakse and Mattson, 2009). NO responsiveness refers to the ability of cells or to detect and respond to the presence of nitric oxide, a signalling molecule which plays a crucial role as in various physiological processes such as neurotransmission, immune responses and inflammation regulation (Rajapakse and Mattson, 2009). The two vitamins, choline chloride and folic acid, and the polyamine, putrescine, are important metabolites during cell growth and are thus commonly found in most mammalian cell culture feeds. Details on the role of each of the above factors during cell growth has been discussed in section 3.7.3.

Pantothenic acid, Histamine and D-Pipecolic acid were not included in the study due to unavailability of the reagents at the time of performing this experiment. The responses analysed in this study included the VCD and culture viability from day 5 until the end of the culture (i.e. day 7). Among these, only the day 6 VCD and culture viability and day 7 VCD and culture viability responses generated significant models (i.e. model p-value < 0.05). The variation in cell growth on day 5 was not significant enough for models to be generated. The ANOVA summary for all the responses are shown in Table 5.31 to 5.36. Essential amino acids (A-term) was the only significant model term in all the responses analysed. The DoE model graphs (Figures 5.27 to 5.30) indicate a positive linear correlation between essential amino acid concentration and both VCD and culture viability. All other factors screened in this study had p-values greater than 0.05 for all the responses analysed.

Table 5.31: ANOVA summary of Day 5 VCD response from screening study 4. Data generated using Design Expert v10 (Stat-Ease, Inc., Minnesota, U.S.A). df is degrees of freedom.

Source	Sum of Squares	df	Mean Squares	F-statistic	p-value
Model ¹	0.000	0			
Lack of Fit	5.45	32	0.17	1.45	0.3968
Pure Error	0.47	4	0.12		

¹ There were no significant terms added to the model using backward p-value elimination with the cut-off at 0.1 i.e. all model terms had a p-value greater than 0.1.

Table 5.32: ANOVA summary of Day 5 culture viability response from screening study 4. Data generated using Design Expert v10 (Stat-Ease, Inc., Minnesota, U.S.A). df is degrees of freedom.

Source	Sum of Squares	df	Mean Squares	F-statistic	p-value
Model	1.76	1	1.76	3.59	0.0665 ¹
C-L-Norvaline	1.76	1	1.76	3.59	0.0665
Lack of Fit	14.38	31	0.46	0.67	0.7721
Pure Error	2.77	4	0.69		

¹ Model p-value > 0.05 therefore it is not significant

Table 5.33: ANOVA summary of Day 6 VCD response from screening study 4. Data generated using Design Expert v10 (Stat-Ease, Inc., Minnesota, U.S.A). df is degrees of freedom.

Source	Sum of Squares	df	Mean Squares	F-statistic	p-value
Model	3.64	1	3.64	27.07	< 0.0001
A-Essential amino acid	3.64	1	3.64	27.07	< 0.0001
Lack of Fit	4.07	31	0.14	1.08	0.5366
Pure Error	0.50	4	0.13		

5.4 | DESIGN OF EXPERIMENTS BASED SCREENING OF FEED SUPPLEMENTS TO INCLUDE IN THE NOVEL FEED FOR ENHANCING 277 CELL LINE GROWTH

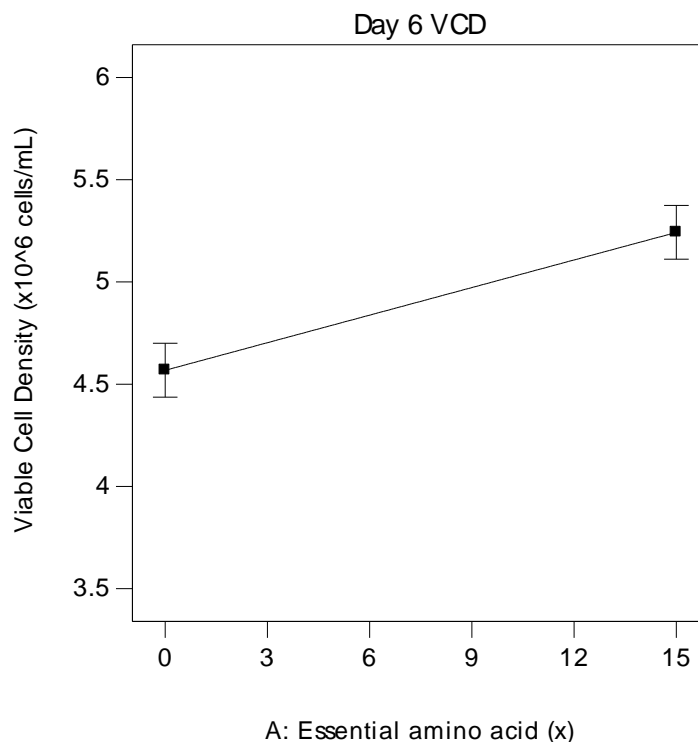


Figure 5.27: Day 6 VCD response model graph from screening study 4. Graph shows effect of essential amino acids (A-term) on day 6 VCD. The x-axis unit ‘x’ refers to times the minimum essential media MEM concentration.

Table 5.34: ANOVA summary of Day 6 culture viability response from screening study 4. Data generated using Design Expert v10 (Stat-Ease, Inc., Minnesota, U.S.A). df is degrees of freedom.

Source	Sum of Squares	df	Mean Squares	F-statistic	p-value
Model	132.44	1	132.44	135.73	< 0.0001
A-Essential amino acid	132.44	1	132.44	135.73	< 0.0001
Lack of Fit	29.63	31	0.99	1.11	0.5224
Pure Error	3.55	4	0.89		

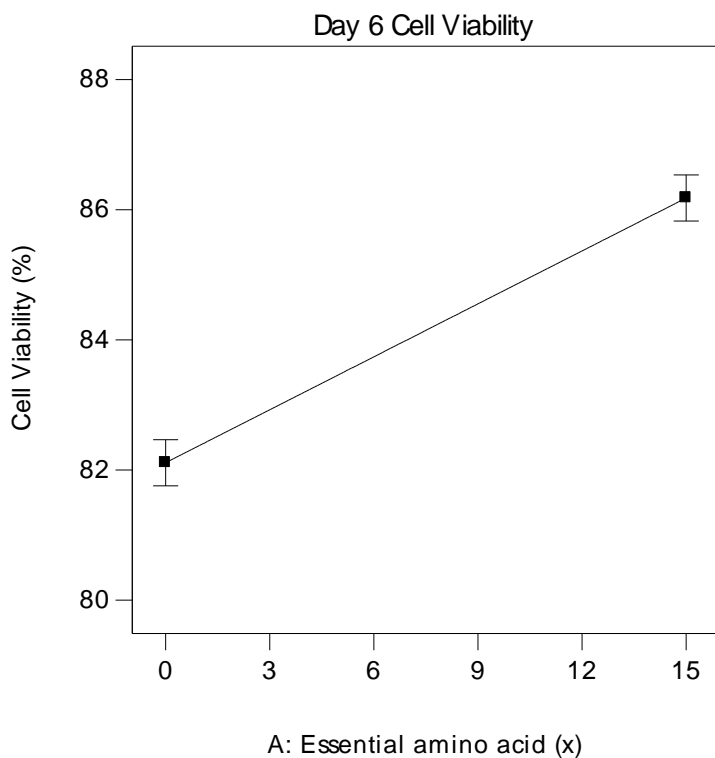


Figure 5.28: Day 6 culture viability response model graph from screening study 4. Graph shows effect of essential amino acids (A-term) on day 6 cell viability. The x-axis unit ‘x’ refers to times the minimum essential media MEM concentration.

Table 5.35: ANOVA summary of Day 7 VCD response from screening study 4. Data generated using Design Expert v10 (Stat-Ease, Inc., Minnesota, U.S.A). df is degrees of freedom.

Source	Sum of Squares	df	Mean Squares	F-statistic	p-value
Model	13.66	1	13.66	173.03	< 0.0001
A-Essential amino acid	13.66	1	13.66	173.03	< 0.0001
Lack of Fit	2.30	31	0.077	0.79	0.6936
Pure Error	0.39	4	0.097		

5.4 | DESIGN OF EXPERIMENTS BASED SCREENING OF FEED SUPPLEMENTS TO INCLUDE IN THE NOVEL FEED FOR ENHANCING 277 CELL LINE GROWTH

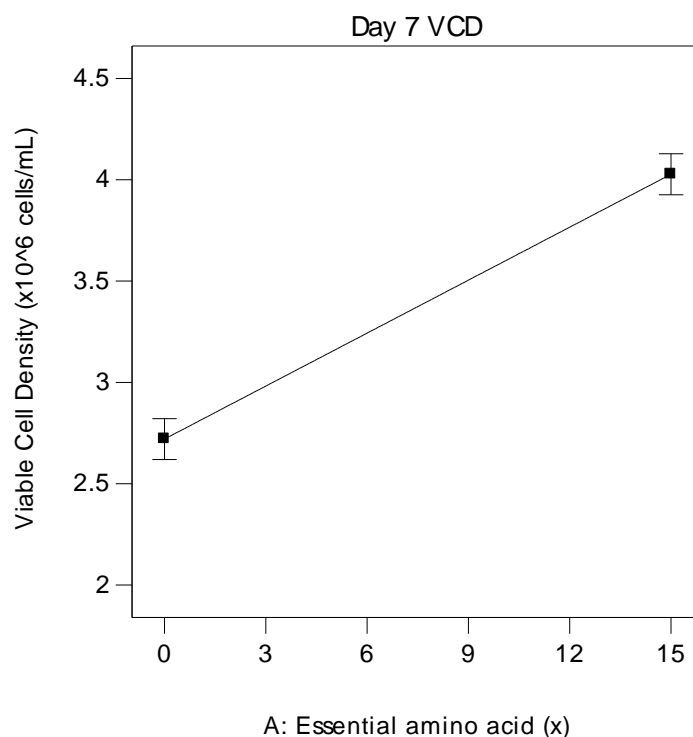


Figure 5.29: Day 7 VCD response model graph from screening study 4. Graph shows effect of essential amino acids (A-term) on day 7 VCD. The x-axis unit ‘x’ refers to times the minimum essential media MEM concentration.

Table 5.36: ANOVA summary of Day 7 culture viability response from screening study 4. Data generated using Design Expert v10 (Stat-Ease, Inc., Minnesota, U.S.A). df is degrees of freedom.

Source	Sum of Squares	df	Mean Squares	F-statistic	p-value
Model	321.31	1	321.31	60.54	< 0.0001
A-Essential amino acid	321.31	1	321.31	60.54	< 0.0001
Lack of Fit	173.83	31	5.79	3.49	0.1154
Pure Error	6.63	4	1.66		

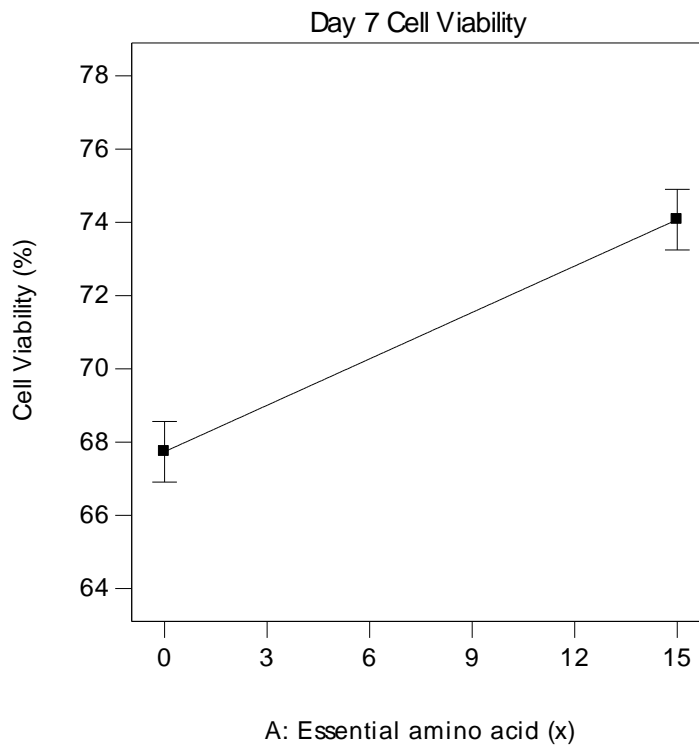


Figure 5.30: Day 7 culture viability response model graph from screening study 4. Graph shows effect of essential amino acids (A-term) on day 7 cell viability. The x-axis unit ‘x’ refers to times the minimum essential media MEM concentration.

Overall, the data from the four screening studies has provided valuable insights into the effect of various feed supplements on 277 cell growth:

- A total of 24 different factors were screened across the four studies. From these, essential amino acids as a complete formulation had the strongest effect on enhancing cell growth. It appeared to be a significant factor in almost all the responses analysed.
- Increasing the concentration of essential amino acids resulted in the highest VCD and culture viability measurements.

5.4 | DESIGN OF EXPERIMENTS BASED SCREENING OF FEED SUPPLEMENTS TO INCLUDE IN THE NOVEL FEED FOR ENHANCING 277 CELL LINE GROWTH

- Factors such as vitamins, polyamines, L-alanyl-L-glutamine and non-essential amino acids exhibited a stochastic effect on growth i.e. they only appeared as significant model terms in a few responses unlike essential amino acids. In the responses where they were significant, their effect on growth was not as strong as essential amino acids.
- Glucose and IGF-1, achieved a negative correlation to 277 cell growth. With glucose, the interaction with essential amino acids was more detrimental to growth than the factor alone. For IGF-1, it is assumed the concentration used in the screening study may not have been optimal for HEK293 cells.
- All the remaining factors screened did not achieve a significant effect on cell growth. It is worth noting that this limited data set may not be conclusive to ascertain whether these metabolites play an important role in HEK293 cell growth. Perhaps, the concentrations evaluated in these screening studies did not result in any effect on growth.

Based on the results from the four screening studies, essential amino acids will be carried forward in the subsequent DoE studies where the focus will be on optimising its concentration. Non-essential amino acids will also be included in the optimisation studies since data from screening study 3 indicated that a feed comprising all 20 amino acids (essential and non-essential) achieved an improved growth profile compared to the condition with no feed.

5.5 OPTIMISING THE NOVEL FEED COMPOSITION AND FEEDING REGIME FOR ENHANCING 277 CELL LINE GROWTH

5.5.1 Optimisation study 1 – Optimising concentration of essential and non-essential amino acids in the novel feed

From all the factors screened in section 5.4, essential and non-essential amino acids were selected to be optimised as components of the novel feed for enhancing 277 cell growth. Essential amino acids in particular was a significant model term in all the screening studies showing a strong positive effect on cell growth. Furthermore, the DoE model graphs indicated a positive linear correlation to growth i.e. increasing the concentration of essential amino acids resulted in improved growth with the highest VCD and culture viability measurements obtained at the highest essential amino acids concentration. In all the screening studies, the concentration of essential amino acids evaluated was between 0–15× MEM. Non-essential amino acids also demonstrated a positive effect on cell growth, although not as significant as essential amino acids. Perhaps, the concentration range tested (i.e. 0–1× MEM) was not wide enough for significant changes on cell growth to be observed. Hence, the goal of the first optimisation study was to evaluate a wider concentration range of the essential and non-essential amino acids using a central composite DoE design. It is the most commonly used fractional factorial design used in response surface modelling (Bhattacharya, 2021).

In this design, the centre points are augmented with a group of axial points which enables the prediction of curvature in the response more accurately (Bhattacharya, 2021). Furthermore, the central composite design helps eliminate the need for a three-level factorial experiment to build a second-order quadratic model, thus reducing the

number of experimental runs without compromising the model response (Bhattacharya, 2021).

According to Costa *et al.*, 2014, the concentration of essential amino acids in mammalian cell culture feeds can be as high as 30× MEM. Hence, the range tested in this study was between 0–30× MEM. For non-essential amino acids, the feed concentration reported is much lower at around 0–1× MEM, since cells are able to synthesize these themselves. This range was already evaluated in the screening studies with little effect on growth observed. Hence, the range of non-essential amino acids tested was extended to 0–10× MEM. Table 5.5 in section 5.2.3 shows the full DoE design summary for this study.

Data from the screening studies showed that the effects of the feed was most apparent on day 6 and day 7. This is when the most variation in VCD and culture viability measurements were observed among the different runs hence generating more significant models compared to earlier time points. Hence, for the optimisation studies, the responses analysed included the VCD and culture viability from day 6 until the end of the culture (i.e. day 7). For response surface designs, the most suitable model is selected based on a set of statistical criteria. Firstly, the highest order model (i.e. smallest p-value) is preferred as it explains significantly more of the variation in the response. Secondly, the model should have an insignificant lack of fit (lack of fit p-value > 0.1). Furthermore, the model maximising the ‘Adjusted R-Squared’ and ‘Predicted R-Squared’ values is preferred. The adjusted R-squared is a measure of the amount of variation around the mean explained by the model, adjusted for the number of terms in the model. The adjusted R-squared decreases as the number of terms in the model increases if those additional terms do not add value to the model. The predicted R-squared is a measure of the amount of variation in new data explained by the model. For a suitable model, the predicted R-squared and the adjusted R-squared have to be within 0.20 of each other.

Using the above criteria, a summary of models selected for each response is given in Table 5.37. The detailed fit summary for all responses is shown in Table 9.18 – 9.21

under Appendix A (section 9.4.4). A linear model was selected for the day 6 VCD response whilst the cubic model was preferred for the day 6 culture viability response. For both day 7 responses, fit summary data shows that the lack-of-fit p-value for all models were significant (i.e. p-value < 0.05) and therefore no model was generated.

ANOVA data was further used to analyse the day 6 responses in order to assess significant model terms. The ANOVA summary is shown in Table 5.38 and 5.39 respectively. For day 6 VCD, the linear term for essential amino acids (A-term) was the only significant term in the model. For day 6 culture viability, both essential and non-essential amino acids were significant model terms. Additionally, the interaction between the two factors (AB-term) was also significant. ANOVA data also shows the presence of curvature in the response since the cubic term for essential amino acids (A³-term) and quadratic term for non-essential amino acids (B²-term) were significant.

Model graphs were generated to illustrate the trend in the day 6 responses as shown in Figure 5.31 and 5.32 respectively. For day 6 VCD, the model graph in Figure 5.31 indicates a strong positive linear correlation between essential amino acids concentration and VCD. Increasing the concentration of essential amino acids resulted in improved cell growth with the highest VCD achieved at 30× MEM concentration. Furthermore, the difference in VCD between 0× and 30× MEM was around 1.5×10^6 cells/mL indicating the importance of essential amino acids concentration in increasing cell proliferation. According to Figure 5.32, both essential and non-essential amino acids were important for the maintenance of high culture viability at day 6. The highest culture viability measurements (i.e. > 92%) were achieved at high concentration of both essential and non-essential amino acids. However, the trend from the DoE model suggests that at the highest concentration of essential amino acids (i.e. 30× MEM), culture viability was independent of non-essential amino acids concentration since high culture viability was achieved at both high and low non-essential amino acids concentration.

As mentioned earlier, model graphs for the day 7 response were not generated due to a significant lack of fit in the data set. Therefore, to better visualise the effect of the

feed over the entire culture period, the conditions with the three highest maximum VCDs were plotted against the 'no feed' condition (i.e. Run 30, 31 and 41). The feed formulations of these top performing conditions termed Feed 4, Feed 6 and Feed 13 are shown in Table 5.40. All three formulations had a high concentration of essential amino acids (i.e. $> 25\times$ MEM) but varied in their concentration of non-essential amino acids.

Feed 4 had a higher concentration of non-essential amino acids at $8\times$ MEM, Feed 6 had $5\times$ MEM whilst Feed 13 did not have non-essential amino acids at all. The cell growth profile shows that higher VCDs (Figure 5.33) and culture viability (Figure 5.34) values were achieved in cultures with feed addition compared to the condition where no feed was added. For all three feed cultures, the maximum VCD was comparable at around 6.7×10^6 cells/mL and was significantly higher than the maximum VCD of 5.2×10^6 cells/mL achieved for the 'no feed' culture. Furthermore, whilst growth arrest was observed after day 5 for the condition with no feed addition, exponential growth was extended until day 6 for the three feed conditions. A steep decline in VCD and culture viability was also observed after day 6 in two of the three feed conditions, specifically Feed 4 and Feed 13. Perhaps the addition of the day 6 feed in these cultures may have been toxic for the cells resulting in cell death. The sudden decline in growth at day 7 for some of the conditions with high essential amino acids concentration may also explain why there was a significant lack of fit in the day 7 response models. Feed 4 and Feed 6 were similar in the sense that both contained essential and non-essential amino acids as part of the formulation albeit at different concentrations. However, the response in VCD and culture viability after day 6 was very different. Between Feed 6 and Feed 13, the key difference was the presence of non-essential amino acids at $5\times$ MEM concentration in the Feed 6 formulation. Hence, this may suggest that non-essential amino acids has a role to play in maintaining culture viability. But more importantly, the balance of essential and non-essential amino acids in the feed is crucial to prevent cell death (Horvat et al., 2020).

Table 5.37: Summary of the models selected for each response in optimisation study 1. For day 7 VCD and cell viability responses, all models had a significant lack of fit.

Response	Model selected	Model p-value	Lack of fit p-value	Adjusted R-square	Predicted R-square
Day 6 VCD	Linear	< 0.0001	0.6513	0.6272	0.5963
Day 6 culture viability	Cubic	0.0077	0.6985	0.8657	0.8079
Day 7 VCD	No model selected due to significant lack of fit				
Day 7 culture viability	No model selected due to significant lack of fit				

Table 5.38: ANOVA summary of Day 6 VCD response from optimisation study 1. Data generated using Design Expert v10 (Stat-Ease, Inc., Minnesota, U.S.A). df is degrees of freedom.

Source	Sum of Squares	df	Mean Squares	F-statistic	p-value
Model	8.94	1	8.94	61.73	< 0.0001
A-Essential amino acids	8.94	1	8.94	61.73	< 0.0001
Lack of Fit	1.60	11	0.15	1.01	0.4646
Pure Error	4.05	28	0.14		

5.5 | OPTIMISING THE NOVEL FEED COMPOSITION AND FEEDING REGIME FOR ENHANCING 277 CELL LINE GROWTH

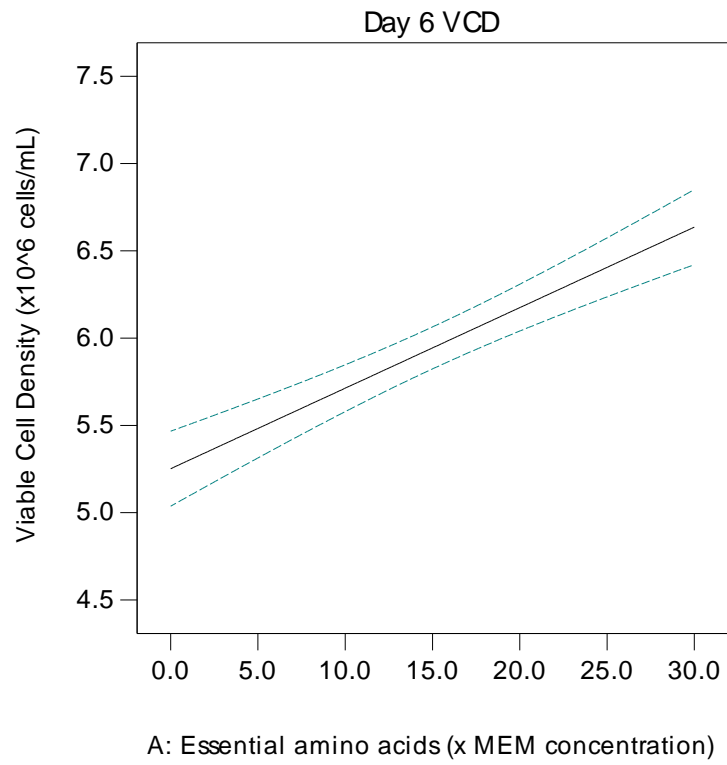


Figure 5.31: Day 6 VCD response model graph from optimisation study 1. Graph shows effect of essential amino acids (A-term) on day 6 VCD. MEM means minimum essential media.

Table 5.39: ANOVA summary of Day 6 culture viability response from optimisation study 1.

Data generated using Design Expert v10 (Stat-Ease, Inc., Minnesota, U.S.A). df is degrees of freedom.

Source	Sum of Squares	df	Mean Squares	F-statistic	p-value
Model	410.17	6	68.36	40.70	< 0.0001
A-Essential amino acids	88.99	1	88.99	52.98	< 0.0001
B-Non-essential amino acids	36.82	1	36.82	21.92	< 0.0001
AB	8.58	1	8.58	5.11	0.0303
B ²	17.66	1	17.66	10.51	0.0027
A ³	17.94	1	17.94	10.68	0.0025
Lack of Fit	10.86	6	1.81	1.10	0.3889
Pure Error	46.24	28	1.65		

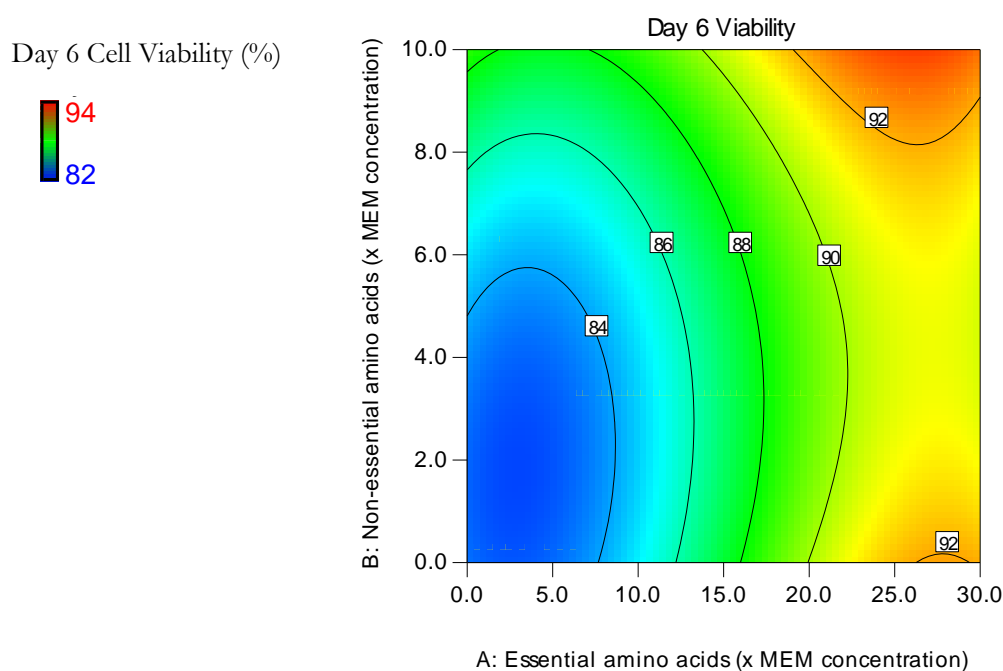


Figure 5.32: Day 6 culture viability response model graph from optimisation study 1. Graph shows interaction between essential amino acids and non-essential amino acids. MEM means minimum essential media.

5.5 | OPTIMISING THE NOVEL FEED COMPOSITION AND FEEDING REGIME FOR ENHANCING 277 CELL LINE GROWTH

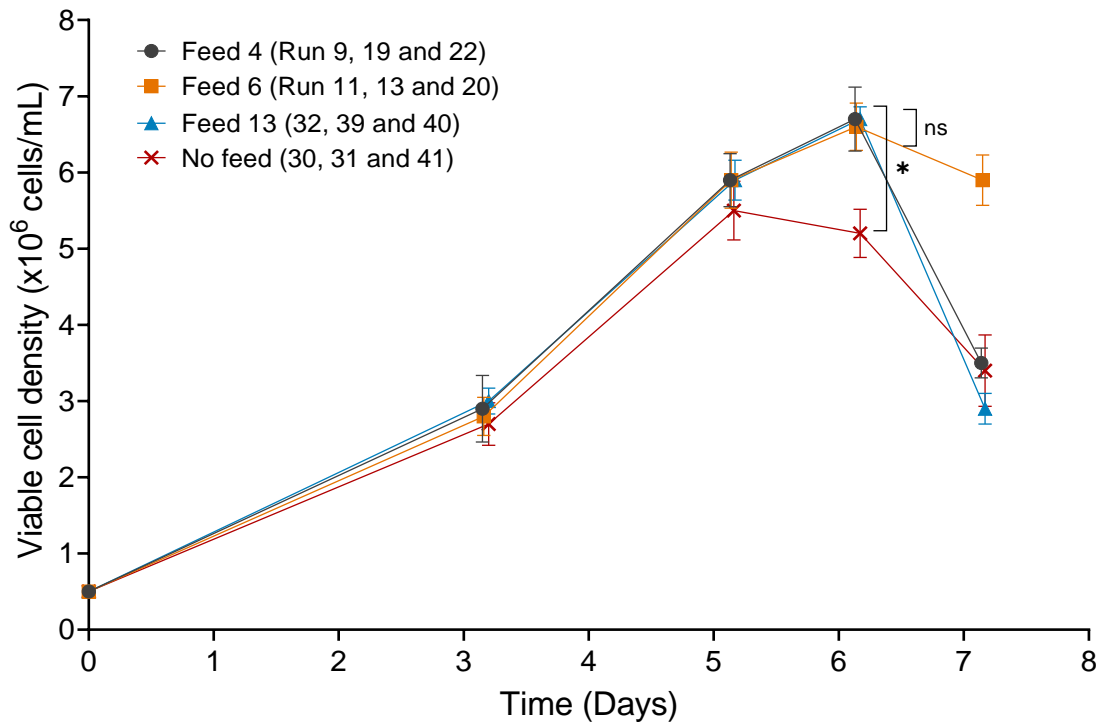


Figure 5.33: Comparison of VCD profile of three top performing feed conditions from optimisation study 1 and no feed condition. Error bars represent one standard deviation about the mean (n=3). Student's t-test was used to compare difference in the day 6 VCDs on the three feeds as well as Feed 6 against 'no feed'; ns: p-value > 0.05; *: p-value ≤ 0.05.

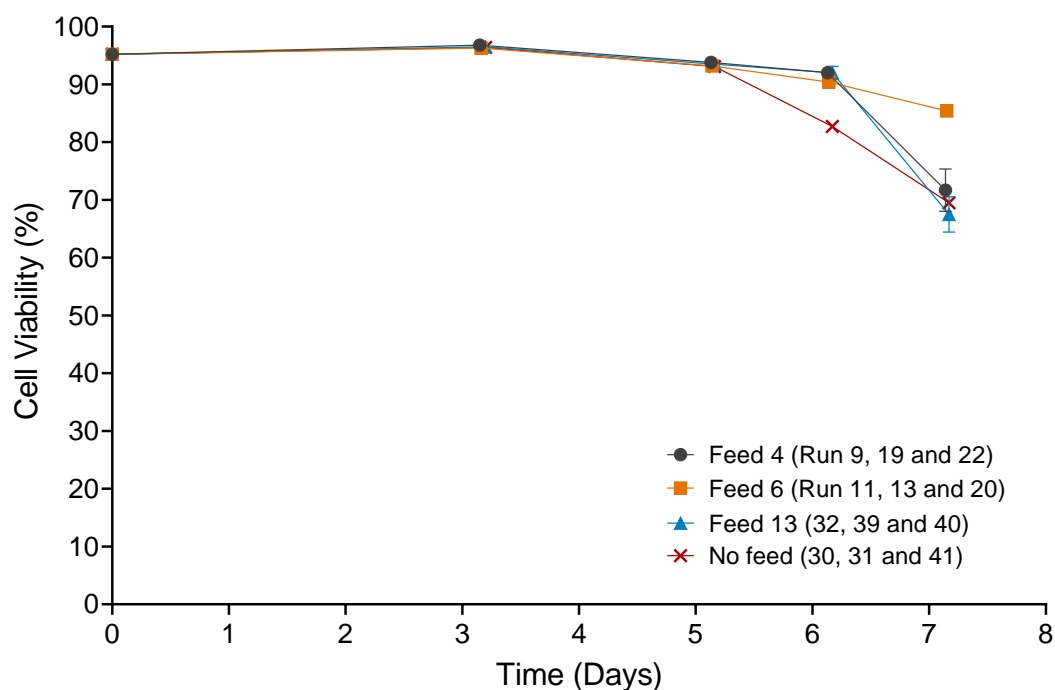


Figure 5.34: Comparison of culture viability profile of three top performing feed conditions from optimisation study 1 and no feed condition. Error bars represent one standard deviation about the mean (n=3).

Table 5.40: Feed formulation of top performing conditions from optimisation study 1.

Feed ID	Run	Essential amino acid (x MEM)	Non-essential amino acid (x MEM)
4	9, 19, 22	25.6	8.5
6	11, 13, 20	30	5
13	32, 39, 40	30	0

5.5.2 Optimisation study 2 – Assessment of essential amino acids concentration higher than 30X MEM

In the previous optimisation study, a wider concentration range of the essential and non-essential amino acids was evaluated using a central composite DoE design. The data showed a strong positive linear correlation between day 6 VCD and essential amino acids concentration. Non-essential amino acids had more of an effect on culture viability rather than VCD. In this study, the aim was to assess essential amino acids concentration higher than 30× MEM in order to evaluate the effect on 277 cell growth. Five different concentrations between 30–50× MEM were tested in increments of 5× MEM. Table 5.6 in section 5.2.3 outlines the conditions tested in this study.

The VCD and culture viability profiles are shown in Figure 5.35 and 5.36 respectively. The data shows that very high essential amino acid concentration was not suitable for cell culture. Concentrations greater than 35× MEM was toxic for the cells and resulted in early cell death. For 45× and 50× MEM, cell death was observed within 24 hours of adding the feed. For 40× MEM, the cells were able to tolerate the day 3 feed addition as demonstrated by a favourable VCD and viability profile at day 5. However, the day 5 feed addition was toxic for the cells resulting in subsequent growth decline.

From the five concentrations tested, 30× MEM achieved the best growth profile. Although a slower growth rate was observed between day 3 to day 5 compared to other conditions with higher concentrations of essential amino acids, there was no apparent decline in VCD throughout the entire culture unlike 35× MEM and 40× MEM where growth decline was observed after day 5. This may indicate that cells were best able to tolerate 30× MEM concentration of essential amino acids in the feed. Furthermore, culture viability at day 7 was >90% suggesting a healthy culture environment was maintained. As also demonstrated in optimisation study 1, 30× MEM concentration achieved a better growth profile compared to the condition without feed addition. In the ‘no feed’ condition, cell growth arrest was observed at day 5 after which VCD and

viability started to drop sharply. However, for 30× MEM, cell proliferation continued past day 5 with maximum VCD being achieved at Day 7.

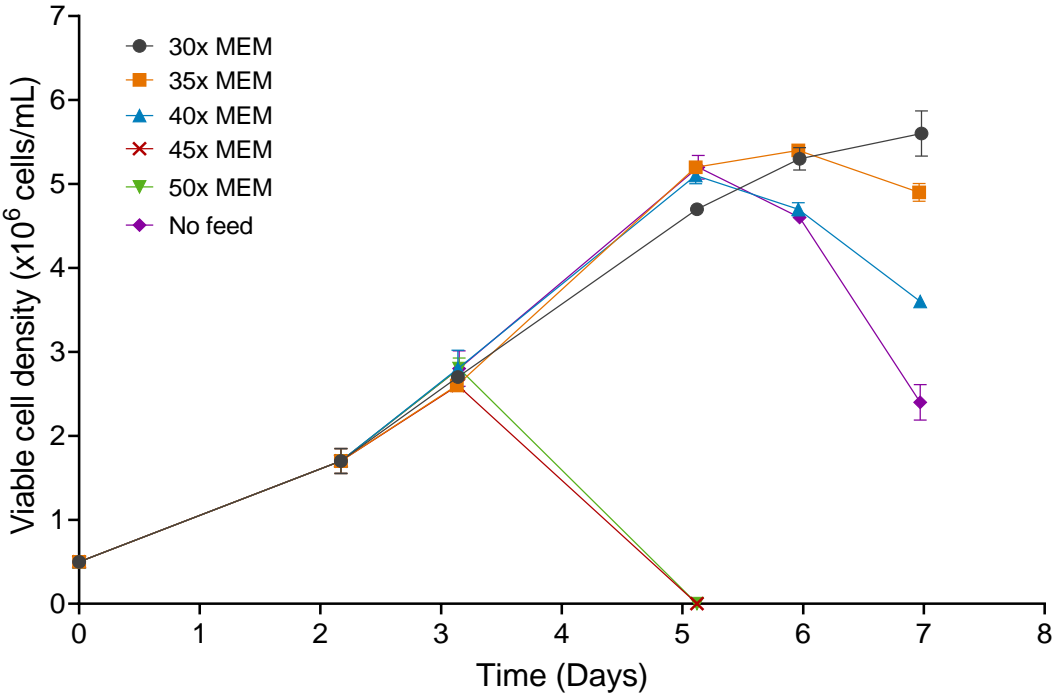


Figure 5.35: Effect of essential amino acids concentration on VCD profile. Error bars represent one standard deviation about the mean (n=2).

5.5 | OPTIMISING THE NOVEL FEED COMPOSITION AND FEEDING REGIME FOR ENHANCING 277 CELL LINE GROWTH

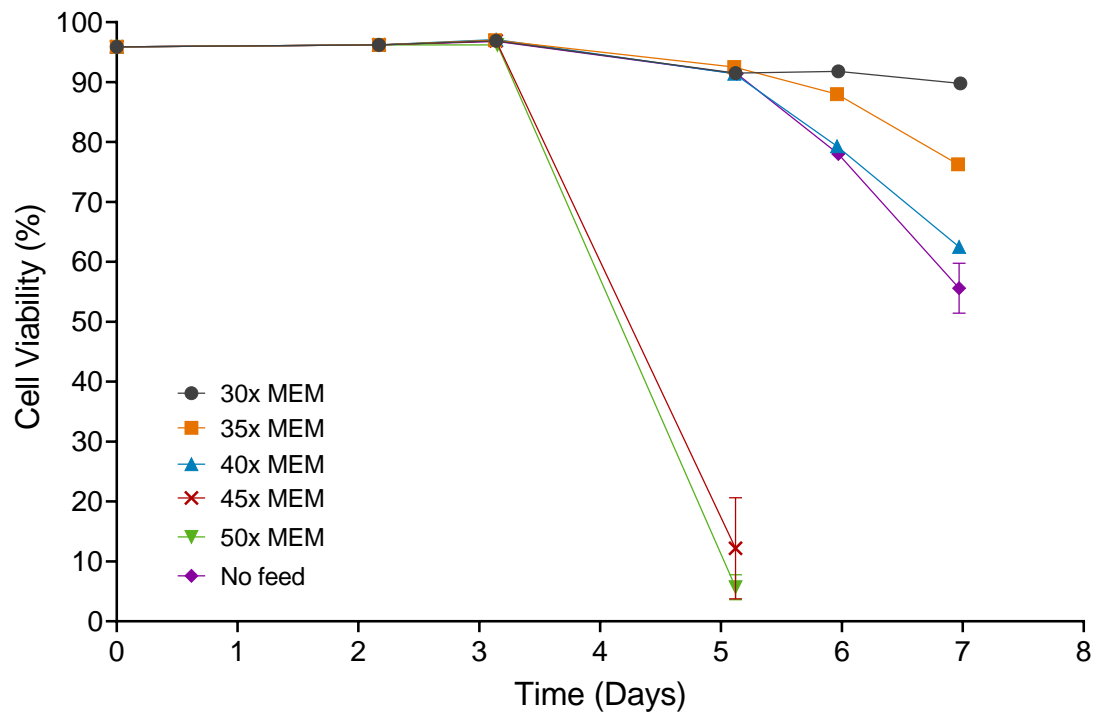


Figure 5.36: Effect of essential amino acids concentration on culture viability profile. Error bars represent one standard deviation about the mean (n=2).

5.5.3 Optimisation study 3 – Assessment of the optimal feeding regime of the novel feed

In optimisation study 1, the highest VCD at day 6 was achieved for conditions with the highest concentration of essential amino acids. However, for these same conditions, adding feed on day 6 resulted in cell death at day 7, perhaps due to a disturbance in the metabolic balance of the cells. Hence the feeding strategy optimised in section 5.3 using the commercial feed may not be applicable for the novel 277 feed due to differences in the formulation. Hence, this study aims to assess optimal feeding regime for the novel feed by addressing the following questions:

1. Which days should the novel feed be added?
2. What concentration of feed should be added on each day?

Four feeding time points were assessed in this study: day 3, day 4, day 5 and day 6. Furthermore, the range of feed amount evaluated on each day was between 0–5% (v/v). The feed formulation used in this study was adapted from the top performing condition from optimisation study 1 (i.e. Feed 6) and is shown in Table 5.41. The DoE design details has already been described in section 5.2.3 and table of factors shown in Table 5.7.

Table 5.41: Summary of feed formulation used in optimisation study 3.

Component	Concentration
Essential amino acids	30× MEM
Non-essential amino acids	5× MEM
Sodium bicarbonate	Add amount to achieve pH 7-7.4

For this study, the responses analysed included the VCD and culture viability from day 6 until the end of the culture (i.e. day 7). For each response, the most suitable model was selected based on the statistical criteria outlined earlier in section 5.5.1. The

detailed fit summary for all responses is shown in Table 9.22 – 9.25 under Appendix A (section 9.4.4). A summary of the models selected for each response is shown in Table 5.42. For day 7 culture viability, no model was selected due to a significant lack of fit.

ANOVA data was further used to analyse each response in order to assess significant model terms. The ANOVA summary is shown in Table 5.43 to 5.45. From the ANOVA output, the VCD at day 6 was affected by feed amounts at day 3, 4 and 5. All three feed additions prior to day 6 achieved the minimum p-value threshold of less than 0.05 in order to be included in the model. Furthermore, the quadratic terms for day 3 (A²-term), day 4 (B²-term) and day 5 (C²-term) feed amounts were all significant terms in the model indicating the presence of curvature. From the three time points, day 4 feed amount had the most significant effect on the VCD at day 6. The day 4 term had the smallest p-value and largest F-statistic suggesting it was the most sensitive factor to the response. The DoE model graph (Figure 5.37) also indicates that the highest VCDs were achieved when the day 4 feed amount was maximised. With regards to day 3 and day 5 feed amounts, there was curvature in the response since high VCDs were achieved at both low and high quantities of day 3 feed, whilst 2.5% (v/v) feed addition at day 5 resulted in the most favourable growth profile.

For day 6 culture viability, all prior feed time points were again significant to the response. In particular, the interaction between day 3 and day 4 feed (AB-term) and day 4 and day 5 feed (BC-term) time points were significant, hence the two-factor interaction (i.e. 2FI) model was selected. Both day 4 and day 5 feed amounts were equally sensitive to the model with the highest culture viabilities being achieved when these two factors were maximised (see Figure 5.38).

For day 7 VCD, all four prior feed additions had a significant effect on the growth profile. The ANOVA data also indicates interaction between the different feed time points with AD, BC, BD and CD terms all achieving p-values less than 0.05. Furthermore, the quadratic terms for day 4 and day 5 feed time points were also significant indicating curvature in the response.

The DoE model graph (Figure 5.39) demonstrates that a high volume feed addition early in the process (i.e. at day 3 and day 4) followed by lower volume feed additions later on resulted in the highest cell densities. The region on the graph with the highest cell density was 5% (v/v) feed addition at day 3 and day 4, 2.5% (v/v) feed addition at day 5 and no feed addition at day 6. The condition corresponding to this feed regime (i.e. Run 21 and 26) achieved the highest maximum VCD of 7.3×10^6 cells/mL. However, analysing the conditions which achieved maximum VCDs greater than 7×10^6 cells/mL demonstrated a trend that was not evident from the DoE model graphs. It was actually a combination of different feed regimes that achieved favourable growth profiles. Table 5.46 summarises the feed regimes of the top 3 conditions from the DoE study. A common pattern in these conditions was that the total amount of feed added in the 4-day period was between 11.5 – 12.5% (v/v). Conditions with total feed addition greater than 12.5% (v/v) resulted in poor VCDs at day 7. And conversely, conditions with total feed addition less 11.5% (v/v) achieved lower peak VCDs.

For LVV production processes, reducing process duration, as well as maximising cell growth and infectious titre, would be advantageous. Therefore, the feed regime corresponding to runs 21 and 26 would be the most preferable option. Not only does it achieve the highest maximum VCD, but feeding is also completed the earliest (i.e. by day 5) with this regime. To assess the performance of the novel 277 feed, the growth profile from the optimised feeding regime (i.e. Runs 21 and 26) was plotted against the no feed control (Runs 22 and 30) as shown in Figure 5.40. According to both the VCD (Figure 5.41) and cell viability (Figure 5.42) graphs, addition of the novel feed significantly enhanced 277 cell growth. Higher VCDs and culture viability measurements were achieved as a consequence of adding the feed. The maximum VCD of 7.3×10^6 cells/mL achieved with the novel feed was significantly higher than that of the ‘no feed’ culture which achieved 5.05×10^6 cells/mL. A Student’s T-test was used to confirm significance at 95% confidence level. Furthermore, for the novel feed, the maximum VCD was obtained at day 6 with the exponential growth period extended by up to 24 hours compared to the ‘no feed’ culture.

With each round of DoE study, there has been a gradual increase in the maximum VCD of the 277 cell line. From the screening studies, the maximum VCD of the top formulations comprising essential amino acids at 15× MEM concentration was between $5.2\text{--}5.9 \times 10^6$ cells/mL. By optimising the concentration of essential and non-essential amino acids in optimisation study 1, the maximum VCD increased to $6.7 \pm 0.4 \times 10^6$ cells/mL. Optimisation of the feeding regime in this study resulted in the highest maximum VCD of $7.3 \pm 0.3 \times 10^6$ cells/mL.

Although this novel feed has improved 277 cell growth, comparing its performance against the commercial feed suggests that there is still further scope for optimising its formulation. The growth profile from the optimal feed regime from this study was plotted against the optimised commercial feed condition (i.e. feed regime 3) from section 5.3 (see Figure 5.43). Although the growth profile between the two feeds were comparable until day 6, the commercial feed culture continued to grow until day 7, thus achieving a higher maximum VCD. Typical mammalian cell culture feeds contain 50–100 components which include trace elements, inorganic salts, energy source, amino acids, vitamins, nucleic acid derivatives, fatty acids and lipids (Landauer, 2014). The balance of each of these components is key to the success of the feed. Achieving the optimal balance requires significant time and resource. In this project, only 24 factors have been screened across 4 studies, providing a suitable proof-of-concept for novel feed development. Further work could be performed in future to continue to develop this novel feed.

Table 5.42: Summary of the models selected for each response in optimisation study 3. For day 7 cell viability response, all models had a significant lack of fit.

Response	Model selected	Model p-value	Lack of fit p-value	Adjusted R-square	Predicted R-square
Day 6 VCD	Quadratic	< 0.0001	0.4830	0.8422	0.7351
Day 6 cell viability	2FI	0.0003	0.1450	0.8217	0.7396
Day 7 VCD	Quadratic	0.0029	0.3854	0.7685	0.6261
Day 7 cell viability	No model selected due to significant lack of fit				

Table 5.43: ANOVA summary of Day 6 VCD response from optimisation study 3. Data generated using Design Expert v10 (Stat-Ease, Inc., Minnesota, U.S.A).

Source	Sum of Squares	df	Mean Squares	F-statistic	p-value
Model	19.05	7	2.72	32.91	< 0.0001
A-Day 3	1.25	1	1.25	15.10	0.0004
B-Day 4	7.28	1	7.28	88.05	< 0.0001
C-Day 5	3.06	1	3.06	37.01	< 0.0001
AB	0.42	1	0.42	5.05	0.0310
A ²	1.43	1	1.43	17.34	0.0002
B ²	0.64	1	0.64	7.79	0.0085
C ²	2.38	1	2.38	28.74	< 0.0001
Lack of Fit	2.78	33	0.084	1.47	0.4855
Pure Error	0.11	2	0.057		

5.5 | OPTIMISING THE NOVEL FEED COMPOSITION AND FEEDING REGIME FOR ENHANCING 277 CELL LINE GROWTH

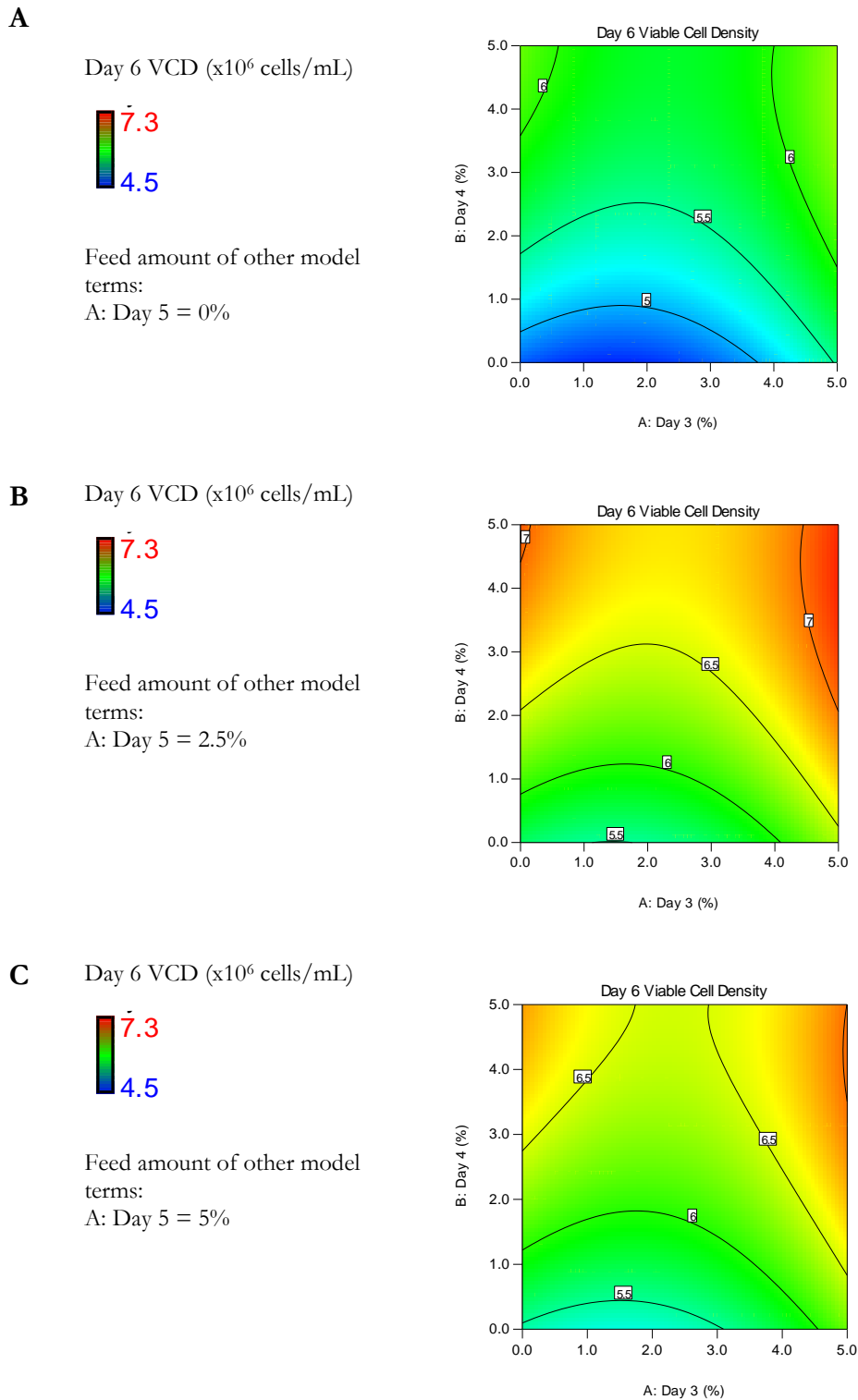


Figure 5.37: Day 6 VCD response model graph from optimisation study 3. Graph shows effect of day 3 and day 4 feed amounts on day 6 VCD. Interaction with day 5 feed amount is also shown: (A) Day 5 = 0% (B) Day 5 = 2.5% (C) Day 5 = 5%. VCD is viable cell density.

Table 5.44: ANOVA summary of Day 6 culture viability response from optimisation study 3.

Data generated using Design Expert v10 (Stat-Ease, Inc., Minnesota, U.S.A).

Source	Sum of Squares	df	Mean Squares	F-statistic	p-value
Model	510.42	5	102.08	42.80	< 0.0001
A-Day 3	33.17	1	33.17	13.91	0.0006
B-Day 4	136.59	1	136.59	57.27	< 0.0001
C-Day 5	129.58	1	129.58	54.33	< 0.0001
AB	17.83	1	17.83	7.48	0.0095
BC	56.81	1	56.81	23.82	< 0.0001
Lack of Fit	87.40	35	2.50	5.91	0.1550
Pure Error	0.84	2	0.42		

5.5 | OPTIMISING THE NOVEL FEED COMPOSITION AND FEEDING REGIME FOR ENHANCING 277 CELL LINE GROWTH

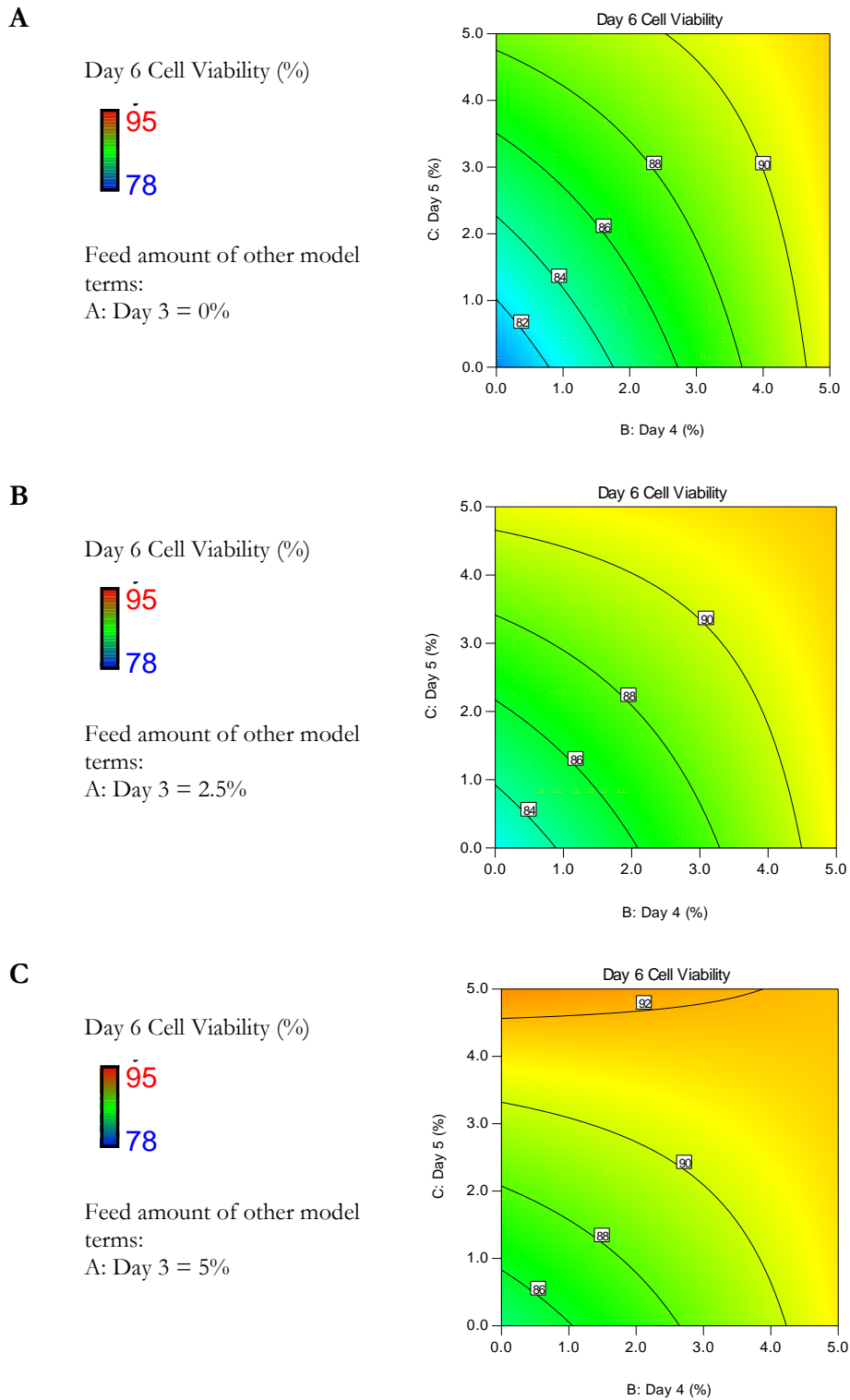


Figure 5.38: Day 6 culture viability response model graph from optimisation study 3. Graph shows effect of day 4 and day 5 feed amounts on day 6 cell viability. Interaction with day 3 feed amount is also shown: (A) Day 3 = 0% (B) Day 3 = 2.5% (C) Day 3 = 5%. VCD is viable cell density.

Table 5.45: ANOVA summary of Day 7 VCD response from optimisation study 3. Data generated using Design Expert v10 (Stat-Ease, Inc., Minnesota, U.S.A).

Source	Sum of Squares	df	Mean Squares	F-statistic	p-value
Model	57.38	13	5.74	11.28	< 0.0001
A-Day 3	0.44	1	0.44	0.86	0.3613
B-Day 4	3.10	1	3.10	6.09	0.0191
D-Day 6	1.50	1	1.50	2.95	0.0957
AD	4.91	1	4.91	9.64	0.0040
BC	7.27	1	7.27	14.29	0.0006
BD	4.06	1	4.06	7.98	0.0081
CD	3.88	1	3.88	7.62	0.0095
B ²	3.82	1	3.82	7.50	0.0100
C ²	2.13	1	2.13	4.19	0.0491
Lack of Fit	15.86	27	0.53	2.53	0.3229
Pure Error	0.42	2	0.21		

5.5 | OPTIMISING THE NOVEL FEED COMPOSITION AND FEEDING REGIME FOR ENHANCING 277 CELL LINE GROWTH

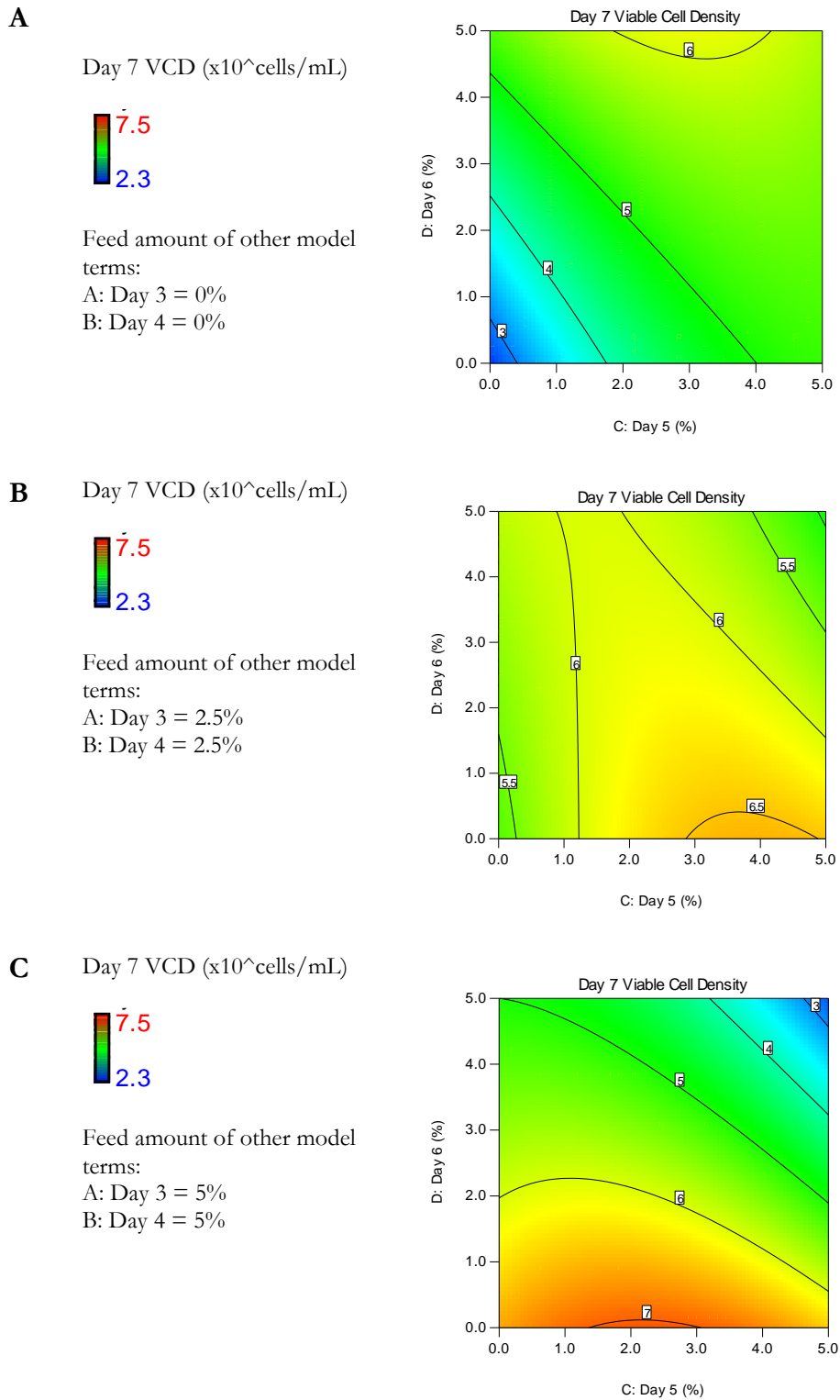


Figure 5.39: Day 7 VCD response model graph from optimisation study 3. Graph shows effect of day 4 and day 5 feed amounts on day 7 VCD. Interaction with day 3 and day 4 feed amount is also

5 | DEVELOPING A NOVEL FEEDING REGIME FOR ENHANCED HEK293T STABLE CELL LINE GROWTH

shown: (A) Day 3 and Day 4 = 0% (B) Day 3 and Day 4 = 2.5% (C) Day 3 and Day 4 = 5%. VCD is viable cell density.

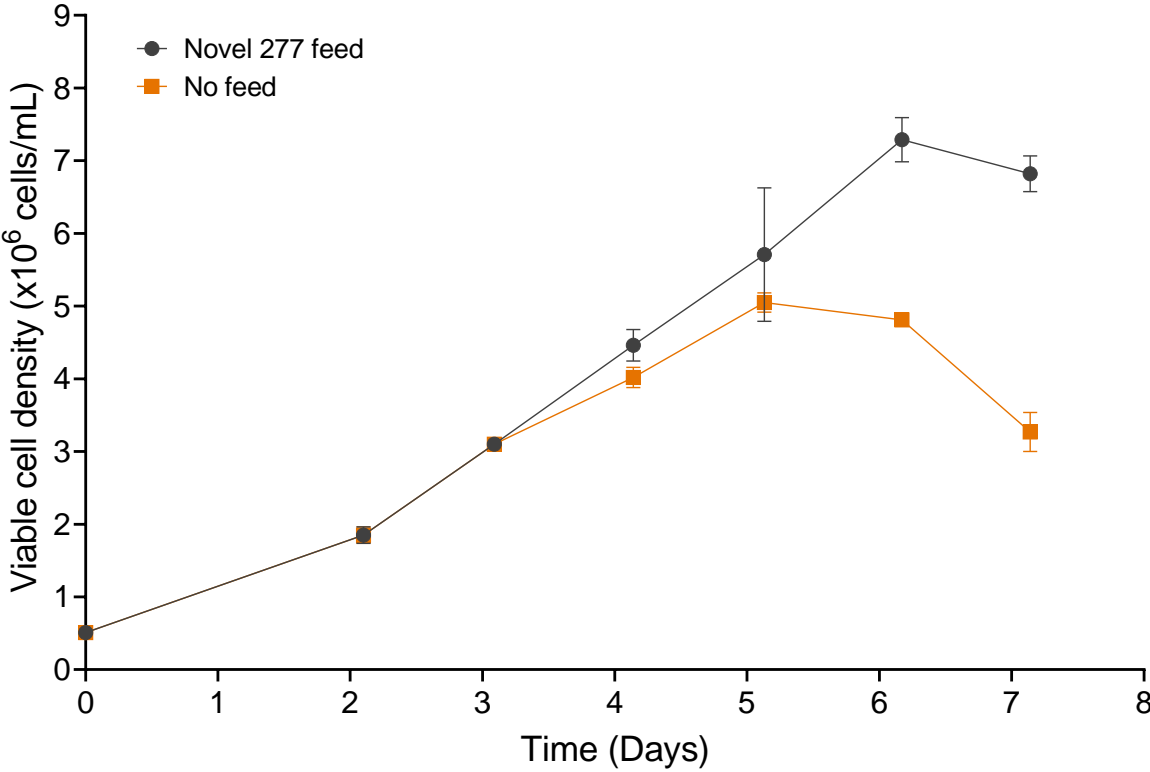


Figure 5.40: Comparison of VCD profile of the top performing feed condition from optimisation study 3 and no feed condition. Error bars represent one standard deviation about the mean (n=2).

5.5 | OPTIMISING THE NOVEL FEED COMPOSITION AND FEEDING REGIME FOR ENHANCING 277 CELL LINE GROWTH

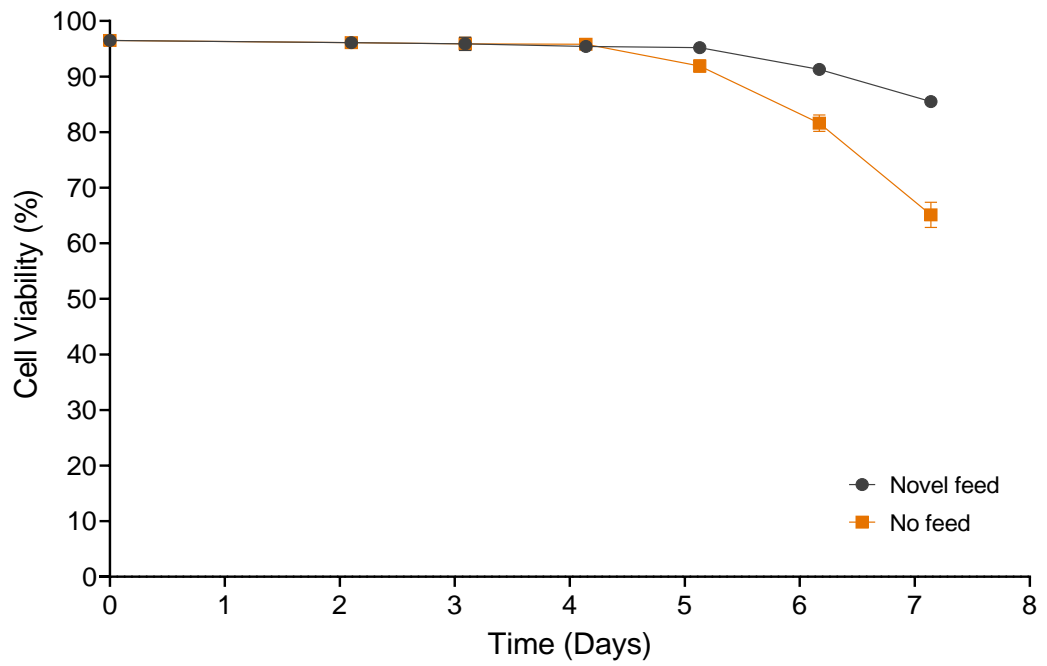


Figure 5.41: Comparison of culture viability profile of the top performing feed condition from optimisation study 3 and no feed condition. Error bars represent one standard deviation about the mean (n=2).

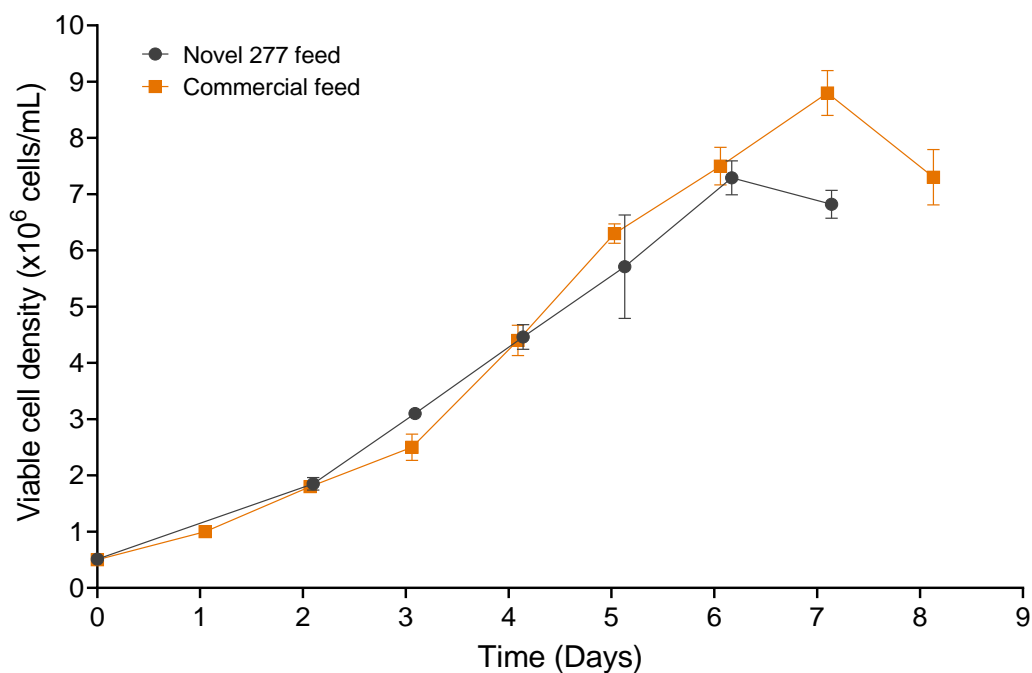


Figure 5.42: Comparison of the VCD profile of the top performing feed condition from optimisation study 3 and the optimal commercial feed condition from section 5.3. Error bars represent one standard deviation about the mean (n=2 for the novel 277 feed; n=3 for the commercial feed).

Table 5.46: Summary of the feed regimes of the top 3 conditions from optimisation study 3.

Run	Day 3 feed (% v/v)	Day 4 feed (% v/v)	Day 5 feed (% v/v)	Day 6 feed (% v/v)	Max VCD (x10 ⁶ cells/mL)
21 and 26	5	5	2.5	0	7.3 ± 0.3
17 and 33	0	5	5	1.5	7.0 ± 0.6
13 and 31	5	2.5	2.5	2.5	7.2 ± 0.2

Table 5.47: Summary of the optimised characteristics of the novel feed.

Feed characteristic	Optimised variable
Feed composition	Essential amino acids - 30× MEM
	Non-essential amino acids - 5× MEM
Feed regime	Day 3 feed amount – 5% v/v
	Day 4 feed amount – 5% v/v
	Day 5 feed amount – 2.5% v/v

5.6 CHAPTER SUMMARY

This chapter has successfully demonstrated the use of DoE methodology to develop a novel feed for enhancing 277 cell growth. A summary of the optimised characteristics of the novel feed is shown in Table 5.47. Below are the key findings from this chapter:

- From the 24 different factors screened in section 5.4, essential amino acids achieved the most significant effect on cell growth. There was a strong positive linear correlation between essential amino acids concentration and VCD. Non-essential amino acids was also considered for optimisation due to its role in maintaining high cell viabilities.
- The composition of the novel feed was optimised in section 5.5.1. The best overall growth profile was achieved with a formulation comprising of 30× MEM essential amino acids and 5× MEM non-essential amino acids.
- In section 5.3, a commercial feed was used to characterise a feeding regime to employ in the DoE studies. However, it was later discovered in section 5.5.1 that the feeding strategy optimised using the commercial feed was not suitable for the novel 277 feed due to differences in the formulation. Hence, the feed regime of the novel feed was optimised in section 5.5.3. The data showed that

a combination of different feed regimes achieved favourable growth profiles provided the total feed addition between day 3 and day 6 amounted to 11.5–12.5% (v/v). The most preferable feed regime consisted of 5% (v/v) addition on day 3, 5% (v/v) addition on day 4 and 2.5% (v/v) addition on day 5. This regime not only achieved the highest maximum VCD of 7.3×10^6 cells/mL but is also most suited for the LVV production process due to the completion of feed addition by day 5.

- Lastly, the novel feed has enabled the exponential growth period to be extended beyond day 5. This permits cells to be induced later than day 3 and at higher VCD's which could potentially increase LVV titres. Hence, in the next chapter, the novel 277 feed will be used to characterise LVV production at high induction cell densities.

6 ASSESSMENT OF LVV PRODUCTION AT HIGH INDUCTION CELL DENSITIES USING THE NOVEL FEED

6.1 INTRODUCTION AND AIMS

In Chapter 3, it was demonstrated that the 277 cell line was unable to reach high cell densities under the current platform conditions. Cell growth arrest was observed as early as day 5 with the culture reaching a maximum VCD of just under 6×10^6 cells/mL. Due to the short period of exponential growth, GSK's current upstream LVV process using the 277 cell line has been optimised for induction around day 3 (i.e. middle of exponential growth) and vector harvest performed approximately 48 hours later. This coincides with an induction cell density in the range of $2\text{--}3 \times 10^6$ cells/mL. In Chapter 5, a DoE approach was used to formulate a novel feed comprising of essential and non-essential amino acids that was able to improve 277 stable cell line growth. The regime of adding the novel feed was also optimised. Addition of the novel feed not only achieved a higher maximum VCD of 7.3×10^6 cells/mL but also increased the period of exponential growth by 1 day (i.e. until day 6 post-inoculation). The maintenance of high VCD and cell viability using the novel feed could allow for the cell culture to be induced after day 3 and at higher cell densities.

Thus, the aim of this chapter is to evaluate the effect of inducing HEK293T stable cell line culture at high cell density on LVV production.

First, the effect of the novel feed on LVV production will be assessed using the 277 cell line cultured in 24-DSW plates. Thereafter, the optimised feeding regime will be evaluated using an alternative proprietary GSK stable producer cell line for production of a LVV encoding for a therapeutic transgene (termed GSK-asset cell line hereafter) in 24-DSW plates. The specific objectives of this chapter are:

- Characterisation of LVV production at high cell densities in 24-DSW plates using the 277 stable cell line
- Evaluating the effect of the novel feed on cell growth and LVV production profile of a GSK-asset stable cell line cultured in 24-DSW plates
- Study interaction between feeding regime, induction timepoint and LVV harvest timepoint

6.2 CHAPTER SPECIFIC MATERIALS AND METHODS

6.2.1 Characterisation of LVV production at high cell densities in 24-DSW plates using the 277 and GSK-asset stable cell lines

The experiments were performed using the 24-DSW plate high-throughput scale down model. Triplicate wells were used for daily sampling. The method pertaining to 24-DSW plate set-up, operation and sampling has been outlined in section 2.5. The method for all analytical techniques used in this study are described in section 2.7. The optimised feed from chapter 5 was used in this study. The feed formulation is

summarised in Table 6.1. The method for preparing the feed is discussed in section 2.2.

Table 6.1: Formulation of the optimised novel feed.

Component	Feed concentration
Essential amino acids	30× MEM
Non-essential amino acids	5× MEM
Sodium bicarbonate (1M)	Add amount to achieve pH 7-7.4

6.2.2 Quantification of infectious titre for LVV produced using the GSK-asset stable cell line

This section is only relevant to section 6.4.

The LVV produced using the GSK-asset stable cell line does not contain the green fluorescence protein (GFP) transgene and hence cannot be quantified using the flow cytometry based method described in section 2.7.4. The method presented below describes the determination of infectious titre of LVVs through quantification of the number of LVVs integrated in transduced SUP-T1 cells by digital droplet polymerase chain reaction (ddPCR). The first step involves transduction of the SUP-T1 cells with serial dilutions of the LVV to be titrated. The SUP-T1 cells were derived from a GSK in-house research cell bank. The cells were grown in a T-25 flask (Corning Inc. New York, U.S.A) and maintained in complete RPMI media (Thermo Fisher Scientific, Massachusetts, U.S.A). Complete formulation of RPMI was achieved by supplementing with 10% Foetal Bovine Serum (FBS) (Thermo Fisher Scientific, Massachusetts, U.S.A) and 2 mM of GlutaMAX (Thermo Fisher Scientific, Massachusetts, U.S.A). Serial dilutions for LVV samples were performed using complete RPMI media. An in-house positive LVV control was also included in the

analysis. The recommended dilutions for the LVV samples and control were performed as per the company's protocol. Transduction of the SUP-T1 wells was performed in 96-well plates (Corning Inc. New York, U.S.A). Transduced cells were then cultured for 3 days at 37°C in a 5% (v/v) CO₂ humidified incubator (Panasonic, Osaka, Japan). On day 3, 100 µL of complete RPMI was added to all wells containing LVV samples and controls. The plates were then returned for incubation for two more days. On day 5, the transduction was terminated and DNA extraction was performed using the KingFisher Flex benchtop automated extraction instrument (Thermo Fisher Scientific, Massachusetts, U.S.A).

The PrepSEQ™ Residual DNA sample preparation kit (Thermo Fisher Scientific, Massachusetts, U.S.A) was used to prepare samples for DNA extraction following the manufacturer's instructions. The DNA extracts were stored at -20°C until used for digital droplet polymerase chain reaction (ddPCR) analysis. ddPCR was performed using a QX200 Droplet Digital PCR system (Bio-Rad, California, U.S.A). The Mastermix for ddPCR included ddPCR Supermix for Probes (no dUTP) (Bio-Rad, California, U.S.A), HIV target gene primer (Life Technologies, California, U.S.A) and RPLP0 reference primer (Bio-Rad, California, U.S.A). The concentration of reagents in the Mastermix used were based on the company's protocol. The generation of droplets was performed by the QX200 Droplet Generator (Bio-Rad, California, U.S.A) according to the manufacturer's protocol. PCR amplification was carried out using QX200 system thermocycler (Bio-Rad, California, U.S.A) with the company's recommended PCR conditions. The plate was stored at 4°C until the droplets were analysed with QX200 Droplet Reader and QuantaSoft software version 1.7.4 (Bio-Rad, California, U.S.A).

6.3 CHARACTERISATION OF LVV PRODUCTION AT HIGH CELL DENSITIES IN 24-DSW PLATES USING THE 277 STABLE CELL LINE

In section 5.5.3, it was demonstrated that the optimised novel feed was able to improve 277 cell line growth by extending the exponential growth period until day 6. To achieve the highest LVV titre, induction is preferred to be carried out in the middle of exponential growth when cells are in the most viable state. Therefore, with the novel feed, cells can now be induced as late as day 4 and vector harvested approximately 48 hours later (i.e. day 6) which corresponds to the time point just prior to growth arrest. The aim of this study, therefore, was to characterise LVV production at high cell densities using the 277 stable cell line. It is important to note that the enhanced 277 growth profile from section 5.5.3 was obtained with the following optimised feeding regime: 5% (v/v) feed addition at day 3; 5% (v/v) feed addition at day 4; 2.5% (v/v) feed addition at day 5. Therefore, inducing the cell culture at day 4 would mean that the day 5 feed from the optimised regime would become a post-induction feed. Hence, this study will also compare different feeding regimes for optimal LVV production. The conditions evaluated in this study are summarised in Table 6.2.

Table 6.2: Summary of conditions used to characterise LVV production at high cell densities in 24-DSW plates using the 277 cell line.

	Day 3 feed addition (5% v/v)	Day 4 feed addition (5% v/v)	Day 5 feed addition (2.5% v/v)	Induction time point
Condition 1	✗	✗	✗	Day 3
Condition 2	✓	✓	✗	Day 4
Condition 3	✓	✓	✓	Day 4
Condition 4	✗	✗	✗	Day 4
Condition 5	✓	✓	✓	Day 5
Condition 6	✗	✗	✗	Day 5

The infectious and physical titre profiles from this study are shown in Figures 6.1 and 6.2 respectively. The data from both graphs demonstrates that the condition with pre-induction feed additions on day 3 and day 4 (i.e. condition 2) achieved the highest infectious and physical titres. The Student's t-test also showed that the difference in titre was significantly higher compared to all other conditions evaluated. Compared to the 277 cell line platform condition with no feed addition and induction on day 3 (i.e. condition 1), condition 2 achieved 1.9-fold higher infectious titre and 2.1-fold higher physical titre. Additionally, it is worth noting that the difference in titres was proportional to the induction viable cell densities. According to the VCD profile shown in Figure 6.3, the induction cell density for condition 2 (i.e. 4.6×10^6 cells/mL) was around 1.8-fold higher than condition 1 (i.e. 2.6×10^6 cells/mL).

The increased LVV production in condition 2 may be due to high culture viability at harvest resulting from feed addition. A control condition with no feed addition and induction on day 4 (i.e. condition 4) was included in the experiment in order to better characterise the effect of the novel feed on LVV production. Figures 6.3 and 6.4 show that the VCD and culture viability at the time of induction was comparable between condition 2 and condition 4. The induction cell densities were 4.6×10^6 cells/mL and 4.5×10^6 cells/mL respectively, and culture viabilities were 97.9% and 98.2% respectively. However, the difference in both infectious (Figure 6.1) and physical titres (Figure 6.2) were significantly higher for condition 2 compared to condition 4. As the induction cell densities were similar, this shows that the higher LVV production observed with condition 2 could be attributed to the effect of the feed.

According to Figure 6.4, the culture viability at harvest was approximately 90.2% for condition 2, which was greater than condition 4 which had an end process viability of around 88%. Perhaps, the presence of more viable cells post-induction may have facilitated higher LVV production. The novel feed formulation used in this study was mainly composed of essential and non-essential amino acids. For CHO cells in particular, several authors have reported that amino acid supplementation can increase culture viability and product titer (Horvat et al., 2020; Kishishita et al., 2015; Torkashvand et al., 2015; Xing et al., 2011b; Xu et al., 2014). For a monoclonal

antibody (mAb) producing CHO cell cultures, Horvat *et al.*, 2020 have demonstrated that supplementation of amino acids resulted in 12% increase in end process culture viability and 0.5 g/L increase in mAb titre. This is in line with the observations from this study.

The data also shows that feed addition post-induction resulted in lower LVV titres. From Figures 6.1 and 6.2, it was found that condition 3 which had pre-induction feed additions on day 3 and day 4 and a post-induction feed on day 5, resulted in significantly lower titres compared to condition 2 which only had the pre-induction feeds on day 3 and day 4. Both conditions were induced on day 4 and the VCD profile (Figure 6.3) shows that their induction cell densities were comparable (4.6×10^6 cells/mL and 4.8×10^6 cells/mL respectively). Hence, the lower titres in condition 3 could be attributed to the effect of the post-induction feed. Figure 6.4 shows that the cell viability at harvest for condition 3 (92.1%) was in fact higher than condition 2 (90.2%). However, the presence of more viable cells did not result in increased LVV production in this case. Perhaps, the post-induction feed addition may have disrupted the cellular metabolic balance and thus negatively affecting the viral production pathways. Studies have reported that initiation of virus production (i.e. point of induction or transfection) causes a change in cell metabolism whereby cellular machinery is directed from cell growth towards virus production (Coroadinha *et al.*, 2006a, 2006b). This leads to an upregulation of pathways involving DNA synthesis, lipid synthesis, polyamine synthesis among others (Rodrigues *et al.*, 2013). Salazar *et al.*, 2016 report that supplementing cells with amino acids without careful consideration of the cell metabolism can cause imbalances which negatively affects mammalian cell culture processes. Hence, the addition of the amino acid-rich feed post-induction may have disturbed the viral production pathways causing lower LVV production. However, this hypothesis can only be proven by understanding the metabolic pathways through detailed proteomic and transcriptomic analysis, and investigating their impact on LVV production.

According to the titre profiles (Figures 6.1 and 6.2), another trend observed was that delaying induction until day 5 resulted in poor LVV production whether feed was

added or not. Where feed was added, the two conditions induced on day 4 (i.e. conditions 2 and 3) achieved significantly higher titres compared to condition 5 which was induced on day 5. Similarly, for the conditions where feed was not added, condition 4 achieved higher titres compared to condition 6. According to the growth profile (Figure 6.3 and 6.4), the VCD and culture viability at induction for the two conditions induced on day 5 was sufficient enough to result in high level of LVV production (i.e. 7.6×10^6 cells/mL and 97.7% respectively for condition 5 and 6.6×10^6 cells/mL and 97.1% respectively for condition 6). However, the culture viability started to decrease immediately after induction with a particularly steep decline in the period between 24 to 48 hours post induction. The viability at harvest was around 81% for condition 5 and 85% for condition 6 suggesting cells were not in an environment suited for LVV production. Usually, the onset of viral release causes a decrease in culture viability. However, at this late stage in the culture (i.e. post day 6), a decline in culture viability would be expected even without inducing the cells.

6.3 | CHARACTERISATION OF LVV PRODUCTION AT HIGH CELL DENSITIES IN 24-DSW PLATES USING THE 277 STABLE CELL LINE

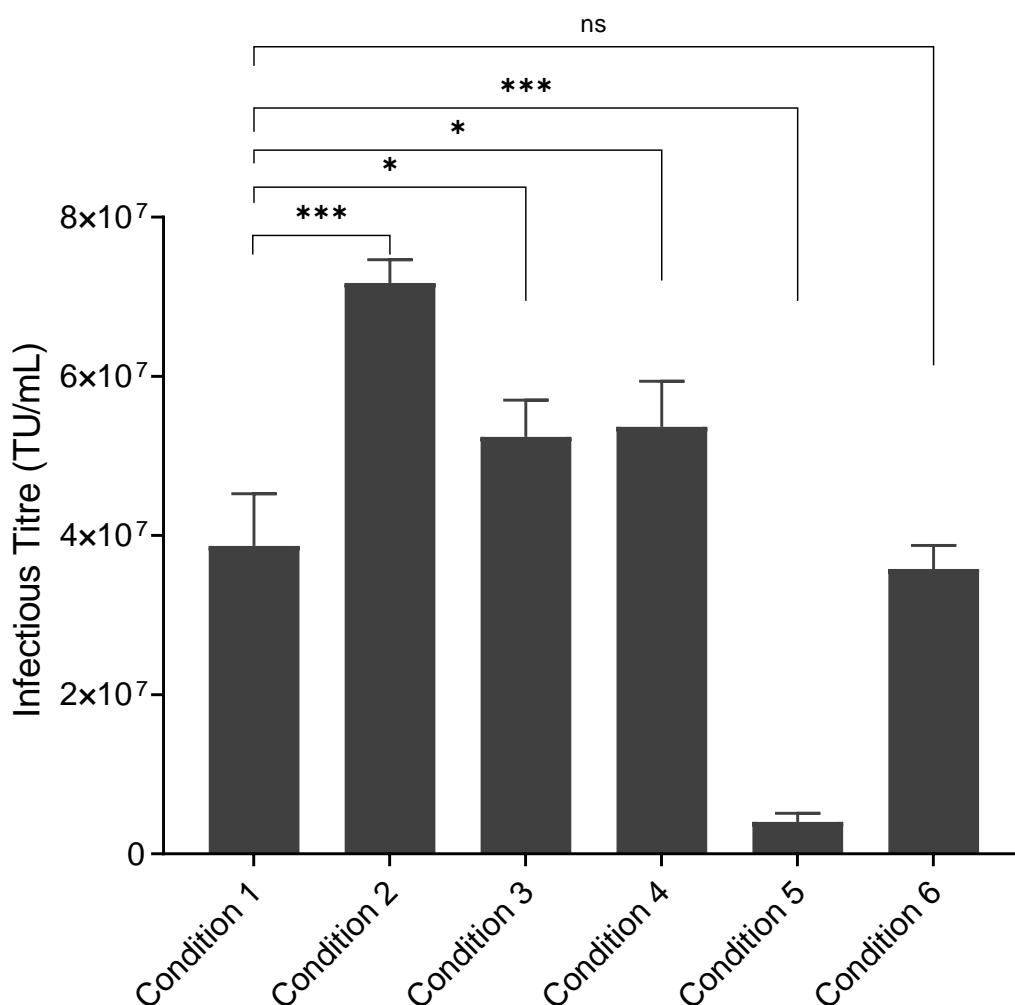


Figure 6.1: Effect of the novel feed on LVV infectious titre profile using the 277 cell line cultured in 24-DSW plates. Condition 1: No feed – Induction at Day 3 (Experimental control i.e. 277 cell line platform process conditions); Condition 2: 5% feed addition at Day 3; 5% feed addition at Day 4 - Induction on Day 4; Condition 3: 5% feed addition at Day 3; 5% feed addition at Day 4; 2.5% feed addition at Day 5 – Induction on Day 4; Condition 4: No feed – Induction on Day 4 (control for conditions 2 and 3); Condition 5: 5% feed addition at Day 3; 5% feed addition at Day 4; 2.5% feed addition at Day 5 – Induction on Day 5; Condition 6: No feed – Induction on Day 5 (control for conditions 5). Error bars represent one standard deviation about the mean (n=3). Statistical comparisons were done using one-way ANOVA analysis followed by post-hoc Tukey multiple comparison test at 95% confidence level: ns: p-value > 0.05; *: p-value ≤ 0.05; **: p-value ≤ 0.01; ***: p-value ≤ 0.001.

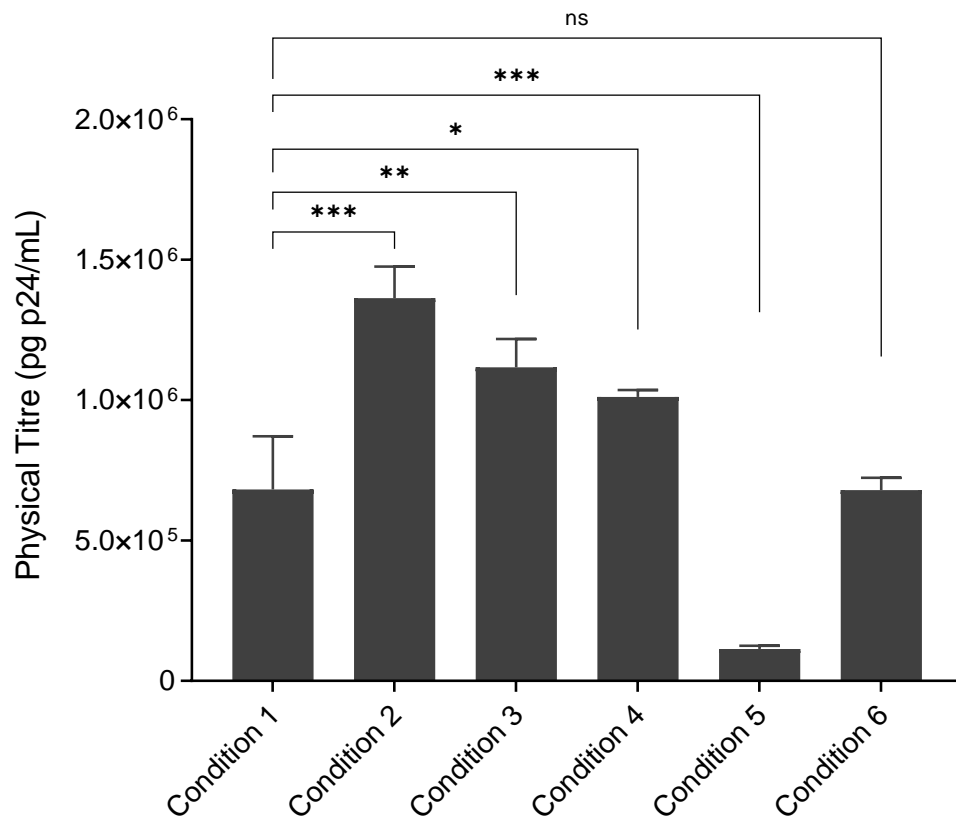


Figure 6.2: Effect of the novel feed on LVV physical titre profile using the 277 cell line cultured in 24-DSW plates. Condition 1: No feed – Induction at Day 3 (Experimental control i.e. 277 cell line platform process conditions); Condition 2: 5% feed addition at Day 3; 5% feed addition at Day 4 - Induction on Day 4; Condition 3: 5% feed addition at Day 3; 5% feed addition at Day 4; 2.5% feed addition at Day 5 – Induction on Day 4; Condition 4: No feed – Induction on Day 4 (control for conditions 2 and 3); Condition 5: 5% feed addition at Day 3; 5% feed addition at Day 4; 2.5% feed addition at Day 5 – Induction on Day 5; Condition 6: No feed – Induction on Day 5 (control for conditions 5). Error bars represent one standard deviation about the mean (n=3). Statistical comparisons were done using one-way ANOVA analysis followed by post-hoc Tukey multiple comparison test at 95% confidence level: ns: p-value > 0.05; *: p-value ≤ 0.05; **: p-value ≤ 0.01; ***: p-value ≤ 0.001.

6.3 | CHARACTERISATION OF LVV PRODUCTION AT HIGH CELL DENSITIES IN 24-DSW PLATES USING THE 277 STABLE CELL LINE

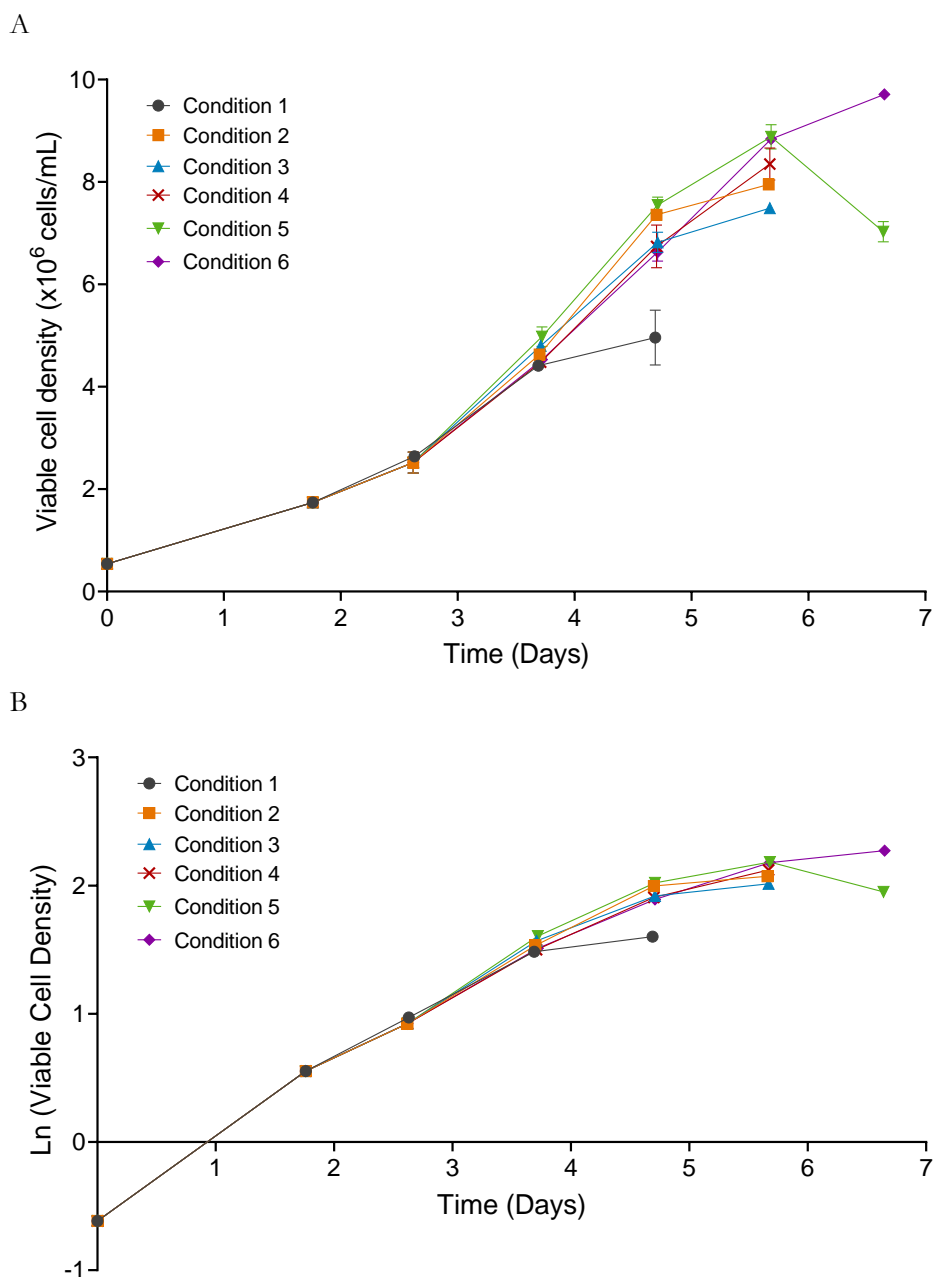


Figure 6.3: (A) Effect of the novel feed on VCD profile during LVV production using the 277 cell line cultured in 24-DSW plates. (B) Natural logarithm of viable cell density plotted against time. Condition 1: No feed – Induction at Day 3 (Experimental control i.e. 277 cell line platform process conditions); Condition 2: 5% feed addition at Day 3; 5% feed addition at Day 4 - Induction on Day 4; Condition 3: 5% feed addition at Day 3; 5% feed addition at Day 4; 2.5% feed addition at Day 5 – Induction on Day 4; Condition 4: No feed – Induction on Day 4 (control for conditions 2 and 3); Condition 5: 5% feed addition at Day 3; 5% feed addition at Day 4; 2.5% feed addition at Day 5 –

6 | ASSESSMENT OF LVV PRODUCTION AT HIGH INDUCTION CELL DENSITIES USING THE NOVEL FEED

Induction on Day 5; Condition 6: No feed – Induction on Day 5 (control for conditions 5). Error bars represent one standard deviation about the mean (n=3).

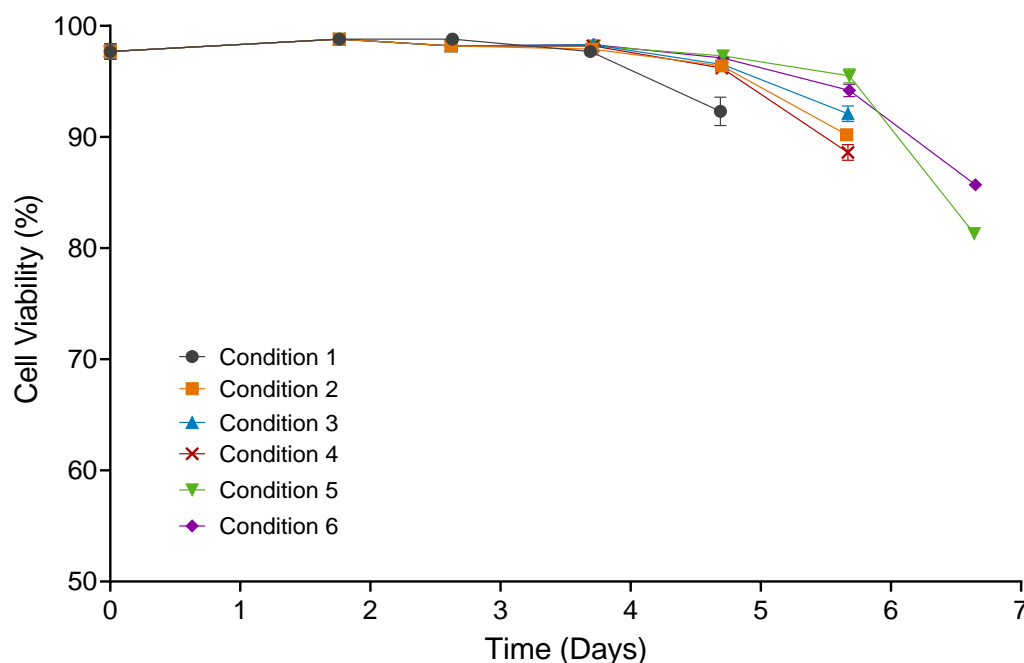


Figure 6.4: Effect of the novel feed on the culture viability profile during LVV production using the 277 cell line cultured in 24-DSW plates. Condition 1: No feed – Induction at Day 3 (Experimental control i.e. 277 cell line platform process conditions); Condition 2: 5% feed addition at Day 3; 5% feed addition at Day 4 - Induction on Day 4; Condition 3: 5% feed addition at Day 3; 5% feed addition at Day 4; 2.5% feed addition at Day 5 – Induction on Day 4; Condition 4: No feed – Induction on Day 4 (control for conditions 2 and 3); Condition 5: 5% feed addition at Day 3; 5% feed addition at Day 4; 2.5% feed addition at Day 5 – Induction on Day 5; Condition 6: No feed – Induction on Day 5 (control for conditions 5). Error bars represent one standard deviation about the mean (n=3).

To confirm the trend in viability decline later in the process, a separate study was carried out to assess the growth profile without induction. Three conditions were evaluated as shown below:

1. Cell growth with feed regime used in condition 2 (i.e. 5% feed addition at Day 3; 5% feed addition at Day 4)
2. Cell growth with feed regime used in conditions 3 and 5 (i.e. 5% feed addition at Day 3; 5% feed addition at Day 4; 2.5% feed addition at Day 5)

3. Cell growth with no feed addition

The VCD and culture viability profile is shown Figures 6.5 and 6.6 respectively. The data shows that even without inducing the culture, a rapid decline in culture viability was observed between day 6 and day 7 for all three conditions. As this corresponds to the period of active viral production in conditions 5 and 6, the low culture viability environment was not ideal for achieving high LVV titres as confirmed by the data. Furthermore, for the two feed regimes, both VCD and culture viability profiles were comparable suggesting the additional feed on day 5 did not add any benefit towards cell growth. In fact, data from Figures 6.1 and 6.2 also demonstrated that the day 5 feed was not favourable for LVV production as well. This was evident from the lower titre profile for condition 3 compared to condition 2 with the only difference being the day 5 feed in condition 3. Additionally, the titre data showed that LVV production for condition 5 was significantly lower than condition 6. Perhaps, the day 5 feed in combination with the delayed induction may have contributed to the poor titre profile in condition 5.

Lastly, for the control conditions where no feed was added, inducing on day 4 (i.e. condition 4) resulted in a more favourable titre profile compared to inducing on day 3 (i.e. condition 1) or day 5 (i.e. condition 6). This observation does not follow the usual trend for this cell line given that the GSK platform process has been optimised with induction around day 3 and vector harvest on day 5. The growth profile of the condition with no feed from Figures 6.5 and 6.6 shows that the 277 cell line used in this study was better growing compared to the same cell line used in studies from the previous chapters (i.e. chapter 3, 4 and 5). To illustrate this, Figures 6.7 and 6.8 compares the VCD and culture viability profiles of the condition with no feed from this study (i.e. from Figure 6.5 and 6.6) and optimisation study 3 (section 5.5.3) from the previous chapter. For the 277 cell line used in optimisation study 3, growth decline was observed around day 5 and hence optimal induction time point was characterised as day 3. However, for the 277 cell line used in the present study, exponential growth was observed until day 6 suggesting day 4 to be the optimal induction time point even without feed addition. Hence, this explains the higher titre achieved with condition 4

compared to condition 1. For condition 6, as mentioned earlier, the delay in induction until day 5 may have contributed to the relatively lower titre compared to condition 4.

The lack of consistent growth improvements suggests that there might be cell line-specific considerations influencing the outcomes. The stability of the 277 cell line could play a role in the observed variations in growth improvements with the amino acid feed. Over time, cell lines can undergo genetic and epigenetic changes (e.g. DNA methylation and histone modifications) that can influence their growth behaviour and response to external stimuli (Ng et al., 2017). These changes can be exacerbated with high passage numbers or prolonged culture periods (Ng et al., 2017). HEK293T cells can also be heterogeneous, and subclones with slightly different characteristics might exist within the same cell line (Stepanenko and Dmitrenko, 2015). These subclones could respond differently to the amino acid feed. Regular quality control measures such as karyotyping, genetic stability assays, and functional assessments, are important in ensuring cell line stability (Stepanenko and Dmitrenko, 2015). Analysing the genetic stability of different 277 cell line subpopulations (i.e. from the working cell bank), and comparing them to the original cell line from the master cell bank can help identify any potential genetic changes that may have contributed to the observed differences in growth responses to the feed.

Overall, this study has demonstrated that optimising feed addition and induction time points is key to maximising LVV titres. In terms of feed addition, only two feeds prior to induction is enough to improve LVV titre by almost 2-fold compared to the 277 cell line platform process. For induction, the ideal time point is around 48 hours prior to cells entering into stationary phase. Data from this study has shown that for the same cell line, different vials from the same cell bank can vary in growth. Therefore, it is important to characterise the growth profile of each cell line in order to identify the optimal time point for induction.

6.3 | CHARACTERISATION OF LVV PRODUCTION AT HIGH CELL DENSITIES IN 24-DSW PLATES USING THE 277 STABLE CELL LINE

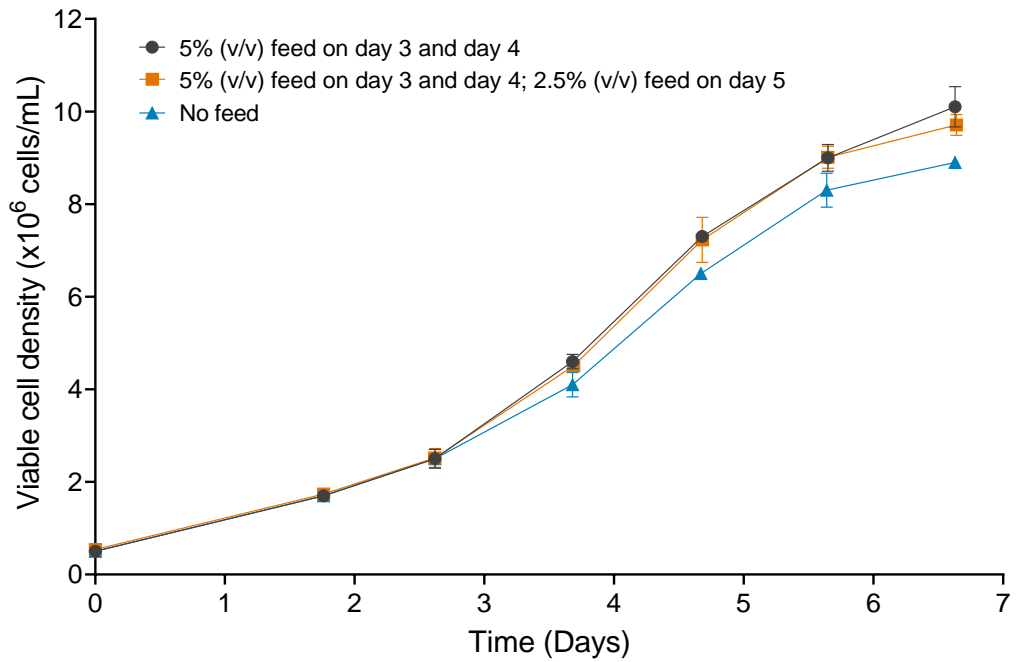


Figure 6.5: Assessment of the VCD profile without induction of the 277 cell line used in section 6.3. Error bars represent one standard deviation about the mean (n=3).

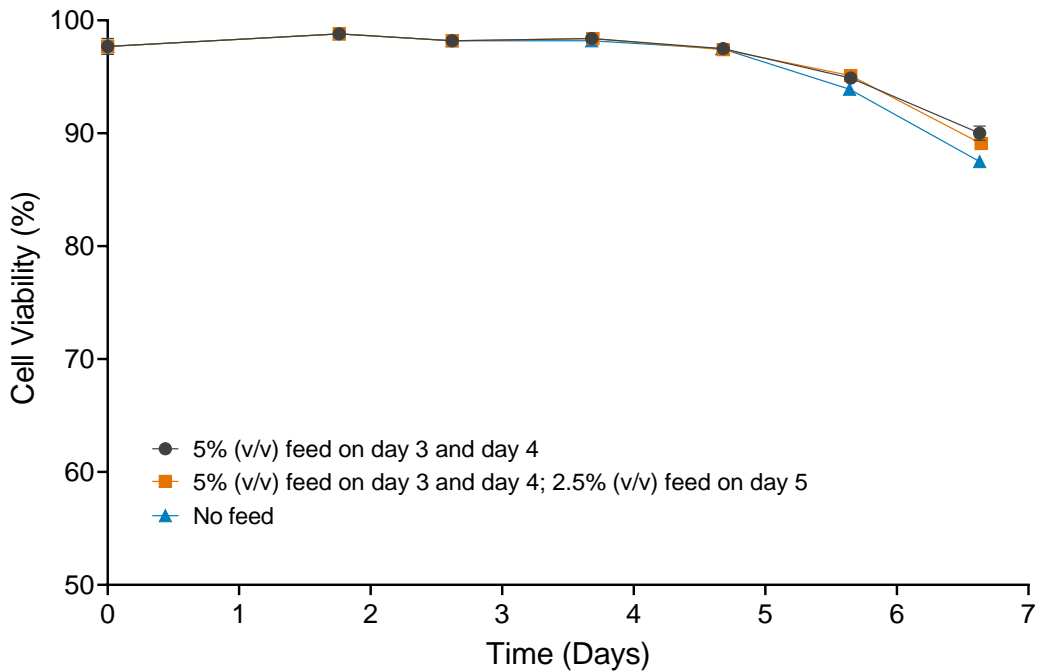


Figure 6.6: Assessment of the culture viability profile without induction of the 277 cell line used in section 6.3. Error bars represent one standard deviation about the mean (n=3).

6 | ASSESSMENT OF LVV PRODUCTION AT HIGH INDUCTION CELL DENSITIES USING THE NOVEL FEED

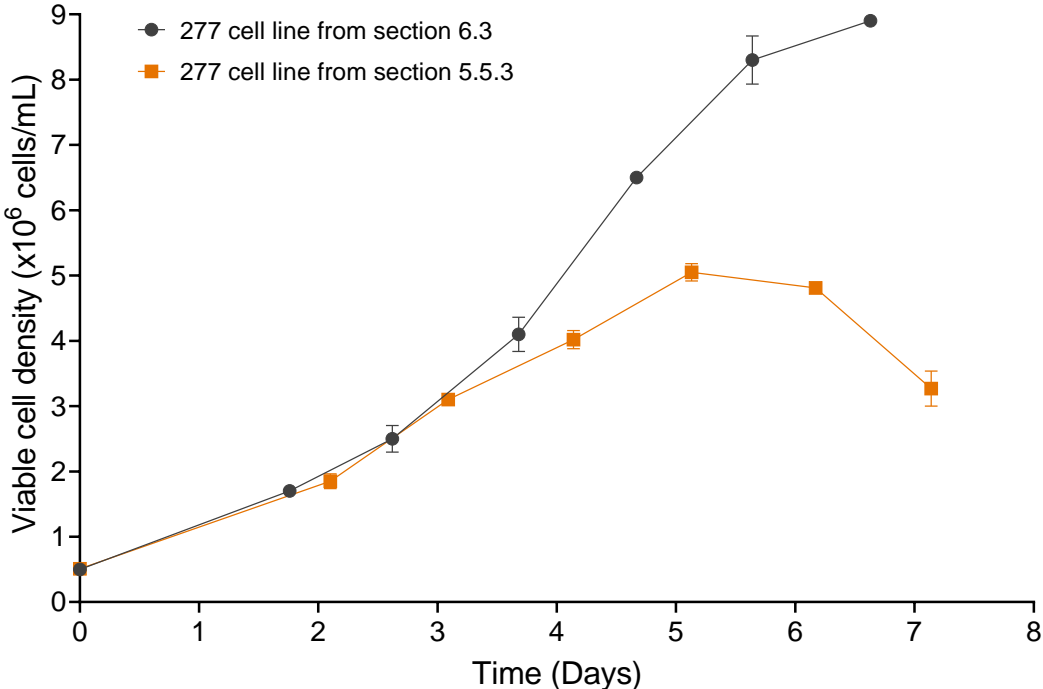


Figure 6.7: Comparison of the VCD profile of the condition with no feed from this study (i.e. from Figure 6.5) and optimisation study 3 (section 5.5.3). Error bars represent one standard deviation about the mean (n=3) for 277 cell line from section 6.3 and n=2 for 277 cell line from section 5.5.3).

6.4 | EVALUATING THE EFFECT OF THE NOVEL FEED ON CELL GROWTH AND LVV PRODUCTION PROFILE OF A GSK-ASSET STABLE CELL LINE CULTIVATED IN 24-DSW PLATES

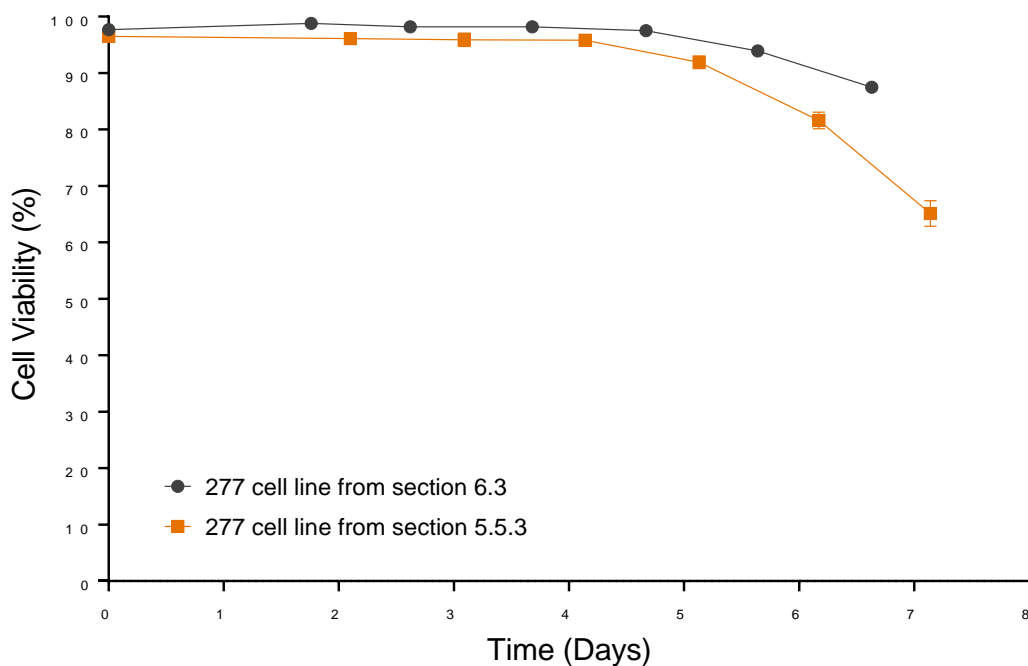


Figure 6.8: Comparison of the culture viability profile of the condition with no feed from this study (i.e. from Figure 6.5) and optimisation study 3 (section 5.5.3). Error bars represent one standard deviation about the mean (n=3) for 277 cell line from section 6.3 and n=2 for 277 cell line from section 5.5.3).

6.4 EVALUATING THE EFFECT OF THE NOVEL FEED ON CELL GROWTH AND LVV PRODUCTION PROFILE OF A GSK-ASSET STABLE CELL LINE CULTIVATED IN 24-DSW PLATES

The efficacy of the novel feed in improving LVV production using the 277 cell line was demonstrated in section 6.3. Addition of the novel feed resulted in a 2-fold increase in LVV production compared to the 277 cell line platform condition with no feed. Hence, the aim of this study was to translate the findings from the 277 cell line to a proprietary GSK-asset cell line which encodes a therapeutic transgene.

As mentioned previously in section 2.1, the 277 cell line is also a proprietary GSK stable cell line. However, it encodes for a GFP transgene and thus is primarily used in platform research work. This is because the fluorescence emitted by the protein can be easily measured by flow cytometry. Furthermore, GFP is non-toxic and can be expressed in living cells, which enables the study of dynamic, physiological processes (Soboleski et al., 2005). As part of its pipeline, GSK have also developed other HEK293T stable cell lines which encode for different therapeutic transgenes. The GSK-asset cell line used for this study encodes for a protein (proprietary knowledge) which is overexpressed on various tumour cells making it a target for CAR-T cell therapy. Upon induction with doxycycline, this cell line produces LVV with an RNA genome encoding for the anti-tumour CAR-T. The LVV is then used to modify patient T cells to express a proprietary CAR-T that targets a marker on cancer cells. In this study, the novel feed was used to assess the GSK-asset cell line growth and LVV production profile in 24-DSW plate cultures. The conditions evaluated in this study are summarised in Table 6.3.

Table 6.3: Summary of conditions used to characterise cell growth and LVV production at high cell densities in 24-DSW plates using the GSK-asset stable cell line.

	Day 3 feed addition (5% v/v)	Day 4 feed addition (5% v/v)	Day 5 feed addition (2.5% v/v)	Induction time point
Condition 1	✘	✘	✘	No induction
Condition 2	✓	✓	✓	No induction
Condition 3	✘	✘	✘	Day 3
Condition 4	✓	✓	✘	Day 4
Condition 5	✘	✘	✘	Day 4

Before studying the LVV production profile, the cell growth of the cell line was first characterised with and without the addition of feed (see conditions 1 and 2 in Table 6.3). The VCD and culture viability profiles from this study are shown in Figures 6.9 and 6.10 respectively. From these graphs, it is evident that addition of the novel feed improved the GSK-asset stable cell line growth profile. Both the VCD and culture

6.4 | EVALUATING THE EFFECT OF THE NOVEL FEED ON CELL GROWTH AND LVV PRODUCTION PROFILE OF A GSK-ASSET STABLE CELL LINE CULTIVATED IN 24-DSW PLATES

viability data show that the cell culture with novel feed addition (i.e. condition 2) performed significantly better compared to the culture with no feed (i.e. condition 1). For condition 2, feed addition was initiated at day 3 and the effect on cell growth was apparent soon after i.e. the data shows that condition 2 achieved consistently higher VCD and culture viability immediately after initiating the feeding regime. Figure 6.9B shows that cells in condition 2 were in exponential growth until day 5. In condition 1, the rate of cell growth appeared to be slowing down after day 3. The maximum VCD prior to cell entering into stationary phase (i.e. day 6) was higher in condition 2 than condition 1 (i.e. 9×10^6 cells/mL and 7×10^6 cells/mL respectively). Furthermore, the culture viability at day 6 was approximately 94% for condition 2 suggesting cells were actively proliferating until this point. culture viability only started to decrease after day 6 for condition 2. However, for condition 1, the cell viability at day 6 was around 89% suggesting cells were already in decline at this stage. By extending the exponential growth period until day 6, the addition of the novel feed thereby allows the GSK-asset cell line to be induced at higher cell densities on day 4. For the process with no feed, the decline in culture viability after day 5 means the desirable induction time point would be around day 3.

6 | ASSESSMENT OF LVV PRODUCTION AT HIGH INDUCTION CELL DENSITIES USING THE NOVEL FEED

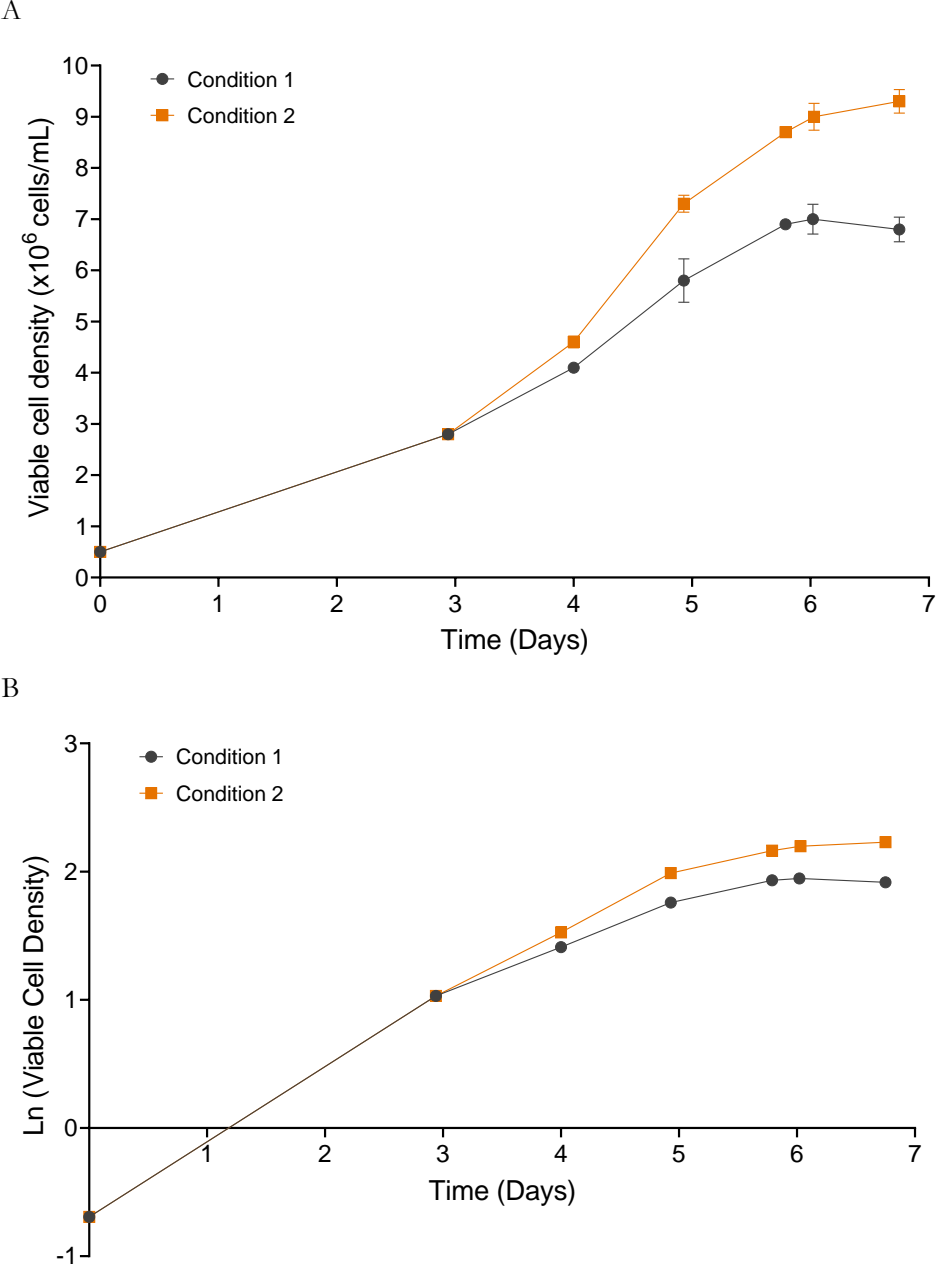


Figure 6.9: (A) Effect of the novel feed on the non-induced VCD profile of the GSK-asset stable cell line (B) Natural logarithm of viable cell density plotted against time. Condition 1: No feed; Condition 2: 5% feed addition at day 3; 5% feed addition at day 4; 2.5% feed addition on day 5. Error bars represent one standard deviation about the mean (n=3).

6.4 | EVALUATING THE EFFECT OF THE NOVEL FEED ON CELL GROWTH AND LVV PRODUCTION PROFILE OF A GSK-ASSET STABLE CELL LINE CULTIVATED IN 24-DSW PLATES

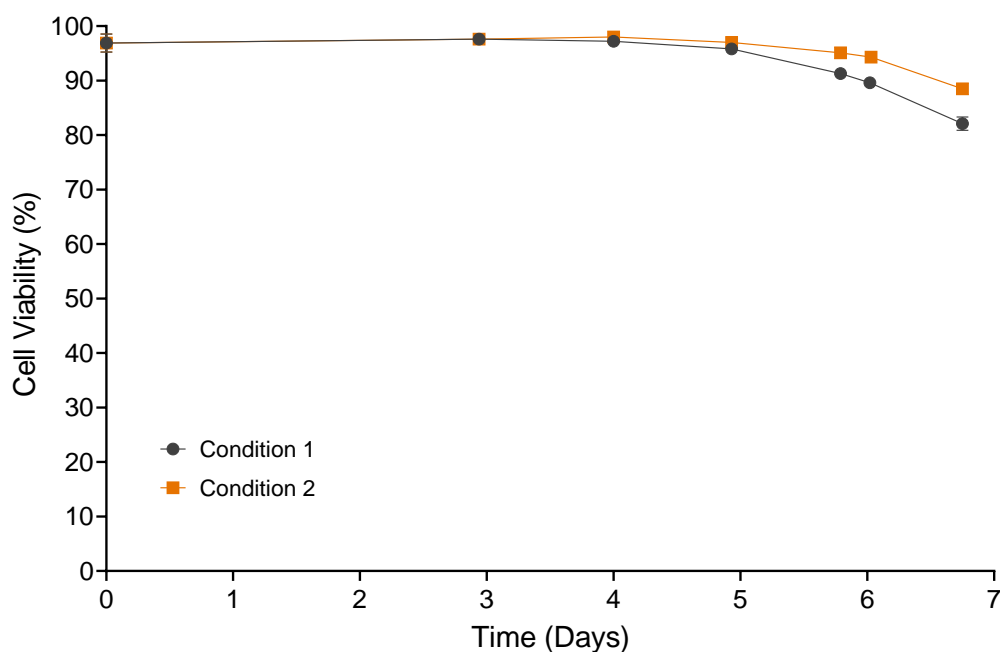


Figure 6.10: Effect of the novel feed on the non-induced culture viability profile of the GSK-asset stable cell line. Condition 1: No feed; Condition 2: 5% feed addition at day 3; 5% feed addition at day 4; 2.5% feed addition on day 5. Error bars represent one standard deviation about the mean (n=3).

As shown in Table 6.3, three conditions were used to assess the effect of the feed on LVV production. Condition 3 was the control condition with no feed addition and induction on day 3. Condition 4 had pre-induction feed additions on day 3 and day 4 and cells induced on day 4. This condition achieved the most favourable titre profile using the 277 cell line from the previous study (see section 6.3). And lastly, condition 5 was the control for condition 4; there was no feed addition and cells were induced on day 4.

The infectious and physical titre profiles are shown in Figures 6.11 and 6.12 respectively. The data from both graphs shows that addition of bespoke feed significantly improved the LVV production profile of the GSK-asset stable cell line i.e. the condition with feed addition (i.e. condition 4) achieved the highest physical and infectious titres. The Student's t-test also showed that the difference in titre was significantly higher compared to the other conditions evaluated. Compared to the

control condition (i.e. condition 3), condition 4 achieved 1.15-fold (i.e. 15%) higher infectious titre and 1.3-fold (i.e. 30%) higher physical titre. Compared to the 277 cell line, the increase in titre achieved with the GSK-asset stable cell line was lower i.e. 1.9-fold and 1.15-fold respectively. Additionally, with the 277 cell line, the improvement in titre was proportional to the increase in the induction viable cell density. However, this proportionality was not observed with the GSK-asset cell line. Although there was a 2-fold increase in the induction cell density by inducing on day 4, the improvement in titre was only 1.15-fold. Studies have reported that some transgenes may present toxic properties in the host cell which can reduce the ability to generate highly concentrated batches of LVV (Bagnis et al., 2014; Schlimgen et al., 2016). As indicated earlier, the transgene present in the 277 cell line is GFP and it is considered to be non-toxic (Soboleski et al., 2005). The transgene present in the GSK-asset cell line encodes for a protein that is used to target tumour cells. Perhaps the host cell toxicity induced from this transgene may account for the difference in the titres between the two stable cell lines. It is hypothesised that toxicity may arise from off-target effects i.e. the transgene may have unintended interactions or interfere with essential cellular pathways. Transcriptomic analysis can be used to investigate this further.

Condition 5 which involved induction on day 4 and no feed addition was included in the experiment as a control for condition 4. Figures 6.13 and 6.14 show that the VCD and culture viability at the time of induction was comparable between condition 4 and condition 5. The induction cell densities were 4.4×10^6 cells/mL and 4.1×10^6 cells/mL respectively, and culture viabilities were 98.0% and 97.3% respectively. However, the difference in infectious (Figure 6.11) and physical titre (Figure 6.12) was significant, with higher titres for condition 4 compared to condition 5. As the induction cell densities were similar, this shows that the higher LVV production observed with condition 4 can be attributed to the effect of the feed. According to Figure 5, the culture viability at harvest was 90.3% for condition 2, which was higher than condition 4 which had an end process viability of 86.5%. As observed with the 277 cell line in section 6.3, perhaps the presence of more viable cells post-induction may have facilitated higher LVV production.

6.4 | EVALUATING THE EFFECT OF THE NOVEL FEED ON CELL GROWTH AND LVV PRODUCTION PROFILE OF A GSK-ASSET STABLE CELL LINE CULTIVATED IN 24-DSW PLATES

For conditions with no feed addition, the data suggests that inducing at day 3 (i.e. condition 3) resulted in higher titres compared to induction on day 4 (i.e. condition 5). This is consistent with the trend observed with the GSK platform stable cell line process. Hence, the platform process has been optimised with induction around day 3 and vector harvest on day 5. Lower infectious and physical titre for condition 5 may be due to poor culture viability observed after day 4. According to Figure 6.9, even without inducing the cell culture, there was a rapid decline in cell viability after day 4 for the ‘no feed’ condition (i.e. condition 1). Hence, without any feed addition, the cell culture environment after day 4 is not suitable for virus production.

To maximise the commercial viability of cell and gene therapy products, there is a strong drive towards decreasing LVV manufacturing costs. According to Comisel *et al.*, 2021, the cost contribution of LVV relative to the CAR-T cost of goods (COG) per patient ranges between 15–20%. The authors describe the application of a decisional tool aimed at investigating the target process performance required to lower LVV-associated costs. For a hypothetical case CAR-T LVV product with a dose size of 2×10^9 transducing units (TU) and fixed demand at 1,000 doses/year, sensitivity analysis showed that upstream harvest titre has a significant impact on reducing the LVV-associated COG per dose ($\text{COG}_{\text{LVV}}/\text{dose}$). For a 200 L scale single-use STR, a 30% increase in harvest titre would decrease the $\text{COG}_{\text{LVV}}/\text{dose}$ by 42%. Other decisional tools developed by the same authors predict that for same culture vessel (i.e. 200 L STR), harvest titres need only to double or triple for the LVV cost contribution to drop to ~1% in the context of the CAR-T product. Hence, for the company, a 15% increase in LVV titre observed with the GSK-asset stable cell line in the present study could potentially result in a significant reduction in the overall manufacturing cost of its CAR-T product. The consequence of this would mean life-saving cell and gene therapy products like CAR-T cell therapy can be more affordable for the patients in need, thereby improving accessibility. However, it is important to note that the additional days of culturing (i.e. due to delaying harvest) comes at a cost since COG may increase due to higher labour costs. A detailed COG analysis would be required to justify the commercial benefit of improving harvest titre at the expense of longer process duration.

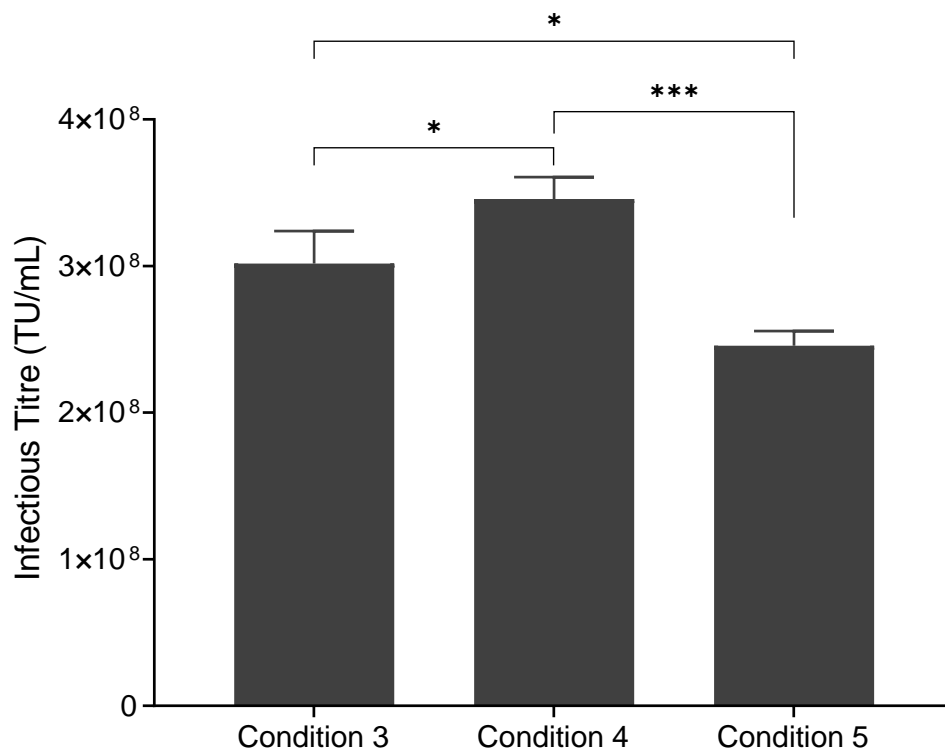


Figure 6.11: Effect of the novel feed on LVV infectious titre profile using the GSK-asset stable cell line cultured in 24-DSW plates. Condition 3: No feed – Induction at Day 3 (Experimental control); Condition 4: 5% feed addition at Day 3; 5% feed addition at Day 4 - Induction on Day 4; Condition 5: No feed – Induction on Day 4 (control for condition 4). Error bars represent one standard deviation about the mean (n=3). Statistical comparisons were done using one-way ANOVA analysis followed by post-hoc Tukey multiple comparison test at 95% confidence level: ns: p-value > 0.05; *: p-value ≤ 0.05; **: p-value ≤ 0.01; ***: p-value ≤ 0.001.

6.4 | EVALUATING THE EFFECT OF THE NOVEL FEED ON CELL GROWTH AND LVV PRODUCTION PROFILE OF A GSK-ASSET STABLE CELL LINE CULTIVATED IN 24-DSW PLATES

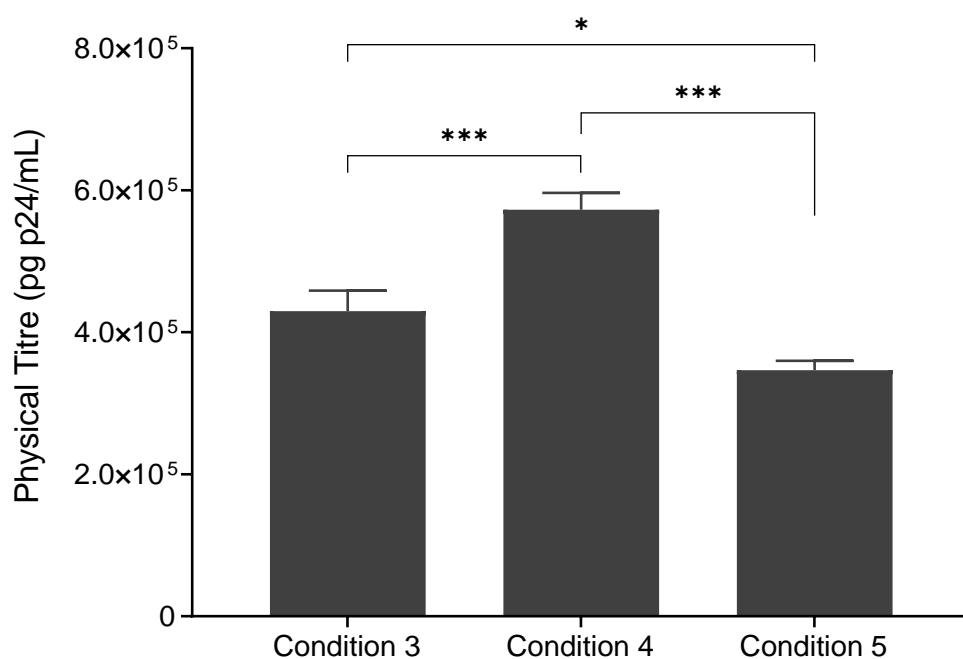


Figure 6.12: Effect of the novel feed on LVV physical titre profile using the GSK-asset stable cell line cultured in 24-DSW plates. Condition 3: No feed – Induction at Day 3 (Experimental control); Condition 4: 5% feed addition at Day 3; 5% feed addition at Day 4 - Induction on Day 4; Condition 5: No feed – Induction on Day 4 (control for condition 4). Error bars represent one standard deviation about the mean (n=3). Statistical comparisons were done using one-way ANOVA analysis followed by post-hoc Tukey multiple comparison test at 95% confidence level: ns: p-value > 0.05; *: p-value ≤ 0.05; **: p-value ≤ 0.01; ***: p-value ≤ 0.001.

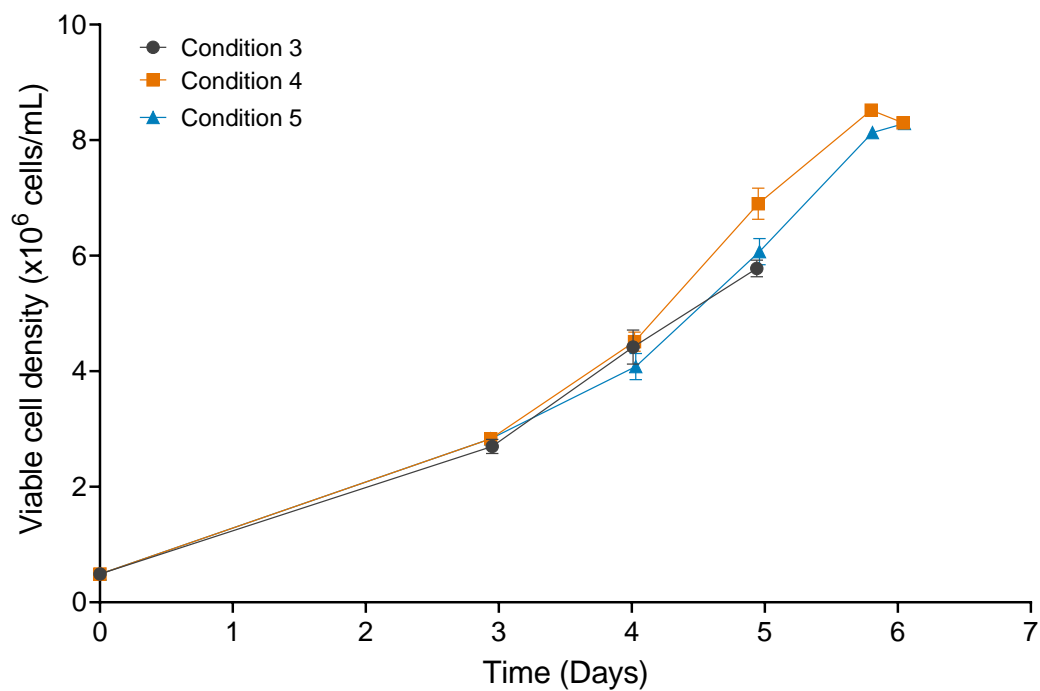


Figure 6.13: Effect of the novel feed on the VCD profile using the GSK-asset stable cell line cultured in 24-DSW plates. Condition 3: No feed – Induction at Day 3 (Experimental control); Condition 4: 5% feed addition at Day 3; 5% feed addition at Day 4 - Induction on Day 4; Condition 5: No feed – Induction on Day 4 (control for condition 4). Error bars represent one standard deviation about the mean (n=3).

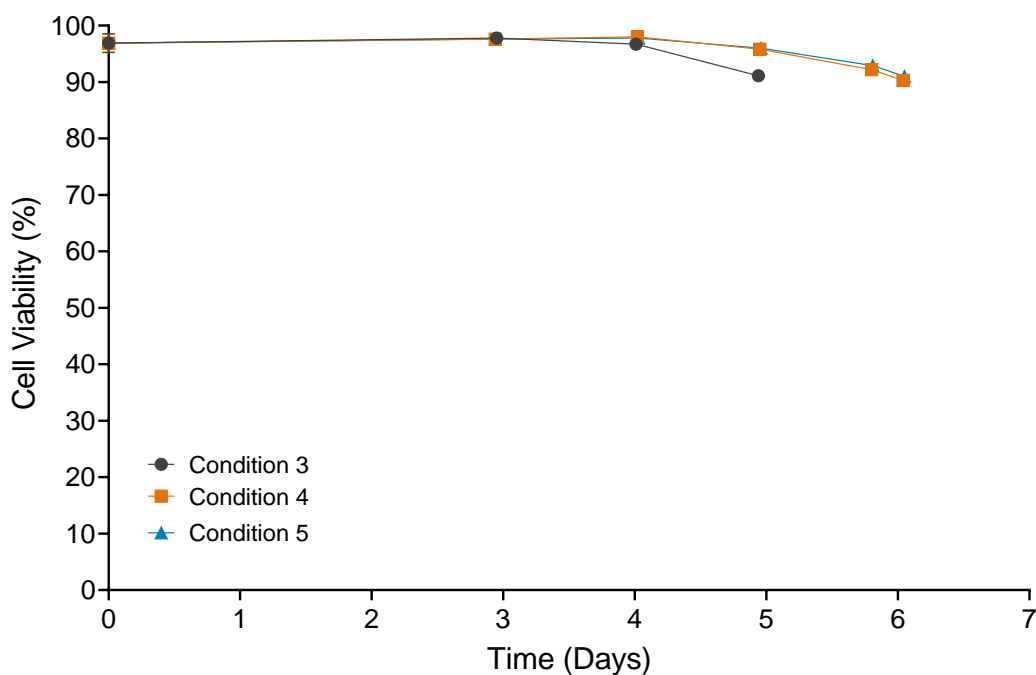


Figure 6.14: Effect of the novel feed on the culture viability profile using the GSK-asset stable cell line cultured in 24-DSW plates. Condition 3: No feed – Induction at Day 3 (Experimental control); Condition 4: 5% feed addition at Day 3; 5% feed addition at Day 4 - Induction on Day 4; Condition 5: No feed – Induction on Day 4 (control for condition 4). Error bars represent one standard deviation about the mean (n=3).

6.5 CHAPTER SUMMARY

This chapter has successfully demonstrated the efficacy of the novel feed in improving LVV production for two different GSK proprietary stable cell lines in 24-DSW plates. Below are the key findings from this chapter:

- For the 277 cell line, addition of the novel feed resulted in a 2-fold increase in LVV infectious titre compared to the platform process control (section 6.3). The increased LVV production with the novel feed may be due to high cell viability at harvest compared to the conditions with no feed.

- The regime of feed addition is important for LVV production. Data from section 6.3 showed that addition of novel feed post-induction resulted in lower LVV titres compared to condition with pre-induction feed only.
- Section 6.4 showed that the novel feed significantly improved the growth and LVV productivity profile of the GSK-asset cell line. Feed addition resulted in 15% higher LVV infectious titre compared to the control condition.

In summary, the novel feed developed in this work shows significant promise towards enhancing GSK's cell and gene therapy LVV production capabilities. The increase in LVV titre may result in a significant reduction in the overall manufacturing costs. Hence, for the company to realise the benefit of the novel feed, the next step is to complete further characterisation, as outlined in chapter 7 (section 7.2).

7 CONCLUSION AND FUTURE WORK

7.1 REVIEW OF PROJECT OBJECTIVES

The overarching goal of this project was to establish a novel feeding strategy for improving the growth profile of a HEK293T-derived LVV stable producer cell line cultured in fed-batch mode, and thereby, enabling the potential for increased LVV production. In line with achieving this goal, this project had three objectives: 1) Assessment of GSK's 277 HEK293T stable cell line cultivation in 2 L stirred tank reactor and identifying potential targets for improving cell growth, 2) Developing an effective high-throughput scale-down model of GSK's platform 277 HEK293T stable cell line cultivation process in 2 L stirred tank reactor, and 3) Developing a novel feeding regime for enhanced HEK293T stable cell line growth and LVV productivity.

An assessment of the 277 cell line demonstrated that under the current operating conditions for this cell line, the maximum VCD achieved before cell growth arrest was approximately 6×10^6 viable cells/mL. The growth profile was also characterised by a short exponential growth phase lasting around 3 to 4 days. The metabolite profile during cell growth was characterised by high levels of glucose consumption and significant lactate accumulation exceeding the concentration reported to be inhibitory for cell growth (5 g/L). Altering the cell metabolism using pH and CO₂ control

successfully prevented glucose depletion and lactate accumulation above 5 g/L. However, this did not translate into improved cell growth, as the culture still entered into stationary phase after 5 days with maximum VCD still approximately 6×10^6 cells/mL. LC-MS analysis of the cell culture supernatant at different stages along the growth phase identified 90 metabolites of interest belonging to 10 different classes of compounds. 33 metabolites showed no significant change in concentration with time. 7 metabolites were accumulating with time; among these, only lactate had growth inhibitory properties reported in literature. 50 metabolites were depleting with time; among these, 22 not only showed significant depletion, but also had a correlation with mammalian cell growth.

Testing the addition of metabolites found to be depleting in the LC-MS analysis in order to develop a novel feed requires a high-throughput scale-down system. Hence, a 24-DSW microwell platform was used to develop a scale-down mimic of GSK's established stable suspension LVV production process model at 2 L STR scale. Mixing time proved to be an effective basis for scale translation. Comparable 277 cell line growth kinetics and LVV productivity profiles were achieved in 24-DSW plate and 2 L STR cultures at matched mixing time. A limitation of the 24-DSW model was the lack of pH control, which was likely to have contributed to differences in the glucose and lactate concentration profiles observed. However, as a screening platform, obtaining comparable growth and LVV productivity profiles was sufficient for the intended purpose.

Next, the 24-DSW scale-down model, together with DoE methodology, was used to screen the addition of metabolites identified to be depleting in LC-MS analysis in order to develop a novel growth enhancing feed. From the 24 different factors screened, essential amino acids achieved the most significant effect on cell growth. There was a strong positive linear correlation between essential amino acids concentration and VCD and cell viability. Non-essential amino acids also had a positive role in maintaining high cell viabilities. These two factors were then optimised in terms of their concentration and feed regime. The highest peak VCD and cell viability profile was achieved with a formulation comprising of 30× MEM essential amino acids and

5× MEM non-essential amino acids. The optimal feed regime consisted of 5% (v/v) addition on day 3, 5% (v/v) addition on day 4 and 2.5% (v/v) addition on day 5. This regime extended the exponential growth period until day 6, which was 24 hours longer than the control condition, achieving a maximum VCD of 7.3×10^6 cells/mL.

Finally, extending the exponential growth period with the novel feed permitted induction of LVV production later in the culture and at higher viable cell densities. For the 277 cell line, addition of the novel feed and inducing on day 4 resulted in a 1.9-fold (i.e. 90%) increase in infectious titre compared to the control condition. For a different GSK proprietary stable cell line encoding a therapeutic transgene, the novel feed resulted in a 1.15-fold (i.e. 15%) increase in infectious titre. Studies have shown that harvest titre is a major driver for reducing LVV-associated manufacturing costs. Hence, the application of the novel feed developed in this work has the potential to reduce the cost of goods for manufacturing of cell and gene therapies and consequently make these transformative medicines more accessible to patients.

In summary, all three objectives have been achieved. While there is no doubt that improvements can be made to the novel feed developed in this project, this work has established a foundation for the company to further develop a novel fed-batch process for enhancing LVV production.

7.2 RECOMMENDATIONS FOR FUTURE WORK

This chapter considers future work related to further optimisation of the novel feed process as well as industrial implementation of this research.

7.2.1 Further optimisation of the novel feed process

7.2.1.1 Improvement in feed design

The LC-MS data from chapter 3 indicated that 50 metabolites were significantly depleting. However, only 24 different factors were screened using the DoE methodology in chapter 5. From these, only essential and non-essential amino acids were included as part of the feed formulation. There is scope to test more compounds from the LC-MS analysis, as well as other growth enhancing metabolites identified from the literature. For the metabolites that were excluded during screening, it is also worth testing different concentration ranges as this may perhaps result in a positive effect on growth.

Quenching of the cell culture medium immediately post sampling was overlooked in this study. As discussed earlier in Chapter 3, quenching is a critical step in metabolite analysis to stop metabolic activity, stabilize metabolites, and preserve the metabolic profile at the time of sampling. Skipping this step may have resulted in alterations in metabolite concentrations and potentially compromising the accuracy and reliability of the analysis results. For future work, the LC-MS analysis can be repeated using quenched cell culture medium samples to verify the reliability of the results.

Furthermore, a targeted LC-MS approach was used for cell culture medium analysis. The method only gave coverage to 110 key metabolites that are usually present in most mammalian cell culture media. The obvious limitation of this method is overlooking

metabolites that are not measured but could be crucial for the cell culture. Therefore, an untargeted LC-MS approach could be explored in order to examine a wider range of metabolites during both phases of LVV production. Conducting these additional studies will enable design of a more robust and comprehensive feed formulation.

7.2.1.2 Feed stability studies

Once the formulation of the feed has been finalised, the stability of the feed should be assessed to determine whether the constituent components of the feed degrade over time. The stability studies should take into account factors such as pH fluctuations, storage conditions (i.e. room temperature vs cold storage) and shelf-life.

7.2.1.3 Assess the effect of the novel feed with other GSK-asset stable cell lines

In chapter 6, the efficacy of the novel feed was demonstrated using two different LVV stable producer cell lines. The feed resulted in an improvement in titre for both cell lines albeit at different fold increments. This variability may be due to transgene-induced toxicity exhibited in some stable cell lines. Hence, to better understand this trend, the feed should be tested using stable producer cell lines for other assets in a company's pipeline. Characterising the performance of the feed across different assets will also enable the establishment of a platform manufacturing process utilising the novel feed which can help to maintain product quality.

7.2.1.4 Optimisation of induction conditions

Given that higher cell densities have been shown to be achievable in this work, another key area for optimisation is the concentration of the chemical agents used for induction. In this project, the same concentrations of doxycycline and sodium butyrate as those used in the platform process for the 277 cell line, in which a lower induction

cell density is used, were maintained when inducing at higher viable cell densities. It is therefore important to understand whether the concentration of the induction agents should be adjusted in proportion with the induction cell density.

7.2.1.5 Explore a two-step feeding strategy for LVV production

The production of LVV is a two-step process. The first phase is cell growth, where the goal is to reach the target induction cell density. The second is the virus production phase which occurs after induction. Here, cellular energy is diverted from cell growth towards virus production. This project focused on developing a feed that was tailored towards improving the first step of the LVV production process i.e. improving HEK293T stable producer cell line growth. This approach assumed that improvement in LVV titre resulted from having higher cell numbers i.e. more virus producing cells. However, the feed may also enhance LVV titre by improving the cell specific virus productivity without necessarily increasing the cell number i.e. the number of LVV particles produced by each cell may change due to the effect of the feed. Therefore, an alternative approach would be to have the main readout as LVV titre instead of solely focusing on cell growth. Some of the feed components tested in the screening experiments were overlooked based on their effect on cell growth. However, their impact on LVV titre was not characterised and therefore remains unknown. For future work, the DoE studies can be repeated by having LVV titre as a main readout to address the limitations discussed above.

Another approach is to investigate a two-step feeding process. Studies have reported that the induction time point triggers metabolic pathways that are specific towards the production of virus (Rodrigues et al., 2013). Thus, cellular metabolic requirements during cell growth are different to those during the virus production phase. Hence, a feed developed for improving cell growth may not be fit for purpose during the virus production phase. To tailor a feed specific to this phase, a similar LC-MS analysis could

be carried out on samples taken post-induction to understand the cells metabolic requirements.

7.2.2 Industrial implementation of the novel feed

As discussed in chapter 6, it has been shown that the novel feed developed in this work has the potential to significantly enhance GSK's LVV production capabilities. The feed improved growth in two different GSK proprietary stable cell lines enabling cells to be induced at higher viable cell densities and thus resulting in higher LVV titres. Although there are potential benefits to introduction of this novel feed regime, other factors must be considered before new feed regimes can be implemented for LVV manufacturing. This section explores the activities relating to the industrial implementation of the novel feed regime as part of the upstream LVV production process.

7.2.2.1 Process validation of the novel feed for upstream LVV production

The sponsoring company, GSK, are developing a pipeline of cell and gene therapy products for the treatment of diseases such as cancer. As is the case for all biopharmaceutical companies, GSK faces important regulatory considerations associated with the development of these medicines for commercial supply.

Biopharmaceutical companies must ensure that their operations are compliant with the regulations set out by the Food and Drug Administration (FDA), European Medicines Agency (EMA) as well as other relevant health authorities. LVV manufacturing processes must meet relevant quality standards to be deemed suitable for clinical supply. When introducing a novel feed regime, comparability between existing and new manufacturing processes must be demonstrated.

Additionally, before introducing a novel feed regime for commercial manufacturing, the regime must be validated, along with the entire LVV manufacturing process, according to the regulatory guidelines. Adherence to these guidelines ensures that the manufacturing process generates a product that routinely and reliably meets the required quality standards and is consequently safe and efficacious for patients. The FDA document “Guideline on General Principles of Process Validation,” defines process validation as “establishing documented evidence which provides a high degree of assurance that a specific process will consistently produce a product meeting its pre-determined specifications and quality attributes.” (U.S. Food and Drug Administration, 2011). Validation is typically performed in three stages: process design, process qualification, and process verification.

During process design, the implementation of the novel feed in the upstream process would first be characterised and then scaled up for clinical production (Castillo et al., 2016). The FDA guidance recommends early process development work to be carried out using high-throughput scale-down models and statistical design of experiments (DoE) to study the interaction of different process parameters (U.S. Food and Drug Administration, 2011). Hence, much of the work described in this thesis falls under early process design in line with the FDA guidance. In Chapter 5, the 24-DSW plate scale down model from Chapter 4 together with a DoE approach was used to develop a novel feed for improving 277 cell line growth. In Chapter 6, the effect of the novel feed on LVV production was characterised using two different stable cell lines. To fully characterise the implementation of the novel feed in the upstream process, the following issues also need to be addressed:

1. **Scale-up performance for upstream processing** – This thesis has successfully demonstrated the effect of the novel feed on improving LVV production in the 24-DSW plates. The next stage of process design is to demonstrate scale-up of the novel feed process up to clinical and/or commercial manufacturing scale. During the scale translation, it is important to be aware of the different pH environments between an STR and 24-DSW plate with the latter being uncontrolled and the former controlled. This

difference in pH resulted in varying metabolite profiles between the two systems, as shown in chapter 4. Therefore, the performance of the feed in the pH controlled STR would need to be characterised as it may differ from the performance in the uncontrolled 24-DSW plate, and may require further optimisation.

The initial scale translation to 2 L STR scale can be performed at matched mixing time. This has already been demonstrated to be a successful parameter for scaling between small-scale culture vessels e.g. 24-DSW plate and 2 L STR as shown in section 4.6. For larger fluid volumes (>50 L scale), very high fluid velocities would be required to achieve the same mixing time. This may lead to excessive foaming and high shear stress level in the bioreactor. Therefore, equal P/V is a more suitable parameter when scaling from small scale STR (e.g. 2 L scale) to larger scale STRs (>50 L scale).

2. **Impact on downstream processing** – It is important to ensure that the novel feed does not have a detrimental impact on downstream processing and final product quality. The acceptable range of LVV recovery should be maintained in each individual downstream unit operation. Furthermore, the viable cell densities achieved with the novel feed would likely be greater than those in the existing process and therefore, its impact on the clarification step will also have to be investigated. The higher viable cell densities also means higher impurity levels are likely to be expected in the upstream harvest (Westoby et al., 2011). Therefore, it must be demonstrated that the required level of impurity clearance is maintained. Lastly, it is also important to characterise the downstream process of the novel feed process at large scale.
3. **Technology transfer from R&D to cGMP manufacturing site** – Change in the process scale can be challenging due to the differences of technology and equipment with scale-up. This is even more pertinent when the process is transferred from an R&D lab setting to a manufacturing site in different parts of the world. Hence, a full technology transfer process must be completed to

ensure that all critical process parameters (CPP's) and critical quality attributes (CQA's) are met.

4. **Engineering runs** – To demonstrate successful tech transfer and to 'lock' the operating parameters of the novel feed process, at least two engineering runs would typically be conducted. This ensures successful scale-up for biopharmaceutical manufacturing. The engineering runs are often carried out in a GMP manufacturing environment and at clinical or commercial manufacturing scale.
5. **Investigational New Drug/Investigational Medicinal Product Dossier application** – The Company will also be required to make changes to CMC (Chemical, Manufacturing and Controls) sections within the IND (FDA) or IMPD (EMA) application. The company has to demonstrate to the regulators that the product is consistently produced with defined attributes using the process incorporating the novel feed. This is a crucial stage of validating the feed since failure to do so can affect the ability to continue through development. Successful completion of the engineering runs, and acceptance of the IND/IMPD content by the regulators, ensures that the vector is safe for clinical supply.

The next two stages of process validation (i.e. process qualification and continued process verification) are usually carried out after obtaining successful clinical data i.e. after phase 3 trials. During process qualification, the aim is to ensure that the manufacturing process is capable of reliably producing viral vector which meets all release criteria during commercial manufacturing (Castillo et al., 2016). The ability to execute the process within those control ranges are verified through process performance qualification (PPQ) (Zingaro et al., 2020). The PPQ batches are performed by trained staff under full cGMP conditions using prequalified equipment in the proposed commercial manufacturing plant (Castillo et al., 2016). For complete process qualification, all aspects of the manufacturing process have to be validated,

such as raw materials used in each unit operation, process equipment and all supporting facilities and utilities (Castillo et al., 2016; Zingaro et al., 2020).

Lastly, the purpose of continued process verification is to monitor the routine commercial production using validated test methods to ensure that the viral vector produced continues to meet all critical quality attributes (CQAs) (Castillo et al., 2016). The production data is collected on an ongoing basis and it should provide strong statistical evidence that all CPPs are within their acceptable ranges (Castillo et al., 2016).

7.2.2.2 Practical, safety and environmental aspects

In addition to process validation, it should be evaluated whether the implementation of the novel feed regime in the company's upstream vector process can be realised from a practical, safety and environmental aspect. Firstly, the company should engage with raw material suppliers and develop a robust supply chain. It is important to engage with multiple suppliers to mitigate risk in the event of supply shortages. The consistency of the raw materials is very important and potential trace impurities (e.g. trace metals) has to be taken into consideration. In addition to the raw materials for feed formulation, the supply chain should also consider single-use consumables such as sterile bottles, bags and tubing which are required for packaging the formulated feed. Regulatory authorities are encouraging companies to better understand their raw material supply chain as this enables a proper assessment of any risks the materials may pose with respect to impacting the quality, safety, and efficacy of the final product (Zingaro et al., 2020).

From a practical perspective, it is also important to engage with the team at the manufacturing facility responsible for preparing media and buffers. This is particularly important during process scale-up when large quantities of the feed would be required. To ensure consistency in the feed preparation, an SOP (standard operating procedure) detailing the method of formulating the feed should be documented. Furthermore, it is important that sterile working practices are adhered to when preparing the feed.

When operating the process at large-scale (e.g. > 50 L), another key practical consideration is the transfer of the feed from the container to the production reactor. A sterile welding machine or sterile connections are often used to facilitate the transfer process. It is important to write an SOP for feed transfer at each scale taking into account the size of tubing and connection method.

In terms of safety, it is important to always ensure containment of the feed. For example, the amino acids in the feed can cause skin and eye irritation when in contact. Hence, suitable PPE must be worn when handling the feed. The feed addition bottles and bags are also pressurised and should therefore be inspected frequently for leaks.

Lastly, the environmental impact of the feed should be captured in a separate risk assessment. Important considerations include disposal of unused feed, as well as single-use components. Guidelines for waste disposal should be adhered to at all times.

8 REFERENCES

- Abaandou, L., Quan, D., Shiloach, J., 2021. Affecting hek293 cell growth and production performance by modifying the expression of specific genes. *Cells* 10. <https://doi.org/10.3390/cells10071667>
- Adamson, L., Walum, E., 2007. Insulin and IGF-1 Mediated Inhibition of Apoptosis in CHO Cells Grown in Suspension in a Protein-free Medium. <https://doi.org/10.1177/026119290703500301> 35, 349–352. <https://doi.org/10.1177/026119290703500301>
- Alberts, A.W., Fergusonj, K., Hennessy, S., Vagelos, P.R., 1974. Regulation of Lipid Synthesis in Cultured Animal Cells*. *OF BIOLOGICAL CHEYIBTBY* 249, 5241–5249. [https://doi.org/10.1016/S0021-9258\(19\)42354-5](https://doi.org/10.1016/S0021-9258(19)42354-5)
- Allen, J., Davey, H.M., Broadhurst, D., Heald, J.K., Rowland, J.J., Oliver, S.G., Kell, D.B., 2003. High-throughput classification of yeast mutants for functional genomics using metabolic footprinting. *Nature Biotechnology* 2003 21:6 21, 692–696. <https://doi.org/10.1038/nbt823>
- Al-Ramadhani, O., 2015. Design and characterisation of a parallel miniaturised bioreactor system for mammalian cell culture. Doctoral thesis, UCL (University College London). .
- Altamirano, C., Paredes, C., Cairó, J.J., Gòdia, F., 2000. Improvement of CHO cell culture medium formulation: simultaneous substitution of glucose and glutamine. *Biotechnol Prog* 16, 69–75. <https://doi.org/10.1021/BP990124J>
- Amanullah, A., Buckland, B.C., Nienow, A.W., 2004. Mixing in the Fermentation and Cell Culture Industries. *Handbook of Industrial Mixing* 1071–1170. <https://doi.org/10.1002/0471451452.CH18>
- Ansorge, S., Henry, O., Kamen, A., 2010. Recent progress in lentiviral vector mass production. *Biochem Eng J* 48, 362–377. <https://doi.org/10.1016/J.BEJ.2009.10.017>

- Ansorge, S., Lanthier, S., Transfiguracion, J., Durocher, Y., Henry, O., Kamen, A., 2009. Development of a scalable process for high-yield lentiviral vector production by transient transfection of HEK293 suspension cultures. *J Gene Med* 11, 868–876. <https://doi.org/10.1002/JGM.1370>
- Ansorge, S., Lanthier, S., Transfiguracion, J., Henry, O., Kamen, A., 2011. Monitoring lentiviral vector production kinetics using online permittivity measurements. *Biochem Eng J* 54, 16–25. <https://doi.org/10.1016/j.bej.2011.01.002>
- Arora, M., 2013. Cell Culture Media: A Review. *Materials and Methods* 3. <https://doi.org/10.13070/MM.EN.3.175>
- Bachrach, U., 2007. Antiviral activity of oxidized polyamines. *Amino Acids* 33, 267–272. <https://doi.org/10.1007/S00726-007-0535-Y>
- Bagnis, C., Zwojczyki, G., Chiaroni, J., Bailly, P., 2014. Off-on polyadenylation strategy as a supplemental mechanism for silencing toxic transgene expression during lentiviral vector production. *Biotechniques* 56, 311–318. <https://doi.org/10.2144/000114178/ASSET/IMAGES/LARGE/FIGURE3.JPEG>
- Baig, F., Pechlaner, R., Mayr, M., 2016. Caveats of Untargeted Metabolomics for Biomarker Discovery. *J Am Coll Cardiol* 68, 1294–1296. <https://doi.org/10.1016/J.JACC.2016.05.098>
- Barrett, T.A., Wu, A., Zhang, H., Levy, M.S., Lye, G.J., 2010. Microwell engineering characterization for mammalian cell culture process development. *Biotechnol Bioeng* 105, 260–275. <https://doi.org/10.1002/BIT.22531>
- Belete, T.M., 2021. The Current Status of Gene Therapy for the Treatment of Cancer. *Biologics* 15, 67. <https://doi.org/10.2147/BTT.S302095>
- Betts, J.I., Baganz, F., 2006. Miniature bioreactors: Current practices and future opportunities. *Microb Cell Fact* 5, 1–14. <https://doi.org/10.1186/1475-2859-5-21/FIGURES/3>
- Bhatia, S., 2015. Plant Tissue Culture. *Modern Applications of Plant Biotechnology in Pharmaceutical Sciences* 31–107. <https://doi.org/10.1016/B978-0-12-802221-4.00002-9>
- Bhattacharya, S., 2021. Central Composite Design for Response Surface Methodology and Its Application in Pharmacy. *Response Surface Methodology in Engineering Science*. <https://doi.org/10.5772/INTECHOPEN.95835>
- Bielser, J.M., Wolf, M., Souquet, J., Broly, H., Morbidelli, M., 2018. Perfusion mammalian cell culture for recombinant protein manufacturing - A critical review. *Biotechnol Adv* 36, 1328–1340. <https://doi.org/10.1016/J.BIOTECHADV.2018.04.011>
- Bokhoven, M., Stephen, S.L., Knight, S., Gevers, E.F., Robinson, I.C., Takeuchi, Y., Collins, M.K., 2009. Insertional gene activation by lentiviral and gammaretroviral vectors. *J Virol* 83, 283–294. <https://doi.org/10.1128/JVI.01865-08>

- Briggs, J.A.G., Wilk, T., Welker, R., Kräusslich, H.G., Fuller, S.D., 2003. Structural organization of authentic, mature HIV-1 virions and cores. *EMBO J* 22, 1707. <https://doi.org/10.1093/EMBOJ/CDG143>
- Butler, M., 2003. Hybridomas, Genetic Engineering of. *Encyclopedia of Physical Science and Technology* 427–443. <https://doi.org/10.1016/B0-12-227410-5/00319-7>
- Capra, E., Gennari, A., Loche, A., Temps, C., 2022. Viral-vector therapies at scale: Today's challenges and future opportunities Viral-vector gene therapies are here to stay. Keeping pace with increasing demand requires consideration of challenges, the potential for standardization, and strategizing for accelerating patient access.
- Castillo, F.C., Cooney, B., Levine, H.L., 2016. Biopharmaceutical Manufacturing Process Validation and Quality Risk Management | Pharmaceutical Engineering [WWW Document]. International Society for Pharmaceutical Engineering. URL <https://ispe.org/pharmaceutical-engineering/may-june-2016/biopharmaceutical-manufacturing-process-validation-and> (accessed 8.27.23).
- Cavazzana-Calvo, M., Payen, E., Negre, O., Wang, G., Hehir, K., Fusil, F., Down, J., Denaro, M., Brady, T., Westerman, K., Cavallesco, R., Gillet-Legrand, B., Caccavelli, L., Sgarra, R., Maouche-Chrétien, L., Bernaudin, F., Giroto, R., Dorazio, R., Mulder, G.J., Polack, A., Bank, A., Soulier, J., Larghero, J., Kabbara, N., Dalle, B., Gourmel, B., Socie, G., Chrétien, S., Cartier, N., Aubourg, P., Fischer, A., Cornetta, K., Galacteros, F., Beuzard, Y., Gluckman, E., Bushman, F., Hacein-Bey-Abina, S., Leboulch, P., 2010. Transfusion independence and HMGA2 activation after gene therapy of human β -thalassaemia. *Nature* 467, 318–322. <https://doi.org/10.1038/NATURE09328>
- Cervera, L., Gutiérrez-Granados, S., Martínez, M., Blanco, J., Gòdia, F., Segura, M.M., 2013. Generation of HIV-1 Gag VLPs by transient transfection of HEK 293 suspension cell cultures using an optimized animal-derived component free medium. *J Biotechnol* 166, 152–165. <https://doi.org/10.1016/J.JBIOTECH.2013.05.001>
- Chalfie, M., 2001. Cell Markers: Green Fluorescent Protein (GFP). *Encyclopedia of Genetics* 311–313. <https://doi.org/10.1006/RWGN.2001.0174>
- Chen, Y., Ott, C.J., Townsend, K., Subbaiah, P., Aiyar, A., Miller, W.M., 2009. Cholesterol supplementation during production increases the infectivity of retroviral and lentiviral vectors pseudotyped with the vesicular stomatitis virus glycoprotein (VSV-G). *Biochem Eng J* 44, 199–207. <https://doi.org/10.1016/J.BEJ.2008.12.004>
- Chen, Y.H., Pallant, C., Sampson, C.J., Boiti, A., Johnson, S., Brazauskas, P., Hardwicke, P., Marongiu, M., Marinova, V.M., Carmo, M., Sweeney, N.P., Richard, A., Shillings, A., Archibald, P., Puschmann, E., Mouzon, B., Grose, D., Mendez-Tavio, M., Chen, M.X., Warr, S.R.C., Senussi, T., Carter, P.S., Baker, S., Jung, C., Brugman, M.H., Howe, S.J., Vink, C.A., 2020. Rapid Lentiviral Vector Producer Cell Line Generation Using a Single DNA Construct. *Mol Ther Methods Clin Dev* 19, 47–57. <https://doi.org/10.1016/J.OMTM.2020.08.011>
- Chisti, Y., Moo-Young, M., 2003. Bioreactors. *Encyclopedia of Physical Science and Technology* 247–271. <https://doi.org/10.1016/B0-12-227410-5/00067-3>

- Chong, W.P.K., Goh, L.T., Reddy, S.G., Yusufi, F.N.K., Lee, D.Y., Wong, N.S.C., Heng, C.K., Yap, M.G.S., Ho, Y.S., 2009. Metabolomics profiling of extracellular metabolites in recombinant Chinese Hamster Ovary fed-batch culture. *Rapid Commun Mass Spectrom* 23, 3763–3771. <https://doi.org/10.1002/RCM.4328>
- Chong, W.P.K., Reddy, S.G., Yusufi, F.N.K., Lee, D.Y., Wong, N.S.C., Heng, C.K., Yap, M.G.S., Ho, Y.S., 2010. Metabolomics-driven approach for the improvement of Chinese hamster ovary cell growth: overexpression of malate dehydrogenase II. *J Biotechnol* 147, 116–121. <https://doi.org/10.1016/J.JBIOTECH.2010.03.018>
- Chong, W.P.K., Yusufi, F.N.K., Lee, D.Y., Reddy, S.G., Wong, N.S.C., Heng, C.K., Yap, M.G.S., Ho, Y.S., 2011. Metabolomics-based identification of apoptosis-inducing metabolites in recombinant fed-batch CHO culture media. *J Biotechnol* 151, 218–224. <https://doi.org/10.1016/j.jbiotec.2010.12.010>
- Chou, M.L., Bailey, A., Avory, T., Tanimoto, J., Burnouf, T., 2015. Removal of transmissible spongiform encephalopathy prion from large volumes of cell culture media supplemented with fetal bovine serum by using hollow fiber anion-exchange membrane chromatography. *PLoS One* 10. <https://doi.org/10.1371/JOURNAL.PONE.0122300>
- Clincke, M.F., Mölleryd, C., Zhang, Y., Lindskog, E., Walsh, K., Chotteau, V., 2013. Very high density of CHO cells in perfusion by ATF or TFF in WAVE bioreactor™. Part I. Effect of the cell density on the process. *Biotechnol Prog* 29, 754–767. <https://doi.org/10.1002/BTPR.1704>
- Comisel, R.-M., Kara, B., Fiesser, F.H., Farid, S.S., 2021. Lentiviral vector bioprocess economics for cell and gene therapy commercialization. *Biochem Eng J* 167, 107868. <https://doi.org/https://doi.org/10.1016/j.bej.2020.107868>
- Coroadinha, A.S., Alves, P.M., Santos, S.S., Cruz, P.E., Merten, O.W., Carrondo, M.J.T., 2006a. Retrovirus producer cell line metabolism: implications on viral productivity. *Appl Microbiol Biotechnol* 72, 1125–1135. <https://doi.org/10.1007/S00253-006-0401-Y>
- Coroadinha, A.S., Ribeiro, J., Roldão, A., Cruz, P.E., Alves, P.M., Merten, O.W., Carrondo, M.J.T., 2006b. Effect of medium sugar source on the production of retroviral vectors for gene therapy. *Biotechnol Bioeng* 94, 24–36. <https://doi.org/10.1002/BIT.20778>
- Costa, A.R., Rodrigues, M.E., Henriques, M., Oliveira, R., Azeredo, J., 2014. Feed optimization in fed-batch culture. *Methods Mol Biol* 1104, 105–116. https://doi.org/10.1007/978-1-62703-733-4_8
- Costariol, Elena, Rotondi, Marco C, Amini, Arman, Hewitt, Christopher J, Nienow, Alvin W, Heathman, Thomas R J, Rafiq, Qasim A, Costariol, E, Rotondi, M C, Amini, A, Rafiq, Q A, Hewitt, C J, Nienow, A W, Heathman, T R J, 2020. Demonstrating the Manufacture of Human CAR-T Cells in an Automated Stirred-Tank Bioreactor. *Biotechnol J* 15, 2000177. <https://doi.org/10.1002/BIOT.202000177>
- Cribbs, A.P., Kennedy, A., Gregory, B., Brennan, F.M., 2013. Simplified production and concentration of lentiviral vectors to achieve high transduction in primary human T cells. <https://doi.org/10.1186/1472-6750-13-98>

- Cruz, H.J., Freitas, C.M., Alves, P.M., Moreira, J.L., Carrondo, M.J.T., 2000. Effects of ammonia and lactate on growth, metabolism, and productivity of BHK cells. *Enzyme Microb Technol* 27, 43–52. [https://doi.org/10.1016/S0141-0229\(00\)00151-4](https://doi.org/10.1016/S0141-0229(00)00151-4)
- Cuisset, L., Tichonicky, L., Jaffray, P., Delpuch, M., 1997. The effects of sodium butyrate on transcription are mediated through activation of a protein phosphatase. *Journal of Biological Chemistry* 272, 24148–24153. <https://doi.org/10.1074/jbc.272.39.24148>
- Das, A.T., Tenenbaum, L., Berkhout, B., 2016. Tet-On Systems For Doxycycline-inducible Gene Expression. *Curr Gene Ther* 16, 156. <https://doi.org/10.2174/1566523216666160524144041>
- Dautzenberg, I.J.C., Rabelink, M.J.W.E., Hoeben, R.C., 2020. The stability of envelope-pseudotyped lentiviral vectors. *Gene Therapy* 2020 28:1 28, 89–104. <https://doi.org/10.1038/s41434-020-00193-y>
- Davis, H.E., Morgan, J.R., Yarmush, M.L., 2002. Polybrene increases retrovirus gene transfer efficiency by enhancing receptor-independent virus adsorption on target cell membranes. *Biophys Chem* 97, 159–172. [https://doi.org/https://doi.org/10.1016/S0301-4622\(02\)00057-1](https://doi.org/https://doi.org/10.1016/S0301-4622(02)00057-1)
- Delignat, S., Peyron, I., El Ghazaly, M., V Kaveri, S., Rohde, J., Mueller, F., Lacroix-Desmazes, S., 2018. Biochemical characterization and immunogenicity of Neureight, a recombinant full-length factor VIII produced by fed-batch process in disposable bioreactors. *Cell Immunol* 331, 22–29. <https://doi.org/10.1016/J.CELLIMM.2018.05.002>
- Diamond, D.L., Syder, A.J., Jacobs, J.M., Sorensen, C.M., Walters, K.A., Proll, S.C., McDermott, J.E., Gritsenko, M.A., Zhang, Q., Zhao, R., Metz, T.O., Camp, D.G., Waters, K.M., Smith, R.D., Rice, C.M., Katze, M.G., 2010. Temporal proteome and lipidome profiles reveal hepatitis C virus-associated reprogramming of hepatocellular metabolism and bioenergetics. *PLoS Pathog* 6. <https://doi.org/10.1371/JOURNAL.PPAT.1000719>
- Diaz, A., Acevedo, F., 1999. Scale-up strategy for bioreactors with Newtonian and non-Newtonian broths. *Bioprocess Engineering* 21, 21–23. <https://doi.org/10.1007/S004490050634/METRICS>
- Doig, S.D., Pickering, S.C.R., Lye, G.J., Baganz, F., 2005. Modelling surface aeration rates in shaken microtitre plates using dimensionless groups. *Chem Eng Sci* 60, 2741–2750. <https://doi.org/10.1016/J.CES.2004.12.025>
- Doran, P., 2013. *Engineering Principles Second Edition*, Academic Press.
- Ducommun, P., Ruffieux, P.A., Von Stockar, U., Marison, I., 2001. The role of vitamins and amino acids on hybridoma growth and monoclonal antibody production. *Cytotechnology* 37, 65–73. <https://doi.org/10.1023/A:1019956013627/METRICS>
- Duetz, W.A., 2007. Microtiter plates as mini-bioreactors: miniaturization of fermentation methods. *Trends Microbiol* 15, 469–475. <https://doi.org/10.1016/J.TIM.2007.09.004>
- Duetz, W.A., Rüedi, L., Hermann, R., O'Connor, K., Büchs, J., Witholt, B., 2000. Methods for intense aeration, growth, storage, and replication of bacterial strains in microtiter

- plates. *Appl Environ Microbiol* 66, 2641–2646.
<https://doi.org/10.1128/AEM.66.6.2641-2646.2000/ASSET/AC3BA13C-1670-419C-B1FC-8469123FE6B7/ASSETS/GRAPHIC/AM0601805003.JPEG>
- Duetz, W.A., Witholt, B., 2004. Oxygen transfer by orbital shaking of square vessels and deepwell microtiter plates of various dimensions. *Biochem Eng J* 17, 181–185.
[https://doi.org/10.1016/S1369-703X\(03\)00177-3](https://doi.org/10.1016/S1369-703X(03)00177-3)
- Eagle, H., 1955. Nutrition needs of mammalian cells in tissue culture. *Science* (1979) 122, 501–504. <https://doi.org/10.1126/SCIENCE.122.3168.501/ASSET/102AEF74-7CDA-4D68-85CF-7CB74B5977D2/ASSETS/SCIENCE.122.3168.501.FP.PNG>
- Enfors, S.O., Jahic, M., Rozkov, A., Xu, B., Hecker, M., Jürgen, B., Krüger, E., Schweder, T., Hamer, G., O’Beirne, D., Noisommit-Rizzi, N., Reuss, M., Boone, L., Hewitt, C., McFarlane, C., Nienow, A., Kovacs, T., Trägårdh, C., Fuchs, L., Revstedt, J., Friberg, P.C., Hjertager, B., Blomsten, G., Skogman, H., Hjort, S., Hoeks, F., Lin, H.Y., Neubauer, P., Van der Lans, R., Luyben, K., Vrabel, P., Manelius, Å., 2001. Physiological responses to mixing in large scale bioreactors. *J Biotechnol* 85, 175–185.
[https://doi.org/10.1016/S0168-1656\(00\)00365-5](https://doi.org/10.1016/S0168-1656(00)00365-5)
- Erickson, L.E., 2011. Bioreactors for Commodity Products. *Comprehensive Biotechnology*, Second Edition 3, 653–658. <https://doi.org/10.1016/B978-0-08-088504-9.00236-1>
- Fan, Y., Jimenez Del Val, I., Müller, C., Wagtberg Sen, J., Rasmussen, S.K., Kontoravdi, C., Weilguny, D., Andersen, M.R., 2015. Amino acid and glucose metabolism in fed-batch CHO cell culture affects antibody production and glycosylation. *Biotechnol Bioeng* 112, 521–535. <https://doi.org/10.1002/BIT.25450>
- Ferreira-Torres, C., Micheletti, M., Lye, G.J., 2005. Microscale process evaluation of recombinant biocatalyst libraries: Application to Baeyer-Villiger monoxygenase catalysed lactone synthesis. *Bioprocess Biosyst Eng* 28, 83–93.
<https://doi.org/10.1007/S00449-005-0422-4/TABLES/3>
- Freund, N.W., Croughan, M.S., 2018. A Simple Method to Reduce both Lactic Acid and Ammonium Production in Industrial Animal Cell Culture. *Int J Mol Sci* 19.
<https://doi.org/10.3390/IJMS19020385>
- Gama-Norton, L., Botezatu, L., Herrmann, S., Schweizer, M., Alves, P.M., Hauser, H., Wirth, D., 2011. Lentivirus production is influenced by SV40 large T-antigen and chromosomal integration of the vector in HEK293 cells. *Hum Gene Ther* 22, 1269–1279. <https://doi.org/10.1089/HUM.2010.143>
- Garnier, A., Côté, J., Nadeau, I., Kamen, A., Massie, B., 1994. Scale-up of the adenovirus expression system for the production of recombinant protein in human 293S cells. *Cytotechnology* 15, 145–155. <https://doi.org/10.1007/BF00762389/METRICS>
- Geraerts, M., Micheils, M., Baekelandt, V., Debyser, Z., Gijssbers, R., 2005. Upscaling of lentiviral vector production by tangential flow filtration. *J Gene Med* 7, 1299–1310.
<https://doi.org/10.1002/JGM.778>

- Gogate, P.R., Beenackers, A.A.C.M., Pandit, A.B., 2000. Multiple-impeller systems with a special emphasis on bioreactors: a critical review. *Biochem Eng J* 6, 109–144. [https://doi.org/10.1016/S1369-703X\(00\)00081-4](https://doi.org/10.1016/S1369-703X(00)00081-4)
- Graham, F.L., Smiley, J., Russell, W.C., Nairn, R., 1977. Characteristics of a human cell line transformed by DNA from human adenovirus type 5. *J Gen Virol* 36, 59–72. <https://doi.org/10.1099/0022-1317-36-1-59>
- Guy, H.M., McCloskey, L., Lye, G.J., Mitrophanous, K.A., Mukhopadhyay, T.K., 2013. Characterization of Lentiviral Vector Production Using Microwell Suspension Cultures of HEK293T-Derived Producer Cells. <https://home.liebertpub.com/hgtb> 24, 125–139. <https://doi.org/10.1089/HGTB.2012.200>
- Haggerty, D.F., Gerschenson, L.E., Harary, I., Mead, J.F., 1965. The metabolism of linoleic acid in mammalian cells in culture. *Biochem Biophys Res Commun* 21, 568–574. [https://doi.org/10.1016/0006-291X\(65\)90523-1](https://doi.org/10.1016/0006-291X(65)90523-1)
- Heaton, N.S., Randall, G., 2011. Multifaceted roles for lipids in viral infection. *Trends Microbiol* 19, 368–375. <https://doi.org/10.1016/J.TIM.2011.03.007>
- HEBY, O., 1981. Role of Polyamines in the Control of Cell Proliferation and Differentiation. *Differentiation* 19, 1–20. <https://doi.org/10.1111/J.1432-0436.1981.TB01123.X>
- Henry, O., Jolicoeur, M., Kamen, A., 2011. Unraveling the metabolism of HEK-293 cells using lactate isotopomer analysis. *Bioprocess Biosyst Eng* 34, 263–273. <https://doi.org/10.1007/S00449-010-0468-9/TABLES/3>
- Hernandez, I., Prasad, V., Gellad, W.F., 2018. Total Costs of Chimeric Antigen Receptor T-Cell Immunotherapy. *JAMA Oncol* 4, 994–996. <https://doi.org/10.1001/JAMAONCOL.2018.0977>
- Hölttä, E., Pohjanpelto, P., 1982. Polyamine dependence of Chinese hamster ovary cells in serum-free culture is due to deficient arginase activity. *Biochimica et Biophysica Acta (BBA) - Molecular Cell Research* 721, 321–327. [https://doi.org/10.1016/0167-4889\(82\)90085-4](https://doi.org/10.1016/0167-4889(82)90085-4)
- Horvat, J., Narat, M., Spadiut, O., 2020. The effect of amino acid supplementation in an industrial Chinese Hamster Ovary process. *Biotechnol Prog* 36, e3001. <https://doi.org/10.1002/BTPR.3001>
- Hossler, P., Mcdermott, S., Racicot, C., Chumsae, C., Raharimampionona, H., Zhou, Y., Ouellette, D., Matuck, J., Correia, I., Fann, J., Li, J., 2014. Cell culture media supplementation of uncommonly used sugars sucrose and tagatose for the targeted shifting of protein glycosylation profiles of recombinant protein therapeutics. *Biotechnol Prog* 30, 1419–1431. <https://doi.org/10.1002/BTPR.1968>
- Hu, Y., Li, Y., 2018. Effect of Low pH Treatment on Cell Cycle and Cell Growth. *The FASEB Journal* 32, 804.49-804.49. https://doi.org/10.1096/FASEBJ.2018.32.1_SUPPLEMENT.804.49

- Ishaque, A., Al-Rubeai, M., 2002. Role of vitamins in determining apoptosis and extent of suppression by bcl-2 during hybridoma cell culture. *Apoptosis* 7, 231–239. <https://doi.org/10.1023/A:1015343616059/METRICS>
- Iwakuma, T., Cui, Y., Chang, L.J., 1999. Self-inactivating lentiviral vectors with U3 and U5 modifications. *Virology* 261, 120–132. <https://doi.org/10.1006/VIRO.1999.9850>
- Kallunki, T., Barisic, M., Jäättelä, M., Liu, B., 2019. How to choose the right inducible gene expression system for Mammalian studies? *Cells*. <https://doi.org/10.3390/cells8080796>
- Karantalis, V., Schulman, I.H., Balkan, W., Hare, J.M., 2015. Allogeneic cell therapy: a new paradigm in therapeutics. *Circ Res* 116, 12–15. <https://doi.org/10.1161/CIRCRESAHA.114.305495>
- Kerviel, A., Thomas, A., Chaloin, L., Favard, C., Muriaux, D., 2013. Virus assembly and plasma membrane domains: which came first? *Virus Res* 171, 332–340. <https://doi.org/10.1016/J.VIRUSRES.2012.08.014>
- Khoo, S.H.G., Al-Rubeai, M., 2007. Metabolomics as a complementary tool in cell culture. *Biotechnol Appl Biochem* 47, 71. <https://doi.org/10.1042/BA20060221>
- Kim, D.Y., Lee, J.C., Chang, H.N., Oh, D.J., 2005. Effects of supplementation of various medium components on Chinese hamster ovary cell cultures producing recombinant antibody. *Cytotechnology* 47, 37–49. <https://doi.org/10.1007/S10616-005-3775-2/METRICS>
- Kishishita, S., Katayama, S., Kodaira, K., Takagi, Y., Matsuda, H., Okamoto, H., Takuma, S., Hirashima, C., Aoyagi, H., 2015. Optimization of chemically defined feed media for monoclonal antibody production in Chinese hamster ovary cells. *J Biosci Bioeng* 120, 78–84. <https://doi.org/https://doi.org/10.1016/j.jbiosc.2014.11.022>
- Kotterman, M.A., Chalberg, T.W., Schaffer, D. V., 2015. Viral Vectors for Gene Therapy: Translational and Clinical Outlook. *Annu Rev Biomed Eng* 17, 63–89. <https://doi.org/10.1146/ANNUREV-BIOENG-071813-104938>
- Krömer, J.O., Dietmair, S., Jacob, S.S., Nielsen, L.K., 2011. Quantification of l-alanyl-l-glutamine in mammalian cell culture broth: Evaluation of different detectors. *Anal Biochem* 416, 129–131. <https://doi.org/10.1016/J.AB.2011.05.019>
- Kudugunti, S., Lin, W.R., Rusche, J., 2015. LONG®R3 IGF-I Boosts IgG Production in CHO.
- Kumar, S., Wittmann, C., Heinzle, E., 2004. Minibioreactors. *Biotechnol Lett* 26, 1–10. <https://doi.org/10.1023/B:BILE.0000009469.69116.03>
- Labbé, R.P., Vessillier, S., Rafiq, Q.A., 2021. Lentiviral Vectors for T Cell Engineering: Clinical Applications, Bioprocessing and Future Perspectives. *Viruses* 13, 1528. <https://doi.org/10.3390/V13081528>
- Landauer, K., 2014. Designing media for animal cell culture: CHO cells, the industrial standard. *Methods in Molecular Biology* 1104, 89–103. https://doi.org/10.1007/978-1-62703-733-4_7/TABLES/9

- Langheinrich, C., Nienow, A.W., 1999. Control of pH in large-scale, free suspension animal cell bioreactors: Alkali addition and pH excursions. *Biotechnol Bioeng* 66, 171–179. [https://doi.org/10.1002/\(SICI\)1097-0290\(1999\)66:3<171::AID-BIT5>3.0.CO;2-T](https://doi.org/10.1002/(SICI)1097-0290(1999)66:3<171::AID-BIT5>3.0.CO;2-T)
- Lavado-García, J., Jorge, I., Cervera, L., Vázquez, J., Gòdia, F., 2020. Multiplexed Quantitative Proteomic Analysis of HEK293 Provides Insights into Molecular Changes Associated with the Cell Density Effect, Transient Transfection, and Virus-Like Particle Production. *J Proteome Res* 19, 1085–1099. <https://doi.org/10.1021/ACS.JPROTEOME.9B00601>
- Ledgerwood, J.E., DeZure, A.D., Stanley, D.A., Coates, E.E., Novik, L., Enama, M.E., Berkowitz, N.M., Hu, Z., Joshi, G., Ploquin, A., Sitar, S., Gordon, I.J., Plummer, S.A., Holman, L.A., Hendel, C.S., Yamshchikov, G., Roman, F., Nicosia, A., Colloca, S., Cortese, R., Bailer, R.T., Schwartz, R.M., Roederer, M., Mascola, J.R., Koup, R.A., Sullivan, N.J., Graham, B.S., 2017. Chimpanzee Adenovirus Vector Ebola Vaccine. *N Engl J Med* 376, 928–938. <https://doi.org/10.1056/NEJMOA1410863>
- Lee, D.Y., Bowen, B.P., Northen, T.R., 2010. Mass spectrometry-based metabolomics, analysis of metabolite-protein interactions, and imaging. *Biotechniques* 49, 557–565. <https://doi.org/10.2144/000113451>
- Levine, B.L., 2015. Performance-enhancing drugs: design and production of redirected chimeric antigen receptor (CAR) T cells. *Cancer Gene Therapy* 2015 22:2 22, 79–84. <https://doi.org/10.1038/cgt.2015.5>
- Li, F., Vijayasankaran, N., Shen, A., Kiss, R., Amanullah, A., 2010. Cell culture processes for monoclonal antibody production. <https://doi.org/10.4161/mabs.2.5.12720> 2, 466–479. <https://doi.org/10.4161/MABS.2.5.12720>
- Li, Y., Ducci, A., Micheletti, M., 2020. Study on mixing characteristics in shaken microwell systems. *Biochem Eng J* 153, 107392. <https://doi.org/10.1016/J.BEJ.2019.107392>
- Li, Y., Ducci, A., Micheletti, M., 2019. Mixing Time in Intermediate-Sized Orbitally Shaken Reactors with Small Orbital Diameters. *Chem Eng Technol* 42, 1611–1617. <https://doi.org/10.1002/CEAT.201900063>
- Lin, J., Takagi, M., Qu, Y., Gao, P., Yoshida, T., 1999. Metabolic flux change in hybridoma cells under high osmotic pressure. *J Biosci Bioeng* 87, 255–257. [https://doi.org/https://doi.org/10.1016/S1389-1723\(99\)89025-2](https://doi.org/https://doi.org/10.1016/S1389-1723(99)89025-2)
- Lindwasser, O.W., Resh, M.D., 2001. Multimerization of human immunodeficiency virus type 1 Gag promotes its localization to barges, raft-like membrane microdomains. *J Virol* 75, 7913–7924. <https://doi.org/10.1128/JVI.75.17.7913-7924.2001>
- Liste-Calleja, L., Lecina, M., Lopez-Repullo, J., Albiol, J., Solà, C., Cairó, J.J., 2015. Lactate and glucose concomitant consumption as a self-regulated pH detoxification mechanism in HEK293 cell cultures. *Appl Microbiol Biotechnol* 99, 9951–9960. <https://doi.org/10.1007/S00253-015-6855-Z>
- Liste-Calleja, L., López-Repullo, J., Lecina, M., Cairó, J.J., 2013. Preliminary studies of cell culture strategies for bioprocess development based on HEK293 cells. *BMC Proc* 7. <https://doi.org/10.1186/1753-6561-7-S6-P52>

- Manceur, A.P., Kim, H., Mistic, V., Andreev, N., Dorion-Thibaudeau, J., Lanthier, S., Bernier, A., Tremblay, S., Gélina, A.M., Broussau, S., Gilbert, R., Ansorge, S., 2017. Scalable Lentiviral Vector Production Using Stable HEK293SF Producer Cell Lines. *Hum Gene Ther Methods* 28, 330–339. <https://doi.org/10.1089/HGTB.2017.086>
- Martínez, V.S., Dietmair, S., Quek, L.E., Hodson, M.P., Gray, P., Nielsen, L.K., 2013. Flux balance analysis of CHO cells before and after a metabolic switch from lactate production to consumption. *Biotechnol Bioeng* 110, 660–666. <https://doi.org/10.1002/BIT.24728>
- Martínez-Monge, I., Albiol, J., Lecina, M., Liste-Calleja, L., Miret, J., Solà, C., Cairó, J.J., 2019. Metabolic flux balance analysis during lactate and glucose concomitant consumption in HEK293 cell cultures. *Biotechnol Bioeng* 116, 388–404. <https://doi.org/10.1002/BIT.26858>
- Matsumoto, S., Yamamoto, S., Sai, K., Maruo, K., Adachi, M., Saitoh, M., Nishizaki, T., 2003. Pipecolic acid induces apoptosis in neuronal cells. *Brain Res* 980, 179–184. [https://doi.org/10.1016/S0006-8993\(03\)02869-5](https://doi.org/10.1016/S0006-8993(03)02869-5)
- McCarron, A., Donnelley, M., McIntyre, C., Parsons, D., 2016. Challenges of up-scaling lentivirus production and processing. *J Biotechnol* 240, 23–30. <https://doi.org/10.1016/J.JBIOTECH.2016.10.016>
- Melton, L.A., Lipp, C.W., Spradling, R.W., Paulson, K.A., 2010. Dismt - Determination of mixing time through color changes. <http://dx.doi.org/10.1080/00986440212077189>, 322–338. <https://doi.org/10.1080/00986440212077>
- Merten, O.-W., Hebben, M., Bovolenta, C., 2016. Production of lentiviral vectors. *Mol Ther Methods Clin Dev* 3, 16017. <https://doi.org/10.1038/mtm.2016.17>
- Micheletti, M., Barrett, T., Doig, S.D., Baganz, F., Levy, M.S., Woodley, J.M., Lye, G.J., 2006. Fluid mixing in shaken bioreactors: Implications for scale-up predictions from microlitre-scale microbial and mammalian cell cultures. *Chem Eng Sci* 61, 2939–2949. <https://doi.org/10.1016/J.CES.2005.11.028>
- Midway, S., Robertson, M., Flinn, S., Kaller, M., 2020. Comparing multiple comparisons: practical guidance for choosing the best multiple comparisons test. *PeerJ* 8, e10387. <https://doi.org/10.7717/PEERJ.10387/SUPP-1>
- Minteer, D.M., Gerlach, J.C., Marra, K.G., 2014. Bioreactors Addressing Diabetes Mellitus. <https://doi.org/10.1177/1932296814548215> 8, 1227–1232. <https://doi.org/10.1177/1932296814548215>
- Mullick, A., Xu, Y., Warren, R., Koutroumanis, M., Guilbault, C., Broussau, S., Malenfant, F., Bourget, L., Lamoureux, L., Lo, R., Caron, A.W., Pilotte, A., Massie, B., 2006. The cumate gene-switch: a system for regulated expression in mammalian cells. *BMC Biotechnol* 6, 43. <https://doi.org/10.1186/1472-6750-6-43>
- Munger, J., Bajad, S.U., Collier, H.A., Shenk, T., Rabinowitz, J.D., 2006. Dynamics of the cellular metabolome during human cytomegalovirus infection. *PLoS Pathog* 2, 1165–1175. <https://doi.org/10.1371/JOURNAL.PPAT.0020132>

- Munger, J., Bennett, B.D., Parikh, A., Feng, X.J., McArdle, J., Rabitz, H.A., Shenk, T., Rabinowitz, J.D., 2008. Systems-level metabolic flux profiling identifies fatty acid synthesis as a target for antiviral therapy. *Nature Biotechnology* 26:10 26, 1179–1186. <https://doi.org/10.1038/nbt.1500>
- Nadeau, I., Jacob, D., Perrier, M., Kamen, A., 2000. 293SF Metabolic Flux Analysis during Cell Growth and Infection with an Adenoviral Vector. *Biotechnol Prog* 16, 872–884. <https://doi.org/10.1021/BP000098L>
- Nadeau, I., Kamen, A., 2003. Production of adenovirus vector for gene therapy. *Biotechnol Adv* 20, 475–489. [https://doi.org/10.1016/S0734-9750\(02\)00030-7](https://doi.org/10.1016/S0734-9750(02)00030-7)
- Naldini, L., Blömer, U., Gallay, P., Ory, D., Mulligan, R., Gage, F.H., Verma, I.M., Trono, D., 1996. In vivo gene delivery and stable transduction of nondividing cells by a lentiviral vector. *Science* 272, 263–267. <https://doi.org/10.1126/SCIENCE.272.5259.263>
- Newsholme, P., Lima, M.M.R., Procopio, J., Pithon-Curi, T.C., Doi, S.Q., Bazotte, R.B., Curi, R., 2003. Glutamine and glutamate as vital metabolites. *Brazilian Journal of Medical and Biological Research* 36, 153–163. <https://doi.org/10.1590/S0100-879X2003000200002>
- Ng, S., Gisonni-Lex, L., Azizi, A., 2017. New approaches for characterization of the genetic stability of vaccine cell lines. *Hum Vaccin Immunother*. <https://doi.org/10.1080/21645515.2017.1295191>
- Nienow, A.W., 2006. Reactor engineering in large scale animal cell culture. *Cytotechnology* 50, 9–33. <https://doi.org/10.1007/S10616-006-9005-8/METRICS>
- Nienow, A.W., 1998. Hydrodynamics of Stirred Bioreactors. *Appl Mech Rev* 51, 3–32. <https://doi.org/10.1115/1.3098990>
- Nordholt, N., Van Heerden, J., Kort, R., Bruggeman, F.J., 2017. Effects of growth rate and promoter activity on single-cell protein expression. *Scientific Reports* 2017 7:1 7, 1–11. <https://doi.org/10.1038/s41598-017-05871-3>
- Ono, A., Freed, E.O., 2001. Plasma membrane rafts play a critical role in HIV-1 assembly and release. *Proc Natl Acad Sci U S A* 98, 13925–13930. <https://doi.org/10.1073/PNAS.241320298>
- Ouellette, M.È., Bérubé, J.C., Bourget, J.M., Vallée, M., Bossé, Y., Fradette, J., 2019. Linoleic acid supplementation of cell culture media influences the phospholipid and lipid profiles of human reconstructed adipose tissue. *PLoS One* 14, e0224228. <https://doi.org/10.1371/JOURNAL.PONE.0224228>
- Ozturk, S.S., Riley, M.R., Palsson, B.O., 1992. Effects of ammonia and lactate on hybridoma growth, metabolism, and antibody production. *Biotechnol Bioeng* 39, 418–431. <https://doi.org/10.1002/BIT.260390408>
- Palfi, S., Gurruchaga, J.M., Scott Ralph, G., Lepetit, H., Lavis, S., Buttery, P.C., Watts, C., Miskin, J., Kelleher, M., Deeley, S., Iwamuro, H., Lefaucheur, J.P., Thiriez, C., Fenelon, G., Lucas, C., Brugières, P., Gabriel, I., Abhay, K., Drouot, X., Tani, N., Kas, A., Ghaleh, B., Le Corvoisier, P., Dolphin, P., Breen, D.P., Mason, S., Guzman, N.V.,

- Mazarakis, N.D., Radcliffe, P.A., Harrop, R., Kingsman, S.M., Rascol, O., Naylor, S., Barker, R.A., Hantraye, P., Remy, P., Cesaro, P., Mitrophanous, K.A., 2014. Long-term safety and tolerability of ProSavin, a lentiviral vector-based gene therapy for Parkinson's disease: a dose escalation, open-label, phase 1/2 trial. *Lancet* 383, 1138–1146. [https://doi.org/10.1016/S0140-6736\(13\)61939-X](https://doi.org/10.1016/S0140-6736(13)61939-X)
- Petiot, E., Ansoerge, S., Rosa-Calatrava, M., Kamen, A., 2017. Critical phases of viral production processes monitored by capacitance. *J Biotechnol* 242, 19–29. <https://doi.org/10.1016/j.jbiotec.2016.11.010>
- Petiot, E., Cuperlovic-Culf, M., Shen, C.F., Kamen, A., 2015. Influence of HEK293 metabolism on the production of viral vectors and vaccine. *Vaccine* 33, 5974–5981. <https://doi.org/10.1016/j.vaccine.2015.05.097>
- Petiot, E., Jacob, D., Lanthier, S., Lohr, V., Ansoerge, S., Kamen, A.A., 2011. Metabolic and Kinetic analyses of influenza production in perfusion HEK293 cell culture. *BMC Biotechnol* 11, 1–12. <https://doi.org/10.1186/1472-6750-11-84/FIGURES/4>
- Pfeifer, A., Brandon, E.P., Kootstra, N., Gage, F.H., Verma, I.M., 2001. Delivery of the Cre recombinase by a self-deleting lentiviral vector: Efficient gene targeting in vivo. *Proc Natl Acad Sci U S A* 98, 11450. <https://doi.org/10.1073/PNAS.201415498>
- Pluta, K., Kacprzak, M.M., 2009. Use of HIV as a gene transfer vector. *Acta Biochim Pol* 56, 531–595. https://doi.org/10.18388/abp.2009_2490
- Potter, H., Heller, R., 2018. Transfection by Electroporation. *Curr Protoc Mol Biol* 121, 9.3.1-9.3.13. <https://doi.org/10.1002/CPMB.48>
- Pulix, M., Lukashchuk, V., Smith, D.C., Dickson, A.J., 2021. Molecular characterization of HEK293 cells as emerging versatile cell factories. *Curr Opin Biotechnol* 71, 18–24. <https://doi.org/10.1016/J.COPBIO.2021.05.001>
- Quinonez, R., Sutton, R.E., 2002. Lentiviral vectors for gene delivery into cells. *DNA Cell Biol* 21, 937–951. <https://doi.org/10.1089/104454902762053873>
- Rabinowitz, J.D., Purdy, J.G., Vastag, L., Shenk, T., Koyuncu, E., 2011. Metabolomics in drug target discovery. *Cold Spring Harb Symp Quant Biol* 76, 235–246. <https://doi.org/10.1101/SQB.2011.76.010694>
- Rajapakse, N.W., Mattson, D.L., 2009. Role of l-arginine in nitric oxide production in health and hypertension. *Clin Exp Pharmacol Physiol*. <https://doi.org/10.1111/j.1440-1681.2008.05123.x>
- Reed, S.E., Staley, E.M., Mayginnnes, J.P., Pintel, D.J., Tullis, G.E., 2006. Transfection of mammalian cells using linear polyethylenimine is a simple and effective means of producing recombinant adeno-associated virus vectors. *J Virol Methods* 138, 85–98. <https://doi.org/10.1016/J.JVIROMET.2006.07.024>
- Ren, M., Zhong, X., Ma, C.Y., Sun, Y., Guan, Q.B., Cui, B., Guo, J., Wang, H., Gao, L., Zhao, J.J., 2008. Insulin-like growth factor-1 promotes cell cycle progression via upregulation of cyclin D1 expression through the phosphatidylinositol 3-kinase/nuclear factor- κ B signaling pathway in FRTL thyroid cells. *Acta Pharmacologica Sinica* 2009 30:1 30, 113–119. <https://doi.org/10.1038/aps.2008.8>

- Roca, B.C., Lao, N., Barron, N., Doolan, P., Clynes, M., 2019. An arginase-based system for selection of transfected CHO cells without the use of toxic chemicals. *Journal of Biological Chemistry* 294, 18756–18768. <https://doi.org/10.1074/jbc.RA119.011162>
- Rodrigues, A.F., Amaral, A.I., Veríssimo, V., Alves, P.M., Coroadinha, A.S., 2012. Adaptation of retrovirus producer cells to serum deprivation: Implications in lipid biosynthesis and vector production. *Biotechnol Bioeng* 109, 1269–1279. <https://doi.org/10.1002/BIT.24410>
- Rodrigues, A.F., Carmo, M., Alves, P.M., Coroadinha, A.S., 2009. Retroviral vector production under serum deprivation: The role of lipids. *Biotechnol Bioeng* 104, 1171–1181. <https://doi.org/10.1002/BIT.22499>
- Rodrigues, A.F., Carrondo, M.J.T., Alves, P.M., Coroadinha, A.S., 2014. Cellular targets for improved manufacturing of virus-based biopharmaceuticals in animal cells. *Trends Biotechnol* 32, 602–607. <https://doi.org/10.1016/J.TIBTECH.2014.09.010>
- Rodrigues, A.F., Formas-Oliveira, A.S., Bandeira, V.S., Alves, P.M., Hu, W.S., Coroadinha, A.S., 2013. Metabolic pathways recruited in the production of a recombinant enveloped virus: Mining targets for process and cell engineering. *Metab Eng* 20, 131–145. <https://doi.org/10.1016/J.YMBEN.2013.10.001>
- Rodriguez, G., Anderlei, T., Micheletti, M., Yianneskis, M., Ducci, A., 2014. On the measurement and scaling of mixing time in orbitally shaken bioreactors. *Biochem Eng J* 82, 10–21. <https://doi.org/10.1016/J.BEJ.2013.10.021>
- Román, R., Farràs, M., Camps, M., Martínez-Monge, I., Comas, P., Martínez-Espelt, M., Lecina, M., Casablanca, A., Cairó, J.J., 2018. Effect of continuous feeding of CO₂ and pH in cell concentration and product titers in hIFN γ producing HEK293 cells: Induced metabolic shift for concomitant consumption of glucose and lactate. *J Biotechnol* 287, 68–73. <https://doi.org/10.1016/j.jbiotec.2018.10.005>
- Sake, C.L., Newman, D.M., Boyle, N.R., 2020. Evaluation of quenching methods for metabolite recovery in photoautotrophic *Synechococcus* sp. PCC 7002. *Biotechnol Prog* 36, e3015. <https://doi.org/10.1002/BTPR.3015>
- Salazar, A., Keusgen, M., Von Hagen, J., 2016. Amino acids in the cultivation of mammalian cells. *Amino Acids* 48, 1161. <https://doi.org/10.1007/S00726-016-2181-8>
- Samuel, B.U., Mohandas, N., Harrison, T., McManus, H., Rosse, W., Reid, M., Haldar, K., 2001. The role of cholesterol and glycosylphosphatidylinositol-anchored proteins of erythrocyte rafts in regulating raft protein content and malarial infection. *J Biol Chem* 276, 29319–29329. <https://doi.org/10.1074/JBC.M101268200>
- Sani, M., Baganz, F., 2016. Mixing time as a criterion for scale translation of cell-culture processes. *Biopharm Int* 29, 47–51.
- Savonnière, S., Zeghari, N., Miccoli, L., Muller, S., Maugras, M., Donner, M., 1996. Effects of lipid supplementation of culture media on cell growth, antibody production, membrane structure and dynamics in two hybridomas. *J Biotechnol* 48, 161–173. [https://doi.org/10.1016/0168-1656\(96\)01392-2](https://doi.org/10.1016/0168-1656(96)01392-2)

- Schlender, M., Hernandez-Villafuerte, K., Cheng, C.Y., Mestre-Ferrandiz, J., Baumann, M., 2021. How Much Does It Cost to Research and Develop a New Drug? A Systematic Review and Assessment. *Pharmacoeconomics* 39, 1243–1269.
<https://doi.org/10.1007/S40273-021-01065-Y>
- Schlimgen, R., Howard, J., Wooley, D., Thompson, M., Baden, L.R., Yang, O.O., Christiani, D.C., Mostoslavsky, G., Diamond, D. V., Duane, E.G., Byers, K., Winters, T., Gelfand, J.A., Fujimoto, G., Hudson, T.W., Vyas, J.M., 2016. Risks associated with lentiviral vector exposures and prevention strategies. *J Occup Environ Med* 58, 1159–1166.
<https://doi.org/10.1097/JOM.0000000000000879>
- Schmidt, F.R., 2005. Optimization and scale up of industrial fermentation processes. *Appl Microbiol Biotechnol* 68, 425–435. <https://doi.org/10.1007/S00253-005-0003-0/FIGURES/1>
- Schnellbaecher, A., Binder, D., Bellmaine, S., Zimmer, A., 2019. Vitamins in cell culture media: Stability and stabilization strategies. *Biotechnol Bioeng* 116, 1537–1555.
<https://doi.org/10.1002/BIT.26942>
- Schweizer, M., Merten, O.-W., 2010. Large-scale production means for the manufacturing of lentiviral vectors. *Curr Gene Ther* 10, 474–486.
<https://doi.org/10.2174/156652310793797748>
- Segura, M.M., Garnier, A., Durocher, Y., Coelho, H., Kamen, A., 2007. Production of lentiviral vectors by large-scale transient transfection of suspension cultures and affinity chromatography purification. *Biotechnol Bioeng* 98, 789–799.
<https://doi.org/10.1002/bit.21467>
- Segura, M.M., Mangion, M., Gaillet, B., Garnier, A., 2013. New developments in lentiviral vector design, production and purification. *Expert Opin Biol Ther* 13, 987–1011.
<https://doi.org/10.1517/14712598.2013.779249>
- Seo, J.Y., Cresswell, P., 2013. Viperin regulates cellular lipid metabolism during human cytomegalovirus infection. *PLoS Pathog* 9, e1003497–e1003497.
<https://doi.org/10.1371/JOURNAL.PPAT.1003497>
- Sharon, D., Kamen, A., 2018. Advancements in the design and scalable production of viral gene transfer vectors. *Biotechnol Bioeng* 115, 25–40.
<https://doi.org/10.1002/BIT.26461>
- Silk, N.J., 2014. High throughput approaches to mammalian cell culture process development.
- Silk, N.J., Denby, S., Lewis, G., Kuiper, M., Hatton, D., Field, R., Baganz, F., Lye, G.J., 2010. Fed-batch operation of an industrial cell culture process in shaken microwells. *Biotechnol Lett* 32, 73–78. <https://doi.org/10.1007/S10529-009-0124-0/FIGURES/3>
- Soboleski, M.R., Oaks, J., Halford, W.P., 2005. Green fluorescent protein is a quantitative reporter of gene expression in individual eukaryotic cells. *The FASEB Journal* 19, 1–20. <https://doi.org/10.1096/FJ.04-3180FJE>
- Sofer, G.K., 2003. Virus inactivation in the 1990s - and into the 21st century. Part 5, disinfection. *Biopharm Int* 16, 44–48.

- Stacey, G.N., Merten, O.W., 2011. Host cells and cell banking. *Methods Mol Biol* 737, 45–88. https://doi.org/10.1007/978-1-61779-095-9_3
- Stepanenko, A.A., Dmitrenko, V. V., 2015. HEK293 in cell biology and cancer research: phenotype, karyotype, tumorigenicity, and stress-induced genome-phenotype evolution. *Gene* 569, 182–190. <https://doi.org/10.1016/J.GENE.2015.05.065>
- Strober, W., 2001. Trypan blue exclusion test of cell viability. *Current protocols in immunology / edited by John E. Coligan ... [et al.] Appendix 3.* <https://doi.org/10.1002/0471142735.ima03bs21>
- Subedi, G.P., Johnson, R.W., Moniz, H.A., Moremen, K.W., Barb, A., 2015. High yield expression of recombinant human proteins with the transient transfection of HEK293 cells in suspension. *Journal of Visualized Experiments* 2015. <https://doi.org/10.3791/53568>
- Tang, Q.L., Gu, L.X., Xu, Y., Liao, X.H., Zhou, Y., Zhang, T.C., 2021. Establishing functional lentiviral vector production in a stirred bioreactor for CAR-T cell therapy. *Bioengineered* 12, 2095–2105. https://doi.org/10.1080/21655979.2021.1931644/SUPPL_FILE/KBIE_A_1931644_SM7099.DOCX
- Tetlow, L.C., Woolley, D.E., 2003. Histamine stimulates the proliferation of human articular chondrocytes in vitro and is expressed by chondrocytes in osteoarthritic cartilage. *Ann Rheum Dis* 62, 991–994. <https://doi.org/10.1136/ARD.62.10.991>
- Tharmalingam, T., Goudar, C.T., 2015. Evaluating the impact of high Pluronic® F68 concentrations on antibody producing CHO cell lines. *Biotechnol Bioeng* 112, 832–837. <https://doi.org/10.1002/BIT.25491>
- Throm, R.E., Ouma, A.A., Zhou, S., Chandrasekaran, A., Lockey, T., Greene, M., De Ravin, S.S., Moayeri, M., Malech, H.L., Sorrentino, B.P., Gray, J.T., 2009. Efficient construction of producer cell lines for a SIN lentiviral vector for SCID-X1 gene therapy by concatemeric array transfection. *Blood* 113, 5104–5110. <https://doi.org/10.1182/blood-2008-11-191049>
- Thuret, I., Ruggeri, A., Angelucci, E., Chabannon, C., 2022. Hurdles to the Adoption of Gene Therapy as a Curative Option for Transfusion-Dependent Thalassemia. *Stem Cells Transl Med* 11, 407–414. <https://doi.org/10.1093/STCLTM/SZAC007>
- Tissot, S., Farhat, M., Hacker, D.L., Anderlei, T., Kühner, M., Comninellis, C., Wurm, F., 2010. Determination of a scale-up factor from mixing time studies in orbitally shaken bioreactors. *Biochem Eng J* 52, 181–186. <https://doi.org/10.1016/J.BEJ.2010.08.005>
- Tomás, H.A., Rodrigues, A.F., Alves, P.M., Coroadinha, A.S., Tomás, H.A., Rodrigues, A.F., Alves, P.M., Coroadinha, A.S., 2013. Lentiviral Gene Therapy Vectors: Challenges and Future Directions. *Gene Therapy - Tools and Potential Applications.* <https://doi.org/10.5772/52534>
- Torkashvand, F., Vaziri, B., Maleknia, S., Heydari, A., Vossoughi, M., Davami, F., Mahboudi, F., 2015. Designed amino acid feed in improvement of production and quality targets

- of a therapeutic monoclonal antibody. *PLoS One* 10.
<https://doi.org/10.1371/journal.pone.0140597>
- Tripathi, N.K., Shrivastava, A., 2019. Recent Developments in Bioprocessing of Recombinant Proteins: Expression Hosts and Process Development. *Front Bioeng Biotechnol* 7. <https://doi.org/10.3389/FBIOE.2019.00420>
- Tsien, R.Y., 1998. The green fluorescent protein. *Annu Rev Biochem* 67, 509–544.
<https://doi.org/10.1146/ANNUREV.BIOCHEM.67.1.509>
- U.S. Food and Drug Administration, 2011. Guidance for Industry Process Validation: General Principles and Practices Guidance for Industry.
- van der Loo, J.C.M., Wright, J.F., 2016. Progress and challenges in viral vector manufacturing. *Hum Mol Genet* 25, R42–R52.
<https://doi.org/10.1093/HMG/DDV451>
- Villas-Bôas, S.G., Noel, S., Lane, G.A., Attwood, G., Cookson, A., 2006. Extracellular metabolomics: a metabolic footprinting approach to assess fiber degradation in complex media. *Anal Biochem* 349, 297–305.
<https://doi.org/10.1016/J.AB.2005.11.019>
- Wallace, H.M., Fraser, A. V, Hughes, A., 2003. A perspective of polyamine metabolism. *Biochem. J* 376, 1–14.
- Wang, L.L.W., Janes, M.E., Kumbhojkar, N., Kapate, N., Clegg, J.R., Prakash, S., Heavey, M.K., Zhao, Z., Anselmo, A.C., Mitragotri, S., 2021. Cell therapies in the clinic. *Bioeng Transl Med* 6. <https://doi.org/10.1002/BTM2.10214>
- Wendler, R., Veith, R., Dancer, J., Stitt, M., Komor, E., 1990. Sucrose storage in cell suspension cultures of *Saccharum* sp. (sugarcane) is regulated by a cycle of synthesis and degradation.
- Westoby, M., Chrostowski, J., De Vilmorin, P., Smelko, J.P., Romero, J.K., 2011. Effects of solution environment on mammalian cell fermentation broth properties: Enhanced impurity removal and clarification performance. *Biotechnol Bioeng* 108, 50–58.
<https://doi.org/10.1002/BIT.22923>
- Wiegmann, V., Martinez, C.B., Baganz, F., 2020. Using a parallel micro-cultivation system (micro-matrix) as a process development tool for cell culture applications. *Methods in Molecular Biology* 2095, 69–81. https://doi.org/10.1007/978-1-0716-0191-4_5/FIGURES/2
- Witting, S.R., Li, L.H., Jasti, A., Allen, C., Cornetta, K., Brady, J., Shivakumar, R., Peshwa, M. V., 2012. Efficient large volume lentiviral vector production using flow electroporation. *Hum Gene Ther* 23, 243–249. <https://doi.org/10.1089/HUM.2011.088>
- Wong, V.V.T., Ho, K.W., Yap, M.G.S., 2004. Evaluation of insulin-mimetic trace metals as insulin replacements in mammalian cell cultures. *Cytotechnology* 45, 107–115.
<https://doi.org/10.1007/S10616-004-6173-2/METRICS>

- Xing, Z., Kenty, B., Koyrakh, I., Borys, M., Pan, S.H., Li, Z.J., 2011a. Optimizing amino acid composition of CHO cell culture media for a fusion protein production. *Process Biochemistry* 46, 1423–1429. <https://doi.org/10.1016/J.PROCBIO.2011.03.014>
- Xing, Z., Kenty, B., Koyrakh, I., Borys, M., Pan, S.H., Li, Z.J., 2011b. Optimizing amino acid composition of CHO cell culture media for a fusion protein production. *Process Biochemistry* 46, 1423–1429. <https://doi.org/10.1016/J.PROCBIO.2011.03.014>
- Xing, Z., Kenty, B.M., Li, Z.J., Lee, S.S., 2009. Scale-up analysis for a CHO cell culture process in large-scale bioreactors. *Biotechnol Bioeng* 103, 733–746. <https://doi.org/10.1002/BIT.22287>
- Xu, P., Dai, X.P., Graf, E., Martel, R., Russell, R., 2014. Effects of glutamine and asparagine on recombinant antibody production using CHO-GS cell lines. *Biotechnol Prog* 30, 1457–1468. <https://doi.org/10.1002/BTPR.1957>
- Yako, H., Niimi, N., Kato, A., Takaku, S., Tatsumi, Y., Nishito, Y., Kato, K., Sango, K., 2021. Role of pyruvate in maintaining cell viability and energy production under high-glucose conditions. *Scientific Reports* 2021 11:1 11, 1–17. <https://doi.org/10.1038/s41598-021-98082-w>
- Yang, J.D., Lu, C., Stasny, B., Henley, J., Guinto, W., Gonzalez, C., Gleason, J., Fung, M., Collopy, B., Benjamino, M., Gangi, J., Hanson, M., Ille, E., 2007. Fed-batch bioreactor process scale-up from 3-L to 2,500-L scale for monoclonal antibody production from cell culture. *Biotechnol Bioeng* 98, 141–154. <https://doi.org/10.1002/BIT.21413>
- Yang, Q., Lucas, A., Son, S., Chang, L.J., 2007. Overlapping enhancer/promoter and transcriptional termination signals in the lentiviral long terminal repeat. *Retrovirology* 4. <https://doi.org/10.1186/1742-4690-4-4>
- Yao, T., Asayama, Y., 2017. Animal-cell culture media: History, characteristics, and current issues. *Reprod Med Biol* 16, 99–117. <https://doi.org/10.1002/RMB2.12024>
- Zhang, H., Lamping, S.R., Pickering, S.C.R., Lye, G.J., Shamlou, P.A., 2008. Engineering characterisation of a single well from 24-well and 96-well microtitre plates. *Biochem Eng J* 40, 138–149. <https://doi.org/10.1016/J.BEJ.2007.12.005>
- Zhong, J.J., 2019. Bioreactor engineering. *Comprehensive Biotechnology* 257–269. <https://doi.org/10.1016/B978-0-444-64046-8.00077-X>
- Zingaro, K., Begos, D.M., Miller, T., 2020. Challenges to Process Validation for Viral Vectors [WWW Document]. URL <https://www.pharmasalmanac.com/articles/challenges-to-process-validation-for-viral-vectors> (accessed 8.27.23).
- Zufferey, R., Dull, T., Mandel, R.J., Bukovsky, A., Quiroz, D., Naldini, L., Trono, D., 1998. Self-inactivating lentivirus vector for safe and efficient in vivo gene delivery. *J Virol* 72, 9873–9880. <https://doi.org/10.1128/JVI.72.12.9873-9880.1998>

9 APPENDIX A: SUPPLEMENTARY MATERIAL

9.1 CELL POPULATION DOUBLING TIME DATA

9.1.1 Cell population doubling time for 277 stable cell line growth culture in 2 L STR (section 3.3)

Table 9.1: Cell population doubling time for 277 stable cell line growth culture in 2 L STR (section 3.3). Doubling time was calculated using equations 2 and 3 as shown in section 2.11.

Time period (days)	Population doubling time (hours)
0 to 1	56.0
1 to 2	22.8
2 to 3	30.3
3 to 4	41.1
4 to 5	47.7
5 to 6	182.3
6 to 7	335.2

9.1.2 Cell population doubling time for 277 stable cell line platform LVV production process in 2 L STR (section 3.4)

Table 9.2: Cell population doubling time for 277 stable cell line platform LVV production process in 2 L STR (section 3.4). Population doubling time was calculated using equations 2 and 3 as shown in section 2.11.

Time period (days)	Population doubling time (hours)
0 to 1	29.4
1 to 2	23.7
2 to 3	33.9
3 to 4	214.0

9.1.3 Cell population doubling time for 277 stable cell line growth culture in 2 L STR at different pH and CO₂ set-point values (section 3.6)

Table 9.3: Cell population doubling time for 277 stable cell line growth culture in 2 L STR (section 3.6). Population doubling time was calculated using equations 2 and 3 as shown in section 2.11. N/A means the cell culture entered into death phase.

Time period (days)	Population doubling time (hours)			
	STR 1	STR 2	STR 3	STR 4
0 to 1	22.4	23.4	29.4	26.5
1 to 2	30.5	30.6	31.9	33.0
2 to 3	27.3	26.6	26.1	26.1
3 to 4	44.2	30.0	49.5	48.0
4 to 5	58.0	51.9	70.5	53.1
5 to 6	86.1	N/A	373.8	317.3
6 to 7	22.4	N/A	N/A	N/A

9.1.4 Cell population doubling time for 277 stable cell line growth culture in 24-DSW plate (section 5.3)

Table 9.4: Cell population doubling time for 277 stable cell line growth culture in 2 L STR (section 5.3). Population doubling time was calculated using equations 2 and 3 as shown in section 2.11. N/A means the cell culture entered into death phase.

Time period (days)	Population doubling time (hours)				
	No Feed	Feeding regime 1	Feeding regime 2	Feeding regime 3	Feeding regime 4
0 to 1	24.5	24.5	24.5	24.5	24.5
1 to 2	29.0	29.0	29.0	29.0	29.0
2 to 3	78.3	41.3	52.1	56.6	59.4
3 to 4	39.5	39.2	33.5	33.7	47.4
4 to 5	47.8	44.7	40.9	43.7	47.4
5 to 6	1090.0	62.4	92.4	98.8	68.9
6 to 7	N/A	116.6	161.8	109.5	50.5
7 to 8	N/A	N/A	N/A	N/A	N/A
8 to 9	N/A	N/A	N/A	N/A	N/A

9.2 LITERATURE REFERENCES USED TO SCORE DEPLETING METABOLITES IN SECTION 3.7.3

Table 9.5: List of literature references for depleting metabolites used in scoring analysis.

	Metabolite	Type	Literature
1	L-Serine	Amino acid	Dietmair et al., 2012; Fan et al., 2015; Henry et al., 2011; Kim et al., 2005; Martínez-Monge et al., 2019; Nadeau et al., 2000; Petiot et al., 2011; Rodrigues et al., 2013; Schwarz et al., 2020; Xing et al., 2011

2	L-Lysine	Amino acid	Dietmair et al., 2012; Fan et al., 2015; Henry et al., 2011; Kim et al., 2005; Landauer, 2014; Martínez-Monge et al., 2019; Nadeau et al., 2000; Rodrigues et al., 2013; Schwarz et al., 2020; Xing et al., 2011
3	L-Valine	Amino acid	Dietmair et al., 2012; Henry et al., 2011; Kim et al., 2005; Landauer, 2014; Nadeau et al., 2000; Petiot et al., 2011; Rodrigues et al., 2013; Schwarz et al., 2020; Xing et al., 2011
4	Choline	Vitamin	Ducommun et al., 2001; Ishaque and Al-Rubeai, 2002; Kim et al., 2005; Kurano et al., 1990; Kuwae et al., 2018; Landauer, 2014
5	L-Leucine	Amino acid	Dietmair et al., 2012; Fan et al., 2015; Henry et al., 2011; Kim et al., 2005; Landauer, 2014; Martínez-Monge et al., 2019; Nadeau et al., 2000; Rodrigues et al., 2013; Schwarz et al., 2020; Xing et al., 2011
6	L-Glutamine	Amino acid	Dietmair et al., 2012; Fan et al., 2015; Henry et al., 2011; Kim et al., 2005; Martínez-Monge et al., 2019; Nadeau et al., 2000; Petiot et al., 2011; Rodrigues et al., 2013; Schwarz et al., 2020; Xing et al., 2011
7	Glucose	Carbohydrate	Coroadinha et al., 2006a; Fan et al., 2015; Henry et al., 2011; Landauer, 2014; Martínez-Monge et al., 2019; Nadeau et al., 2000; Petiot et al., 2011; Quek et al., 2010; Rodrigues et al., 2013; Wong et al., 2005
8	L-Arginine	Amino acid	Capella Roca et al., 2019; Dietmair et al., 2012; Henry et al., 2011; Kim et al., 2005; Landauer, 2014; Petiot et al., 2011; Rodrigues et al., 2013; Schwarz et al., 2020; Xing et al., 2011
9	Aspartic acid	Amino acid	Dietmair et al., 2012; Henry et al., 2011; Kim et al., 2005; Landauer, 2014; Martínez-Monge et al., 2019; Nadeau et al., 2000; Petiot et al., 2011; Schwarz et al., 2020
10	Folic acid (Vitamin B9)	Vitamin	Borman and Branda, 1989; Ducommun et al., 2001; Ishaque and Al-Rubeai, 2002; Kim et al., 2005; Landauer, 2014; Schnellbaecher et al., 2019; Stoll et al., 1996; Takagi et al., 2001
11	L-alanyl-L-glutamine	Peptide	Christie and Butler, 1994; Imamoto et al., 2013; Krömer et al., 2011b; Liste-Calleja et al., 2013; Salazar et al., 2016
12	Isoleucine	Amino acid	Dietmair et al., 2012; Henry et al., 2011; Landauer, 2014; Nadeau et al., 2000; Rodrigues et al., 2013; Schwarz et al., 2020
13	Asparagine	Amino acid	Duarte et al., 2014; Landauer, 2014; Nadeau et al., 2000; Rodrigues et al., 2013; Schwarz et al., 2020; Xing et al., 2011

9.2 | LITERATURE REFERENCES USED TO SCORE DEPLETING METABOLITES IN SECTION 3.7.3

14	L-Ornithine	Amino acid	Baich, 1983; Capella Roca et al., 2019; Hölttä and Pohjanpelto, 1982; Mounce et al., 2017; Steglich et al., 1985; Yamamoto and Niwa, 1993
15	L-Methionine	Amino acid	Kim et al., 2005; Landauer, 2014a; Rodrigues et al., 2013; Xing et al., 2011
16	Pantothenic acid (Vitamin B5)	Vitamin	Ducommun et al., 2001; Ishaque and Al-Rubeai, 2002; Kim et al., 2005; Landauer, 2014; Schnellbaecher et al., 2019; Stoll et al., 1996; Takagi et al., 2001
17	L-Phenylalanine	Amino acid	Landauer, 2014; Rodrigues et al., 2013
18	Histamine	Organic compound	None
19	L-Norvaline	Amino acid	None
20	Putrescine	Polyamine	Capella Roca et al., 2019; Hölttä and Pohjanpelto, 1982; Igarashi and Kashiwagi, 2010; Mounce et al., 2017; Pohjanpelto et al., 1981; Rodrigues et al., 2013; Sugahara et al., 2008
21	2-Aminoisobutyric acid	Amino acid	None
22	D-Pipecolic acid	Acid	None
23	Ascorbic acid (Vitamin C)	Vitamin	Chepda et al., 2001; Kim et al., 2005; Landauer, 2014
24	L-Cystine	Amino acid	Kim et al., 2005; Landauer, 2014
25	L-Histidine	Amino acid	Kim et al., 2005; Landauer, 2014
26	L-Tryptophan	Amino acid	Landauer, 2014; Xing et al., 2011
27	L-Tyrosine	Amino acid	Kim et al., 2005; Landauer, 2014
28	Acetylcysteine	Amino acid derivative	Ezeriņa et al., 2018; Mi et al., 2010
29	Glycine	Amino acid	Henry et al., 2011; Landauer, 2014
30	L-Glutamic acid	Amino acid	Landauer, 2014; Nadeau et al., 2000
31	L-Proline	Amino acid	Landauer, 2014; Martínez-Monge et al., 2019
32	Citrulline	Amino acid	Yamamoto and Niwa, 1993
33	L-Alanine	Amino acid	Landauer, 2014
34	Succinic acid	Acid	Argentova et al., 2020
35	2-Aminoethanol	Fatty acids and Lipids	Landauer, 2014
36	Glycyl-L-glutamine	Peptide	Christie and Butler, 1994

37	Oleic acid	Acid	None
38	β -Alanine	Amino acid	None
39	DL-2-Aminoadipic acid	Amino acid	None
40	Homocystine	Amino acid	None
41	L-Pyroglutamic acid	Amino acid derivative	None
42	Transhydroxyproline	Amino acid derivative	None
43	Lipoic acid	Vitamin	Landauer, 2014
44	Ethylenediamine	Organic compound	None
45	Phosphorylcholine	Fatty acids and Lipids	None
46	Cystathionine	Amino acid	None
47	Gamma-aminobutyric acid	Amino acid	None
48	DL-Methionine sulfoxide	Amino acid derivative	None
49	Carnosine	Peptide	None
50	L-Threonic acid	Acid	None
51	Malic acid	Acid	None

9.3 COMPARISON OF SAMPLING METHODS USED FOR 24-DSW PLATE CULTURES

The VCD profile of two different sampling methods used for 24-DSW plate cultures in Figure 9.1 below. Same well sampling means a single well is used for sampling during the entire culture duration. In sacrificial well sampling, one well is dedicated for each days sampling. Hence, multiple wells are required to cover sampling over the whole culture period.

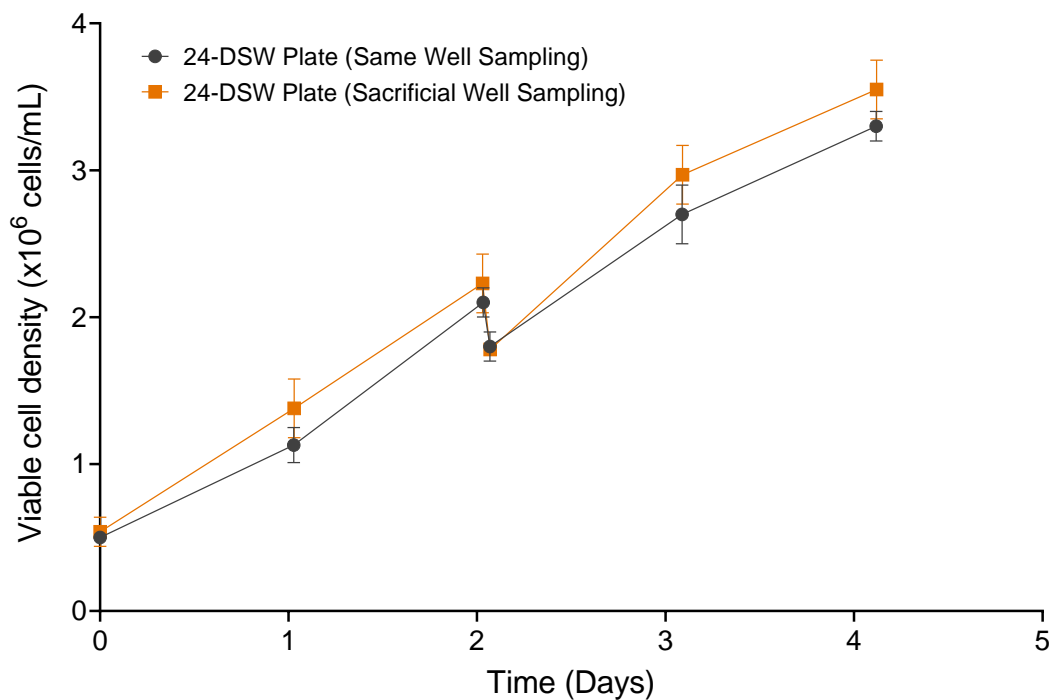


Figure 9.1: Viable cell density profile of HEK293T stable producer cell line culture in 24-DSW plates using same well sampling and sacrificial well sampling methods. Error bars represent one standard deviation about the mean (n=3).

9.4 DESIGN OF EXPERIMENTS STUDIES

9.4.1 Experimental design space for DoE screening studies generated using Design Expert software (section 5.4)

Table 9.6: Experimental design space for DoE screening study 1 (section 5.4.1). Design was generated using Design Expert v10 (Stat-Ease, Inc., Minnesota, U.S.A).

Run	Essential amino acids (× MEM)	Non-essential amino acids (× MEM)	Glutamine (× MEM)	Vitamins (× MEM)	Glucose (× MEM)	Polyamines (× MEM)
1	0	1	0	0	8	1
2	15	1	15	4	8	1
3	15	1	0	4	0	0
4	0	0	0	0	0	0
5	7.5	0.5	7.5	2	4	0.5
6	15	0	15	0	0	1
7	15	1	0	0	0	1
8	0	1	0	4	8	0
9	0	1	15	0	0	0
10	0	0	0	4	0	1
11	7.5	0.5	7.5	2	4	0.5
12	15	0	0	0	8	0
13	15	0	0	4	8	1
14	0	0	15	4	8	0
15	0	1	15	4	0	1
16	7.5	0.5	7.5	2	4	0.5
17	0	0	15	0	8	1
18	15	0	15	4	0	0
19	15	1	15	0	8	0
20	15	0	0	4	8	1
21	0	1	0	0	8	1
22	15	0	0	0	8	0
23	7.5	0.5	7.5	2	4	0.5
24	0	0	0	0	0	0
25	0	0	0	4	0	1
26	15	1	0	4	0	0
27	15	1	15	0	8	0
28	15	1	0	0	0	1
29	0	1	15	0	0	0
30	0	0	15	4	8	0
31	7.5	0.5	7.5	2	4	0.5
32	0	0	15	0	8	1
33	0	1	15	4	0	1
34	15	0	15	0	0	1
35	7.5	0.5	7.5	2	4	0.5
36	15	0	15	4	0	0
37	0	1	0	4	8	0

38 15 1 15 4 8 1

Table 9.7: Experimental design space for DoE screening study 2 (section 5.4.2). Design was generated using Design Expert v10 (Stat-Ease, Inc., Minnesota, U.S.A).

Run	Essential amino acid (× MEM)	L-alanyl-L-glutamine (× MEM)	Lipids (dilution)	Inorganic salts (× MEM)	Insulin (mg/mL)	IGF-1 (µg/mL)	Sodium pyruvate (mM)	Feed mixture (relative concentration)
1	15	15	0	0	0	2.5	1	0
2	0	0	0.05	1	2.5	0	0	1
3	7.5	7.5	0.025	0.5	1.25	1.25	0.5	0.5
4	15	15	0.05	1	2.5	2.5	1	1
5	15	0	0.05	1	0	0	1	0
6	15	15	0.05	0	2.5	0	0	0
7	0	15	0.05	0	0	0	1	1
8	15	15	0	1	0	0	0	1
9	0	0	0	1	0	2.5	1	1
10	0	15	0.05	1	0	2.5	0	0
11	15	0	0	0	2.5	0	1	1
12	7.5	7.5	0.025	0.5	1.25	1.25	0.5	0.5
13	0	0	0	0	0	0	0	0
14	15	0	0.05	0	0	2.5	0	1
15	0	0	0.05	0	2.5	2.5	1	0
16	7.5	7.5	0.025	0.5	1.25	1.25	0.5	0.5
17	15	0	0	1	2.5	2.5	0	0
18	0	15	0	1	2.5	0	1	0
19	0	15	0	0	2.5	2.5	0	1
20	7.5	7.5	0.025	0.5	1.25	1.25	0.5	0.5
21	7.5	7.5	0.025	0.5	1.25	1.25	0.5	0.5
22	15	15	0	1	0	0	0	1
23	0	15	0.05	0	0	0	1	1
24	0	0	0.05	1	2.5	0	0	1
25	15	0	0.05	0	0	2.5	0	1
26	0	15	0.05	1	0	2.5	0	0
27	15	15	0	0	0	2.5	1	0
28	0	0	0	1	0	2.5	1	1
29	0	15	0	0	2.5	2.5	0	1
30	15	0	0	0	2.5	0	1	1
31	15	0	0.05	1	0	0	1	0
32	15	15	0.05	1	2.5	2.5	1	1
33	0	0	0.05	0	2.5	2.5	1	0
34	0	15	0	1	2.5	0	1	0

35	0	0	0	0	0	0	0	0
36	7.5	7.5	0.025	0.5	1.25	1.25	0.5	0.5
37	15	0	0	1	2.5	2.5	0	0
38	15	15	0.05	0	2.5	0	0	0

Table 9.8: Experimental design space for DoE screening study 3 (section 5.4.3). Design was generated using Design Expert v10 (Stat-Ease, Inc., Minnesota, U.S.A).

Run	L-Aspartic acid (g/L)	L-Leucine (g/L)	L-Valine (g/L)	L-Lysine hydrochloride (g/L)	L-Isoleucine (g/L)	L-Arginine hydrochloride (g/L)	L-Serine (g/L)	L-Asparagine (g/L)
1	0.4	1.6	0	0	0	3.8	0.3	0
2	0.4	0	1.4	2.2	0	0	0.3	0
3	0	1.6	0	2.2	1.6	0	0.3	0
4	0	0	0	2.2	0	3.8	0.3	0.4
5	0	0	1.4	2.2	1.6	0	0	0.4
6	0.4	1.6	0	2.2	0	0	0	0.4
7	0.4	0	1.4	0	0	3.8	0	0.4
8	0.4	1.6	0	2.2	0	0	0	0.4
9	0.2	0.8	0.7	1.1	0.8	1.9	0.15	0.2
10	0.4	0	0	0	1.6	0	0.3	0.4
11	0	0	1.4	2.2	1.6	0	0	0.4
12	0.4	1.6	1.4	0	1.6	0	0	0
13	0	1.6	1.4	0	0	0	0.3	0.4
14	0.4	1.6	1.4	2.2	1.6	3.8	0.3	0.4
15	0	1.6	1.4	0	0	0	0.3	0.4
16	0	0	1.4	0	1.6	3.8	0.3	0
17	0	0	0	0	0	0	0	0
18	0	1.6	0	2.2	1.6	0	0.3	0
19	0.4	0	0	0	1.6	0	0.3	0.4
20	0.4	1.6	1.4	0	1.6	0	0	0
21	0	1.6	1.4	2.2	0	3.8	0	0
22	0.4	0	1.4	2.2	0	0	0.3	0
23	0	1.6	0	0	1.6	3.8	0	0.4
24	0.4	0	0	2.2	1.6	3.8	0	0
25	0	1.6	1.4	2.2	0	3.8	0	0
26	0	0	0	2.2	0	3.8	0.3	0.4
27	0.4	0	1.4	0	0	3.8	0	0.4
28	0.2	0.8	0.7	1.1	0.8	1.9	0.15	0.2
29	0	0	1.4	0	1.6	3.8	0.3	0
30	0	0	0	0	0	0	0	0
31	0.4	1.6	0	0	0	3.8	0.3	0
32	0.4	1.6	1.4	2.2	1.6	3.8	0.3	0.4

33	0.4	0	0	2.2	1.6	3.8	0	0
34	0.2	0.8	0.7	1.1	0.8	1.9	0.15	0.2
35	0	1.6	0	0	1.6	3.8	0	0.4

Table 9.9: Experimental design space for DoE screening study 4 (section 5.4.4). Design was generated using Design Expert v10 (Stat-Ease, Inc., Minnesota, U.S.A).

Run	Essential amino acids (× MEM)	L-Ornithine (g/L)	L-Norvaline (g/L)	2-Aminoisobutyric acid (g/L)	Choline chloride (g/L)	Folic acid (g/L)	Putrescine dihydrochloride (g/L)
1	15	0	5	5	0	0	1
2	15	5	5	0	5	0	0
3	15	0	5	0	0	0.5	0
4	0	5	5	0	0	0	1
5	0	0	5	5	5	0	0
6	0	0	5	0	5	0.5	1
7	15	5	0	0	0	0.5	1
8	15	0	0	0	5	0	1
9	0	5	0	0	5	0.5	0
10	7.5	2.5	2.5	2.5	2.5	0.25	0.5
11	0	0	0	5	0	0.5	1
12	15	0	0	5	5	0.5	0
13	0	0	0	0	0	0	0
14	15	5	5	5	5	0.5	1
15	0	5	0	5	5	0	1
16	7.5	2.5	2.5	2.5	2.5	0.25	0.5
17	7.5	2.5	2.5	2.5	2.5	0.25	0.5
18	0	5	5	5	0	0.5	0
19	15	5	0	5	0	0	0
20	15	5	5	0	5	0	0
21	15	0	0	5	5	0.5	0
22	0	0	0	5	0	0.5	1
23	7.5	2.5	2.5	2.5	2.5	0.25	0.5
24	0	5	5	5	0	0.5	0
25	15	5	0	0	0	0.5	1
26	0	5	5	0	0	0	1
27	15	0	5	5	0	0	1
28	0	5	0	5	5	0	1
29	0	0	5	0	5	0.5	1
30	7.5	2.5	2.5	2.5	2.5	0.25	0.5
31	7.5	2.5	2.5	2.5	2.5	0.25	0.5
32	15	5	0	5	0	0	0
33	15	5	5	5	5	0.5	1

34	15	0	5	0	0	0.5	0
35	0	0	0	0	0	0	0
36	15	0	0	0	5	0	1
37	0	5	0	0	5	0.5	0
38	0	0	5	5	5	0	0

9.4.2 Experimental design space for DoE optimisation studies generated using Design Expert software (section 5.5)

Table 9.10: Experimental design space for DoE optimisation study 1 (section 5.5.1). Design was generated using Design Expert v10 (Stat-Ease, Inc., Minnesota, U.S.A).

Run	Essential amino acids (× MEM)	Non-essential amino acids (× MEM)
1	15.0	0.0
2	15.0	10.0
3	25.6	1.5
4	4.4	1.5
5	4.4	1.5
6	4.4	8.5
7	25.6	1.5
8	15.0	5.0
9	25.6	8.5
10	0.0	5.0
11	30.0	5.0
12	15.0	5.0
13	30.0	5.0
14	15.0	5.0
15	15.0	5.0
16	4.4	1.5
17	4.4	8.5
18	25.6	1.5
19	25.6	8.5
20	30.0	5.0
21	0.0	5.0
22	25.6	8.5
23	4.4	8.5
24	15.0	5.0

25	15.0	10.0
26	15.0	10.0
27	15.0	0.0
28	0.0	5.0
29	15.0	0.0
30	0.0	0.0
31	0.0	0.0
32	30.0	0.0
33	20.0	0.0
34	20.0	0.0
35	10.0	0.0
36	20.0	0.0
37	10.0	0.0
38	10.0	0.0
39	30.0	0.0
40	30.0	0.0
41	0.0	0.0

Table 9.11: Experimental design space for DoE optimisation study 3 (section 5.5.3). Design was generated using Design Expert v10 (Stat-Ease, Inc., Minnesota, U.S.A).

Run	Day 3 feed amount (% v/v)	Day 4 feed amount (% v/v)	Day 5 feed amount (% v/v)	Day 6 feed amount (% v/v)
1	0.0	0.0	3.6	0.0
2	2.2	2.5	2.5	2.5
3	5.0	0.0	5.0	2.5
4	0.8	5.0	5.0	5.0
5	3.1	4.9	4.8	2.1
6	3.1	2.5	5.0	0.0
7	5.0	2.5	0.0	5.0
8	3.7	1.7	0.0	2.3
9	3.0	5.0	0.0	2.5
10	4.3	0.0	0.0	0.0
11	0.0	0.0	0.0	3.6
12	3.1	0.0	2.5	5.0
13	5.0	2.5	2.5	2.5
14	4.4	5.0	5.0	5.0
15	0.0	5.0	1.4	5.0
16	2.2	2.5	2.5	2.5
17	0.0	5.0	5.0	1.5
18	0.0	3.6	0.0	0.0
19	2.5	2.5	2.5	2.5
20	0.0	1.4	5.0	5.0

21	5.0	5.0	2.5	0.0
22	0.0	0.0	0.0	0.0
23	4.3	0.0	0.0	0.0
24	0.0	3.6	0.0	0.0
25	5.0	0.0	5.0	2.5
26	5.0	5.0	2.5	0.0
27	0.0	0.0	0.0	3.6
28	4.4	5.0	5.0	5.0
29	2.5	2.5	2.5	2.5
30	0.0	0.0	0.0	0.0
31	5.0	2.5	2.5	2.5
32	0.0	1.4	5.0	5.0
33	0.0	5.0	5.0	1.5
34	0.8	5.0	5.0	5.0
35	3.1	0.0	2.5	5.0
36	5.0	2.5	0.0	5.0
37	0.0	0.0	3.6	0.0
38	3.0	5.0	0.0	2.5
39	3.7	1.7	0.0	2.3
40	3.1	2.5	5.0	0.0
41	3.1	4.9	4.8	2.1
42	0.0	5.0	1.4	5.0
43	2.2	2.5	2.5	2.5
44	2.2	2.5	2.5	2.5

9.4.3 Complete formulations of the commercially available pre-formulated reagents used in the DoE studies (Section 5.4 and 5.5)

Table 9.12: Complete formulation of MEM Essential Amino Acids Solution (50X) (ThermoFisher Scientific, U.S.A).

Components	Concentration (mg/L)
L-Arginine hydrochloride	6320.0
L-Cystine	1200.0
L-Histidine hydrochloride-H ₂ O	2100.0
L-Isoleucine	2620.0
L-Leucine	2620.0
L-Lysine hydrochloride	3625.0

L-Methionine	755.0
L-Phenylalanine	1650.0
L-Threonine	2380.0
L-Tryptophan	510.0
L-Tyrosine	1800.0
L-Valine	2340.0

Table 9.13: Complete formulation of MEM Non-essential Amino Acids Solution (100X) (ThermoFisher Scientific, U.S.A).

Components	Concentration (mg/L)
Glycine	750.0
L-Alanine	890.0
L-Asparagine	1320.0
L-Aspartic acid	1330.0
L-Glutamic Acid	1470.0
L-Proline	1150.0
L-Serine	1050.0

Table 9.14: Complete formulation of MEM Vitamins Solution (100X) (Thermofisher Scientific, U.S.A).

Components	Concentration (mg/L)
Choline chloride	100.0
D-Calcium pantothenate	100.0
Folic Acid	100.0
Nicotinamide	100.0
Pyridoxal hydrochloride	100.0
Riboflavin	10.0
Thiamine hydrochloride	100.0
i-Inositol	200.0
Sodium Chloride (NaCl)	8500.0

Table 9.15: Formulation of Polyamine supplement (1000X) (MilliporeSigma, U.S.A).

Components	Concentration
Putrescine	Proprietary
Spermine	Proprietary
Spermidine	Proprietary

Table 9.16: Complete formulation of chemically defined lipid concentrate (ThermoFisher Scientific, U.S.A).

Components	Concentration (mg/L)
Arachidonic Acid	2.0
Cholesterol	220.0
DL-alpha-Tocopherol Acetate	70.0
Ethyl Alcohol 100%	confidential
Linoleic Acid	10.0
Linolenic Acid	10.0
Myristic Acid	10.0
Oleic Acid	10.0
Palmitic Acid	10.0
Palmitoleic Acid	10.0
Pluronic F-68	90000.0
Stearic Acid	10.0
Tween 80®	2200.0

Table 9.17: Complete formulation of Hanks' Balanced Salt Solution (10X) (ThermoFisher Scientific, U.S.A).

Components	Concentration (mg/L)
Potassium Chloride (KCl)	4000.0
Potassium Phosphate monobasic (KH ₂ PO ₄)	600.0
Sodium Chloride (NaCl)	80000.0
Sodium Phosphate dibasic (Na ₂ HPO ₄ ·7H ₂ O)	900.0
D-Glucose (Dextrose)	10000.0

9.4.4 DoE model fit summary data from optimisation studies (section 5.5)

Table 9.18: Fit summary data for day 6 VCD from optimisation study 1. Data generated using Design Expert v10 (Stat-Ease, Inc., Minnesota, U.S.A).

Source	Sequential p-value	Lack of Fit p-value	Adjusted R-Squared	Predicted R-Squared	
<u>Linear</u>	<u>< 0.0001</u>	<u>0.6513</u>	<u>0.6272</u>	<u>0.5963</u>	<u>Suggested</u>
2FI	0.8772	0.5712	0.6174	0.5755	
Quadratic	0.6328	0.4702	0.6060	0.5430	
Cubic	0.9305	0.1426	0.5669	0.4449	

Table 9.19: Fit summary data for day 6 cell viability from optimisation study 1. Data generated using Design Expert v10 (Stat-Ease, Inc., Minnesota, U.S.A).

Source	Sequential p-value	Lack of Fit p-value	Adjusted R-Squared	Predicted R-Squared	
Linear	< 0.0001	0.0088	0.7804	0.7530	
2FI	0.2063	0.0092	0.7841	0.7422	
Quadratic	0.0220	0.0402	0.8165	0.7700	
<u>Cubic</u>	<u>0.0077</u>	<u>0.6985</u>	<u>0.8657</u>	<u>0.8079</u>	<u>Suggested</u>

Table 9.20: Fit summary data for day 7 VCD from optimisation study 1. Data generated using Design Expert v10 (Stat-Ease, Inc., Minnesota, U.S.A).

Source	Sequential p-value	Lack of Fit p-value ¹	Adjusted R-Squared	Predicted R-Squared	
Linear	0.6013	< 0.0001	-0.0248	-0.1581	
2FI	0.9663	< 0.0001	-0.0525	-0.2688	
Quadratic	< 0.0001	< 0.0001	0.4651	0.3196	
<u>Cubic</u>	<u>0.0006</u>	<u>< 0.0001</u>	<u>0.6734</u>	<u>0.5532</u>	<u>Suggested</u>

¹ All models have a significant lack of fit i.e. lack of fit p-value < 0.05.

Table 9.21: Fit summary data for day 7 cell viability from optimisation study 1. Data generated using Design Expert v10 (Stat-Ease, Inc., Minnesota, U.S.A).

Source	Sequential p-value	Lack of Fit p-value ¹	Adjusted R-Squared	Predicted R-Squared	
Linear	0.4415	< 0.0001	-0.0083	-0.1408	
2FI	0.4090	< 0.0001	-0.0164	-0.2288	
Quadratic	< 0.0001	< 0.0001	0.5817	0.4613	
<u>Cubic</u>	<u>0.0003</u>	<u>< 0.0001</u>	<u>0.7591</u>	<u>0.6539</u>	<u>Suggested</u>

¹ All models have a significant lack of fit i.e. lack of fit p-value < 0.05.

Table 9.22: Fit summary data for day 6 VCD from optimisation study 3. Data generated using Design Expert v10 (Stat-Ease, Inc., Minnesota, U.S.A).

Source	Sequential p-value	Lack of Fit p-value	Adjusted R-Squared	Predicted R-Squared	
Linear	< 0.0001	0.2532	0.6423	0.5803	
2FI	0.1797	0.2716	0.6732	0.5969	
<u>Quadratic</u>	<u>< 0.0001</u>	<u>0.4830</u>	<u>0.8422</u>	<u>0.7351</u>	<u>Suggested</u>

Table 9.23: Fit summary data for day 6 cell viability from optimisation study 3. Data generated using Design Expert v10 (Stat-Ease, Inc., Minnesota, U.S.A).

Source	Sequential p-value	Lack of Fit p-value	Adjusted R-Squared	Predicted R-Squared	
Linear	< 0.0001	0.0851	0.6833	0.6129	
<u>2FI</u>	<u>0.0003</u>	<u>0.1450</u>	<u>0.8217</u>	<u>0.7396</u>	<u>Suggested</u>
Quadratic	0.1375	0.1588	0.8398	0.6887	

Table 9.24: Fit summary data for day 7 VCD from optimisation study 3. Data generated using Design Expert v10 (Stat-Ease, Inc., Minnesota, U.S.A).

Source	Sequential p-value	Lack of Fit p-value	Adjusted R-Squared	Predicted R-Squared	
Linear	0.6150	0.1038	-0.0322	-0.2506	
2FI	< 0.0001	0.2734	0.6466	0.5526	
<u>Quadratic</u>	<u>0.0029</u>	<u>0.3854</u>	<u>0.7685</u>	<u>0.6261</u>	<u>Suggested</u>

Table 9.25: Fit summary data for day 7 cell viability from optimisation study 3. Data generated using Design Expert v10 (Stat-Ease, Inc., Minnesota, U.S.A).

Source	Sequential p-value	Lack of Fit p-value ¹	Adjusted R-Squared	Predicted R-Squared	
Linear	0.8707	0.0029	-0.0705	-0.3129	
2FI	< 0.0001	0.0163	0.8126	0.7437	
<u>Quadratic</u>	<u>< 0.0001</u>	<u>0.0371</u>	<u>0.9191</u>	<u>0.8575</u>	<u>Suggested</u>

¹ All models have a significant lack of fit i.e. lack of fit p-value < 0.05.